The Consequences of Human land-use Strategies During the PPNB-LN Transition

A Simulation Modeling Approach

by

Isaac Ullah

A Dissertation Presented in Partial Fulfillment
of the Requirements for the Degree
Doctor of Philosophy

Approved December 2012 by the
Graduate Supervisory Committee:

C Michael Barton, Chair
Edward Banning
Ramon Arrowsmith
Geoffrey Clark

ARIZONA STATE UNIVERSITY

May 2013

ABSTRACT

This dissertation investigates the long-term consequences of human land-use practices in general, and in early agricultural villages in specific. This pioneering case study investigates the "collapse" of the Early (Pre-Pottery) Neolithic lifeway, which was a major transformational event marked by significant changes in settlement patterns, material culture, and social markers. To move beyond traditional narratives of cultural collapse, I employ a Complex Adaptive Systems approach to this research, and combine agent-based computer simulations of Neolithic land-use with dynamic and spatially-explicit GIS-based environmental models to conduct experiments into long-term trajectories of different potential Neolithic socio-environmental systems. My analysis outlines how the Early Neolithic "collapse" was likely instigated by a non-linear sequence of events, and that it would have been impossible for Neolithic peoples to recognize the long-term outcome of their actions. The experiment-based simulation approach shows that, starting from the same initial conditions, complex combinations of feedback amplification, stochasticity, responses to internal and external stimuli, and the accumulation of incremental changes to the socio-natural landscape, can lead to widely divergent outcomes over time. Thus, rather than being an inevitable consequence of specific Neolithic land-use choices, the "catastrophic" transformation at the end of the Early Neolithic was an emergent property of the Early Neolithic socio-natural system itself, and thus likely not an easily predictable event. In this way, my work uses the technique of simulation modeling to connect CAS theory with the archaeological and geoarchaeological record to help better understand the causes and consequences of socio-ecological transformation at a regional scale. The research is broadly applicable to other archaeological cases of resilience and collapse, and is truly interdisciplinary in that it draws on fields such as geomorphology, computer science, and agronomy in addition to archaeology.

This dissertation is dedicated to Leah Abriani.

Leah, I could never have done this without you.

ACKNOWLEDGMENTS

I would first like to acknowledge the support of my committee members, Michael Barton, Ted Banning, Geoff Clark, and Ramon Arrowsmith. Michael Barton supported my graduate career with excellent research opportunities, funding, mentorship, and advice, and allowed me to take a leadership role in the Mediterranean Landscape Dynamics Project. This dissertation would not have been possible with his support, direction, and instruction. Ted Banning has supported my research over numerous years, and introduced me to the Neolithic Archaeology of Wadi Ziqlab. My participation in the Wadi Ziqlab Project, including fieldwork opportunities, directly facilitated much of my dissertation research. Geoff Clark has provided abundant advice and mentoring, and his guidance as I formulated my dissertation proposal greatly aided the structure and nature of this dissertation. Ramon Arrowsmith provided essential instruction and advice on field geomorphology and erosion modeling, which became core aspects of my research agenda.

I would also like to thank my colleagues in the Mediterranean Landscape Dynamics project. Helena Mitasova provided invaluable advice on the landscape evolution modeling aspects of this research. Alexandra Miller compiled and facilitated the climate modeling that is used in this research. Mariela Soto-Berelov provided the paleovegetation modeling that is used in this research. Erin Dimaggio and Sidney Remple georectified much of the imagery and other GIS data. Finally, Gary Mayer, Hessam Sarjoughian, and especially Sean Bergin were instrumental in the construction of the Agent-Based simulation environment used in this research. Gabriel Popescu helped to compile some of the ethnographic data used to parameterize the simulation.

Much of the archaeological data used in this dissertation was compiled and analyzed by Wadi Ziqlab Project members Seiji Kadowaki, Kevin Gibbs, Lisa Maher, and Danielle MacDonald. They, and other members of the Wadi Ziqlab field crews, have made fieldwork in Wadi Ziqlab exceedingly enjoyable!

I'd like to thank Ian Kuijt and Meredeth Chesson for their support and hospitality, and for helping me secure employment during the final stages of dissertation writing. Ian Kuijt provided invaluable advice and motivation, which has greatly improved this dissertation.

I would finally like to thank my friends and fellow ASU cohort members —especially Sean Bergin, Christopher Roberts, Bulent Arikan, Alexandra Miller, Mason Thompson, Sophia Kelly, Matt Peeples, Melissa Kruse-Peeples, and Julien Riel-Salvatore—for stimulating discussion, general collegiality, advice, critiques, and friendship. Without good friends like these, graduate school would have been a much poorer experience.

Significant financial support for this dissertation came from NSF award BCS-0410269 , the Arizona State University Dean's Advanced Scholarship, and the Arizona State University Dean's Dissertation Writing Fellowship. Fieldwork was supported by various grants from the Social Studies and Humanities Research Council of Canada.

TABLE OF CONTENTS

Page

CHAPTER Page

CHAPTER Page

CHAPTER Page

CHAPTER Page

LIST OF TABLES

Table page

LIST OF FIGURES

Figure page

Figure page

Figure page

1. INTRODUCTION

1.1. Introduction

This dissertation investigates the "collapse" of the Early (Pre-Pottery) Neolithic lifeway, which was a major transformational event that occurred approximately 8500 years ago, which was marked by significant changes in settlement patterns, material culture, and social markers.

The instigation for this transition remains unclear, but human-caused landscape degradation, rapid climate change, social upheaval, the rise of pandemic disease, conscious reorganization to take better advantage of resources have all been suggested as likely candidates. Little consensus exists among scholars, mainly because the fragmentary nature of the archaeological record from this period prohibits a conclusive understanding of this transition using traditional archaeological techniques alone. To move beyond traditional narratives of cultural collapse, I employ a Complex Adaptive Systems (CAS) approach to this research, and combine agent-based computer simulation models of Neolithic land-use with dynamic and spatially-explicit GIS-based environmental models to conduct experiments into long-term trajectories of different potential Neolithic socio-environmental systems.

The goal of all archaeological modeling is to better understand the trajectory of events that created the archaeological record, but for years archaeologists have relied on narrative models that drew together myriad bits of archaeological evidence that were then tied together with paradigmatic understandings of the nature of human systems. The archaeological record is fragmentary, however, and at best only provides partial clues into ancient peoples' actual daily activities. Furthermore, it is exceedingly difficult, and usually impossible, for archaeologists to know—based on the archaeological data alone—if the clues they have recovered actually reflect real day-to-day economic patterns, or are a consequence of discard biases and site formation processes (Hayden and Cannon, 1983; Schiffer, 1987). Whole subdisciplines of archaeology (e.g., geoarchaeology, ethnoarchaeology, microarchaeology, etc.) have arisen as ways of mitigating these issues, but still typically culminate in narrative models of potential past lifeways. The simulation approach used in this research combines computer simulation modeling with the available archaeological proxy data as a way to move beyond the limitations of the narrative approach: simulation studies allow an examination of socio-natural processes that must have operated in the past, but for which we have little direct evidence.

My analysis outlines how the Early Neolithic "collapse" was likely instigated by a non-linear sequence of events, and that it would have been impossible for Neolithic peoples to recognize the long-term outcome of their actions. The experiment-based simulation approach shows that, starting from the

same initial conditions, complex combinations of feedback amplification, stochasticity, responses to internal and external stimuli, and the accumulation of incremental changes to the socio-natural landscape, can lead to widely divergent outcomes over time. Thus, rather than being an inevitable consequence of specific Neolithic land-use choices, the ”catastrophic” transformation at the end of the Early Neolithic was an emergent property of the Early Neolithic socio-natural system itself, and thus likely not an easily predictable event. In this way, my work uses the technique of simulation modeling to connect CAS theory with the archaeological and geoarchaeological record to help better understand the causes and consequences of socio-ecological transformation at a regional scale.

Studying this phenomenon in the Neolithic period provides the time-depth necessary for a more complete understanding of the deleterious consequences of subsistence decisions, because we can examine their effect at several different temporal scales. Many people in the developing world continue to live a lifestyle of subsistence farming and herding, and so face similar dilemmas as their Neolithic ancestors. A better understanding of the consequences of the cumulative actions of ancient farmers and herders will help us to better predict the future effects of agropastoralism in developing countries today.

1.2. The Geography, Climate, and Geology of Northern Jordan

The natural geography, general geology, and modern climate of northern Jordan has been described by numerous authors (Al-Jaloudy, 2006; Bender, 1975; Bender and Khdeir, 1974; e.g., Burdon and Quennell, 1959, 1959; Cordova, 2007; Davies and Fall, 2001; Fisher et al., 1966; Horowitz, 2001; Schulman, 1962; Sneh et al., 1998; Wagner, 2011), and the brief overview provided here draws from these sources. The bedrock in northern Jordan is largely calcareous lightly metamorphosed sedimentary rocks dating to the Cretaceous and Late Tertiary. The sediment from which these rocks are formed derives mainly from oceanic sedimentation on the floor of the Tethys Sea, and these rocks are sometimes unconformably overlain by early quaternary conglomeritic rocks of terrestrial origin, especially along the margins of the Jordan Valley. The Jordan Valley—locally referred to as al Ghor—is composed of recent fine-grained alluvial soils with high organic content, which overlay marl and shale lake sediments deriving from the ancient Lake Lisan that filled the valley in the Late Pleistocene. The Jordan Valley is part of the greater Jordan Rift zone, which formed as the Arabian Plate moved away from the African Plate, and which stretches from the Red Sea in the south, through the Wadi al Arabah and the Dead Sea up to the Sea of Galilee (Lake Kinneret/Lake Tiberias) and the Hula Basin in the north. The Valley itself is entirely below sea level, and stretches from the Sea of Galilee in the north (at 212 mbsl) to the Dead Sea in the south (at 423 mbsl). The modern alluvial soils of the valley are a combination of overbank deposits from the Jordan River that flows along its length, and outwash deposits from the numerous

tributary streams and seasonal washes that empty into the Valley from both the Judean and Samaran Hills to the west, and the Jordanian Highlands to the east.

The Jordanian Highlands—also referred to as the Mountain Ridge Province—form the eastern edge of the Jordan-Arabah rift zone, and were formed by a combination of synclinal horst and graben subsidence along the strike/slip fault in the Rift Zone and local uplift related to constriction along the fault. Thus, numerous structural features are present in the uplands, including localized and regional deformation and tilting of bedding planes, and a series of translational faults running perpendicular to the main Jordan Rift fault.

The Northern Highlands encompass most of the area between Umm Qais and Madaba (Figure 1.1), and is most typified by the characteristics of its "heartland" in the region between the Yarmouk and Zarqa rivers. The Northern Highlands are composed primarily of calcareous sedimentary rocks of marine origin. The limestones of the upper member of Northern Highlands formation are crystalline, and are thus more resistant to erosion than the chalk/marls found in the lower member. The differing hardness of these members creates a narrow, highly incised, relatively flat-topped plateau of marls directly bordering the Jordan Valley, from which rises the steeper slopes of the harder crystalline limestones. A band of flint-bearing limestones lies between the upper and lower members, providing easy access to tool-stone across the entire region. The eastern edge of the Northern Highlands is gentler than the western edge, and slopes fairly gently towards the central Jordanian Plateau.

Elevations in Northern Highlands range from 700-1200 meters, and the entire region is at a relatively higher elevation than the Southern Highlands. The Northern Highlands are characterized by a Mediterranean climate with cool wet winters, and hot dry summers, and an average precipitation of between 300-600 mm. The higher elevations are mantled in an oak and pistachio woodland, with interspersed pines and junipers becoming more dominant in the lower elevations. Portions of these areas are covered in fairly dense oak/pistachio Maquis or scrub Garrigue, and large tracts have been converted to olive-growing or cultivation of cereal crops. The lowest portions of the Northern Highlands are dominated by open grasslands, especially on the eastern flanks as they descend through the Northern Steppes towards the Eastern Hamada. Vegetation in the wadi-bottoms includes canes, oleanders, and leafy shrubs and forbs, and can be quite dense, especially if there are perennial streams flowing in the wadi-bottom.

In contrast, the Southern Highlands—which span from Wadi Zarqa to Wadi Rumm (Figure 1.1)—are dominated by sandstones, basalts, and granitic bedrocks, and are more highly incised by wadi systems than are the northern highlands. These wadis typically drain into the Dead Sea via the Wadi al Arabah, although those that drain the southernmost stretches of the highlands drain southward into the Red Sea. Although occasional peaks in this region top out at almost 1800 meters, the region is generally at a lower average elevation than are the Northern Highlands, and the topography is considerably rougher and more

varied than in the north as well. Although a significant proportion of the region is still considered to have a Mediterranean climate, the region receives quite a bit less rainfall than the north, and those parts of the region below about 700 meters asl fall into the Iran-Turanian climate zone, with precipitation of 150-300 mm per year. Consequently, there is a wider range of vegetation communities in this region, with much of the area currently covered by shrub-steppe and scrublands.

Wadi Ziqlab is one of a series of linear incised valleys that line the western edge of the northern reaches of the Jordanian Highlands (Figure 1.1). These crosscutting wadis are tributaries of the Jordan River, ultimately draining into the Dead Sea. Most of the Wadis, including those in the Ziqlab region, have perennially flowing streams in their lower portions (below bout 200 masl), fed by a multitude of springs emerging from the limestone bedrock of the wadis (Maher, 2005), whereas their upper portions are seasonally inundated dry riverbeds.

1.3. Organization of the Dissertation

In Chapter 2, I examine the archaeological record of the Neolithic period in the Northern Highlands, and provide a traditional narrative model of the sequence of events that led to the PPN-LN transition. In Chapter 3, I examine the existing ideas about the character of the transition, and for the motivating/instigating factors that caused it. I critique these ideas, and present a new approach to understanding the PPN-LN transition based on Complex Adaptive Systems (CAS) theory and the idea of Soical-Ecological Systems (SES). I discuss the basic concepts of CAS theory, examine the evidence for complexity in human subsistence systems, and provide a heuristic model of the PPNB subsistence system as a regional SES. I also provide some test implications and guiding questions that frame the research presented in the remaining portions of the dissertation. In Chapter 4, I introduce the idea of simulation modeling and discuss the basics of the simulation modeling approach. I then describe the components and structure of the MedLanD Modeling Laboratory (MML), which is the simulation modeling platform used in this research (an agent-based model of subsistence agropastoralism, a vegetation dynamics modeling engine, a soil dynamics modeling engine, a climate modeling engine, and a landscape-evolution modeling engine). In Chapter 5, I discuss the concept of spatially explicit paleoenvironmental reconstruction, and discuss the methods I use to achieve it. I also discuss the results of previous and new geoarchaeolgical fieldwork conducted in Wadi Ziqlab, and their implications for paleoenvironmental reconstruction and as a source of comparison for the simulation model-output. In Chapter 6, I describe how I used ethnographic and archaeological data to parameterize the MML to simulate Neolithic subsistence. I form a series of twelve modeling experiments to better understand the long-term dynamics of potential Neolithic subsistence strategies. In Chapter 7, I examine the output of these modeling experiments to look for patterns relating to issues of resilience, vulnerability,

flexibility, rigidity, and other CAS concepts. I examine the dynamic and recursive interconnections in the simulations, and examine how similar initial conditions could lead to vastly different outcomes. In Chapter 8, I investigate the implications of this research for our understanding of the PPN-LN transition in specific, but also of the concept of "collapse" and the long-term sustainability of SES in general.

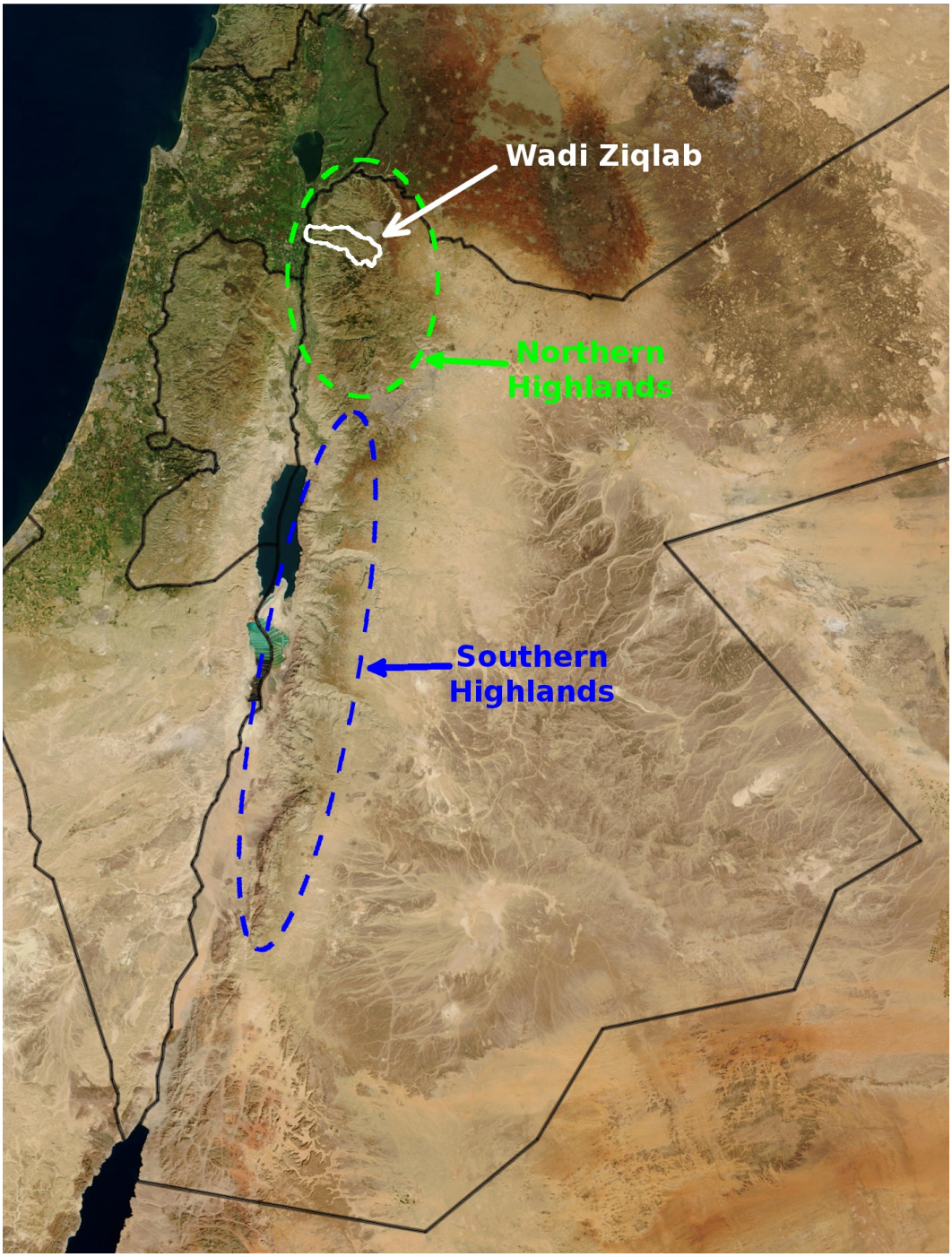

Fig. 1.1. Composite satellite image of Jordan, showing the physical terrain. The green dashed line delimits the approximate extent of the Northern Highlands region, the blue dashed line delimits the approximate extent of the Southern Highlands region, and the solid white line delimits the Wadi Ziqlab catchment.

2. THE NEOLITHIC PERIOD IN NORTHERN JORDAN

2.1 Chapter Introduction

In this Chapter, I provide a basic narrative sequence of the Neolithic period in the Northern Jordanian Highlands region, with special regard to the archaeological record of Wadi Ziqlab. The purpose of this narrative is to provide a basic background to the PPN/LN transition that is the main focus of this dissertation, and to contextualize the simulation experiments described in later chapters. Here, I provide the basic archaeological facts upon which the simulations are based, and the narrative that they are meant to compliment. Therefore, in my overview, I focus specifically on those aspects of the archaeological record that inform us about society, economy, and the relationship between people and their surrounding environment. I do not expect to have covered all the specifics of every site in the region; such a detailed review is outside the purview of this dissertation. I do, however, summarize the major diachronic trends over the entire Neolithic, and I identify the specific aspects of Neolithic material culture and economy that seem to have changed drastically at the PPN/LN transition. Following the basic narrative, I provide extra details about the known Neolithic sites in Wadi Ziqlab.

2.2. The Neolithic Period in the Northern Jordanian Highlands

Although there are several alternative chronological sequences used in different parts of Southwest Asia, in this research, I have chosen to follow the most widely used scheme for the Neolithic of the Southern Levant. The scheme has two major divisions – Prepottery Neolithic (PPN) and Late Neolithic (LN) – each with their own internal divisions, so that the sequence of named periods proceeds: PPNA, EPPNB, MPPNP, LPPNB, PPNC, Yarmoukian, and Wadi Rabah. In this dating schema, the PPN/LN transition occurs during the PPNC period. These periods have general dates assigned to them (Figure 2.1), but the actual timing of occupation phases can be quite different in the various sub-regions of the Levant, and even from site to site within a particular subregion (Banning, 2007a). I provide here a brief outline of the course of the Neolithic in the Northern Jordanian Highlands (see Chapter 1 for a location map) in the vicinity of Wadi Ziqlab, with particular emphasis on the events preceding the PPN/LN transition in the PPNB/C and those that immediately followed in the Yarmoukian[1].

1 This summary will specifically focus on the archaeology of northern Jordan. Several excellent recent general summaries of the Neolithic in all parts of the Levant already exist (e.g., Banning, 1998; Kuijt, 2000; Rollefson, 2001; Kuijt and Goring-Morris, 2002; Simmons, 2007; Twiss, 2007), and much of the detail presented in them will not be replicated here.

2.2.1. Final Natufian/PPNA

Although there are abundant earlier Epipaleolithic remains in the region (Maher, 2011, 2005; Maher et al., 2002; Maher and Banning, 2001), there is very little evidence for Natufian or PPNA occupation in northern Jordan. This is likely more to do with preservation biases due to erosion of the landforms most used in these periods (see Chapter 3 for more information about the source of these biases) than that region was actually abandoned. The evidence from Iraq ed-Dubb —the only site in the region with preserved Late Natufian and PPNA occupations —corroborates this, and suggests that a network of small PPNA sites likely existed throughout the region (Goodale and Kuijt, 2006; Kuijt, 2004; Kuijt et al., 1991). Located in the upper portion of Wadi el-Yabis, about 10 kilometers due south of Wadi Ziqlab, Iraq ed-Dubb is a cave site situated high up on the southern flank of the Wadi, and this unique location is likely the reason this site was preserved while most other sites of this period were not. Two circular, semi-subterranean houses, and the intervening intramural area were excavated, and statistical and spatial analysis of the faunal remains at Iraq ed-Dubb (Martin and Edwards, 2007) suggests that the site was occupied year round, but perhaps was not continually occupied for more than a few years at a time[2]. No domestic fauna were discovered, but a high diversity of wild species were present in the faunal assemblage, with an emphasis on hunted and trapped mammals (especially gazelle, squirrel, fox, hare, and boar) (Martin and Edwards, 2007). Interestingly, the pattern of animal exploitation did not change significantly between the Late Natufian and PPNA layers, indicating both a high degree of continuity between the periods, and that floral and faunal resources were not depleted by the occupants of the site (i.e., they were living below the carrying capacity of the local catchment). Iraq ed-Dubb also boasts some of the earliest evidence of domesticated cereals (carbonized wheat and barley grains dated to 11600 – 11475 cal. BP [Colledge, 2001; Colledge et al., 2004]), suggesting that, if not farmer themselves, the occupants of the site at least had access to domesticated grains. Recent excavations at PPNA sites in the Jordan Valley indicate that these sites had extensive storage granaries, and that use of domesticated or pre-domesticate plant foods intensified during this period (Kuijt and Finlayson, 2009). Several non-native shell and bone ornaments were also discovered at the site, indicating the presence of regional or supra-regional trade networks. It is possible that different sites existed with various specialties (e.g., farming, hunting, bead-making, etc.), and that goods were traded on a regular basis. Regardless of the nature of the trade network, it is clear that a variety of interconnected permanent or semi-permanent Natufian/PPNA settlements existed throughout the hilly regions of the eastern flank of the Jordan Valley, including in Wadi Ziqlab.

Microwear evidence from PPNA sickle-elements (identified by morphology and presence of silica sheen) recovered from sites in the Middle-Euphrates river valley indicates that PPNA sickles were compound tools

2 Originally, it was thought that the site was a seasonally-occupied hunting camp (Kuijt et al., 1991).

constructed in a manner broadly similar to the compound projectile points common in earlier periods (Ibáñez et al., 2007), which indicates that the focus of technological innovation had shifted from hunting tools to farming tools by this period. The sickles shafts were apparently straight (i.e., PPNA sickles were not actually "sickle-shaped"), however, and so the way PPNA peoples must have harvested cereals—by gathering bunches of grass in one hand, and slicing the stalks with the sickle held in the other—was quite laborious and inefficient (Ibáñez et al., 2007). These findings indicate that although the technology of farming was becoming of central importance to PPNA peoples, they had yet to innovate technological solutions that would allow increased harvesting efficiency.

2.2.2. Early PPNB

Like the Natufian and PPNA, there is very little evidence for the Early PPNB period anywhere in the Ziqlab region, but it is less clear, however, if this absence of evidence is also due to preservation biases. It seems that most of the PPNA sites in the Jordan Rift Valley were abandoned at the end of the PPNA (and there is no evidence for any EPPNB sites in the Valley), and it may be that the Northern Jordanian Highlands were also depopulated at this time too (Kuijt and Goring-Morris, 2002). The only possible EPPNB site in the Northern Highlands region—the site of er-Rahib—is, interestingly, also located in the Wadi el-Yabis. Only very minimal excavations were carried out at the site, however, and the site may actually primarily date to the early MPPNB (Kuijt and Goring-Morris, 2002). The EPPNB is thus best known from sites in the Northern Levant (e.g., from Syria and Anatolia [Twiss, 2007a]), but recently, EPPNB remains were discovered directly overlaying PPNA layers at Zahrat adh-Drah` in southern Jordan, suggesting a cultural continuity at that site (Edwards et al., 2004). Although very few EPPNB sites have been excavated, there is a trend towards the adoption of rectilinear house-shapes in the northern areas (occurring first in the West and then later east of the Jordan) during this period, although not in the southern desert areas (Simmons, 2007).

2.2.3. Middle PPNB

The Middle PPNB period is best known from sites in the south, such as Beidah (Byrd, 1994) Shaqarat Mazyad (Kaliszan et al., 2002), and 'Ain Abu Nukhela (Henry et al., 2003), or from west of the Jordan at sites such as Jericho (Gebel, 2004), Kfar haHoresh (Goring-Morris et al., 1998), Nahal Hemar (Bar-Yosef, 1985; Bar-Yosef and Alon, 1988), Yiftahel (Garfinkel, 1987), and others (see Twiss [2007a]). There are only three sites in the highlands of northern Jordan with known MPPNB occupations: 'Ain Ghazal (Rollefson et al., 1992), Wadi Shu'eib (Simmons et al., 2001), and Tell Abu Suwwan (Al-Nahar, 2010). The MPPNB layers at these three sites are modest compared to the substantial LPPNB layers that overlay them, but apparently these northern MPPNB sites are larger than those in the south and west (Kuijt and Goring-Morris, 2002). Furthermore,

the Northern Highlands sites all seem to have been newly established town sites, whereas many of the southern and western sites show marked continuity from earlier periods (Edwards et al., 2004; Gebel, 2004). Of the three northern sites, the MPPNB layers at 'Ain Ghazal provide the largest and best sample of northern MPPNB remains. One pattern that occurs in the MPPNB layers of 'Ain Ghazal, and which is of particular interest to the current research, is that the diameter of structural wooden posts decreased throughout the MPPNB at 'Ain Ghazal[3], suggesting the gradual depletion of mature forests in the surrounding region (Rollefson et al., 1992). Room size also decreased over time, in part due to remolding of interior spaces during (the many) renovations of houses, but also possibly due to the aforementioned lack of large beams (Banning and Byrd, 1987; Rollefson et al., 1992). The typical house-form (called "pier houses") consists of a single rectilinear room, subdivided by stone (or sometimes wooden) "piers", creating a series of chambers along the side. Houses were all about the same size (20-30 m^2), and most domestic activities appeared to have occurred outside the dwelling (e.g., on the roof) (Banning, 2003; Twiss, 2007a). Banning (2003) suggests that the layout and uniformity of these houses indicates inhabitation by nuclear families, in control of their own food storage, but not in competition with each other.

Faunal and botanical evidence shows an increased reliance on goats at the expense of gazelle in the MPPNB, especially at 'Ain Ghazal (Twiss, 2007a; Wasse, 2002). Although it is morphometrically unclear if these goats were fully domesticated, there is an abundance of circumstantial evidence that suggests they were: 1) paleoenvironmental data suggests 'Ain Ghazal was not within an ancestral range of the wild goat progenitor population, 2) goats make up 64% of the faunal assemblage, which is much larger than is known from hunter-gatherer sites, and 3) mortality profiles suggest that animals were culled from a kept herd, and not a wild population (Wasse, 2002). There is a great deal of difficulty in interpreting culling patterns (Marom and Bar-Oz, 2009), and the survivorship curves from the MPPNB layers at 'Ain Ghazal (and Yiftah'el (Horwitz and Lernau, 2003)) do not seem to match well with any published ethnoarchaeologically derived survivorship curves. Marom and Bar-Oz (2009) suggest that survivorship data can be more easily interpreted if binned into "immature", "subadult", and "adult". Doing so does "level" the differences between the two sites, as survivorship at MPPNB 'Ain Ghazal bins to 7.3%, 48.5%, and 44.1% in the three age groups respectively, and survivorship at Yiftah'el bins to 3%, 53%, and 44% respectively, but these data do not neatly fit into any of the three heuristic categories provided by Marom and Bar-Oz (2009) for "meat-only", "milk", or "wool" herds. They might, however, fit *between* the "meat-only" and "wool" categories, suggesting that meat and wool production were very important for MPPNB pastoralism, but that milk was yet to be included in the suite of pastoral products. There also is a wide range of body sizes in MPPNB herds at 'Ain Ghazal, suggesting that the animals were in the initial

3 Post hole diameters reduced from 50-60cm in the earliest phases of the MPPNB, to only 15-20cm in the later phases.

stages of domestication, thus exhibiting both wild and domestic morphological traits within the same herd (Wasse, 2002). Although wild game continue to be an important source of food, it appears, then, that MPPNB people had begun to rely on animal husbandry to provide a regular source of protein, lipids, and micronutrients[4]. It should be noted, however, that goats (domestic or otherwise) are not present in the faunal assemblages of all MPPNB sites (Kuijt and Goring-Morris, 2002), so clearly MPPNB people were still in the initial stages of incorporating pastoral production into their subsistence economies.

In a recent summary of the botanical evidence, Asouti and Fuller (2012) and Fuller et al. (2012) describe a highly variable spread of crop types present at different sites, which calls the idea of a regional agricultural system (i.e., the "Neolithic Package") into question. Not only does this new view show that the process of domestication proceeded at different rates in different places, but it seems that, while agricultural products certainly provided the bulk of MPPNB diets, MPPNB people were still actively experimenting with various combinations of cultivar species and land-races. The main species recovered from MPPNB sites include varieties of wheat (*Triticum aestivum*, *T. monococcum*, and *T. dicoccum*), barley (*Hordeum spontaneum*, *H. vulgare*, and *H. sativum*), pulses and legumes (*Lens culinaris, Pisum sativum, Vicia faba, V. ervilia,* and *Cicer arietinum*), and various other domesticates (*Ficus, Cucumis,* etc.), and frequency analysis of these botanicals suggest that cereals and legumes were the staple crop-types at MPPNB sites in the Mediterranean zone (Banning, 1998; Fuller et al., 2012). The presence of open-field weeds in the botanical record at MPPNB sites indicates that farmed fields were left fallow from time to time, perhaps according to planned crop rotation schemes (swiddening or extensive agriculture) (Banning, 1998). Sickle technology had improved by the MPPNB, and sickle shafts were now "curved" (i.e., actually "sickle shaped"), potentially doubling harvesting efficiency (i.e., over that in the PPNA) because the tool itself could now both gather the grass blades together and cut them in one stroke (Ibáñez et al., 2007).

Several researchers have suggested that the MPPNB was period of major social change in the Neolithic world, and that the Jordanian highlands were "colonized" during this period by migrants emigrating from several of the earlier-established sites west of the Jordan (e.g., Jericho) (Edwards et al., 2004; e.g., Gebel, 2004). Bienert et al. (2004) (and others) point to the fact that the all the known Northern Highlands MPPNB sites were founded in this period on virgin soil, and many of the Southern Highlands MPPNB sites, though mostly not founded anew, show significant changes in architectural style and size (i.e., the MPPNB "pier house" form, [Banning, 2003]). Bienert et al. (2004) go so far as to suggest that the completion of the switch to rectilinear houses that began in the EPPNB (and continued through the MPPNB) was caused by the introduction of a new cultural paradigm brought by migrants to the highlands from west of the Jordan. If that is the case, then sites in the southern desert areas (such as 'Ain Abu Nukhela, Shaqarat Mazyad, and Beidha) must have maintained their autonomy, as

4 See Vigne (2011) for an excellent recent discussion of how this process may have occurred.

they continued to use circular or ovate house-forms throughout those periods[5]. Bar-Yosef (2002, 2001), on the other hand, interprets this phenomenon as evidence for the existence of a series of regional "PPNB cultures", each assigned a particular set of socio-economic traits (e.g., "farmer-herders", "herder-hunters", "foragers"). The unique characteristics of the MPPNB sites in the Jordanian Highlands, in his view, are the result of interaction between the settled, agricultural PPNB "core" west of the Jordan, and a periphery filled with mobile foragers in the eastern and southern deserts. In this scheme. The Jordanian Highlands are the "interaction zone" between the two areas, and the unique characteristics of sites in this region derive from this duality of cultural and economic influences. Whatever the reason, it is clear that the MPPNB was a time of change throughout the Jordanian Highlands, and that divergent social (or socio-ecological) processes were occurring in each of the different sub-regions.

2.2.4. Late PPNB

The Late PPNB period is widely considered to be the florescence of PPN culture (Simmons, 2007). At the start of the LPPNB, most of the known MPPNB sites west of the Jordan were abandoned, and accelerated site growth and foundation of new sites occurs in the Jordanian Highlands and the desert regions. Several of these sites grew to sizes exceeding 10 ha and housing several hundred households (perhaps up to 3000 people or more) (Kuijt, 2000b; Kuijt and Goring-Morris, 2002; Rollefson and Kafafi, 2007). Almost all these so-called "megasites" are found east of the Jordan—mainly concentrated in the Jordanian Highlands—and they all seem to have experienced the same dramatic site growth at the beginning of the LPPNB—presumably from the final influx of new immigrants from the recently abandoned towns west of the Jordan (Gebel, 2004; Kuijt and Goring-Morris, 2002; Rollefson and Kafafi, 2007). The LPPNB settlement system was multi-tiered, and not every LPPNB village grew to "megasite" proportions. In the Northern Highlands, there are only three known "megasites": 'Ain Ghazal (Rollefson et al., 1992), Wadi Shu'eib (Simmons et al., 2001), and Tell Abu Suwwan (Al-Nahar, 2010).[6] Interestingly, unlike the southern "megasites" which seem to have all been newly-founded, the three northern "megasites" grew out of smaller, preexisting MPPNB settlements (Al-Nahar, 2010; Rollefson et al., 1992; Simmons et al., 2001). Not all LPPNB sites grew to "megasite" proportions, however, and the one known LPPNB site in Wadi Ziqlab—Tell Rakkan I—was likely only about only about 1 ha in size (see Section 2.3.1 below).

---

5 Although there are many southern sites that *did* adopt rectilinear architecture (e.g., Baja, Basta, 'Ain Jammam, Wadi Feinan 16, Wadi Fidan 1, es Sifiya, and Ghwair I), all of these sites are in the highland ecozone rather than the lowland desert ecozone.

6 The unexcavated LPPNB site of Kharaysin, also located in the northern highlands, may also be "megasite", as surface finds extended for nearly 36 ha (Edwards and Thorpe, 1986). Until excavations can confirm the size of Kharaysin, its status as a "megasite" cannot be substantiated.

LPPNB culture seems to have been slightly less heterogeneous than that of the MPPNB, and while some researchers argue for the presence of a number of regional sub-cultures (e.g., Gebel, 2004), most known LPPNB sites exhibit a common set of material cultural traits, including: 1) a highly standardized "naviform" blade-based stone tool technology, 2) advanced knowledge of plaster-making, 3) a similar style of multistory dwellings with many rooms known as "corridor buildings", 4) a style of small clay animal figurines, and 5) mortuary practices that involved the secondary burial of skulls covered in plaster facial models (Banning, 1998; Kuijt, 2008a). This last practice (secondary skull burial) had been continually conducted throughout the Levant (and was *not* practiced in neighboring regions) since the Natufian (Rollefson et al., 1998), which indicates a reasonable degree of cultural continuity in the region up through the LPPNB. Finally, in some of the "megasites", such as 'Ain Ghazal, Baja, and Tell Abu Suwwan, large statuary, painted plaster walls, and possible ritual or public space also occurred (Rollefson and Kafafi, 2007; Simmons, 2007).

At 'Ain Ghazal, sheep—virtually non-existent in the MPPNB—now join goats in almost equal numbers in the faunal record, in domestic herds, and the two species account for 69% of all faunal remains from this period (Wasse, 2002), and a similar pattern holds true for other LPPNB sites in the region (Simmons et al., 2001). LPPNB survivorship profiles from 'Ain Ghazal show increased kill-off of younger animals compared to the MPPNB profile (Wasse, 2002), and, although not exactly matching published ethnoarchaeologically determined kill-off patterns, the LPPNB patterns relatively closely approximate the ideal kill-off patterns proposed by Vigne and Helmer (2007) for "Type B meat", "Type B milk", or "wool" herds, as well as those proposed by Payne (1973) for "meat" or "wool" herds. Following the "binning" method espoused by Marom and Bar-Oz (2009) shows an LPPNB herd profile of 22% immature, 41.5% subadult, and 36.5% adult, which suggests that meat was the main pastoral resource, but does not rule out the idea that milk was becoming an important pastoral commodity at this time, especially if meat remained important and milk production in early domesticated ovicaprids was not as copious or continuous as it is in modern breeds. It is likely that cattle, too, had been brought under cultural control (if not completely domesticated) by this time, and although cattle are not over-abundant in the LPPNB faunal record of 'Ain Ghazal, they are prominent in the assemblages of other LPPNB sites in the Jordanian Highlands, such as Wadi Fidan 1 (Twiss, 2007b; Wasse, 2002; Zeder, 2008). The addition of sheep and cattle to the domestic mix added diversity to the suite of LPPNB pastoral economies and reaffirms the hypothesis that secondary products were becoming important[7]. The addition of sheep also changed the degree to which grazing by domestic herds may have impacted the local environment; sheep and goats have different dietary preferences (sheep prefer graze, while goats prefer browse), and

7 In addition to producing wool, sheep also produce more milk than goats, and most modern subsistence pastoralists utilize sheep mainly for these secondary products (Degen, 2007; Maltz and Shkolnik, 1980; Meged' et al., 2008). Modern cattle pastoralists also extract most of their pastoral calories in the form of milk products (Smith, 1992).

combination herds can more efficiently (or more thoroughly) exploit the available fodder in grazing patches (Le Houérou, 1980; Ngwa et al., 2000; Stuth and Kamau, 1989). Combination grazing greatly suppresses the regrowth of woody vegetation, and if grazing pressures are high enough, this leads to an increase in the overall diversity of plant communities in frequently grazed areas, and potentially to an increased prevalence of open grasslands in regions that would otherwise have remained forested (Adler et al., 2001; Carmel and Kadmon, 1999; HilleRisLambers et al., 2001; Osem et al., 2002; Perevolotsky and Seligman, 1998). Finally, sheep are also well-matched with cereal agriculture, being able to take more full advantage of field stubbles and straw than can goats (Thomson, 1987), suggesting that their addition may be related to the adoption of an integrated agropastoral subsistence system during this period.

A co-occurring intensified reliance on agricultural products, the fractionalization of the LPPNB agricultural system from one based on communally held plots or pooled labor, to a set of independent autonomous household holdings, and an increase in risk in the LPPNB agricultural system is attested to via a number of lines of evidence. Firstly, the most commonly recovered LPPNB tools are highly-standardized sickle-elements made on naviform blades (a characteristic type of bi-directional blade core). The high level of standardization of LPPNB sickle elements decreased the time and effort to replace a worn element "in the field", and also increased the efficiency of the harvest. Microwear analysis shows that sickle elements were now attached to the sickle-shaft in a manner so that each individual element protruded at an oblique angle to the shaft (i.e., like "teeth"), which was now even more curved than the sickle-shafts of the MPPNB (Ibáñez et al., 2007). This further increased the cutting efficiency of each stroke, allowing more grass stems to be cut with the same amount of effort, and may also have increased the amount of grain that could be harvested in a given amount of time[8], suggesting that 1) limiting harvesting energy expenditure was important to LPPNB peoples (e.g., because daily energy budgets were becoming smaller, or caloric margins slimmer), 2) harvest time/labor requirements may have become a restricting factor on the overall amount of grain that could be produced (especially if production had switched to the household level, as discussed below), and 3) reduction of waste during harvest was increasingly important (i.e., that the margins for error between the amount planted, and the amount required to harvest was becoming smaller). Each of these three correlates point to increasing risk in the LPPNB agricultural

8 Although Simms and Russell (1997) report that experimental and ethnoarchaeological research among Bedouin groups who hand-harvest wheat and barley (i.e., they use no cutting implements) indicates that the study subjects were capable of reaping slightly more grain per hour with their hand-harvesting method than with an advanced lithic sickle, 1) the Bedouins they observed were not accustomed to using sickles but were very adept at hand-harvesting, 2) their observations were made on modern cultivars of wheat/barley in perfect growing conditions in sandy soils, and 3) they found that using sickles was still more energetically efficient than hand-harvesting. Furthermore, they point out that while advanced sickles may or may not offer advantages of higher harvest rates/efficiency, they *do* offer advantages of intensification, especially when it is necessary to utilize sub-optimal growing patches.

system, but in any case, the level of technological investment directed toward this basic farming tool indicates that farming was an exceedingly important activity to LPPNB people. Secondly, the increase in dedicated storage features in LPPNB houses also attests to intensifying reliance on agricultural products (Gebel, 2004). These storage systems were likely both necessary to, and a consequence of the larger populations of the LPPNB megasites; that is, LPPNB agriculture was clearly capable of producing a surplus that could support a large population, but returns may have been quite variable from year to year, requiring long-term storage of grains for that population to make it through "lean" years (Goodale, 2009; Kuijt, 2009, 2008b; Spielmann et al., 2011). Thirdly, that LPPNB storage areas were increasingly hidden from outside view suggests that agricultural labor had become concentrated at the household level (Kuijt and Finlayson, 2009), and that 1) there was a need/wish to decrease the scope of "formal" food sharing (Enloe, 2003; Kent, 1993) [9] and/or the extent food sharing networks (e.g., by hiding surpluses from people you may be otherwise obligated to share with) (Halstead, 1999; Hitchcock, 1987), and/or 2) that there existed variability in the agricultural returns taken by individual households but that social norms still dictated a general attitude of egalitarianism (i.e., that it was possible to have a larger surplus than your neighbors, but that it was socially advantageous not to flaunt this difference). Fourthly, food preparation areas (such as the location of milling slabs, ovens, and hearths), which were generally placed in publicly viewable in EPPNB and MPPNB houses, are now also located in private, secluded parts of LPPNB houses, suggesting that informal food sharing (the sharing of meals) with non-household members was also curtailed in this period (Wright, 2000), supporting the idea that households were growing more autonomous and inwardly focused. Taken together, the privatization of food storage, preparation, and consumption areas could also suggest that agricultural risk management networks—often connected to food sharing (Hegmon, 1991)—were now circumscribed by the boundaries of the household and/or the extended family, and that the basic unit of agricultural production—and therefore risk—was the nuclear family (Flannery, 1993).

Finally, rather than expand the settlement outward in response to population growth, LPPNB peoples chose to build inwards and upwards. For example, at 'Ain Ghazal, LPPNB houses were built closer together than during the MPPNB, were multi-stories, and show a trend towards the increased compartmentalization of domestic space over time (Banning, 2003; Kuijt, 2000b). Thus, as the LPPNB progressed, villages begin to exhibit ever-increasing aggregation of dwellings, infilling of previously open space, reduction in

9 I use the term "formal" in the sense proposed by Kent (1993), which relates to the sharing of raw or unprocessed foodstuffs typically through established or formalized systems of obligate sharing. Enloe (2003) further delineates this type of sharing into "primary" and "secondary" sharing by the exact type of social or merit conditions that obligate sharing, and which shape and define the character of the act of sharing. Formal food sharing is opposed to "informal" (or what Enloe calls "primary") sharing, which is typically the sharing of cooked foods with guests as a form of hospitality.

domestic floor-space, and the innovation of multi-storied houses in LPPNB villages (Gebel, 2004). This suggests that 1) the need to conserve all available arable land around the site was of great importance to LPPNB villagers (Gebel, 2004), 2) the initial criteria for LPPNB site-founding did not include the potential for rapid growth (i.e., that the rapid population growth of LPPNB villages was neither predicted nor desired by the founding populations of LPPNB sites), and 3) these factors forced people to live in closer proximity to their neighbors than they might otherwise prefer. If agricultural land was at a premium, and was owned or tenured at the level of the household or nuclear family, tensions between households may have increased due to competition for access to the most productive plots, and these tensions would have been exacerbated by the close living quarters of the LPPNB villages. Some scholars suggest that this increase in social stress fueled the increased need for privacy, secrecy, and the inward focus of households (Kuijt, 2000b). In addition to increased tensions related to differential access to agricultural land, the increased size of LPPNB towns may have led to other sources of social stress. For example, "scalar stress" associated with the increased number of interpersonal interactions accompanying larger settlement populations (Johnson, 1982) would have increased exponentially. Tacit cultural or subcultural differences may have sparked or fueled social conflicts arising between members of different clans or lineages now living close together in the LPPNB towns, especially if these social divisions derived from the amalgamation of different immigrant groups that came to the region during the preceding MPPNB period. At the largest LPPNB "megasites" it was likely no longer possible to personally know every individual in the community, which would potentially produce a general ethos of mistrust for all people outside of one's immediate family or lineage, especially if effective mechanisms for mediation between individuals or corporate groups were not fully established (McIntosh, 1991). Rollefson and Kafafi (2007) suggest that the proliferation of non-residential spaces[10] in the built environment of LPPNB villages indicates a social response to these stresses, and that these communal spaces were locations where community bonding events could occur to promote social healing. In any case, it is clear that size and density of many LPPNB villages would have presented their residents with hitherto unknown social problems that needed novel solutions.

2.2.5. PPNC/Final PPNB

In Northern Jordan, the PPNC is only known from the sites of 'Ain Ghazal and Wadi Shuieb[11]. The PPNC period fills a "gap" that was previous postulated to

10 Rollefson and Kafafi (2007) refer to these spaces as "religious/ritual space" or "cult buildings", but I prefer to refer to them simply as "non-residential", "communal", or "community" spaces, because the case for religious, ritual, or cult activities occurring in these spaces is not conclusive.

11 There may be a PPNC layer at Tell Rakkan I, but the limited excavations at that site were unable to positively identify it. Outside of the northern Highlands, PPNC layers have been

have existed between the end of the PPN and the start of the LN, mostly based on the stratigraphy of Jericho (Kenyon, 1960). The length of this period is not well defined, nor does there exist general consensus that the PPNC should be considered as fundamentally "different" from the LPPNB. Indeed, several researchers suggest that "Final PPNB" is a better designation (see [Kuijt and Goring-Morris, 2002]).

Several important economic changes are identified with the PPNC. At 'Ain Ghazal, sheep now outnumber goats in the faunal assemblage by nearly 2 to 1. Sheep account for 48.3% of all faunal remains, and goats for 22%, and thus domesticated ovicaprids account for 70.3% of all fauna (Wasse, 2002). The increased amount of sheep in the faunal profile suggest 1) localized expansion of natural or artificial grasslands that increased the ratio of graze to browse in the site grazing-catchment[12], 2) tighter integration of the herding and agricultural economies so that herds needed to be able take better advantage of field stubbles and fodder crops[13], 3) increased importance of wool and meat[14] in the pastoral economy, or 4) any combination of these factors. Binned according to the method espoused by Marom and Bar-Oz (2009), the transitional LPPNB/PPNC and PPNC herd survivorship patterns for ovicaprids at 'Ain Ghazal (19.8% immature, 42.7% subadult, 37.4% adult; and 25.5% immature, 36.6% subadult, 37.8% adult, respectively [Wasse, 2002]) are not significantly different than they were in the LPPNB (see section 2.2.4, above), but the ovicaprid survivorship curve from the PPNC layers at Yiftah'el (0% immature, 77% subadult, and 33% adult [Horwitz and Lernau, 2003]) are suggestive of a herd kept for milk—especially the "Type B" milk production strategy of Vigne and Helmer (2007). The difference in the faunal record between 'Ain Ghazal and Yiftah'el is interesting, as it suggests that a variety of pastoral strategies may have been practiced in the Mediterranean zone at this time. Wild game—mainly gazelles (11.8%) and pigs (11%)—continue to included in the diet in roughly the same proportions at 'Ain Ghazal as during the LPPNB. Interestingly, at nearby Wadi Shu'eib, sheep and goat comprise only 46.1% of the PPNC faunal assemblage, and pigs compose a much larger proportion of the fauna (15.4%) than do gazelle (0.5%) (Simmons et al., 2001).

---

tentatively identified at several other sites (See [Kuijt and Goring-Morris, 2002]), such as Yiftah'el west of the Jordan (Horwitz and Lernau, 2003) and Basta in the southern Highlands (Rollefson, 1989).

12 Sheep have a preference for graze, and require more available graze in their diets than do goats (Bartolome et al., 1998; Rogosic et al., 2006). Too much browse can cause tooth loss and premature death of sheep, so successful sheep husbandry requires a diet composed mainly of graze (Nablusi et al., 1993).

13 Ethnographic research in Syria has show that the yearly grazing cycle and needs of sheep can be successfully combined with cereal farming, especially if barley is grown mainly as a fodder crop (Thomson, 1987; Thomson and Bahhady, 1983).

14 Comparative study of culled sheep and goats found sheep meat to be more calorie rich and to yield a larger amount of meat per animal (Gaili and Ali, 1985; Sen et al., 2004). In any case, among modern pastoral populations, the sheep to goat ratio increases when wool production or sale/consumption of meat becomes more important (Khazanov, 1994).

This may be due to Wadi Shu'eib's location closer to the Jordan Valley, which was likely prime habitat for wild boar (Simmons et al., 2001), and further indicates that there was a wide degree of intra-regional variation in subsistence practices at this time. In all cases, however, herding is clearly the dominant focus of animal usage in this period.

Technological and cultural changes occur in the PPNC that show drastic departures from the fairly homogeneous and long-lived PPN cultural complex, and which also indicate a continuity with the subsequent Late Neolithic periods that follow. For example, at 'Ain Ghazal and Wadi Shu'eib the ratio of flakes to blades in the lithic assemblages, which was close to 1:1 in the MPPNB and LPPNB, changes to about 2:1 in the PPNC (Rollefson, 1990; Rollefson and Köhler-Rollefson, 1993; Simmons et al., 2001), which is similar to the trend towards flakes in the LN (see section 2.2.6 below). The blades produced in the PPNC were also less regular, produced by plain percussion rather than indirect bunch percussion, and were more apt to bear significant amounts of cortex than in the PPNB, indicating a decrease both in standardization and in the level of technology invested in blade production, as in the Yarmoukian (Rollefson, 1990). Other components of the PPNC lithic tool kit exhibit broad similarity to the Yarmoukian, including adzes, axes, and knives (Rollefson, 1993). There was also a reduction in the quality and quantity of plaster floors, which are now made mostly of crushed marls than of lime plaster (Kuijt and Goring-Morris, 2002), and are similar to the types of "huwar" plaster being used in the Late Neolithic (Banning, 2010). PPNC contexts at 'Ain Ghazal also provide a small sampling of ceramics, indicating an early experimentation with a technology that is to become common in the Late Neolithic (Rollefson, 1993). Finally, it also appears that the number of small fired-clay animal and human figurines declines in this period, and the (very) long-lived secondary-mortuary practice of skull removal and re-burial is largely discontinued (Rollefson, 1993; Rollefson and Köhler-Rollefson, 1993).

There is evidence, however, to suggest some cultural continuity from the previous PPN periods. Cumulative frequency charts of burin geometry at 'Ain Ghazal and Wadi Shu'eib show a gradual and continual change throughout the entire Neolithic, from the MPPNB through the Yarmoukian (Rollefson, 1993; Simmons et al., 2001). The frequency of projectile points, while always quite low, also remains fairly constant across the transition at the two sites as well, although the size of the points decreases with time (Rollefson and Köhler-Rollefson, 1993; Simmons et al., 2001).

Still other pieces of evidence suggest that this was a period of rapid innovation and experimentation. For example, there is increase in the diversity of projectile point types during the PPNC at Wadi Shu'ieb, suggesting that this was a period of rapid experimentation and innovation in—at least—hunting technology (Simmons et al., 2001). At 'Ain Ghazal, as opposed to the high level of dwelling standardization seen in the LPPNB, the PPNC layers exhibit a diversity of house types, with the two major types being rectilinear, semi-subterranean, corridor

buildings, and square, single-room, above-ground dwellings (Rollefson and Köhler-Rollefson, 1993).

Absolute dates compiled from radiocarbon assays of the PPNC layers at 'Ain Ghazal and other Levantine sites suggest that the period lasted about 350 years, from about 8600 cal. BP to 8250 cal. BP (Kuijt and Goring-Morris, 2002). However, in a more recent analysis of the radiocarbon evidence using Bayesian methods and also including dates from Late Neolithic sites, Banning (2007a) places the boundary between the PPNC and the Yarmoukian at about 8450 cal. BP, suggesting that the PPNC or Final PPNB period only lasted about 100-150 years. Thus, if the PPNC/Final PPNB is looked at as a transition rather than discrete period, then the transition occurred fairly quickly—over the space of three to four generations[15].

2.2.6. Late Neolithic (Yarmoukian and Wadi Rabah)

The Late Neolithic period in the northern Jordanian highlands is known mainly from the sites in Wadi Ziqlab, but also from the sites of Abu Thawwab (south of Jerash) (Kafafi, 1993, 1992), 'Ain Rahub (north of Irbid) (Muheisen et al., 1988), 'Ain Ghazal (Rollefson, 1993), and Wadi Shu'eib (Simmons et al., 2001). The period itself has been mainly defined by the assemblages at larger sites in the Jordan Valley, such as Sha'ar Ha-Golan, Munhatta, and Jericho, and those on the coastal plain, such as Wadi Rabah. The Late Neolithic period is generally split into two sub-periods—the Yarmoukian period, and the Wadi Rabah period[16]. These two sub-periods were originally conceived of as synchronic culture-areas, based on the assemblages recovered from the two type sites (Sha'ar Ha-Golan and Wadi Rabah, respectively), but Bayesian analysis of the radiocarbon evidence at a

15 Recent cross-cultural research by Fenner (2005) into the generation intervals for developed nations, developing nations, and hunter-gatherers reveals a mean generation length of 29.1, 30.1, and 28.6 years respectively. It should be noted that demographic research by Eshed et al. (2004) indicates that the average age at death during the Neolithic was about 32 years, which is similar to the mean generation interval reported by Fenner. However, as Eshed points out herself in a later publication (Eshed et al., 2008), we are missing the remains of *most* of the PPN adult population due recovery biases, especially because most bodies seem to have been disposed of offsite in non-cemetery contexts. The adult skeletal matter that *has* been recovered has been subjected to significant postmortem manipulation of skeletal matter before secondary burial of only a few select individuals, and shows a distinct bias against the secondary burial of wome. Furthermore, there is a large bias towards the recovery of infants and children at most PPN sites, as these age groups are the only ones that seem to have been regularly buried in primary contexts on site. It is therefore uncertain if it is even possible to adequately estimate the average human lifespan during the Neolithic from the extant demographic data. Finally, regardless of whether or not their estimates are representative, 22.4% of the sample population studied by Ershed et al. (2004) lived to be older than 40, and between 8.3% and 15.2% of the population at various Neolithic sites lived to be older than 50, which suggests that a generation interval estimate of 30 is not inappropriate.

16 Alternate designations do exist for the Late Neolithic, such as those based on the assemblages from Jericho, and or for the southern desert sites (Banning, 2007b).

regional scale has shown these differences to be diachronic; the Yarmoukian period lasted from about 8450 (±75) cal. BP to about 7875 (±113) cal. BP, and, depending upon the particular Bayesian model used, the Wadi Rabah period began either directly at the end of the Yarmoukian (i.e., at around 7875 cal. BP), or, if one postulates a gap, at around 7760 (±52) cal. BP and ended at about 7200 (±85) cal. BP (Banning, 2007a, 2007a). Although there may be some interesting differences between the two sub-periods, for the purposes of this review, I examine the Late Neolithic period of the Northern Highlands as single entity, which exhibits some striking differences from the preceding periods, and the Late Neolithic in other parts of the Levant (Simmons, 2000). Firstly, pottery is now common, and it is the regional and diachronic variation in pottery styles, rather than in stone tools, that now provide the basis of the temporal and regional distinctions made by archaeologists. The pottery itself is of fairly coarse temper, and most recovered sherds are fairly utilitarian plainwares—although some incised, painted/slipped, and burnished decorations exist (Banning et al., 2011; Gibbs et al., 2006; Lovell et al., 2007). Secondly, domestic architecture is quite non-standardized. There is a remarkably wide diversity of house types seen at different LN sites, varying from circular or semi-circular to apsidal to rectilinear in shape, semi-subterranean to completely above-ground, single to multi-room, and with a wide variety of internal and external features such as hearths, benches, storage pits, patios, etc. (Banning, 2003; Kafafi, 1993). Architecture varies between sites in Wadi Ziqlab itself, with reasonably well-built rectilinear single-room houses being the norm at Tabaqat al-Buma, and small circular structures, and wall-less cobbled surfaces (perhaps tent-enclosed?) being the norm at al-Basitan (Blackham, 1997; Gibbs et al., 2010). Thirdly, burial styles are dramatically different than the preceding period. The practice of secondary interment of skulls is now completely stopped, and is replaced with a wide variety of burial practices, including jar burial, communal burial, cist-burial, burial under tumuli, flexed burial, extended position burial, burial with and without grave goods, secondary and primary burials, and burials with and with out skull removal (Banning, 1998). Fourthly, the once common fired-clay animal figurine is largely replaced by “coffee-bean eyed” humanoid figurines (Kafafi, 1993). And finally, major changes in the lithic technology also occur in the LN. Cores are now single-platform or amorphous multi-platform types and are non-standardized (Kadowaki 2005). Blades, which used to be the most common formal lithic tools in the LPPNB, are now extremely rare (for example, making up only 5-7% of the lithic assemblages of the LN phases at Tabqat al-Buma) (Kadowaki, 2007). The most common lithic tool types are non-formal flake tools, chipped and ground adzes, cortical scrapers, and highly retouched and denticulated sickle-elements, but the most common lithic artifact are unretouched flakes (for example making up 97% of the lithic assemblage at al-Basitan) (Gibbs et al., 2010). Although projectile points have been recovered from Abu Thawwab, Wadi Shu'eib and 'Ain Ghazal (Kafafi, 1993; Rollefson, 1993; Simmons et al., 2001), the Ziqlab sites have almost no projectile points at all (Banning et al., 2011).

There are several types of basalt and limestone grinding/pounding implements at LN sites, including large querns, pestles, loaf-shaped handstones, and shallow grinding basins (Banning and Siggers, 1997; Gibbs et al., 2010). There is no local source of basalt in Wadi Ziqlab—the nearest source is over 6.5 km to the north, and the next nearest source is almost 20 km to the east—so the presence of large basalt grinding implements at Ziqlab sites suggests either a fairly high degree of residential mobility, regular logistical forays for raw material acquirement, or participation in a regional trade network. The sickle-elements, heretofore the pinnacle of LPPNB technological innovation, are still more standardized than any other type of stone tool used in the LN, but are now made from a variety of blank types (blades or flakes), and are exhibit quite a bit more variety in size and shape than do PPNB sickle-elements. Nevertheless, LN sickle-elements remain fairly standardized, especially in relation to the rest of the LN lithic tool kit (Banning and Siggers, 1997). The sickles are typically truncated at each short edge, steeply retouched along on one long edge, and may be denticulated along the other (Kadowaki, 2005). This standardization indicates that farming is still very important to Late Neolithic peoples, and the presence of several types of grinding implements on imported materials at Late Neolithic sites supports this assertion.

Late Neolithic sites in northern Jordan are rather dispersed, and vary widely in size and complexity. While a few LN sites were as big or bigger than the largest LPPNB "megasites" (e.g., Sha'ar ha-Golan at ~20 ha), and some the size of more modest LPPNB villages (e.g., Abu Thawwab at 6 ha) most known LN sites are quite a bit smaller than any of the known LPPNB villages, and many LN sites, including those in Wadi Ziqlab, are more on the order of 500 m^2 or less, and so are better described as farmsteads than villages (Banning, 2003, 2001, 1998; Kafafi, 1992; Twiss, 2007a). Some sites—such as 'Ain Ghazal, Wadi Shu'eib, and Tell Rakkan I—exhibit continuity between the LPPNB/PPNC and the LN, but most are founded on virgin soil at the beginning of this period (Banning, 2001; Kafafi, 1992).

There is also a fairly wide array of settlement patterns in this period. Abu Thawwab, for example, seems to have been the nucleus for a constellation of smaller sites that surrounded it (Kafafi, 1992). Excavations have not been conducted at any of these satellite sites, so it is unclear if they are perfectly contemporaneous with Abu Thawwab[17], but if they are, then they may represent special-purpose sites (e.g., field-houses or herding stations), they may be part of a system of seasonal "pulsatory" transhumance (sensu Johnson [1969]), or they may be part of a true two-level site hierarchy[18]. This type of two-level site hierarchy has been considered as the typical settlement pattern of the Late

17 The sites were identified by Gordon and Knauf (1987) during the Er-Rumman Survey in 1985, and were dated to the LN based on the types of surface finds recovered.

18 If the smaller sites are not perfectly contemporaneous with Abu Thawwab, then the Abu Thwwab region would represent an interesting case of dispersal (or contraction) of settlement density that occurred *during* the Late Neolithic.

Neolithic of the southern Levant, and that the larger sites served as a focus of ritual and/or community activities (Banning, 2001), but it seems that a different settlement system existed in Wadi Ziqlâb, which is typified by a series small hamlets or farmsteads of about 500-600 m^2 in size each[19] linearly dispersed along a single drainage, and home to perhaps 1-3 households each (Banning, 2001, 1998; Gibbs, 2008; Kadowaki et al., 2008). Four such small farmsteads—al Basitân, al-Aqaba, Tabaqat al Bûma, and the upper levels of Tell Rakkan—have been discovered and at least partially excavated in the Wadi Ziqlâb drainage (Banning, 2001, 1995, 1992a; Banning and Najjar, 1999; Kadowaki et al., 2008). There are also several other as-yet undated sites in the Wadi that could also date to the Late Neolithic, so it is quite possible that the dispersed LN system of farmsteads in Ziqlab consisted of perhaps 5-10 farmsteads (Kadowaki et al., 2008). Recent discovery of similar LN sites in Wadis Tayiba and Qusieba to the north of Ziqlab (see section 2.3.5 below) suggests that the Wadi Ziqlab pattern may be repeated throughout the tributary wadis of the eastern flank of the Jordan Valley. Furthermore, a similar pattern of small Late Neolithic settlements has been recently noted in the vicinity of Wadi Far'ah, west of the Jordan (Bar and Rosenberg, 2011). The Wadi Far'ah sites are in a geo-ecological context very similar to that of the Ziqlab sites, as they are dendritically dispersed along wadi-systems draining the eastern flanks of the Samarran Hills into the Jordan Valley.

The Ziqlab farmsteads are within easy walking distance of each other (the sites are spaced within a 7 km transect), and radiocarbon and stratigraphic evidence suggests that they were occupied roughly contemporaneously (Banning, 2007a, 2001; Kadowaki, 2005; Kadowaki et al., 2008). Banning (2001, p.153) even suggests that "the inhabitants of many such small settlements in one wadi system may have thought of themselves as a single community". In a study of the stylistic and functional attributes and construction sequence of sickle-elements from two of the farmsteads (Tabaqat al-Buma and al-Basitan), Kadowaki (2005) shows that there are more similarities in construction between sickle elements found at the two sites than there are between these sites and Late Neolithic sites in other parts of the region. Kadowaki suggests that this may indicate a large degree of social cohesion between the sites. That the occupants of the two sites constructed and used sickles similarly also suggests that they likely pooled labor during the harvest period, and thus perhaps did so for other subsistence tasks (field-clearance, planting, herding) as well. In a comparison of stylistic, functional, and construction of pottery recovered from Tabaqat al-Buma, al-

19 It should be noted that Tabaqat al-Buma is the only LN site in Wadi Ziqlab for which we can be absolutely certain of site size. Excavations exposed about 350 m^2 of the site (Banning et al. 2011), which was probably about 600 m^2 all together. It was not possible to fully explore the the LN component of Tell Rakkan (Banning and Najjar, 1999), so it is unclear how large the LN occupation might have been. Al Aqaba is a highly disturbed site, making it difficult to determine the size of the original site, but its location and the similarity in artifact types suggest that it was likely similar in size to Tabaqat al-Buma (Kadowaki et al., 2008). Al Basitan could be slightly larger Tabaqat al-Buma, but we tested a reasonably large proportion of the terrace during excavations at the site, so it is unlikely to be much bigger than 600 m^2, and certainly not bigger than 1000 m^2.

Aqaba, and al-Basitan, Gibbs (Gibbs, 2008) finds broad similarity in pottery construction and function between the three farmsteads, suggesting a high level of social relation between the sites, but also discovered crucial stylistic differences that suggest subtle or tacit cultural boundaries existed and that the individual farmsteads maintained at least partially unique identities. Thus, although the individual communities likely worked together to accomplish difficult or risky subsistence activities, it is likely that ownership and basic subsistence decision-making resided at the level of the individual hamlet.

Botanical evidence is extremely scarce at the Ziqlab sites, and although specific charred grains have yet to be identified from LN deposits, the presence of sickle-elements clearly indicates the farming of cereal grains, and it is highly likely that pulses and legumes were also farmed (Banning, 2001; Banning et al., 1994). Interestingly, botanical evidence is also very scarce at 'Ain Ghazal and Wadi Shu'eib, where no grains could be identified in the many flotation samples taken from these sites (Rollefson, 1993; Simmons et al., 2001). Luckily, botanical remains *have* been recovered from the sites of Abu Thawwab and 'Ain Rahub. Emmer wheat (*Triticum dicoccum*), barley (*Hordeum distichum*), field pea (*Pisum sativum*), lentils (*Lens culinaris*), pistachio, and almond were recovered from Abu Thawwab (Kafafi, 1992), and Emmer wheat (*Triticum dicoccum*), Einkorn wheat (*Triticum monococcum*), and flax (*Linum usitatissimum*) were recovered from 'Ain Rahub (Muheisen et al., 1988).

Faunal preservation at the Ziqlab sites is also unremarkable, and although finely detailed species differentiation or mortality profile analysis is not possible, preliminary faunal analyses have nevertheless revealed some interesting intersite variability (Kadowaki et al., 2008). The recovered faunal assemblage at Tabaqat al-Buma is strangely dominated by the remains of cervid and canines (accounting for 57.8% of the analyzed sample). The remainder of the Tabaqat assemblage consists of cattle (4.4%), pigs (3.8%) and ovicaprids (34%). The faunal assemblage at al-Basitan, on the other hand, is overwhelmingly dominated by ovicaprids (68.3%), but also has significantly more pigs (13.3%) and much fewer deer and canine bones (together only accounting for 2.9% of the analyzed sample). There is also a relatively higher proportion of cattle at al-Basitan, acounting for 11.8% of the faunal assemblage. Only about half of those (5.6% of the total assemblage) were positively identified as likely to have been domestic, and while it is unclear if the remainder were domesticated, cattle are clearly more important at al-Basitan than at Tabaqat al-Buma. Although the poor preservation of ageable features on the recovered bones make for a tenuous assessment of ovicaprid herd mortality curves, those data that do exist suggest that management practices were not significantly different from preceding periods. At al-Basitan, 17.2% of ageable remains were immature, 44.8% were subadult, and 37.9% were adult, which, according to the heuristic framework provided by Marom and Bar Oz (2009), is suggestive of a herd kept for meat, and also perhaps for wool, but not for dairying. Isotopic analysis of potsherds recovered from al-Basitan can neither confirm nor deny the processing of milk, but do confirm that the site's

inhabitants regularly cooked and ate the meat and/or marrow of goats/sheep and pigs (Gregg et al., 2009). The ovicaprid herding-species composition data suggests a sheep-dominated herding ratio of about 3:1, ostensibly supporting the case for wool production, but the sample size of species-identifiable ovicaprid bones is so small as to make these results virtually meaningless (only about 10% of the ovicaprid remains could be identified to the species-level). Herd mortality, ovicaprid speciation, and pot sherd isotopic data are not yet available for Tabaqat al-Buma, but based on the overall differences in the faunal assemblages between the two sites, it would not be surprising if these data are shown to differ between the sites as well. In any case, it seems apparent that the inhabitants of al-Basitan specialized in the herding of ovicaprids, and possibly cattle, and also focused on the hunting of wild boar, while the inhabitants of Tabaqat al-Buma focused on the hunting of deer and the herding of ovicaprids, but the latter to a lesser degree than at al-Basitan.

The faunal evidence from the Ziqlab sites is in general alignment with that of other LN sites in the area. At Abu Thawwab, abundant remains (68% of the total faunal assemblage) of domesticated goat and sheep, moderately abundant remains of wild gazelle and cattle, and scant remains of wild boar and onager were recovered (Kafafi, 1992). The Yarmoukian layers at 'Ain Ghazal, produced a faunal assemblage where sheep and goat make up 72.5% of the total LN faunal assemblage (Wasse, 2002), and Wadi Shu'eib, where sheep and goat make up 47.6% of the total LN faunal assemblage (Simmons et al., 2001). Of these sites, only faunal analysis detailed enough to differentiate sheep and goat remains comes from 'Ain Ghazal, where sheep compose 49.1% of the LN faunal assemblage and goats compose only 23.4% (Wasse, 2002). This also indicates a sheep-dominated herding ratio (in this case of 2:1), but it is again unclear if the reliance on sheep is common to all LN sites. The binned LN herd survivorship data from 'Ain Ghazal are not significantly different from the PPNC and LPPNB curves (20.7% immature, 39% subadult, and 41.3% adult [Wasse, 2002]), and again, although this is indicative of meat production, it does not rule out milk or wool production (and wool in particular, considering the predominance of sheep in the LN faunal record at 'Ain Ghazal).

Taken as a whole, the faunal evidence recovered from LN sites in the Northern Highlands indicates that Late Neolithic people relied heavily on domestic flocks of sheep and goat, but occasionally supplemented their diets with animal proteins derived from potentially domesticated cattle and pig, and/or from wild game such as deer or wild boar. That the proportion of hunted wild game species differs between sites suggests that individual hamlets may have been purposefully located to take advantage of specific game species. For example, the larger amount of pig bones at al-Basitan may relate the sites location near the main perennial springs and the more deeply entrenched portions of the Wadi, which today are filled with thick riparian vegetation that provides excellent habitat for an abundant amount of wild boar, whereas the larger proportion of deer bones at Tabaqat al-Buma may relate to its closer proximity to the wooded

uplands, which were presumably excellent deer habitat in the Late Neolithic. Economic specialization may have extended beyond the realm of hunting, however, as the much larger proportion of ovicaprid bones at al-Basitan, combined with the more ephemeral style of the architecture discovered there, suggest that its occupants might have specialized in pastoralism, perhaps centered around the production of dairy and other secondary products. Tabaqat al-Buma (and perhaps al-Aqaba), on the other hand, may have specialized more in cereal production, especially considering the numerous fertile alluvial terraces in close proximity to the site. Thus, each small hamlet may have been a semi-specialized "node" in an economically integrated sub-regional network of sites, spaced out along each major Wadi system so as to take better advantage of localized variation in wild resource availability and suitability for agriculture and herding. This idea is in congruence with the material cultural evidence discussed above suggesting subregional cultural cohesion with subtle, but distinct, cultural boundaries between sites.

2.2.7. The End of the Late Neolithic

The end of the Late Neolithic period is still unclear in the Northern Highlands. In Wadi Ziqlab, there is evidence for some minor upheaval at Tabaqat al-Buma prior to another social, economic, and settlement reorganization at the beginning of the Chalcolithic. One of the major trends in material culture at Tabaqat al-Buma was a gradual reinvestment in complex blade-based sickle technology over the Late Neolithic suggests that people were once again intensifying their agricultural strategies (Banning et al., 2011). The brief abandonment before the relatively short final reoccupation of the site (Blackham, 1997) at the very end of the Late Neolithic period suggests that people were once again experimenting new settlement strategies. The specific motivation for this experimentation is currently unclear, but in any case, it seems that two totally new settlements were founded at the start of the Chalcolithc, and, of all the Neolithic settlements, only Tell Rakkan I remained occupied . The first new Chalcolithic site—located near the modern village of Tubna—settlement was established high in the uplands, perched on a hill-top well above the upper reaches of Wadi Ziqlab, and the second new Chalcolithic site—the site of Tell Fendi—was established out in the Jordan Valley proper, near the confluence of the Ziqlab stream with the Jordan River (Banning, 1999; Banning et al., 1998; Blackham et al., 1997). These sites were larger than the previous Late Neolithic sites, and their vastly different locations and different material culture indicate the emergence of a new socio-economic system at this time.

2.3. Neolithic Sites in Wadi Ziqlab

Banning (Banning, 1983, 1982; Banning and Fawcett, 1983) began the early stages of what was to become the long-lived Wadi Ziqlab Project (WZP)

with an archaeological survey in 1981 that culminated in his PhD dissertation work concerning ancient human land use in the region (Banning, 1985). The Neolithic occupation of Wadi Ziqlab has been a focus of the WZP since its inception, and continues to be so today. To date, four Neolithic sites have been positively identified and excavated by the WZP in Wadi Ziqlab, three to four other locations have been identified in the Wadi where smaller amounts of Neolithic material have been recovered, and four more possible Neolithic sites have been tentatively identified during survey in the neighboring wadis. In this section, I provide a brief overview of the main details of these sites.

2.3.1. Tell Rakkan I

Tell Rakkan I (originally referred to as 'Ain Jahjah) is a stratified PPNB through Chalcolithic site (see Figure 2.1) located on a small terraced promontory in the lower western section of Wadi Ziqlab, adjacent to the second knick point (and waterfall) and the perennial artesian spring, 'Ain Jahjah (Figures 2.3 and 2.4). Paleoenvironemental modeling (see Chapter 5) suggests that the site was located at border of the Mediterranean Woodland and Savannoid (Savannah) ecozones in their configuration during the LPPNB period. The site was first investigated in 1995 by surface survey, which noted several stratified deposits, numerous PPNB artifacts, plastered surfaces, and stone walls eroding from a 100 meter-long bull dozer cut made in the mid 1980's when some concrete fish ponds were installed on the site (Figure 2.4). Excavations were carried out in 1999, and consisted of four step trenches along the edges of the site near the dozer cut, which yielded Chalcolithic, LN, and PPNB/C artifacts (Banning, 1999; Banning and Najjar, 1999).

Two radiocarbon dates taken on charcoal associated with the lowest plaster floors in the exposed dozer cut yielded calibrated dates of 9427 (±122) cal. BP and 9040 (±250) cal. BP (Banning, 2001; Banning and Najjar, 1999). These plaster floors directly overlaid sterile subsoil (tufaceous earths), and so the earliest documented occupation of the site is likely not earlier than the mid 10th millennium BP (i.e., the latter part of the MPPNB). The lower contexts yielded characteristic LPPNB artifacts such as Naviform sickle blades, crested blades, and Amuq and Byblos points, plaster “white ware” vessels, as well as characteristic LPPNB architectural features such as fine plastered floors and double-leaf stone walls (Banning and Najjar, 1999).

The LN layers at Tell Rakkan directly overlay the LPPNB layers, suggesting that the site may be one of the few sites in the region displaying continuity over the PPN/LN transition. Although no architecture (except for the possibility of a single wall) was found in the LN layers, and no absolute dates have been processed for these layers, Banning (2001) estimates the main period of occupation at the site to be from about 9300-7000 cal. BP (i.e., from the start of the LPPNB through the end of the LN5 phase of Tabaqat al-Buma, see Figure

2.1). Several characteristic LN artifacts were found in the upper layers of the site, including sherds exhibiting characteristic Yarmoukian "herring bone" incised decoration, red slipped pottery, and pottery of similar friable fabric to that recovered at Tabaqat al-Buma and al-Aqaba (although not with the same cross-hatched/combing incised decoration) (Banning and Najjar, 1999).

Determining the size of the site itself is complicated by the level of disturbance to the main deposits (Figure 2.4). The two tiered terrace upon which the site is situated is about 4 ha, and the upper tier upon which the site is directly located is about 3 ha. The original excavators estimated the size of the LPPNB occupation of the site to have been between 0.75 and 1.5 ha[20], meaning that it could have housed no more than about 300 people (but likely housed less)[21]. The LN occupation was poorly represented in the excavation units, which were located towards the periphery of the LPPNB occupation area, suggesting that the LN occupation of the site was on a smaller scale than the PPN occupation. It is therefore quite likely that the LN occupation of the site was as a small hamlet similar in size to Tabaqat al-Buma or al-Basitan.

2.3.2. LN Tabaqat Al Buma

The site of Tabaqat al-Bûma is located on a small alluvial terrace near the active channel of the Wadi Ziqlab drainage in the upper portion of the middle Ziqlab near the confluence of two major tributaries (Figures 2.3 and 2.5). Paleoenvironmental modeling (Chapter 5) suggests that the site was located firmly within the Mediterranean Woodland ecozone during the Neolithic period. The site was occupied from the Epipaleolithic until modern times, with the main occupation period during the Late Neolithic. The site was discovered in 1987 using a systematic subsurface testing strategy (Banning, 1996), and excavations continued at the site until 1992. The site has been subject of many publications (Banning, 1992a, 1992b; Banning et al., 1996, 1992, 1989; Blackham, 1997; Dodds, 1987; Ullah, 2012, 2009), and is currently the best-documented Late Neolithic hamlet in Northern Jordan.

The architecture at the site is characterized by free-standing stone masonry structures with a variety of floor substrates, including low-quality plaster, cobbled surfaces, and packed earth surfaces (Blackham, 1997). The houses themselves are

20 Banning and Najjar (1999) report the site to be between 1 and 1.5 ha, but Banning (2001) reports it to be between 0.75 and 1 ha. I have chosen to use the outside intervals of these two sources because my own efforts to judge the size of the site (including two site visits) showed it to be difficult to estimate due to modern disturbances (particularly by the construction of the fish ponds and terracing for pomegranate orchards).

21 Population estimates are derived by using the technique first published by Schacht (1981) where population is estimated by regression against site size [P = 85 + (107.55 x A), where A is the area in hectares]. Internal MedLanD research has updated the original regression with additional ethnographic data so that the estimates provided here derive from the following equation: P = 83 + (159 x A)

of a variety of sizes and shapes, but they are all geometric (non-circular) four-walled structures, and the majority are square or rectilinear (Kadowaki, 2007). A total of ten structures were discovered at the site, with between two and three houses in used in any occupational phase (although some structures seem to have been reused as storage areas, refuse disposal areas, or animal pens in subsequent phases) (Blackham, 1997). There are a variety of internal features in the houses, including plastered and other hearths, basalt and limestone grinding querns, floor-level door or entry-ways, and possibly windows (Kadowaki, 2007; Ullah, 2012). The pottery recovered from the site shares some general traits with Wadi Rabah and Yarmoukian types, but is also unique enough to defy absolute correlation with established pottery "cultures" of the region (Banning et al., 2011). The lithic assemblage is also consistent with Wadi Rabah assemblages, although the proportion of sickle-element types is different at Tabaqat al-Buma than at "typical" Wadi Rabah sites (Banning et al., 2011). Interestingly, it appears that sickles not only become more common over time at the site, but they also become more technologically sophisticated, indicating a temporal trend of increased importance of sickles with specific morphological traits (Banning et al., 2011).

The Late Neolithic occupation at Tabaqat al-Bûma occurred in five distinct architectural phases (designated LN1-5) from ca. 8600 to 6200 cal. BP (Figure 2.1) (Banning et al., 2011; Blackham, 1997; Kadowaki, 2007). The site was apparently not abandoned between each phase, with the possible exception of an abandonment between phases LN4 and LN5 (Banning, 2007a). The first Neolithic usage of the site (phase LN1) was as a cemetery, and two slab-covered and rock-lined cist tombs, dug into the Epipaleolithic paleosol, were encountered in the excavation units (Banning et al., 2011). No domestic artifacts or architecture were recovered from this phase, indicating that the special-purpose usage of the site as a cemetery in this phase. Only two of the four radiocarbon dates that exist from this phase are reliable, and Bayesian analysis constraining the start of this phase to the end of the PPNC suggests that it lasted from about 8625 (±61) cal. BP to about 8104 (±202) cal. BP (Banning et al., 2011). Very little of the second phase was captured in the excavation units, but it seems that this phase marked the beginning of domestic occupation at the site, as evidenced by the mainly destroyed remains of two to three houses. No radiocarbon dates exist for this phase, but if constrained by the dates from the previous and subsequent phases, it would have lasted from around 8000 cal. BP to 7600 cal. BP (Banning et al., 2011). The LN3 is the first well represented occupational phase, and the site seems to have been a small farmstead with two clusters of domestic buildings housing perhaps 2-3 families (Banning et al., 2011). Kadowaki (2007) finds the spatial patterning of artifacts from this phase to be suggestive of a small cooperative unit, with shared outdoor workspaces and common areas where communal food preparation possibly occurred. Microrefuse analysis of one of the house floors from this phase suggests that food processing and meal preparation took place indoors, however, which would indicated that the occupants were attempting to reduce informal sharing of cooked foods (Ullah, 2012). Bayesian analysis of the radiocarbon dates from this phase indicates that it began at about

7624 (±82) cal. BP and ended at about 7357 (±70) cal. BP (Banning et al., 2011). The LN4 phase is marked by the construction of one new structure, and the abandonment and collapse of two of the structures from the previous phase, with the other structures being reused (Banning et al., 2011). While Kadowaki (2007) sees evidence for more constricted use of space in the architecture, and less communality of food preparation in the spatial patterning of the larger artifacts, suggesting that the occupants of the site were less cooperative than in the previous phase. Microrefuse analysis of one of the domestic structures, however, suggests that food preparation no longer took place indoors, indicating an *increase* in the informal sharing of cooked foods, which is contra to the expectations of decreasing communality of resources (Ullah, 2012). Bayesian analysis of the radiocarbon dates from this phase, with a small abandonment gap postulated before the reoccupation of the site in phase LN5 and constrained by the earliest dates from the nearby Chalcolithic site of Tubna, estimates this phase to have lasted from about 7357 (±70) cal. BP to 7174 (±102) cal. BP (Banning et al., 2011).[22] The final phase seems to have been a reoccupation of the site after a brief hiatus, and is marked by the construction of two new structures. Kadowaki (2007) interprets the architectural and artifact patterning as once again indicative of a small cooperative farmstead of two-three families who shared communal open-space and food preparation activities. Domestic microrefuse data is currently unavailable from this phase, but it will be interesting to see if the contrasting patterns of the previous two phases continues in this one. Bayesian analysis of provides a very rough estimate of the length of this occupation, and suggests that it lasted from about 7100 cal. BP to about 7000 cal. BP.

2.3.3. LN al-Basatîn

The site of al-Basitan is a Late Neolithic and Early Bronze Age site located about a kilometer downstream from Tell Rakkan I on a large bench terrace elevated above the current course of the Wadi by about 100 meters (Figures 2.3 and 2.6). Paleoenvironmental modeling (Chapter 5) suggests that the site would have been firmly within the Mediterranean Savannoid (grassland) ecozone during the Neolithic. The site was initially discovered during geoarchaeological testing in 2000, test excavations in 2002 located the main subsurface deposits, and large scale excavations were undertaken in 2004, 2008, and 2009 (Banning et al., 2004; Gibbs et al., 2010, 2006; Kadowaki et al., 2008; Maher and Banning, 2001), and abundant Late Neolithic material has been recovered. There is insufficient evidence for the determination of distinct phases of occupation at al-Basitan, but radiocarbon dates taken from the LN layers of the site suggest an occupation from between 7700 to 7300 cal. BP (Figure 2.1) (Kadowaki et al., 2008). These dates place the site roughly contemporaneous to the LN3/4 occupation layers at Tabaqat al-Buma, or during the Wadi Rabah

22 Banning et al. (2011) admit that this estimate probably underestimates the date for the end of the LN4.

cultural phase of the regional chronology (see Figure 1). However, it should be noted that stratigraphic analysis of the site is not complete, so it is unclear if these dates reflect the entirety of the occupational period at the site. Given the large degree of culture affinity between the two sites (see below), it is highly likely that the founding and abandonment of al-Basitan would coincide with the timing of phase changes at Tabaqat al-Buma. Therefore, until definitively proven otherwise, we should consider the main period of occupation at al-Basitan to coincide with the LN2 and LN3 phases of Tabaqat al-Buma, which would mean an occupation that began around 7900 cal. BP, and ended around 7200 cal. BP.

Lithic and pottery styles at al-Basitan and Tabaqat al-Buma share more similarities with each other than they do with other LN sites in the southern Levant, suggesting a close cultural affinity (Gibbs, 2008; Kadowaki, 2005). Al-Basitan differs from Tabaqat al-Buma in some significant ways, however, including some of the specifics of pottery and lithics manufacture and style (Gibbs, 2008; Kadowaki, 2005). But there are some difference that are more striking. For example, in contrast to the abundance of domestic structures and indoor areas discovered at Tabaqat al-Buma, mostly outdoor surfaces with flat-lying debris have been discovered at al-Basitan. Also, aside from a few short alignments of stones, no rectilinear structures have been discovered at al-Basitan either. In fact, only two features have been discovered that could be interpreted as "houses" in the traditional sense of the word, and they are both circular structures of around 2 to 3 meters in diameter. The interpretation of these buildings as domestic derives mainly from the discovery of an ashy feature in the interior portion of one of the structures that was likely a hearth. Future analysis of detailed microarchaeological samples taken from these structures will aid in their final interpretation. By far the most common architectural feature at the site are cobbled surfaces of varying quality and geometry that are not associated with any walls. To date, at least five, and perhaps six (one may be a natural cobble layer) of these surfaces have been discovered. The best constructed of these surfaces is also the most geometric, being a perfect circle of about 2 meters in diameter. The largest cobbled surface is about 4 meters along its longest dimension, and was likely rectilinear in shape, although only one corner of it appeared in the excavation unit. These surfaces were mainly devoid of artifacts, indicating that they were likely cleaned on a regular basis. A cache of refittable flint flakes, a stone axe, and a paired handstone and pestle were, however, discovered *in situ* on the largest of the surfaces, and preliminary analysis of flotation samples recovered from this surface revealed the presences of charcoal, olive pit fragments, and unidentifiable seeds (Kadowaki et al., 2008). Future analysis of detailed microarchaeological samples taken from these surfaces will aid in the interpretation of their use, but currently it is hypothesized that they were either used in relation to the processing and storage of agricultural products and tools (Kadowaki et al., 2008), or that they may have been the floors for tents (Gibbs et al., 2010). Three stone-filled storage pits were also discovered at the site, and a large basalt grinding slab was discovered in the bottom of one of these.

2.3.4. Al-Aqaba

Al-Aqaba (first referred to by its site number, WZ 310) is a highly eroded LN site located about 600 meters downstream and on the opposite bank from Tabaqat al-Bûma (Figures 2.3, 2.5, and 2.7). Al-Aqaba was discovered with the same systematic trenching strategy that revealed Tabaqat al-Bûma (Banning, 1996), and minor excavations at al-Aqaba were conducted concurrently with the excavations at Tabaqat al-Bûma. The pottery, sickle elements, and other artifacts recovered from al-Aqaba are of identical style to those recovered from Tabaqat al-Buma, suggesting a strong relationship between the two sites. The exact nature of this relationship is unclear, but at the very least, the occupants of the two sites were in very close and very frequent cultural contact with each other. Although no radiocarbon dates exist for the site, it is clearly contemporaneous with at least part of the occupation at Tabaqat al-Buma (Figure 2.1) (Banning, 1999).

Very little architecture was discovered at the site, and most artifacts were found to be in secondary colluvial contexts, originating from further up the slope, and now overlaying later deposits (Bronze Age pits). No in situ material was found on the upper slopes, however, leading the excavators to believe that the original site has been totally destroyed, perhaps due to a land-slide or other mass wasting processes (Banning, 1999). It is thus very difficult to determine the original size and exact nature of the site, but it seems likely that it was also a small farmstead of 1-3 households.

2.3.5. Other Locations in Wadi Ziqlab with Neolithic Material

Between the years of 1986 and 1992, 18 trenches were dug into 15 of the small alluvial terraces of the middle and upper Ziqlab drainage (Banning, 1996). Aside from the discovery of the sites of Tabaqat al-Buma and al-Aqaba by two of the test trenches (as discussed above), the subsurface testing recovered small amounts of Neolithic or probable Neolithic materials from four of the other sampled terraces (Figure 2.3 and 2.8). Although significant locational sampling biases may be present in the dataset (only one or two trenches were dug per terrace), the very low density of the recovered Neolithic material, and the close proximity of the terraces to either Tabaqat al-Buma or al-Aqaba, suggest that they were utilized for agriculture rather than habitation (Banning, 1996). One of these locations—WZ-312—is also significant because it appears that flint nodules may have been quarried from an outcrop directly upslope from the terrace, and it seem that the raw nodules were at least partially processed on location (Banning, 2001, 1996). Another flint source has been identified in the lower reaches of the Wadi (see Figure 2.3), which may have been a potential source of tool stone for the inhabitants of al-Basitan and Tell Rakkan I (Kadowaki et al., 2008).

Small amounts of Late Neolithic material have also been recovered at the site of 'Uyun al-Hammam, which is located a few hundred meters downstream from Al-Aqaba and Tabaqat al-Buma (see Figure 2.3), and is more important for the abundant Epi-Paleolithic remains that are preserved in an ancient paleosol below the colluvial layers (Maher, 2011, 2007; Maher et al., 2002). The most interesting potential Neolithic feature at 'Uyun al-Hammam is a bundle burial in stone-lined rubble-filled pit (Maher, 2007). Although no absolute dates yet exist for this feature or burial, and despite the fact that no diagnostic grave goods were recovered, the presence of a few LN potsherds recovered in the upper layers of the rubble fill, the general style of the burial (similar to the LN cist-tombs), and the previously documented presence of LN dug into the Epi-Paleolithic layers at nearby Tabaqat al-Buma are all indicative that this burial dates from the Late Neolithic. In any case, the pit itself appears to have been first used as a storage feature (also similar to some of the burials from Tabaqat al-Buma), and considering that 'Uyun al-Hammam is located on what was once a broad alluvial terrace (until being largely destroyed by modern road building) very near to a perennial spring (Maher, 2011), it is quite likely that the terrace was farmed, and perhaps even occupied during the Late Neolithic.

Finally, in addition to these locales, 18 other “unremarkable” surface lithic scatters were detected in the original survey of the Wadi in 1981 (Banning, 2001, 1983; Banning and Fawcett, 1983). The “unremarkable” aspects of these scatters related to the lack of diagnostic lithics, and it is quite possible that some or all of these scatters date from the Late Neolithic, which, as I have discussed above, is characterized by a fairly “unremarkable” lithic assemblage. Without excavation, the function of these sites are unknown, and although it is supposable that at least some of them may be related to other small Neolithic hamlets, they may also be related extensive farming, pastoral, or hunting activities in the Wadi (Banning, 2001).

2.3.6. Neolithic Sites in Neighboring Wadis

The multicomponent site of WT-4, discovered during geoarchaeological survey in Wadi Tayiba (Figure 2.3) in 2000 and 2001 (Maher et al., 2002; Maher and Banning, 2001), seems have had a substantial PPNB occupation (although it is not possible to determine if it is LPPNB). Based on an investigation of a large bulldozer cut that bisects the site (Figure 2.9) and the spatial extent of surface finds collected during two brief site visits in 2006 and 2008, I believe the PPNB occupation at WT-4 was probably very similar to that of Tell Rakkan, and that it was likely a small village of not more than 1-2 ha in size. WT-4 may also have a Late Neolithic component, but without excavation, it is unclear exactly how large the LN occupation at WT-4 may have been.

A recently completed survey of Wadi Qusieba (to the immediate north of Wadi Tayiba) in the summer of 2012 has discovered two possible PPNB sites in that Wadi as well (Figure 2.3, sites WQ-121, also known as 'Ain Quseiba, and

WQ-115) (Banning, pers. com.). These two sites, identified by surface finds of a few PPNB-style blades, are both located in the lower stretch of Wadi Quseiba, near its outlet to the Jordan Valley on two very small alluvial terraces. Although located on opposite banks of the Wadi, they are only about 300 meters distant from each other, and so may be two components of a single PPNB site. The artifacts that were discovered on the surface seem to derive from recent cutbanks, and although the surface collections of each site were conscribed to two very small outcrops of about 500 m^2 each, there are likely to be more substantial subsurface remains that have been covered by large amounts of colluvium (as is common for most Neolithic sites in the region). It is thus still unclear exactly how large these sites (site) may have been, nor whether they date to the LPPNB or to an earlier part of the PPNB.

At least one well-preserved Late Neolithic site (Figure 2.3, the site of WQ-117) was also discovered during this latest survey (Banning, pers. com.). The surface assemblage at WQ-117 appears to cover about 550 m^2, which is very similar to the size of Tabaqat-al Buma. Artifacts recovered from the site suggest that it dates to the Yarmoukian, and so was likely contemporaneous with the sites in Ziqlab.

As of yet, and despite fairly intensive formal and informal survey, no Neolithic sites have been discovered in Wadi Abu Ziad. However, there are two sources of high quality flint in Wadi Abu Ziad (see Figure 2.3), which may have been the quarry for much of the stone used to construct tools in Wadi Ziqlab (Kadowaki et al., 2008). Although no comprehensive sourcing analysis has been undertaken, there is abundant evidence that this flint was quarried in antiquity, including the likely remnants of extensive quarries at the Bronze Age site of 'Ain Beidah near the outlet of Abu Ziad.

2.4. Chapter Summary

In this chapter, I have provided a basic archaeological narrative model of course of the Neolithic period in the Northern Highlands of Jordan, with specific emphasis on the view of this trajectory from Wadi Ziqlab. The basic picture is one of continual intensification and reliance on domesticated plants and animals and a general increase in material cultural, social, and settlement complexity from the advent of domestication economies in the PPNA until the culmination of “Pre-Pottery Neolithic Culture” in the LPPNB. In the following Late Neolithic period, we see a drastic reorganization in all of these aspects of the Neolithic lifeway. At some sites, researchers see a period of reorganization connecting these periods, which has been labeled variously the PPNC or the Terminal PPNB (and could just as easily be labeled the Early Late Neolithic). In many parts of Northern Jordan, this period is evidenced by the slow abandonment of the so-called PPNB “Mega-sites”, which are eventually only used on a seasonal or intermittent basis in the following Late Neolithic.

In Wadi Ziqlab, while the picture of the transitional period itself is less clear, the picture of what was transitioned to is much clearer. Even though the one known LPPNB site in the Wadi is much smaller than any of the Mega-sites, it seems that the population of that site moved to various other parts of the Wadi. Thus, in Wadi Ziqlab, across the transition, people dispersed from a settlement system where most people lived together in one small village situated at the border of the Mediterranean Woodland and Savannoid ecozones, to one where multiple small hamlets were spread linearly along the Wadi, spreading the population throughout both ecozones. In the LPPNB, Tell Rakkan I would have served as a "central place" from which logistical forays to either ecozone for wild game, pasture, and other resources would have been launched. It is unclear if these activities would have been undertaken communally, but there is evidence from other LPPNB sites that suggests not (i.e., that subsistence activities took place at the level of the nuclear family or household). In the Late Neolithic, however, each hamlet likely specialized in the gathering or production of those particular resources most available in, or most suitable for production in, its own ecozone. This specialization was not all-encompassing, however, and, in addition to semi-regular trading or sharing of excess "specialized" resources between hamlets, each hamlet also seemed to have engaged in all types of subsistence activities to greater or lesser degrees. Thus, each hamlet can be considered a single unit of production/consumption making up one semi-autonomous node in a wider net of interconnected hamlets.

Finally, the reader will have no doubt noticed that, although I have stated in Chapter 1 that this dissertation investigates the *cause* of this reorganization, I have not discussed possible causes in this chapter. There is a history of archaeological thought concerning the PPN/LN transition, to which I wish to add my own thoughts. Because these ideas are central to the theme of this dissertation, I believe they require their own space, and so will be the sole focus of the next chapter.

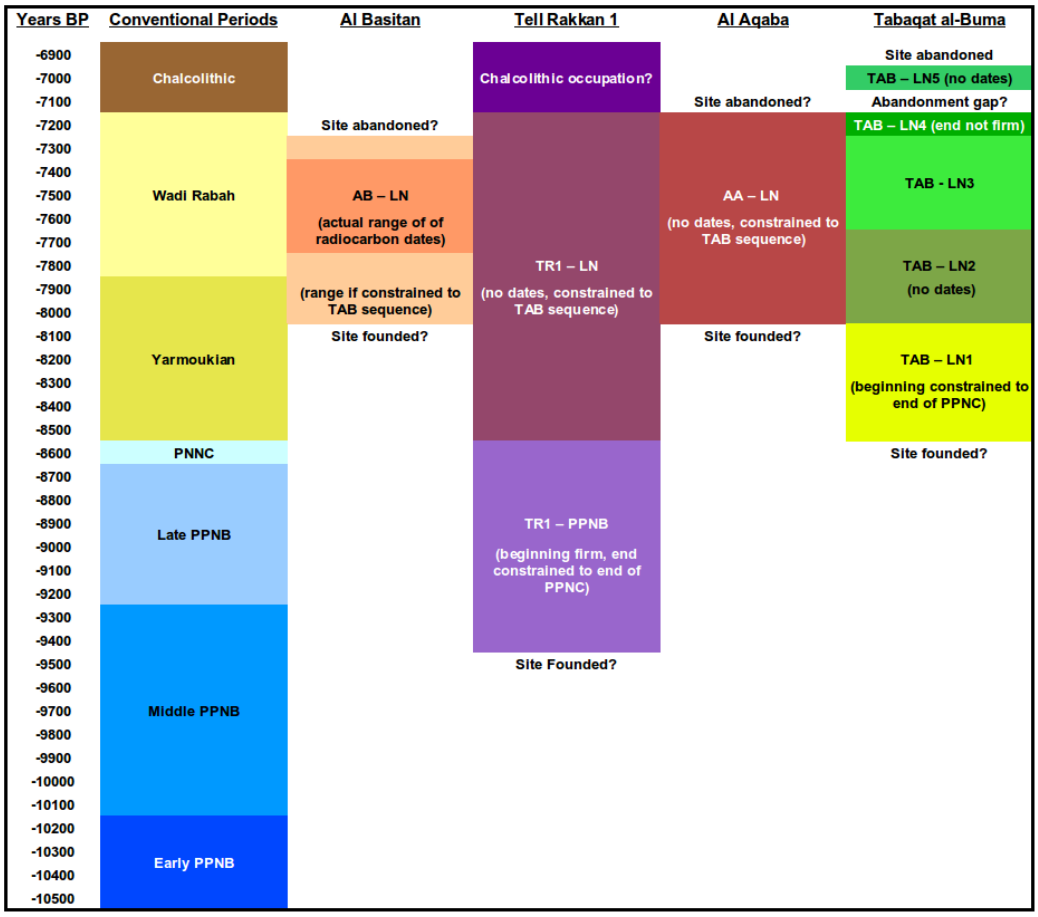

Fig. 2.1. Chronological diagram of the Neolithic in Northern Jordan. The regional "techno-typological" chronology appears on the left, and the absolute or inferred chronology of each of the excavated Ziqlab Neolithic sites appears as a separate column on the right.

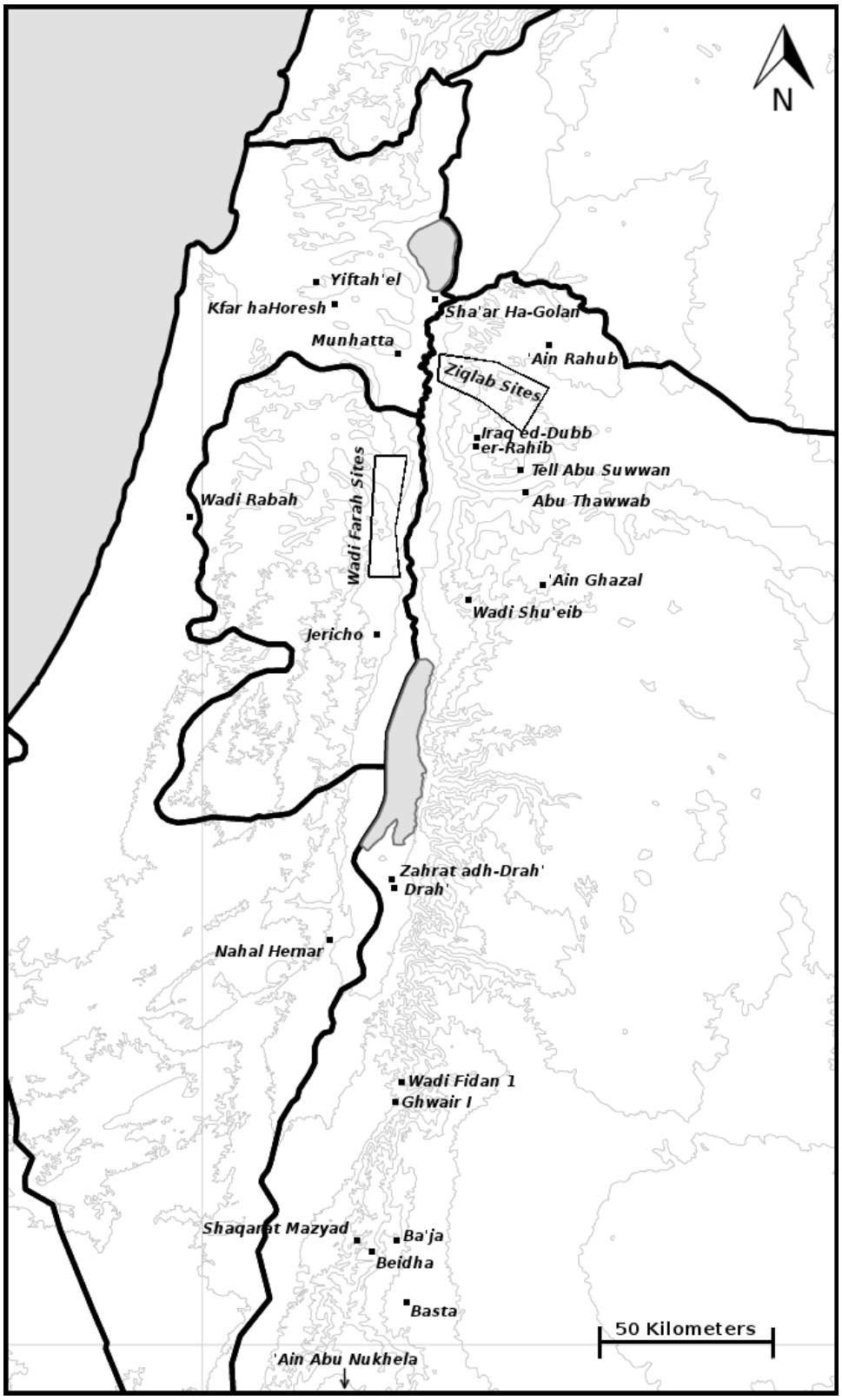

Fig. 2.2. Map of Neolithic sites mentioned in the text.

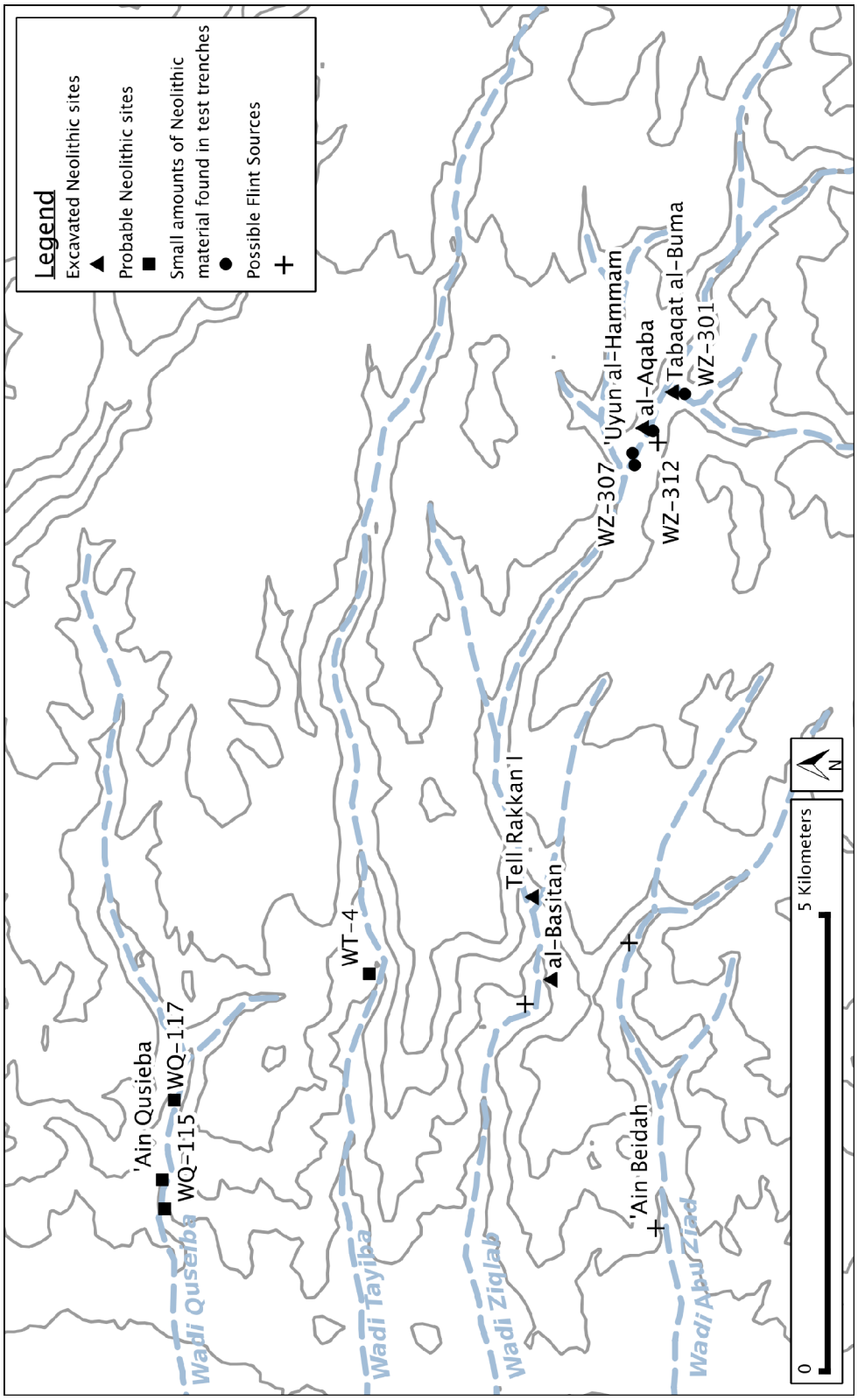

Fig. 2.3. Map showing the known Neolithic sites and potential flint sources in Wadi Ziqlab and the neighboring Wadis

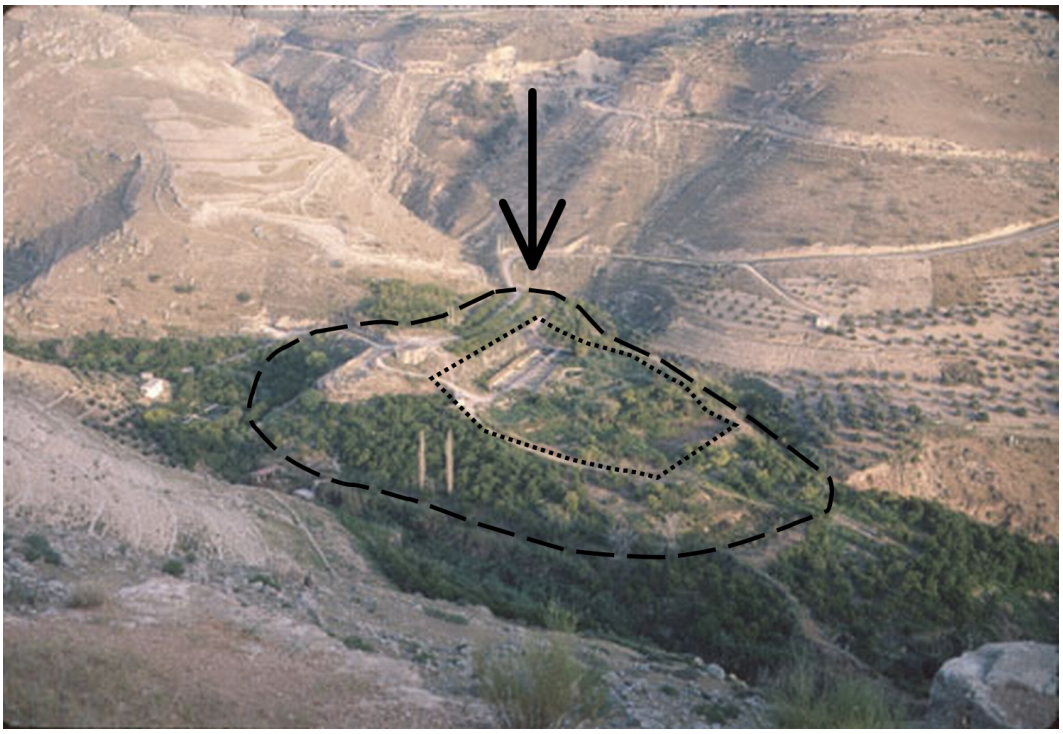

Fig. 2.4. Overview of Tell Rakkan I. Dotted line denotes the area of bulldozer disturbance, dashed line denotes the probable border of the Neolithic village.

Fig. 2.5. Overview of Tabaqat al-Buma. The site plan has been overlayed at approximately the correct scale and orientation. The arrow in the back points to the location of the nearby site of Al Aqaba.

Fig. 2.6. Overview of the al-Basitan terrace. The dotted line shows the approximate extent of the main excavation grid.

Fig. 2.7. The Al Aqaba terrace. The arrow indicates the approximate location of the original excavation trench.

Fig. 2.8. Site WZ-301, one of the terraces where small amounts of Neolithic material was recovered in test trenches.

Fig. 2.9. Overview of the WT-4 terrace, showing the long bulldozer cut that bisects the site. The main portion of the Neolithic site is indicated by the arrow.

3. THEORETICAL APPROACHES TO THE PPN-LN TRANSITION

3.1. Chapter Introduction

In this chapter, I examine the five leading explanations for the instigation of the PPN-LN transition. I critically review each idea, and discuss the current state of research. I then introduce a new approach to understanding the PPN-LN transition, which draws on Complex Adaptive Systems theory (CAS) and Resilience Theory (RT). I describe the salient portions of each theory, discuss how they can be applied to archaeological phenomena, and provide empirical evidence for the existence of complex adaptive phenomena within human subsistence economies. Finally, I sum up a narrative model of how complex phenomena may have led to the PPN-LN transition, and present new, CAS and RT-informed hypotheses for the PPN-LN transition, and examine their test implications.

3.2. Existing Hypotheses About the PPN-LN Transition

There are five leading schools of thought regarding the terminal PPNB/C to LN transition, which I have labeled: 1) the "Climatic-Forcing Hypothesis, 2) the "Human-Induced Environmental Catastrophe Hypothesis", 3) the "Epidemiological Hypothesis", 4) the "Social Breakdown Hypothesis", and 5) the "Settlement Reorganization Hypothesis". In this section, I summarize the main arguments of each hypothesis, and examine their critiques.

3.2.1. The Climatic-Forcing Hypothesis

The basic tenet of the Climate-Forcing Hypothesis is that rapid or radical climate-change was the main driver of the social change seen at the end of the PPN. Its earliest proponents were Davis and Simmons[23] (Davis et al., 1990) and the idea was subsequently taken up by Bar-Yosef (Bar-Yosef, 2001; Bar-Yosef and Meadow, 1995) and Belfer-Cohen and Goring-Morris (Belfer-Cohen and Goring-Morris, 1997). All see the abandonment of the PPNB "Megasites" as corresponding with general climatic changes occurring in the region at that time. Both Bar-Yosef and Davis and Simmons referenced the results of the Cooperative Holocene Mapping Project's (COHMAP) GCM climate-modeling results, published in a 1988 article in the journal *Science* (Anderson et al., 1988), while Belfer-Cohen and Goring-Morris referenced proxy records (pollen and

23 Simmons no longer supports climatic forcing as the main driver of the PPN-LN transition, but instead now supports a combination of social pressures and environmental change (see section 3.2.4., below).

speleothems) from the Levant. In the COHMAP model, in addition to the winter storms coming from the Mediterranean, the Indian monsoon penetrated far enough inland to bring summer storms to the Southern Levant in the first part of the Holocene. According to the model, the monsoon started to retreat to its current extent around 9000 BP, returning the Southern Levant to a classic Mediterranean climate, and coinciding with the depopulation of the megasites. Bar-Yosef connects this climate-change event with the contraction of summer grazing areas, which would have put pressure on the pastoral component of the PPNB economy. Simmons, on the other hand, sees this event connected with increased erosion rates on harvested fields that would have occurred during the PPNB summer monsoons. Rather than the recession of the monsoon, in Simmons' model, it is the cumulative effects of the monsoonal erosion on arable land throughout the PPNB that eventually leads to the abandonment of the megasites, and the reorganization of the population to areas previously forested, and thus where the soil has been conserved. Simmons connects this with the so-called "Neolithic cobble layers" that have been found interspersed between the PPN and LN occupation layers at 'Ain Ghazal, Wadi Shu'eib, and other sites. Belfer-Cohen and Goring-Morris also see accumulating environmental degradation in-part due to human land-use, but suggest that it was a brief climatic reversal (which they see occurring at 7900 BP) that pushed the already-weakened PPNB food-system over the brink of collapse. It is important to note that none of these early proponents of the Climate-Forcing Hypothesis promote climate-change as the *only* factor of the abandonment; all authors indicate that the natural effects of climate-change were amplified by human action. For example, Bar-Yosef postulates that the effect of the reduction in natural summer grazing could have been amplified by a general increase in grazing pressure and woodcutting by PPNB peoples. All three sets of authors, however, implicitly or explicitly suggest that the major cultural and social transformation that occurred across the PPN-LN transition were somehow directly related to climate change.

A new wave of Climate-Forcing Hypothesis papers have been published in the last several years (Berger and Guilaine, 2009; Clare, 2010; Migowski et al., 2006; Pross et al., 2009; e.g., Staubwasser and Weiss, 2006; Weninger et al., 2009, 2006). These writers, referencing newer climate reconstructions, point to a "global climate event" occurring around 8200 BP. This event was a change in the thermohaline current system brought on by an influx of meltwater from the retreating Laurentide icesheet (Abrantes et al., 2012) and is supposed by the proponents of the Climate-Forcing Hypothesis to have been the trigger that led to a reduction in the range of the Indian Monsoon, and a rapid drying of the Eastern Mediterranean. These researchers postulate the drying to have precipitated a massive change to terrestrial ecosystems of the Eastern Mediterranean, and that these ecological changes would have, in turn, massively affected Neolithic cultures of the time[24]. In their view, this was not only the instigation for the

24 For example, Clare (2010) goes so far as to postulate that the climatic deterioration would have caused wide-spread warfare and the rise of chiefs or "big-men".

terminal PPNB societal transformation in the Levant, it also spurred the first waves of Neolithic migration into mainland Europe.

Perhaps the biggest critique that can be leveled against the Climate-Forcing Hypothesis is not that climate-change *could not* have been a factor in the abandonment of the PPNB megasites, but rather that it is the *causal* factor for the change. The main issue for the Climate-Forcing Hypothesis is that, while the date of the 8200 BP event is well established[25], the exact timing of the PPNB-LN transition remains unclear. The timing and effect of the event in northern Jordan is confirmed by recent sedimentological and radiocarbon analysis of Dead Sea cores, which show a dramatic drop in lake-level beginning at 8200 BP—likely caused by a rapid decrease in the amount of precipitation falling in the Sea's catchment (e.g., the Jordanian Highlands)—and lasting until about 7800 BP (Migowski et al., 2006). Weninger et al. (2006) attempt to show a positive correlation between the 8200 BP event and major changes in the occupational sequence of several sites in Eastern Mediterranean, but only succeed by "stretching" the radiocarbon chronology at these sites to fit their model by referring to the possibility of "dates from old wood" or "time lag" between trigger and abandonment. The most current analysis of the radiocarbon evidence from Northern Jordan suggests that the PPN-LN transition occurred around 8500 years ago (see Chapter 2), which is 300 years *before* the 8200 BP event, and thus too early to have been caused by it (Maher et al., 2011).

Interestingly, the "8200 BP event" is not well expressed in the AMCM climate model used in this research (see Chapter 5, Section 5.4.2, and Figures 5.40 to 5.42)[26]. Minimal precipitation impact of the 8200 BP event in the southeastern portion of the Mediterranean basin is corroborated by other GCM paleoclimatic reconstructions (e.g., Brayshaw et al., 2011), and it has been suggested that the impacts of the 8200 BP event were not globally uniform. Furthermore, both the AMCM and the model of Brayshaw et al. (2011) indicate that the early Holocene climate of the southeastern Mediterranean was never affected by the Indian Monsoon. If the major impact of the 8200 BP event was to the strength of summer rainfall, it follows that the event would have had a minimal impact in areas with minimal summer rainfall. Thus, this event was unlikely to have adversely affected people living in the Eastern Mediterranean in any case.

3.2.2. The Human-Induced Environmental Catastrophe Hypothesis

The main premise of the Human-Induced Environmental Catastrophe Hypothesis is that human-caused deterioration of the environment around PPNB

25 There is evidence for the "8200 BP event" in ice cores taken from the Greenland ice sheets, sediment cores taken from the Red, Dead, and Mediterranean Seas, and in pollen cores from various locations in southern Europe and North Africa.

26 The AMCM instead shows the largest drop in annual precipitation to have occurred between 9500-9200 BP—near the end of the MPPNB.

sites was the main driving factor of the social transformation occurring at the PPN-LN transition. The hypothesis was first described in two publications in the late 1980's by Köhler-Rollefson (1988) and Rollefson and Köhler-Rollefson (1989), and elaborated in later publications by the same authors (Kohler-Rollefson, 1992; Kohler-Rollefson and Rollefson, 1990; Rollefson, 1997; Rollefson and Kohler-Rollefson, 1992). Their hypothesis is derived from the data they were recovering from their excavations at 'Ain Ghazal, and especially from the PPNC layers at the site. A major focus of these publications was the diachronic pattern of the utilization of wood resources at 'Ain Ghazal. Calculation of the amount of domestic fuel-wood, architectural wood, and the fuel-wood needed for plaster production yielded very high numbers that seemed to Rollefson and Kohler-Rollefson to have been completely unsustainable in the long-term. The evidence they were uncovering from the PPNC layers at 'Ain Ghazal seemed to support this idea: the wood used for architectural components was becoming scarcer, and posts, beams, etc. were becoming smaller, the quality of plaster was declining, and there was increasing evidence for the use of small brush and dung as fuel in domestic hearths.

Kohler-Rollefson and Rollefson also saw evidence for localized environmental deterioration in the economic data recovered from 'Ain Ghazal. Their interpretation of the faunal evidence (reduction in the amount of woodland species over time) suggested that the local hunting catchment was becoming increasingly deforested. The rapid increase in the proportion of domestic ovicaprids relative to wild species suggested the local pastoral catchment was under increasing pressure, and was likely become overgrazed. Citing the prevalence of pasture on slopes greater than 4% in the direct vicinity of 'Ain Ghazal, they suggest that local denudation by ovicaprids would have led to widespread erosion of these slopes, which eventually bled over into the adjacent agricultural lands. Furthermore, they postulated that these early domestic herds were originally kept in a site-tethered pastoral system (animals return to the site every day, or every few days), which, as herd sizes increased, created increasingly difficult-to-solve scheduling conflicts between pastoral and agricultural activities at the site.

In their view, these human-induced environmental pressures led to two significant outcomes: First, overgrazing—mainly by goats—lead to a general suppression of woody vegetation that caused increased erosion and ineffective fallowing of farm fields, and thus eventual fertility-decline and reduced cereal-yields. Secondly, scheduling conflicts between agriculture and pastoralism—exacerbated by declining yields—eventually led to the need for long-distance seasonal pastoral movement, which in turn led to the development of a specialized pastoral component of PPNB society. In their model, the accrual of deleterious impacts to the local environment eventually made life in the PPNB towns untenable. More and more people left the towns to engage in specialized pastoralism in the steppe and desert regions, eventually only using 'Ain Ghazal as a temporarily occupied way station in their series of seasonal migrations. The

Human-Induced Environmental Catastrophe Hypothesis suggests that it is this lifestyle change that also accounts for the radicle change in material culture and settlement pattern across the transistion.

A major critique of the Human-Induced Environmental Catastrophe Hypothesis has been the lack of targeted geoarchaeological assays of the extent of early Holocene erosion and soil fertiltiy decline in and around the vicinity of the large PPNB sites; the only geological evidence presented in the original articles was anecdotal (e.g., references to "Neolithic cobble layers". See Section 3.2.1, above.). Recent detailed analysis of depositional sequences in Wadi al-Hasa in central Jordan by Schuldenrein (2007) has confirmed that the Early and Middle Holocene was characterized by increased rates of erosion, but Schuldenrein considers this erosion to be driven by tectonic changes in the Dead Sea rift and exacerbated by the overall wetter climate of that period, rather than anthropogenic in nature. Furthermore, in a review of the archaeological evidence for landscape degradation at 'Ain Ghazal, Campbell (2010) questions Rollefson and Kohler-Rollefson's assertions on the basis of a numerical model based on ethnographic data about subsistence farming practices. The results of Campbells' model suggest that Neolithic subsistence could not have been intensive enough to cause serious degradation around the site. Finally, researchers such as Perevelotsky and Seligman (1998) and Barton et al. (2010b) have begun to rethink the idea of degradation itself. What has traditionally been seen as only a negative (e.g., *over*grazing leads to vegetation *deterioration,* hillslope *denudation* leads to *erosion* of soils, etc.), can also be looked at a positive (i.e., heavy grazing *increases* biodiversity in the ecosystem, erosion from hillslopes *replenishes* soils in valleys and plains, etc.). Thus, it is unclear if the environmental impacts of Neolithic agropastoralism, if any, would have even have been deleterious to the Neolithic subsistence system at all.

In response to these critiques, Rollefson and colleagues recently returned to 'Ain Ghazal, and undertook a detailed sedimentological study of the stratigraphy in four the original test trenches, as well as limited geoarchaeological survey in the vicinity of the site, and LiDAR surface modeling of the site itself (Zielhofer et al., 2012). Together, the four studied stratigraphic columns span from the MPPNB through the Chalcolithic (but missing the Yarmoukian) occupation of the site, and include instances of a "rubble layer" in three of the profiles. In order to differentiate between anthropogenic, alluvial, and colluvial depositional processes between the layers of the studied stratigraphic columns, a variety of analyses were conducted on samples taken from each layer, including granulometry, lithology, magnetic susceptibility, carbonate content, pH level, total organic carbon content, and radiometric dating assays of carbonized materials. The rubble layers were found to consist of *ex situ,* but of local origin, fist-sized (4-6 cm diameter) stones, of overwhelmingly limestone lithology (limestone:flint ration of 6:1), which differ significantly from other layers (which have a limestone:flint ratio closer to 1:1, and a greater variety of clast sizes). The clasts are not sorted, or imbricated, and they are surrounded by a matrix of fine

silt, with little sand or clay. Local geoarchaeological survey could not discover any "rubble layers" in non-site contexts, even in topographically lower areas, and LiDAR surface modeling revealed no geomorphological evidence for substantial past gullying, landsliding, or mass wasting that could be responsible for the rubble layers. Interestingly, there is also some evidence for occupational surfaces (compaction, etc.) existing within the rubble layers, although there is no evidence for substantial architecture or other evidence of sustained human occupation (accumulations of artifacts or midden deposits) from these layers, despite their thickness[27].

These data suggest to Rollefson and colleagues that the rubble-layers are actually anthropogenic features, contradicting earlier assessments postulating deposition by natural process exacerbated by either or both of climatic change and human alteration of vegetation on nearby slopes (e.g., Rollefson, 2009; Weninger et al., 2009). Rollefson and colleagues cannot definitively characterize the exact anthropogenic process by which the layers were deposited, but they do rule out the possibility that they were caused by collapsing of abandoned buildings. Their reanalysis has also led to a new understanding of the chronology of these features. Radiocarbon assays and stratigraphic analysis showed there to be two chronologically separate rubble layers: Of the three studied rubble-layers, two date near the end of the LPPNB[28] (one radiocarbon date of 8800 cal. BP), and the third dates from the beginning of the Chalcolithic (several radiocarbon dates between 7300 and 6400 cal. BP[29]). These dates contradict earlier suppositions that these layers dated to the Yarmoukian period (e.g., Rollefson, 2009). This idea was based on the discovery of abundant Yarmoukian potsherds in some of these rubble-layers at the site, but the new analysis finds these sherds to have been secondarily deposited in the now-dated "Chalcolithic" rubble layer.

Two other interesting stratigraphic discoveries were also made during Rollefson and colleagues' re-analysis of the site's stratigraphy. Firstly, the team discovered evidence of localized slope erosion during the PPNB (evidenced by filled rills and colluviation), but of decreased erosion and relative soil stability *during and after* the PPNC (evidenced by increased rates of pedogenesis). This suggests that erosion actually *decreased* through the PPNB/C, which directly contradicts the central test implication of the Human-Induced Environmental Catastrophe Hypothesis (i.e., increased erosion over time due to human impacts). The final new stratigraphic find was the discovery of a previously-unknown erosional unconformity underlying the Chalcolithic deposits. This suggests another period of erosion at the end of the Yarmoukian/LN occupation of the site, and indicates that erosion rates at the site fluctuated over time. Interestingly, none

27 The PPNC rubble layer was found to be nearly 3 m thick, while the Chalcolithic rubble layer was found to be several meters thick.

28 Rollefson and colleagues interpret this date to be in the PPNC, but they are only using the sequence of dates from 'Ain Ghazal, and not the regional chronology.

29 It is interesting to note that these dates place the third "Chalcolithic" rubble layer roughly contemporaneous to the last phases of occupation at Tabaqat al Buma.

of the rubble features or erosional episodes at the site align with periods of climatic drying (e.g., the 8200 BP event), but instead seem to align with periods of relative wetness (as determined from the Dead Sea lake level record). Although the PPNB/C and PPNC/LN transition of the site do not line up with the largest dessication event (i.e., the 8200 BP event), Rollefson and colleagues suggest that they do align with smaller periods of aridity, and so now support a climatic driver for these cultural phase-changes (i.e., they have now adopted the Climate-Forcing Hypothesis).

3.2.3. The Epidemiological Hypothesis

The Epidemiological Hypothesis is a relatively new hypothesis for the PPN-LN transition, put forth by Goring-Morris and Belfer-Cohen (2010), who previously championed a climatic cause of the transition (see Section 3.2.1, above). The main premise of this hypothesis is that the new, densely populated, larger villages of the LPPNB, combined with a closer association of humans and animals than ever before in human history to create an ideal environment for the rapid evolution and spread of disease. Goring-Morris and Belfer-Cohen also point to the decreased nutrition, and increased labor requirements inherent to the new Neolithic lifeway, and suggest that the LPPNB population was also more susceptible to infection by these new pandemic diseases. They suggest that LPPNB people, previously unfamiliar with pandemic disease, had not yet developed appropriate mechanisms for maintaining public hygiene in their villages, and that accumulated trash middens, polluted water-sources, and general uncleanliness would have exacerbated the situation even more. They see some evidence for increased awareness of hygiene in the LPPNB (e.g., the presence of wells at Atlit-Yam, the frequent re-plastering of floors at LPPNB sites), but suggest that eventually these initial steps were inadequate to stem the spread of disease, and that the only option was to disperse from these densely populated LPPNB towns, and to live in widely-separated hamlets and small villages.

A major critique of this hypothesis is that, while perfectly plausible, Goring-Morris and Belfer-Cohen provide no genetic or other paleopathological evidence that would confirm the presences of early pandemic diseases in PPNB villages. They cite increased rates of multiple burials at some LPPNB sites as evidence for epidemic outbreaks, but this is circumstantial at best. Until solid genetic and paleopathological evidence is found, the Epidemiological Hypothesis remains an interesting, but unprovable hypothesis for the changes that occurred over the PPN-LN transition.

3.2.4. The Social Breakdown Hypothesis

Kuijt (2000b) provides a third alternative scenario of the PPN-LN transition, and others researchers have endorsed this idea (e.g., Simmons, 2007,

2000; Verhoeven, 2002), and have expanded upon it. In the Social Breakdown Hypothesis, a new social paradigm emerged in the PPNB: the kin-based networks of earlier times were gradually replaced or expanded by social networks grounded in other types of social bonds, economic ties, or by mortuary and other rituals. However, the Social Breakdown Hypothesis suggests that the organizational changes necessary to promote total group solidarity within the village did not occur concomitantly. Thus, there was insufficient means for governing the new social stresses that would inevitably stem from these new social relationships, as well as from things like population crowding, reduction in privacy, and loss of autonomous control of living spaces. In this scenario, these stresses eventually led to serious fragmentations in the social life of the large LPPNB villages, that in turn led to a disintegration of late PPNB/C social structures and ritual beliefs. Proponents of the Social Breakdown Hypothesis do not dismiss environmental degradation (or climate change); they, in fact, embrace the idea. In the Social Breakdown Hypothesis, it is the *combination* of the new social stresses (and lack of social stress-relief) with increasing resource stress caused by mounting human-caused environmental degradation that led to the disintegration of the PPNB/C culture. The fragmentation of social bonds made it easier for individual families to leave the large villages (i.e., the social consequences of leaving were greatly reduced), and that as resource stress increased, more and more families found it advantageous to "get out of town", move to smaller sites, and to return to a more egalitarian, kin-based social organization system.

Proponents of the Social Breakdown Hypothesis point to the diminishing size and increasing fragmentation of interior domestic spaces, the in-filling of outdoor spaces at PPNB sites, changes in mortuary practices, and evidence of environmental deterioration (e.g., as in the Human-Induced Environmental Catastrophe Hypothesis) to support this hypothesis. However, there is currently little evidence for the emergence of social inequality, hierarchy, or interpersonal violence that would likely have accompanied these suggested social changes and strifes. This lack has led some proponents of the Social Breakdown Hypothesis (e.g., Simmons, 2007) to place more emphasis on the environmental component of the argument, but all proponents of the Social Breakdown Hypothesis believe that the novel social stresses of life in the first large farming villages must have played some role in their eventual abandonment. Furthermore, there is no clear reason why a reversion to a simpler lifestyle was the preferred choice at this time, rather than an escalation in social complexity, as occurs at the end of LN/Chalcolithic.

3.2.5. The Settlement Reorganization Hypothesis

Finally, Banning (2001) provides a fundamentally different hypothesis for the impetus of the PPN-LN transition. Banning believes that shifting to a dispersed settlement system gave the people of the Late Neolithic many social, ecological, and economic benefits, including less competition for, and easier

access to, agricultural fields and pastures. Banning suggests that the shift would have spread agricultural risk over many ecotones, and reduced conflict between agricultural and pastoral land-use—all without the need for fundamental change to social or ritual institutions, (nor drastic environmental degradation) in the preceding period. If the first four hypotheses focus on internal or external "push" factors that could have *actively induced* change in the LPPNB social or economic systems (i.e., *pushing* them towards a new way of doing things), then Banning's hypothesis focuses on a potent "pull" factor that could have *passively attracted* these same changes (i.e., *pulling* them towards a new way of doing things). Banning does not completely ignore push factors, however; he suggests that access to suitable grazing and farming land around the large PPNB sites became more constricted over time, and that this likely led to scheduling problems between the agricultural and the pastoral components of the PPNB food production system. In many ways, Banning's narrative model of the PPN-LN transition can be looked at as an extension of the Social Breakdown Hypothesis, but one that emphasizes the potential benefits of settlement reorganization over the difficulties of life in LPPNB villages, and so is subject to some of the same critiques (specifically the critique that it is difficult to explain why dispersal was a better choice for LPPNB peoples than intensification).

3.2.6. Summary and Critique of Existing Hypotheses

The preceding discussion has summarized the basic arguments for several of the leading hypotheses about the instigation of the PPN-LN transition, and has provided some critiques of each. All are plausible, but none are fully satisfactory. The most recriminatory critiques range from an over-emphasis on monocausal drivers to a basic lack of supporting archaeological evidence. The best of the existing ideas tie together multiple factors (e.g., environmental degradation *and* social stress), and take a long-term view (i.e., that these problems escalated over time). The implicit message is that there were some critical thresholds in social-strife or environmental-effects that the LPPNB socio-economic system eventually surpassed, but they all lack a basic theory that explains rapid change in a dynamic and recursive socio-natural system. Such theory exists, however, and the remainder of this chapter provides a discussion of how this theory can be applied to instances of rapid change in coupled human-natural systems in general, and to the PPN-LN transition in specific.

3.3. A Complex Adaptive Systems Approach to the PPN-LN Transition

"Complex adaptive systems", or CAS, is a body of theory[30] that has evolved out the work of researchers across a variety of disciplines (but particularly ecologists and computer scientists) who, in the latter half of the 20th century, began to rethink previously accepted notions about the linear nature of

30 Often also referred to as "complex systems" or "complexity theory," among other epithets.

natural phenomena (Kohler, 2012). Foremost among the ideas being questioned was the idea that the outcome of a series of stimulus events on natural systems could be accurately predicted, if only the "right" equation were found. In other words, researchers began to question the validity of the quest for unified causal explanations. A reexamination of the linkages between stimuli and results, largely informed by the advent of computer-based simulation modeling, lead to the idea of feedback loops and uncertainty; "predictability" was replaced by "emergent properties" as the epitomizing factor of natural systems (Lansing, 2003).

CAS is, in essence, a framework for investigating how the independent decisions and actions of individual components of a system interact to 1) self organize into a coherent system, 2) adapt to work in the interest of the system as a whole, 3) are dynamic and change over time, and 4) derive novel, unpredictable, emergent properties of the system (Miller and Page, 2007; Mitchell, 2009). Thus the focus of CAS has been to use alternative methods of analysis—namely simulation with agent-based models—to understand these properties of a variety of complex systems, including human social systems, in a way that cannot be done from a reductionist approach.

The type of complex system of most interest to archaeologists are what is termed "Coupled Natural and Human" systems, or (as preferred here) Socio-Ecological Systems (SES). SES has been most recently defined by Glaser et al. (2012:4) as "a complex, adaptive system consisting of a bio-physical unit and its associated social actors and institutions. The spatial or functional boundaries of the system delimit a particular ecosystem and its problem context." Importantly, this means that SES are "real", tangible things, that exist in the physical world, have distinct boundaries in time and space, and so can be observed and studied empirically. Thus, SES can be thought to be regionally distinct analytical units (Bourgeron et al., 2009), which is particularly helpful for archaeologists, who are accustomed to analytical units segregated at a regional scale.

CAS is far from being a monolithic theory, however, and considerable debate exists into the nature of CAS as an integrative or unified theory (Miller and Page, 2007; Mitchell, 2009). This is issue is further complicated by the presence of a separate, but clearly related body of theory, commonly referred to as "Resilience Theory" (RT). Resilience theory is the brainchild of C.S. Holling (first described in Holling, 1973), and has been formalized into a more coherent body of theory in two recent edited volumes (Gunderson et al., 2010; Gunderson and Holling, 2002). Although also developed as a critique of reductionist science, RT is intellectually distinct from CAS. If CAS can be thought of as "a new kind of science" (sec. Wolfram, 2002), then RT is "a new kind of systems theory". In large part, the divide is due to a focus of CAS researchers on smaller-scale issues, such as complex behavior among social insects, whereas RT researchers have focused on larger-scale issues such as the succession and dynamics of entire ecosystems. The traditions are further divided by preferred methodology: CAS largely relies on computational approaches (largely, agent-based models) aimed at understand specific dynamics and properties of complex systems, whereas RT has

been based on a more narrative approach centered on the production of heuristic devices that aid general understanding of the long term behavior of complex systems.

That is not to say that RT is incapable of producing testable hypotheses or tangible research directions, or that CAS approaches are incapable of providing insights into general process or large-scale system behavior. On the contrary, the two techniques are quite complementary, and the current study utilizes a general cross-pollenization of ideas from each. In particular, I use two related suites of concepts (each colligated variably under RT or CAS) that are particularly useful analytical frameworks for interpreting change in the archaeological record of regional SES: 1) the interrelated ideas of the adaptive cycle, resilience, and "panarchy" (Folke, 2006; Gotts, 2007; Gunderson et al., 2010; Gunderson and Holling, 2002; Redman, 2005; Redman et al., 2009; Walker et al., 2006), and 2) the parallel ideas of critical transitions, catastrophic regime shifts, "tipping points", "basins of attractions", and alternative stable states (Abel et al., 2006; Folke et al., 2004; Kinzig et al., 2006; Lamberson and Page, 2012; Lansing, 2003; Scheffer, 2009; Scheffer and Carpenter, 2003). Large bodies of literature exist on these topics (see in particular Bentley and Maschner, 2003; Gunderson et al 2010; Gunderson and Holling 2002; Miller and Page, 2007; Mitchell, 2009; and Scheffer, 2009), but it is useful to briefly discuss them here.

3.3.1. The Adaptive Cycle and Resilience

The adaptive cycle is a heuristic device for understanding change in complex systems. Originally envisioned as a 2-D diagram (Figure 3.1a), it has since been expanded into 3 dimensions (Figure 3.1b) (Holling and Gunderson, 2002). The axes of the diagram correspond to system potential, system connectedness, and system resilience. The potential of a system is a measure of its capacity (typically thought of in terms of accumulated resources), the connectedness of a system is a measure of the amount of integration present in the system (typically thought of as the tightness of the coupling between elements of the system), and the resilience of a system is a measure of its ability to adapt to new conditions (typically thought of as its flexibility or adaptability, and measured in terms of things like degree of specialization, etc.). The "figure 8" diagram of the adaptive cycle is formed as the state of the system proceeds through time in the 3-dimensional space of potential, connectedness, and resilience. There are four phases of the adaptive cycle as its state proceeds: 1) exploitation (r), 2) conservation (κ), release (Ω), and reorganization (α). The exploitation phase is a phase of initial growth. In this phase both connectedness and potential remain low, but resilience increases as the phase progresses. This can be thought of as a phase of "colonizing" a new niche, where multiple strategies for survival in the niche coexist within the same system (thus resilience remains high). Eventually, the system begins to narrow in and to focus on fewer options, system potential and connectedness begin to increase, and the

conservation phase is entered. As the conservation phase proceeds, fewer options exist, and so resilience is lost, and the components of the system become increasingly tightly coupled. The conservation phase may last for some time, but eventually something affects the system (an internal or external stimulus) to which it cannot adapt (due to reduced resilience and increased coupling), the system a rapid decline in both potential and connectedness occurs. This is the release phase. As the release phase continues, resilience remains low, and the previously tightly coupled portions of the system become increasingly independent (i.e., connectedness goes lower). As the individual components of the system are released from their tight bonds, resilience is regained as its components are freed to explore new options, and this new activity begins to grow the potential of the system once again. In this phase, the system is at its most unstable point, and it is here that the system can either re-emerge into a totally new niche[31], or remain in the same niche, but return to its initial state. In either case, the system expends much of its newly regained potential in the process, and the exploitation phase begins again as the new system state is explored. But why does the adaptive cycle, cycle at all? As Scheffer (2009:78) puts it, "there is a fundamental trade-off between being adaptive and being efficient"; in other words, increased resilience can only be had at the expense of decreased potential.

How can this concept be applied to archaeology? First, it is important to note that there is no axis of time in this rendering of the adaptive cycle. The absolute time taken to pass through any of the four phases is not necessarily to the scale of the diagram: each of the four phases can last for any amount of time, cumulatively summing to any size of "cycle width". The archaeological record is historical, however, so time must be explicitly linked to the adaptive cycle for any sort of correlation to archaeological phenomena. To do so, we can borrow a key concepts from another body of theory, known as the "constructal law" (Bejan, 2007; Bejan and Lorente, 2011). Although differing in orgin, scope, and approach, constructal law theory nonetheless parallels CAS in several important ways. Most importantly, however, constructal law theory provides an explicit method for temporalizing change in systems over time: the idea of "S-curves"[32]. "S-curves" are logistical curves that occur when a material aspect of a complex phenomenon is plotted against time. Contstructal law has specific terms for particular curve-shapes, and theory for why they are shaped the way they are, but these are largely outside the scope of this discussion. What is important is that the "S-curve" provides a method for tracking complex phenomena over time. We can borrow this idea to track the expected form of the "S-curve" for "potential", "connectedness", or "resilience" over time to produce heuristic time-series graphs of the adaptive cycle working over time (Figure 3.2). These heuristic graphs can be used to help analyze/explain patterning in time-series plots of proxies for

31 I am using the term "niche" here in a semantically similar manner to its use in ecology (i.e., an "ecological niche"), but I want to be clear that I use the term in a wider sense.

32 The term "S-curve" concept is also commonly used in economics to as one of series of "curves" that describe specific patterns of economic growth (e.g., Bahmani-Oskooee and Hegerty, 2010).

"potential" (e.g., village population, number of farmed plots, crop yields, capital, infrastructure, etc.), "connectedness" (e.g., number of living households in a village, heterogeneity of vegetation), and "resilience" (similar proxies as those for "connectedness", but reversed metrics) over time.

3.3.2. Panarchy and Long-term Trends

Now, let us turn to issues of scale and interconnectivity. Holling et al. (2002) have envisioned an system of interconnection between adaptive cycles at different scales, which they term "Panarchy". Panarchies are hierarchically arranged systems of differently-sized adaptive cycles, scaled logarithmically as a function of time and space (Figure 3.1c). It is perhaps best to envision this as "adaptive cycles within adaptive cycles". That is, smaller adaptive phenomena (e.g., a household) exist as independent cycles within larger adaptive phenomena (e.g., a village). Each type of adaptive phenomenon will have its own areal footprint, and will have its own "cycle width" (length of time it takes to complete an entire circuit of the adaptive cycle). The concept of hierarchy is important here; as the scale increases, larger numbers of smaller adaptive cycles are subsumed (e.g., multiple people in a household, multiple households in a village, multiple villages in a regional culture group, multiple regional culture groups in geographic region, etc.). There are two types of possible "feedback" connections between adjacent scales: "remember", and "revolt" (Figure 3.1d). "Remember" is a negative feedback relationship that reflects the conservative influence of larger, slower adaptive cycles on faster, smaller adaptive cycles. "Revolt" is a positive feedback relationship that reflects the radical influence of faster, smaller adaptive cycles on larger, slower adaptive cycles. Envisioned this way, we can see these two forces as terms in a balancing equation that determines the stability state of the entire panarchy[33]. Although conceptually simple, "complexity" is achieved in the panarchy as a function of the differences in the "cycle width" of all the different scales of adaptive phenomena in the panarchy, and the relative alignment of the adaptive states of the adaptive pheonmena at each scale. Thus, small-scale stability or growth can be maintained via large-scale "remember" feedback, even if local conditions should seem to require release and reorganization. Conversely, failure (release) of the larger scale system can occur via an amalgamation of small-scale "revolt" feedback events in the subsystem, even if the larger-scale cycles were nominally stable.

Figure 3.3 shows a heuristic time-series graph of system potential over several sequential cycle widths of an adaptive system. Starting from time *t1*, the overall amount of system potential can increase, decrease, or remain basically constant over time, depending upon the balance of revolt and remember in the panarchy at that point in time. If the balance of the panarchy tends towards conservation (remember) the system experiences net growth of potential and

33 This is similar to the concept of "metastable" equilibrium in traditional systems theory (e.g., Butzer, 1982)

connectedness over time (though at the expense of resilience), resulting in a pattern of compounding success. If the balance tends towards release and reorganization (revolt) then the panarchy experiences net reduction of potential and connectedness over time (but regains resilience), resulting in a pattern of cascading failure. If the forces of conservation and release/reorganization are well balanced between the various levels of the panarchy (a phenomenon I term "remain"[34]), then the panarchy experiences no (or insignificant) net change over time, resulting in a pattern of long-term stability. It is important to note that at any time *t*, a new cycle begins, and the system can depart anew on any of these three courses. Thus, the trajectory from the system state at time *t1* to any of the possible system states at time *t4* is neither linear nor predictable, and it is impossible to predict which particular system state will be achieved at time *t4*. That is, given any set of initial conditions, there are multiple pathways (combinations of Revolt, Remember, or Remain over time) to each possible system state at any later time, which is what makes the system "complex".

3.3.3. Critical Transitions and Alternative Stable States

The discussion of the temporalization of system components (potential, connectedness, and resilience) and panarchical relationships between scales of adaptive components of SES in the preceding section shows how gradual changes can occur in SES to eventually change the system state over time. System state change can occur more rapidly, however, and understanding this rapid type of change is particularly important for a CAS approach to the PPN-LN transition. Scheffer and colleagues (Folke et al., 2004; Janssen et al., 2003; Janssen and Scheffer, 2004; Scheffer, 2010, 2009; Scheffer et al., 2012, 2009; Scheffer and Carpenter, 2003; van Nes and Scheffer, 2005) have been the foremost thinkers on this topic, and have built a comprehensive theory of rapid system change centered around the two key concepts of the concepts of "critical transitions" (also sometimes referred to as "tipping points", but see Lamberson and Page [2012] for a discussion on how that term has been variably used and abused) and alternative stable states. Scheffer and colleagues have developed a series of heuristic graphs to explain these phenomenon, and it is useful to briefly discuss these here. Figure 3.4 shows three different patterns of system state change over time. Figure 3.4a shows the steady-state change as described in section 3.3.2 above where there is a linear relationship between the system state (y-axis) and some critical variable (x-axis). Figure 3.4b shows a more complex relationship between the system state and the critical variable, where change is more rapid over some subsection of variable values, and less rapid in others. In this figure, the steeper zone of the curve is less stable than the flatter portions, but there is still a fixed relationship between the critical variable and the state of the system (i.e., if one is known, the other can be predicted). Figure 3.4c shows yet another relationship between the

34 Holling et al. (2002) do not specifically identify this phenomenon, but it clearly exists as one possible state of the panarchy.

system state where there is a "zone of vulnerability" where two alternative systems states are possible for the same value of the critical variable. Scheffer and colleagues label this type of curve a "catastrophe curve". The dashed portion of the curve cannot be traveled smoothly, so at critical points F1 and F2, the system state "jumps" from one portion of the curve to the other (Figure 3.4d). An important aspect of this type of curve is that even if the critical variable returns to its value from *before* the critical transition (e.g., point F2), the system remains in the alternative system state, and will remain there until the other critical threshold is surpassed (e.g., point F1). In fact, it is possible for the system to enter into a cyclical recurrence between these two stable states as the critical resource varies between the two critical thresholds, which is called "hysteresis" (Scheffer, 2009).

Scheffer and colleagues use another heuristic device—the "stability landscape"—to provide more detail on this phenomenon (Figure 3.5). A stability landscape is a graph where the slope of the line represents the rate of change (Scheffer, 2009). Thus, if the slope is zero, the rate of change is zero. Scheffer uses the analogy of a "ball in a cup", such that if the stability landscape is concave, the ball will always fall to the bottom of the "trough". Such troughs can thus be thought of as "basins of attraction", or, more formally "attractors". Attractors are essentially the stable state of the system under a specific set of conditions (i.e., the conditions that set the current stability landscape). Where the stability landscape is convex, the ball will always fall away from the "peak". Such peaks can thus be thought of as "repellors". If conditions are such that there is only one stable system state, there will be only one attractor (or none at all) on the stability landscape. In the case of two (or more) possible stable system states, then there will be two (or more) attractors, separated by a repellor. Thus, if the perturbation is large enough to overcome the force of the separating repellor, it is possible for the system state (the "ball") to fall into one or the other attractor. It is this dual attraction and repulsion that results in the rapid pace of change across critical transitions.

Furthermore, the width and depth of the "basins of attraction" can be thought of as measures of the system resilience under the given conditions (Figures 3.5 and 3.6). Thus, a deep, wide attractor is highly resilient, and even large perturbations will not "knock the ball out of the cup" (Figure 3.6a). However, a shallow, narrow attractor is highly vulnerable to change, and a relatively minor perturbation may be sufficient to induce system state change (Figure 3.6b). This is exemplified in Figure 3.5, which shows a series of stability landscapes for different positions on a "catastrophe curve": as the system nears the critical transition point (F2), the resilience of the original attractor reduces, and the amount of perturbation required to switch to the alternate attractor lessens. Related to this, systems that are vulnerable to critical transitions are also characterized by higher degrees of subsystem homogeneity and connectivity (Scheffer et al., 2012) (Figure 3.7). Ironically, these homogeneous and highly connected systems are actually more stable in the short-term, as they continually act to resist change until the critical threshold is surpassed.

Scheffer and colleagues have recently begun to examine what they call "early warning signs" that indicate that a system is approaching a critical transition (Scheffer, 2010; Scheffer et al., 2012, 2009), and some of these warning signs these are of particular interest for analyzing archaeological data and model output. Firstly, systems that are at risk for a critical transition will exhibit slower recovery after a minor perturbation than will highly resilient systems. This will be observable on a time-series plot of system state (e.g., system potential) as difference in the slope of "recovery lines" after a reduction in system potential (Figure 3.6, c and d). Resilient systems will have very steep recovery lines (Figure 3.6c), and systems at risk for critical transitions will have less steep recovery lines (Figure 3.6d). Secondly, the system state of highly resilient systems will be less variable over time than will systems at risk for a critical transition. This is also observable on time-series plots of system potential (Figure 3.6, e and f), where the variation in system potential in resilient systems will have higher amplitude and be more stochastic (Figure 3.6e), and the variation in system potential in at-risk systems will be more regular and have lower peak amplitudes. Finally, related to the idea that at-risk systems have higher connectivity and homogeneity, at-risk systems should appear to "resist" adaptation in the face of changing socio-environmental conditions. Thus, at-risk systems should show a disparity between the pattern of change on a time-series plot of system potential compared to the pattern of change on a times-series plot of key environmental variables (Figure 3.6h), while the patterns should be correlated in highly resilient systems (Figure 3.6f).

3.4. Are There Alternative Stable States of Human Subsistence?

Before using CAS to draw insights into the PPN-LN transition, a more fundamental question must be answered: Can CAS theory actually explain the variability in human subsistence strategies? The tendency in anthropology in recent decades is to view human variation in terms of continua or unsegmented fields of variation (e.g., Binford, 1980; Feinman and Neitzel, 1984; Kelly, 1995, 1983). But, if viewed from a CAS perspective, we would expect that the unique socio-natural conditions of particular subsistence activities would tend to push societies engaging in them into similar adaptive milieus. That is to say, there would be multiple stable and non-overlapping human socio-conomic "system states". So, is it necessary to model PPN land-use as a continuum of variability (e.g., by continuous parameter-sweeps)? Or is it more accurate to model a series of discrete behavioral systems (e.g., by set parameters with limited variation)? Furthermore, is there evidence to suggest that human economies exist as a series of discrete multi-stable states, arranged as a series of attractors and separated by repellors? These questions are essential to the application of the idea of critical transitions to human systems and I turn to the ethnographic record to answer them.

The use of ethnographic data—especially from modern and historical hunter-gatherer groups—to create ethnoarchaeological models for interpreting archaeological patterns has become mainstream since the advent of "the new archaeology" in the 1960's and '70's (Yellen, 1977). "Classic" ethnoarchaeological modeling involves field work with a specific group or groups of people engaging in traditional lifeways (e.g., hunter-gatherers, pastoralists, small scale agriculturalists, etc.), and subsequent transformation of data collected during the field work into "small-scale" models designed to address a specific archaeological problems (such as site formation, settlement patterning, or lithic use-wear) (e.g., Binford, 1980; Lewis R Binford, 1977; Brooks and Yellen, 1987; Deal, 1985) or to create "middle range theory" to connect smaller aspects of archaeological phenomena to larger-scale theories of human behavior (e.g., Bettinger, 1987; Binford, 1983; Lewis R. Binford, 1977). These technique have relied less on cross-cultural comparisons than they have on abstraction from particular case-studies. More recently, a new style of ethnoarchaeological research uses cross-cultural datasets to search for global patterns within human behavior (Feinman and Neitzel, 1984) or to *derive* general models of human behavior (Binford, 2001). In this research, I approach cross-cultural data from a different perspective that combines sophisticated, automated pattern-searching techniques with an external explanatory model derived from the core concepts of CAS theory. In particluar, I seek to identify attractors and repellors in the patterning of human subsistence variability within an extensive cross-cultural dataset that would indicate the presence of critical transitions in human subsistence behavior. The dataset used in this analysis is the Standard Cross Cultural Sample (SCCS, [Murdock and White, 2006]), which is a unique database of over 2000 cultural variables coded for 186 societies.

Although the SCCS data are appropriate for the problem being investigated, they are not without limitations. For example, the SCCS is numerically biased towards groups studied by ethnographers in the modern era, and thus, rather than being a true representative sample of all traditional human lifeways, it is a sample of traditional human lifeways after the effects of colonialism/imperialism. Also, because the data for each group included in the database were collected by many different people at many different times, the creators of the SCCS code most of the variables either as interval-scale data at a very coarse resolution[35], or as nominal-scale data. While there is little to be done about the former, the latter can be accounted for by converting all the SCCS variables to ordinal data types (e.g., by "binning" or conversion to a binary "presence/absence"), and choosing analysis methods appropriate for categorical data.

35 Although the resolution of these data can be considered "coarse" by ethnographic standards, their resolution is actually on-par with, or better than most archaeological data.

3.4.1. Method of Cross-Cultural Analysis

I have developed a "heuristic workflow"[36] designed to graphically identify and intuit natural divisions in the SCCS mobility and economic data by combining the result of multivariate clustering with dimensional reduction analyses. The workflow uses KNIME – a robust Free and Open Source Software (FOSS)[37] "data-mining" platform developed specifically for cluster/classification analysis (Berthold et al., 2009, 2008). KNIME's "graphical-modeling" interface allows for multiple data-mining operations to be "daisy-chained" in a save-able order (i.e., a "workflow"), which facilitates rapid data exploration.

The workflow begins with a K-medoids clustering routine. K-medoids is similar to the better-known K-means routine in that it iteratively assigns input data points to one of a predefined number of clusters based on a distance metric (in this case, Euclidean) and an iteratively defined cluster "center"; but, while k-means uses the mean of the coordinates of all input data points included in a cluster (i.e., a "centroid") as the cluster center , k-medoids uses the most centrally located of the input datapoints in the cluster (i.e., a "medoid") (Park and Jun, 2009). This is advantageous because clustering routines that rely on calculating an "average", such as k-means, cannot be used with categorical data types (Řezanková, 2009), and are also more susceptible to outliers and "noise" in the input dataset (Park and Jun, 2009; Řezanková, 2009).

The workflow continues with a Multidimensional Scaling (MDS) analysis. MDS is a dimensional reduction procedure appropriate techniques for analysis of categorical data-types that is designed to help researchers understand the structure of a multidimensional data set by scaling the variability present in that dataset to a smaller number of dimensions (in this case, two) (Borg and Groenen, 2005). The input data points are projected into the space created by the two most dominant MDS dimensions, and can be viewed as a scatter plot where the physical proximity of the projected points denotes a multidimensional affinity (i.e., the closer two points are on the MDS plot, the more similar their input variables are).

On the output plots (Figures 3.8 and 3.9), individual input cases (SCCS societies) are plotted in MDS space, but colored according to the results of a K-medoid clustering routine (clusters are highlighted by convex hulls). This provides a graphical representation of the degree of cluster separation (the amount of empty space between clusters), the tightness of the clustering itself (the physical proximity of points within each cluster), and the uniformity of each cluster (the overall size and shape of the cluster). In the output plots, the input variables (column loadings) can be considered "weighted" positively or negatively on each axis, such that their "pull" on the input cases is what creates the 2-D spatial pattering of the MDS plots. In other words, the MDS plots also

36 I specifically use the term "heuristic workflow" here in preference to "method", because this analysis is more of an experimental process than a linear step-by-step procedure.

37 As with all other software tools used in this dissertation, I have chosen to use FOSS in order to keep the procedure as transparent and as widely accessible as possible.

provide a graphical representation of the amount of influence that each of the input variables have on the creation, separation, and character of each of the identified clusters. On any of these heuristic plots, distinct clustering would indicate the presence of adaptive basins in subsistence strategies[38], a continuous distribution (e.g., linear, logistical, power, parabolic, etc.) would suggest the presence of a continua of subsistence behavior, and diffuse spatial patterning would indicate that subsistence choice follows no distinct pattern (i.e., choice of subsistence strategy is random).

3.4.2. Results of Cross-Cultural Analysis

I conducted analyses at two scales. At the largest scale, I included as many SCCS societies as possible. Because the focus of my research is on low-level subsistence systems, I *a priori* excluded all SCCS groups engaged in complex or state level systems (e.g., "Chinese", "Vietnamese") and, in order to avoid inaccuracy due to historical biases, I also exclude those SCCS societies that are based on ancient accounts (e.g., "Hebrews", "Romans"), leaving 163 remaining SCCS societies in my initial sample pool (Table 3.1). Using the workflow outlined above, I conducted a series of explorations of the variability with the SCCS data in which I varied the included SCCS variables to better understand which ones are most important for showing and explaining variability in subsistence systems between groups. I began with all SCCS variables related to subsistence, settlement, and population. All continuous variables (e.g., the percentage of reliance on agricultural products) were first "binned" into ordinal categories, and during the course of the exploratory analysis some of the originally nominal-scale variables were converted into a series of dichotomous ordinal categories (e.g., the nominal-scale variable "major crop type" was converted to the following binary "presence/absence" categories: "cereals", "roots/tubers", "tree fruit")[39]. I eventually determined a set of core subsistence, mobility, and social organization to be used in this macro-scale analysis, which are reported in Table 3.2 in italics.

Using this set of core input variables, an analysis of all the remaining SCCS societies showed a very pronounced spatial separation of a 3-cluster K-Medoids result in MDS space (Figure 3.8)[40]. The wide spacing in MDS space between the three K-Medoids clusters, and their relatively tight internal configuration, indicates the presence of three discrete subsistence systems, with little or no overlap between them. Investigation of the K-Medoids "loadings" (i.e., the multidimensional characteristics of the medoids) makes it clear that these

38 I am using the term "adaptive basin" in the sense of Scheffer's (2009:98) idea of "basins of attraction". See in particular his Figure 6.3 (Scheffer, 2009:100) for how these basins would appear on a 2-D plot (like the MDS and CA plots produced in this analysis).

39 See Table 3.2 for a complete list of all data transformations.

40 See Table 3.1 for the membership of each cluster ("pastoralists", "agriculturalists", and "hunter-gatherers").

clusters relate to the subsistence systems of "agriculture", "pastoralism", and "hunting/gathering". It appears that, at the macro-level, human subsistence systems adhere to the pattern expected of discrete adaptive basins, centered around attractors and separated by repellors. It is also likely, then, that any transition between these three basins would occur as a critical transition.

A closer look at the spatial pattering of the macro-scale MDS plot suggests that there is some internal variability in these large-scale clusters, that may relate to finer-scale attractors. I therefore repeated the analysis for a small subset of SCCS societies, using some additional, more detailed input variables in hopes of further illuminating these small-scale patterns. To keep the analysis focused, I first removed all groups identified as "hunter-gatherers" in the macro-scale analysis (see Table 3.1)[41], and further exploration led me to also remove tropical farming groups[42]. The remaining groups are identified in Table 3.3, separated according to the results of a 6-cluster K-Medoids solution. Looking at the MDS plot for this smaller-scale analysis, several interesting patterns are apparent. First, pastoralism and agriculture remain large-scale adaptive basins, distinct from one another. Secondly, there appears to be three internal adaptive basins within agriculture, and three adaptive basins within pastoralism. Looking at the Medoid loadings for each of the six identified clusters, it is clear that the three smaller scale agricultural adaptive basins center around 1) high sedentism and intensive agriculture with low reliance on pastoral products (Medoid: Uttar Pradesh), 2) semi-sedentary extensive agriculture with a high reliance on hunting wild game (Medoid: Lakher), and 3) small-scale "agropastoralists" who emphasize the agricultural component above the pastoral (Medoid: Amhara) (Table 3.3)[43]. The small-scale pastoral adaptive basins seem to relate to 1) full-time fairly nomadic pastoralists (Medoid: Pastoral Fulani), 2) very nomadic pastoralist-hunters (Medoid: Chuckchee), and 3) "specialized" pastoralists who are very mobile, but still very reliant on agricultural products brought in by trade/raid (Medoid: Teda)[44]. Some interesting things are of note when the two scales of analysis are

41 Several interesting sub-clusters exist within the main "hunter-gatherer" cluster, but these results are outside the scope of the current research, and will not be presented here.

42 This is justified by the focus of this paper on Mediterranean (an temperate) environments. Removal of these tropical groups simply made the resultant MDS plot easier to see/interpret, but did not largely affect the spatial patterning of the groups that remained. These groups likely represent a specialized tropical agriculture adaptive basin that shares attributes of the other agricultural basins identified in this analysis, but which is distinct in that it can only be practiced in humid tropical areas. Interestingly, the removed groups were all dependent on pig-raising or wild game, and focused on tree or root crops almost exclusively.

43 It should be noted that 105 of the 163 input societies (the vast majority, see Table 3.1) were classified as agriculturalists by the initial clustering routine, so there is significantly more data-points to help define internal variation than in the pastoral or hunter-gatherer clusters.

44 Such "economic specialist" pastoralists were also identified by Johnson (2002) in a less sophisticated multidimensional analysis of pastoral groups. In her analysis, Johnson finds three "types" of pastoralism: "agropastoralists", "subsistence pastoralists", and "economic specialists". Johnson defines "agropastoralists" as households that engage in a "broad mix of subsistence strategies", including pastoralism and agriculture; "subsistence pastoralists" as

compared: 1) the Abkhaz are lumped with the pastoral macro-cluster in the large-scale analysis, but are placed in the "agropastoral" micro-cluster in the small-scale analysis, albeit well out from the agropastoral cluster center in the direction of the general pastoral basin of attraction, and 2) the Teda and Tuareg (i.e., the "specialized" pastoralism micro-cluster) and the Abkhaz (discussed in point 1, above) occupy a tenuous space in the small-scale MDS, which is somewhere between the main pastoral and agricultural basins of attraction. Looking at the multidimensional signatures of these groups, they are unique from all other groups in that they all seem to have a relatively even reliance (i.e., close to 50/50) on both agricultural and pastoral products. In fact, the Teda/Tuareg mainly differ from the Abkhaz in overall mobility and in community size. I would suggest that these three societies are engaging in subsistence strategies that are at high risk for critical transition, and that given a little perturbance (for example, disruption of the trade network that brings agricultural products to the Tuareg), they would "fall" into one or the other of the major agricultural or pastoral basins. Further, based on the way the small-scale analysis classifies these societies, all else being equal, I would predict the Tuareg/Teda to fall towards the pastoral macro-basin if perturbed, and the Abkhaz to fall towards the agriculture macro-basin if perturbed.

3.4.3. Conclusions of Cross-Cultural Analysis

This analysis suggests that discrete subsistence strategies *do* exist in human subsistence behaviors, meeting the expectations of CAS for the existence of multiple stable states centered around attractors and separated by repellors, and validating the idea that a series of discrete subsistence behaviors should be modeled (rather than a continuum). Furthermore, there are at least two scales at which such adaptive basins exist, aligning with the idea of Panarchy, and suggesting that panarchical relationships may exist across multiple scales and types of SES. At the macro-scale, societies focusing on hunting and gathering are distinctly separated from those engaged in herding or agriculture, and these latter two are also separate from each other. At the finer scale, there are adaptive milieus related to specific types of agriculture and herding (and also likely for different types of hunting/gathering too). Each of these identified clusters is defined by a unique suite of subsistence behaviors, which vary only within a small range of options. While individual behaviors might be present in more than one cluster, the total combination of behaviors that define a cluster are unique and do

---

households who focus on the husbandry of small stock almost to the complete exclusion of agriculture; and "economic specialists" as pastoralists who raise stock mainly for trade. These categories may loosely overlap with those I've identified here, but it is important to note that only 17 of the 163 input societies were classified as pastoralists by the initial cluster separation (see Table 3.1). This is likely too small a sub-sample of pastoral groups to show all the variability in this adaptive basin. I have begun expanding the original database with ethnographic data from additional pastoral groups, and it is probable that this additional data will help to define some internal variation in future analyses.

not overlap. In other words, although each individual basin encompasses a zone of variability *within* each subsistence strategy, there is no "continuum" of subsistence variability *between* each strategy. The attributes of the particular resource-type that a society focuses on limits the variability of its subsistence endeavors to a particular sphere of behavioral choices. These spheres appear to act as "attractors" (*sensu* Scheffer [2009]), drawing in and holding groups within them, and a major change in the system state is necessary for a group to escape from its current sphere. Such change can come from many sources: external influence, technological advancement, social change, evolutionary change, environmental change, climate change, or any combination of these. "Escaped" groups cannot exist in the space between spheres for very long, however, as these "in between" spaces constitute zones of highly unstable behavioral suites, which act as "repellors". Thus, groups that exit a particular basin of attraction due to perturbation will tend to be very quickly pulled back into one of the "attractors" in a classic "critical transition". Finally, the spatial distribution of the individual societies within the basins of attraction (the clusters) in MDS space suggests some additional relationships under CAS theory. Those societies that plot near the edges of a basin of attraction (e.g., the Tuareg, Teda, and Abkhaz) could be considered at-risk for a critical transition, and should thus display all the characteristics of at-risk systems discussed in Section 3.3.3, above (e.g., high levels of connectedness, low amounts of resilience, high amounts of sub-system homogeneity, etc.). Conversely, those societies that plot near the center of a basin (e.g., the various "Medoid" societies) might be expected to be highly resilient systems with all the correlates of such systems (e.g., subsystem heterogeneity, low connectedness, etc.)[45].

3.5. A Complex Adaptive Systems Hypothesis for the PPN-LN Transition

How can the concepts discussed in this chapter be applied to the PPN-LN transition? There are a variety of test implications and expectations that can be derived from CAS theory, but it is more useful to first create a sketch of Neolithic farming communities as components of panarchical regional SES. This sketch will help to narrow down the particular test implications that are relevant to understanding the nature and causes of major transformational events such as the PPN-LN transition. Furthermore, the narrative will also help us better understand the scale complexity of the issue, and which will inform our choice of analytical techniques for a more quantitative analysis of the PPN-LN transition.

3.5.1 A Narrative Model of PPN Regional Social-Ecological Systems

Theoretically, the finest meaningful panarchical scale of the Neolithic SES (or any SES for that matter) is logically that of individual agents (which would

45 This final idea requires additional testing before any strict conclusions about its validity can be made, but that is outside the scope of the current project.

include individual humans, animals, and plants). However, considering the resolution of archaeological data in general, and the information known about PPN socio-economic organization in specific (see Chapter 2), it is most intuitive or useful to envision a multi-tiered panarchy with the smallest meaningful scale being individual households and landscape patches. Each household is connected to a finite number of landscape patches, which are chosen according to a variety of preferences and needs related to subsistence tasks, and which have their own unique and dynamic properties. Thus, the household and its landholdings can be seen as a small-scale autonomous "regional" SES in its own right, with a definable regional footprint (i.e., a "catchment'), and an observable adaptive "cycle width". The exact cycle width and spatial scale at which each household operates will be determined by the size of each household (number of people), the basic needs of each person (e.g., per capita food requirements), the social and economic structure of the household (e.g., the subsistence system), and the state of the local environment (e.g., localized abundance or depletion of critical resources). Thus, similarly-sized households engaged in similar socio-economic practices would cycle through the four phases of the adaptive cycle at similar paces, and act within similar spatial scales.

Each household is panarchically subsumed under the larger adaptive phenomenon of the "village" to which it belongs (and where its inhabitants physically reside). The combined land-use of all households in the village defines the spatial scale at which the village operates and interacts with the landscape (i.e., the village's catchment). The village cycles through the phases of its own adaptive cycle, which has a longer cycle width than any of the individual households[46]. Thus, the cycle width and spatial scale of the village is in part determined by the sum of all the system-states of its households, but the village can also be thought of as an autonomous regional SES in that the fate of the village is independent from any particular household (i.e., the total is greater than the sum of the parts).

Finally, it is possible to envision another, larger, scale of this panarchy, where multiple villages are connected into a regional network (e.g., tied by trade, pooled labor, marriage, ritual). This regional network is another autonomous SES, moving at an even slower cycle width, and operating on an even larger scale, and is composed of all the villages of the network and their catchments. Again, the cycle-width and spatial scale of this largest-scale of the Neolithic panarchy is in part determined by the sum of its constituent villages, but it is independent of the fate of any one village.

46 The exact ratio of a village's cycle width to that of its constituent households is likely to be quire variable under different socio-economic and socio-ecological conditions. Understanding how this ratio changes under different conditions will be the focus of future research.

3.5.2 Gradual and Critical Transitions in PPN Regional Social-Ecological Systems

What are the panarchical relationships that exist within this sketched Neolithic panarchy, and how do they relate to the overall vulnerability of the Neolithic SES to critical transition[47]? It is useful to begin by examining the timing of adaptive cycling in the different levels of the Neolithic panarchy. Starting at the household level, in a highly unconnected, resilient SES, there would be no uniformity of adaptive "cycle width" between households, and households would not be synchronized in any particular adaptive phase (r, κ, Ω, or α). Thus, as long as the resilience of the sketched PPN SES remains high, the life-cycle of households would remain unsynchronized, and the success or failure of any one household would have little effect on the others, or on the village as a whole. Other correlates of high resilience will be heterogeneity in household form (e.g., population size, house forms) and subsistence practices, and that households will not rely on each other for basic subsistence tasks or goods[48] (i.e., connectedness between households will be low). In this loosely connected village, the disrupt force of "revolt" from each autonomous household prevents the village from coalescing into a static identity, and it remains a flexible, highly adaptive SES. If the resilience of the PPN SES decreases, however, the conservative force of "remember" from the village will begin to act as sort of "virtual syncing mechanism", holding and extending the κ phase of each household's cycle so that they appear to remain in phase with each other over the short-term (i.e., increasing overall synchronization in the panarchy). Here, "remember" may be a purely social force (e.g., an inherited set of beliefs about the "right" way to live), or may be a socio-natural force (e.g., an inherited state of environmental productivity, inherited resource surplus, inherited livelihood options, etc.[49]). In any case, one of the main ways that this conservative force is operationalized is by reducing the number of choices available to households, thereby increasing subsystem homogeneity (e.g., less variety in household form and subsistence practices), and increasing connectedness (e.g., households will begin to *rely* on pooled labor or sharing). The force of "remember" from the village will increase if the village itself is in a κ phase of its own adaptive cycle.

It is easy to see how similar interactions could occur between the village and the regional village network. In a resilient village network, villages will be largely independent, and will not rely heavily on inter-village trade or regional labor pools. Villages will maintain relatively independent identities, perhaps reflected in local variation of artifact and building styles, ritual or mortuary practices, and economic practices. Each village will have its own life-cycle width,

47 Although I focus on the relationship between households in villages in this discussion, the relationship between villages and the regional network is analogous.

48 It is important to note that this does not imply that pooled labor or sharing will not exist. It only implies that households will not need to rely on these things for basic survival.

49 This is equivalent to the idea of "ecological inheritance" used in Niche Construction Theory (Day et al., 2003; Laland et al., 2001, 1999; Odling-Smee et al., 2003).

and the villages will not be in phase with each other as they proceed through the adaptive cycle. This loosely connected regional network remains highly adaptable, and the autonomy of each village prevents the regional network from solidifying into an overarching political framework (i.e., through the disruptive force of "revolt" from each of the villages). However, if village autonomy decreases, and the villages come to rely on each other in a more tightly connected system of trade or labor pooling, then the force of "remember" from the regional system can begin to act to align and synchronize them. Further, the strength of "remember" will increase if multiple tiers of the panarchy are aligned; if the regional network of villages is in a κ phase, and a village is itself in a κ phase, then the strength of "remember" acting upon an individual household in that village will be even stronger.

How might the balance of these panarchical interactions change over time? The simplest and most basic way – and one that is common to all complex systems – is through the effects of stochasticity in the system. That is, there is always a chance that cycle-widths between and among the various scales of adaptive phenomena in the Neolithic SES may align simply due to random chance, and so the balance of "revolt" and a "remember" might shift due to this chance occurrence. In any case of stochastically-induced change, there would be a fairly rapid and unpredictable increase in system connectedness, coupled with a decrease in resilience, but without an accompanying increase in system potential.

Another way to change the panarchical balance of the SES is through the interference of an external event. This event may be climate or environmental change, an influx of migrants, a social conflict or any other type of external interference. The event would simultaneously affect all households to a similar degree, which might work to restart the "adaptive clock" at the same time for all of them, resulting in a very synchronized panarchy. The event need not be drastic or even extremely rapid to have this effect[50], and there may even be significant lag-time between the onset of the event and its consequences. Thus, in cases of external influence, there would be a fairly rapid transition to a more connected, less-resilient system following shortly after evidence of an external intrusion, and there need not be an accompanying increase in system potential.

However, the most likely way to achieve a shift in the balance of "revolt" and "remember" over time stems from the self-organizing nature of the system itself. In this scenario, the effect of history within the system acts to increasingly limit the subsistence choices available to households so that it becomes more and more probable that households will be doing the same types of things, at the same scales, and at the same time[51]. What historical factors would act to limit choice? The scope of possible subsistence choices in an SES is largely determined by the combination of social/cultural, technological, and ecological characteristics of the

50 In fact, if the event is too rapid or drastic, it might instead instigate a critical transition in the system (see below).

51 This aligns with the concept of "Path Dependence" as originally outlaid by David (2007, 2001, 1993, 1988).

SES. Some of these are relatively constant factors (e.g., the amount of labor a person can exert, the amount of food needed for good nutrition, the dietary requirements of herd animals), some of are dynamic and change over time (birth and death rates, climate, soil fertility and depth, cereal yields, fodder availability), and some could be variably constant or dynamic (e.g., factors that largely depend on human agency, such as cultural proscriptions on certain behaviors, systems of land tenure, ideas about work-ethic, ideas about sharing or wasting, etc.). The interplay between the dynamic and static variables—especially the interplay between ecological and social factors—can work to limit decision possibilities over time. For example, a newly-founded Neolithic SES in a pristine environment would likely have more choices available for the location of subsistence activities than one existing in an environment that has been used for a number of years and so has fewer "good" locations for subsistence due to depletions of soil fertility, erosion of topsoils, and reductions to fodder availability that have accrued over time. Thus, any human-caused environmental "degradation" need not be severe to have an effect on the resiliency of the system. Choices would be limited further if social or cultural conditions also were such that specific activities were not allowed or were socially unfeasible. In any case affected by such historical contingency, there would be a gradual increase in system connectedness over time, coupled with a general decrease in resilience and an increase in system potential.

The previous examples have shown how a regional SES might change over time – both gradually and more rapidly – but how might a critical transition in such a panarchy be entered into or avoided? First, it is important to realize that critical transitions can happen at any time, at any scale, and to any individual component of the panarchy, but in a highly resilient system, they do so *without* affecting or being influenced by other components of the panarchy. Conversely, a vulnerable system is so connected that a critical transition in any of the system's subcomponents may cascade throughout the system.

It is this idea—synchronized critical transition occurring at a regional level—that is of most interest for our CAS approach to understanding the PPN-LN transition. How might this occur? Remembering that the disruptive force of "revolt" from lower scales of the panarchy affects the stability of the entire panarchy, we can imagine that as synchronization of the adaptive cycles of households increases, the disruptive force of "revolt" on the village—enacted as a household enters into a less-stable phase of its adaptive cycle (Ω, but to a lesser degree also α or r)—increases. If a sufficient number of households enter into an unstable phase in relatively rapid succession (which is more likely if household cycles are synchronized and connected), the concurrent disruptive force of all these "revolts" could be large enough to pull the village into an unstable state of of its own (i.e., into an Ω phase). If other levels of the panarchy are also synchronized and highly connected, then this type of event could result in a "cascade" of rapid instability throughout the panarchy, both downwards from the village to other previously unaffected households, but also upwards to larger-scale

adaptive phenomena in the panarchy such as the regional trade network (and perhaps even beyond). It is thus possible to imagine a lengthy period of apparent synchronization and stability within our fictive panarchy, but where system resilience is greatly reduced, and so the panarchy is at high risk for a critical transition (i.e., we would see the patterns in Figures 3.6b and 3.7b, e, f, and h).

On the other hand, a highly synchronized system is also more vulnerable to outside disturbance. Thus, even if internal "revolts" fail to happen, a system that has become overly-connected and less resilient may be more easily "pushed" into a critical transition by an external event. If that event is very rapid and intense (e.g., rapid climate change, an invading army, an influx of refugees, etc.), then the chances that the system will cascade into a critical transition are increased.

What about resilient systems? If households remain unsynchronized (and thus less connected and more heterogeneous), then the disruptive force of any individual "revolts" are spread over a larger period of time, and can be absorbed at the village level. In this case, individual households and villages in the regional network can succeed or fail independently depending upon the conditions of each subcomponent as an autonomous SES, and the risk of failure at the village level is not increased if some of its households have failed (i.e., because individual system components are not highly connected). If conditions are such that failures of subcomponents (e.g., households) begin to occur at an increased rate, the staggered timing of these failures means that the potential of the entire system simply reduces with each failure (i.e., we would see the patterns in Figures 3.6a and 3.7a, c, d, and g). Resilient systems are more resistant to external pressures as well. Each component of a loosely connected resilient system is free to adapt to new conditions in its own way, so there is less chance that even a relatively drastic external event would trigger simultaneous failure of all system components. Thus, a highly synchronized, tightly interconnected panarchical regional SES is at much higher risk for a large-scale critical transition than a non-synchronized, loosely connected panarchical regional SES.

3.6. Chapter Summary

So, what has this narrative model achieved? Firstly, it shows how CAS and RT theory can update, consolidate, and reformulate the existing ideas about the instigating factors for the PPN-LN transition – re-framing it as a critical transition. The model shows how stochasticity, external events, and internal historical contingency can act – together or separately – to change the balance of "revolt" and "remember" in the regional SES, leading to a less resilient, more connected system that was at risk for critical transition. That transition could have been instigated by the internal socio-natural dynamics of the PPN SES itself, through a series of simultaneous "revolts" that resulted in cascading failure of the entire system[52]. The model also shows how an external event could have "pushed"

52 This scenario essentially subsumes the "human-induced environmental catastrophe", "social breakdown", and "settlement reorganization" hypotheses.

a relatively stable PPN SES into a critical transition that might not have otherwise occurred[53]. These two ideas are not mutually exclusive, as an external event could have pushed an already-unstable PPN SES into a critical transition that was likely to happen anyway. It should be noted that the magnitude of the external event in this third possibility could be much smaller than that needed in the second. Finally, the model also shows how the PPN-LN transition may not have been a critical transition at all, but instead could have been the response of a resilient system to internal or external pressures that resulted in a relatively rapid decrease in system potential and connectedness over several decades (but in a way that was *not* a critical transition).

Which of these scenarios is most plausible for the PPN-LN transition in northern Jordan? The review of the archaeological record of the region in Chapter 2 and of the specific pieces of evidence supporting and controverting existing hypotheses in Section 3.2 (above) have provided only tantalizing snippets of evidence. The fragmented archaeological record is sufficient for a general reconstruction of possible Neolithic lifeways, but has yet proven generally insufficient as a detailed source of information about past land-use dynamics, system resilience, synchronization, and homogeneity, or the exactitudes of regional chronologies and their connections with climate change events. Those snippets of evidence that do exist[54] can be construed to support the idea that the resilience and scope of subsistence choices within the PPNB system were reducing over time, while its homogeneity, connectedness, and potential were increasing, but it is very difficult to understand how these characteristics pattern over time and space. The dynamics of ancient SES are not preserved, and so not only is it unclear exactly how vulnerable the PPN SES was to a critical transition by the end of the PPNB/C, we are also lacking an understanding of the processes and interactions that could have led to vulnerability or to resilience—to continuing long-term success or to a catastrophic failure and reorganization. The best method to use to facilitate and understanding of these issues is simulation modeling, which is the focus of the next chapter.

53 This scenario essentially subsumes the "epidemiological" and the "climate forcing" hypotheses.

54 For example, the increased reliance on domesticates (and reduced use of wild resources), the technological effort spent increasing efficiency of harvest, and the increased standardization of tools suggests that system potential and homogeneity were increasing, but also indicates a restriction of subsistence choice, and therefore a reduction in overall system resilience. Also, the reduced variability of house forms, the infilling of open space in villages, the potential existence of community-bonding ritual activities suggest increased connectedness (although the proliferation of private storage facilities is somewhat contradictory to this).

Table 3.1. Table of SCCS societies used in the macro-scale analysis, organized by K-medoids cluster results.

#	Society Name	#	Society Name	#	Society Name	#	Society Name
Pastoralists		28	Azande	101	Pentecost	*Hunter-Gatherers*	
1	Nama Hottentot	29	Fur (Darfur)	102	MbauFijians	9	Hadza
25	Pastoral Fulani	30	Otoro Nuba	103	Ajie	13	Mbuti
34	Masai	31	Shilluk	104	Maori	77	Semang
36	Somali	32	Mao	105	Marquesans	80	Vedda
38	Bogo	33	Kaffa (Kafa)	106	Western Samoans	90	Tiwi
40	Teda	35	Konso	107	Gilbertese	91	Aranda
41	Tuareg	37	Amhara	108	Marshallese	96	Manus
46	Rwala Bedouin	39	Kenuzi Nubians	109	Trukese	118	Ainu
52	Lapps	42	Riffians	110	Yapese	119	Gilyak
53	Yurak Samoyed	47	Turks	111	Palauans	120	Yukaghir
55	Abkhaz	48	Gheg Albanians	112	Ifugao	122	Ingalik
58	Basseri	56	Armenians	113	Atayal	124	Copper Eskimo
61	Toda	57	Kurd	141	Hidatsa	125	Montagnais
65	Kazak	59	Punjabi (West)	142	Pawnee	126	Micmac
66	Khalka Mongols	60	Gond	143	Omaha	127	Saulteaux
121	Chukchee	62	Santal	144	Huron	128	Slave
159	Goajiro	63	Uttar Pradesh	145	Creek	129	Kaska
		64	Burusho	146	Natchez	130	Eyak
Agriculturalists		67	Lolo	149	Zuni	131	Haida
3	Thonga	68	Lepcha	150	Havasupai	132	Bellacoola
4	Lozi	69	Garo	151	Papago	133	Twana
5	Mbundu	70	Lakher	152	Huichol	134	Yurok
6	Suku	72	Lamet	154	Popoluca	136	Yokuts (Lake)
7	Bemba	74	Rhade	155	Quiche	137	Paiute (North.)
8	Nyakyusa	75	Khmer	156	Miskito	138	Klamath
10	Luguru	78	Nicobarese	157	Bribri	139	Kutenai
11	Kikuyu	81	Tanala	158	Cuna (Tule)	140	Gros Ventre
12	Ganda	82	Negri Sembilan	160	Haitians	147	Comanche
14	Nkundo Mongo	83	Javanese	161	Callinago	148	Chiricahua
15	Banen	84	Balinese	163	Yanomamo	162	Warrau
16	Tiv	85	Iban	165	Saramacca	164	Carib (Barama)
17	Ibo	87	Toradja	166	Mundurucu	174	Nambicuara
18	Fon	88	Tobelorese	167	Cubeo (Tucano)	178	Botocudo
19	Ashanti	89	Alorese	168	Cayapa	179	Shavante
20	Mende	92	Orokaiva	169	Jivaro	180	Aweikoma
21	Wolof	93	Kimam	170	Amahuaca	182	Lengua
22	Bambara	94	Kapauku	172	Aymara	183	Abipon

23	Tallensi	95	Kwoma	176	Timbira	185	Tehuelche
24	Songhai	97	NewIreland	177	Tupinamba	186	Yahgan
26	Hausa	98	Trobrianders	181	Cayua		
27	Massa (Masa)	99	Siuai	184	Mapuche		

Table 3.2. Table of SCCS variables included in the analyses, with data transformations listed. Variables not in italics were used for the macro-scale clustering analysis of the groups in Table 3.1. Variables in italics were added for the smaller-scale clustering analysis of those groups in Table 3.3.

Data Type	**SCCS Attribute**
Ordinal	Agricultural contribution
Ordinal	Agricultural dependence
Binary	*No agriculture*
Binary	*Casual agriculture*
Binary	*Horticulture*
Binary	*Extensive agriculture*
Binary	*Intensive agriculture*
Binary	*Irrigated intensive agriculture*
Binary	*No major crop*
Binary	*Cereals major crop*
Binary	*Roots or tubers major crop*
Binary	*Tree fruit major crop*
Ordinal	Pastoral contribution
Ordinal	Pastoral dependence
Binary	*Milking*
Binary	*Bovine herding*
Binary	*Ovicaprid herding*
Binary	*Equid herding*
Binary	*Pig raising*
Binary	*Deer herding*
Binary	*Camelid herding*
Binary	*No large domestics*
Ordinal	*Fish contribution*
Ordinal	*Fishing dependence*
Binary	*True Fish*
Binary	*Shellfish*
Binary	*Two or more fished*
Binary	*No storage*
Binary	*Individual storage*
Binary	*Communal storage*
Binary	*Economic agent controls storage*
Binary	*Political agent controls storage*

Data Type	**SCCS Attribute**
Ordinal	Hunting contribution
Ordinal	Hunting dependence
Binary	*Large game hunted*
Binary	*Small mammals hunted*
Binary	*Birds hunted*
Binary	*Two plus hunted*
Ordinal	Gathering contribution
Ordinal	Gathering dependence
Binary	*Animal products gathered*
Binary	*Fruit seeds nuts berries gathered*
Binary	*Herbs leaves blossoms gathered*
Binary	*Roots or tubers gathered*
Binary	*Tree pith gathered*
Binary	*Two plus gathered*
Ordinal	Amount traded as food source
Binary	*Food surplus*
Binary	*Year round food supply*
Binary	*Annual variation in food supply*
Binary	*Seasonal variation in food supply*
Binary	*Daily variation in food supply*
Binary	*Imported food supply*
Binary	Migratory settlements
Binary	Periodically moved settlements
Binary	Seminomadic then migratory
Binary	Semisedentary and some migratory
Binary	Rotate between two plus settlements
Binary	Permanent settlements
Binary	Compact permanent settlements
Binary	Compact impermanent settlements
Binary	Semisedentary
Binary	Seminomadic
Binary	Nomadic
Binary	Separated hamlets

Binary	Community size	Binary	Complex settlements
Binary	Population density	Binary	Neighborhoods of homesteads

Table 3.3. Table of selected agricultural or pastoral SCCS societies used in the smaller-scale analysis, organized by K-Medoids cluster result.

#	Society Name	#	Society Name	#	Society Name
Intensive Agriculturalists		30	Otoro Nuba	72	Lamet
17	Ibo	31	Shilluk	81	Tanala
35	Konso	32	Mao	87	Toradja
56	Armenians	37	Amhara	141	Hidatsa
63	Uttar Pradesh	42	Riffians	142	Pawnee
69	Garo	47	Turks	143	Omaha
74	Rhade	48	Gheg Albanians	149	Zuni
82	Negri Sembilan	57	Kurd	152	Huichol
83	Javanese	59	Punjabi (West)		
155	Quiche	60	Gond	*Hunter-Pastoralists*	
160	Haitians	62	Santal	1	Nama Hottentot
		68	Lepcha	52	Lapps
Agropastoralists		75	Khmer	53	Yurak Samoyed
55	Abkhaz	84	Balinese	121	Chukchee
16	Tiv	184	Mapuche		
18	Fon			*Pastoralists*	
172	Aymara	*Extensive Agriculturalist-Hunters*		25	Pastoral Fulani
12	Ganda	6	Suku	34	Masai
3	Thonga	14	Nkundo Mongo	36	Somali
4	Lozi	15	Banen	38	Bogo
10	Luguru	19	Ashanti	46	Rwala Bedouin
11	Kikuyu	156	Miskito	58	Basseri
20	Mende	8	Nyakyusa	61	Toda
21	Wolof	39	Kenuzi Nubians	65	Kazak
22	Bambara	5	Mbundu	66	Khalka Mongols
23	Tallensi	7	Bemba	159	Goajiro
24	Songhai	33	Kaffa (Kafa)	*Transitional (Specialist?)*	
26	Hausa	64	Burusho	*Pastoralists*	
27	Massa (Masa)	67	Lolo	40	Teda
29	Fur (Darfur)	70	Lakher	41	Tuareg

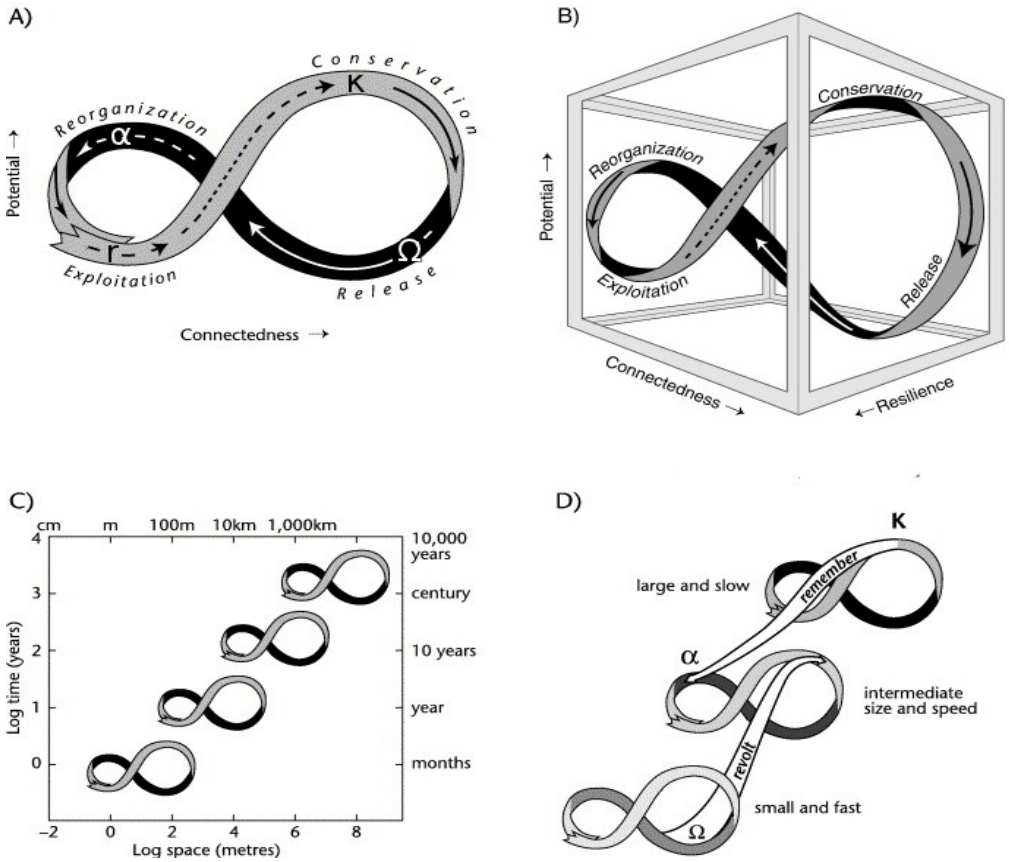

Fig. 3.1. A) 2-D representation of the adaptive cycle showing the four phases of Eploitation, Conservation, Release, and Reorganization. B) A 3-D representation of the adaptive cycle showing the relationship between potential, connectedness, and reslilience during the different phases of the cycle. C) An illustration showing how differnt adaptive cycles can exist at different scales. D) An illustration of the concept "Panarchy" showing the connection (Remember, Revolt) between different scales of adaptive systems. This figure is a composite of illustrations from Slaymaker (2006, 2007), used by permission from Elsevier press, and exemplifying concepts originally published by Gunderson and Holling (2001).

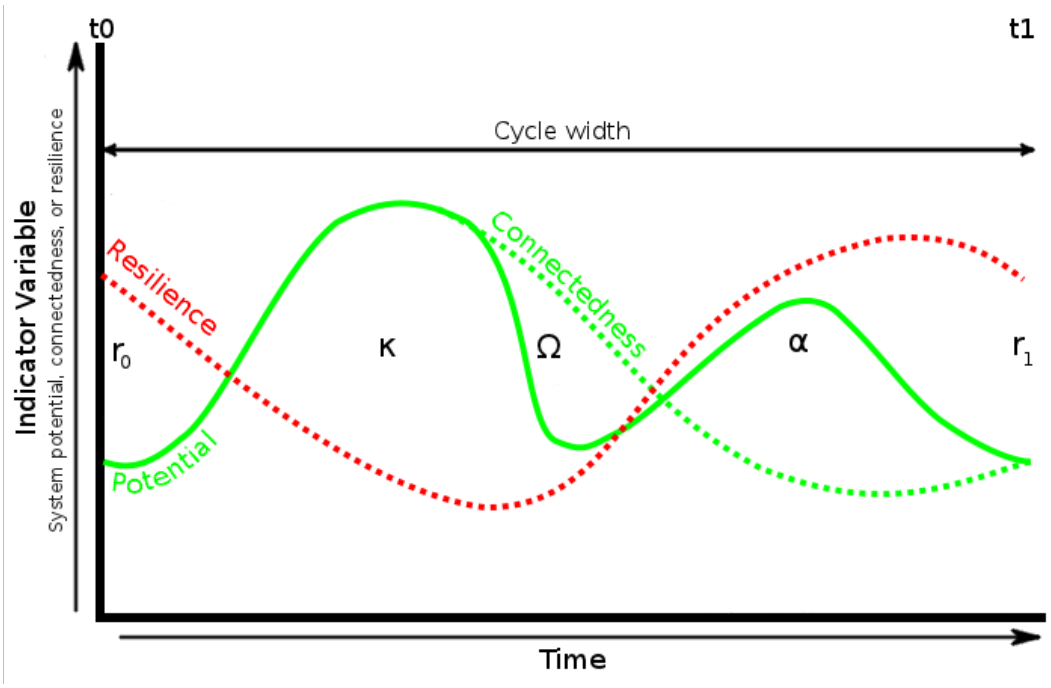

Fig. 3.2. The adaptive cycle plotted as a time series graph. The x-axis is time, and the y-axis is an indicator variable for system potential, connectedness, or resilience. The solid green line shows the expected pattern for system potential, the dashed green line shows the expected pattern for system connectedness over time, the dashed red line shows the expected pattern for resilience over time.

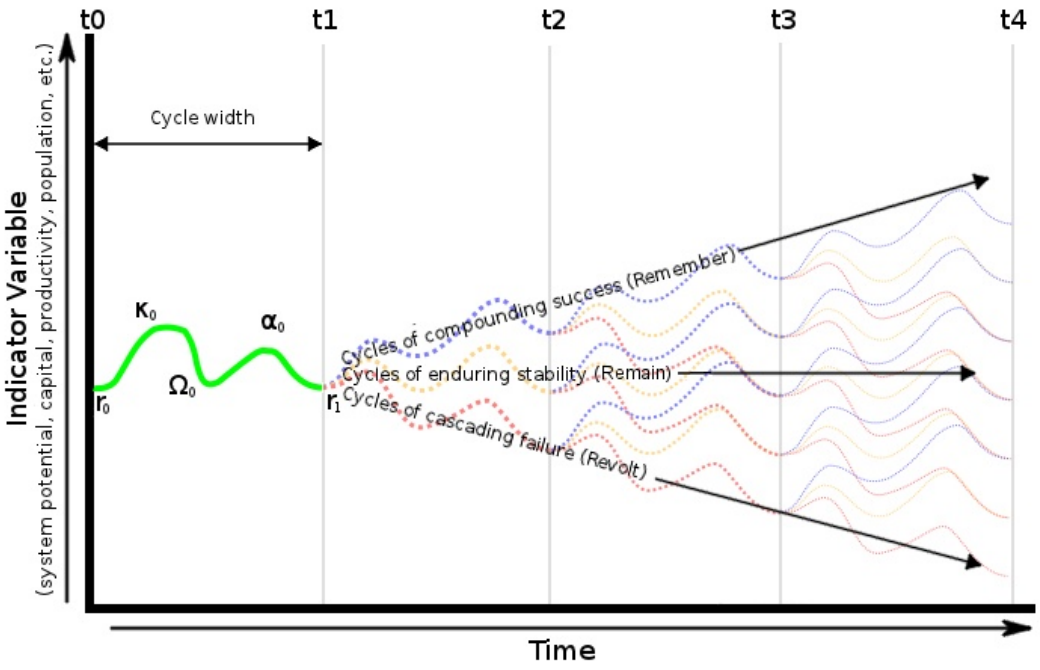

Fig. 3.3. Diagram of potential trajectories of an adaptive system over time. At any time *t*, a new cycle begins. Arrows indicate steady-state trajectories for continual Remember, Revolt, or Remain, but note that multiple pathways (combinations of Remember, Revolt, or Remain between any time *t*) could have been taken to achieve any of the potential system states at time *t4*.

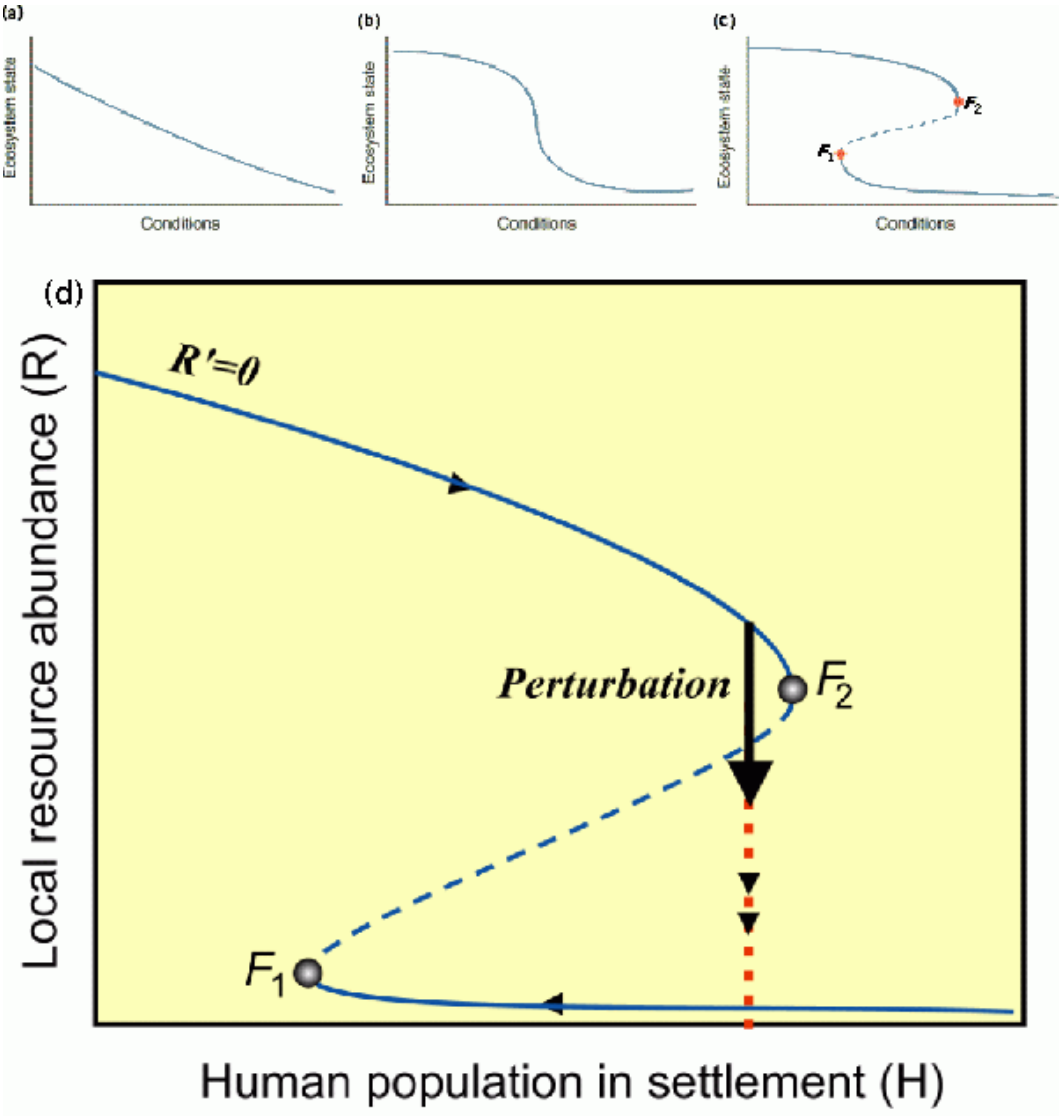

Fig. 3.4. Diagram of different types of system state change. The line in (a) represents linear steady-state change over time. The line in (b) represents a more complex pattern of change, where change occurs more rapidly under certain ranges of conditions. The line in (c) represents a system with a "critical transition", and (d) shows an example of this type of transition in an SES. Modified from Scheffer and Carpenter (2003) and Jensen and Scheffer (2004) with permission.

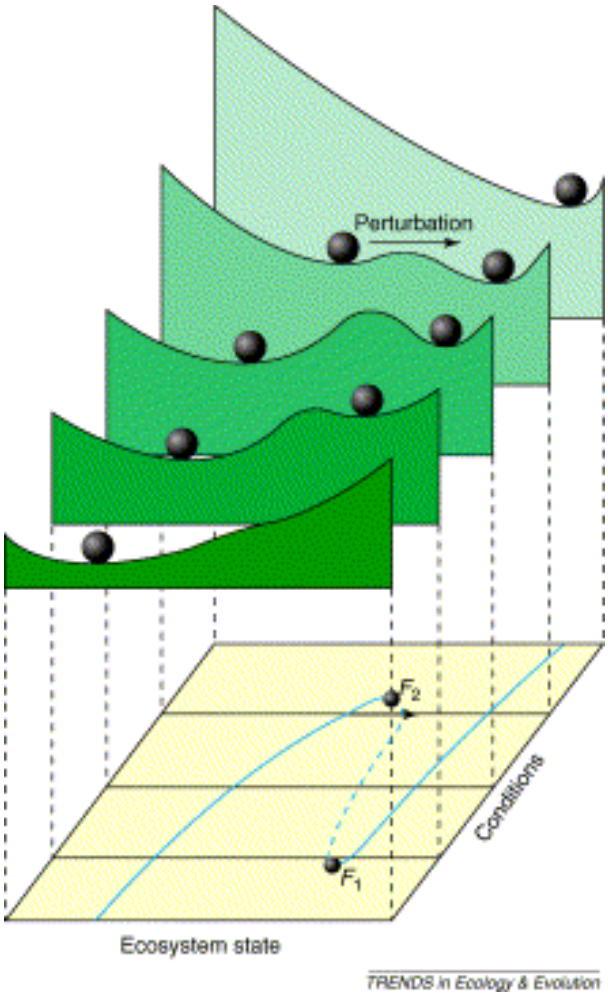

Fig. 3.5. A time series of "stability" landscapes crossing over a critical transition point. Note that initially there is only one attractor (stable state), but as the system is stressed, another attractor develops. When the system is stressed past the critical threshold (F2), it is pulled to the second attractor, and a new stable state is achieved. The depth of the “basin of attraction” indicates amount of system resilience. Reproduced from Scheffer and Carpenter (2003) with permission.

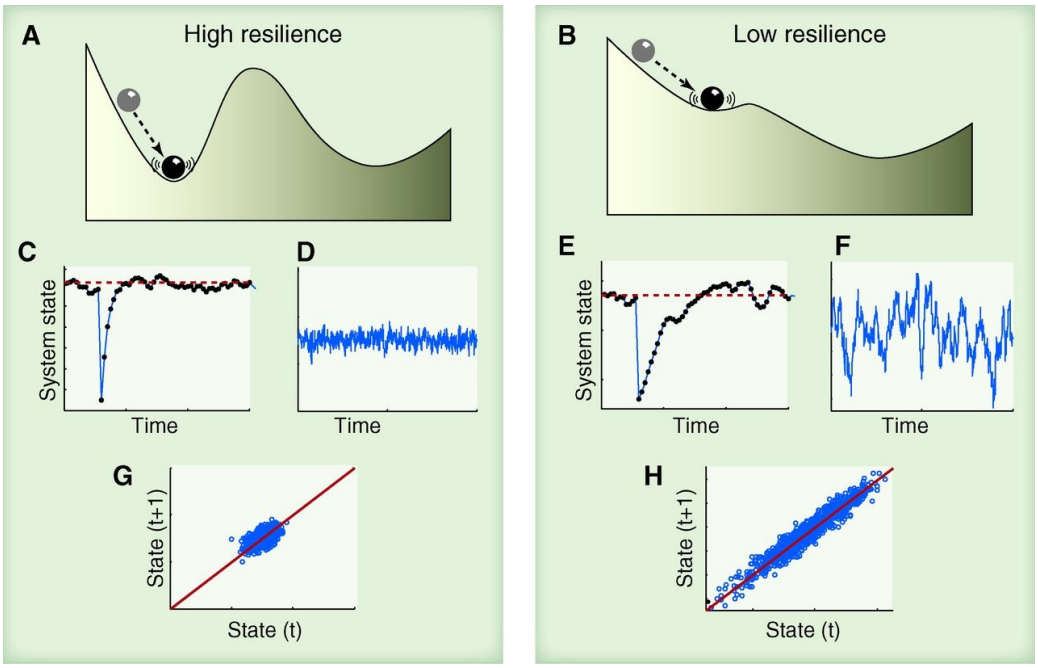

Fig. 3.6. Heuristic graphs showing the time-series indicators for a "stable" system (a) and for a system that is approaching a critical transition (b). The unstable system is characterized by a loss of resilience ("shallowing" of the basin of attraction), which is visible in the time-series graph as a larger degree of variation and stochasticity over time. Reproduced from Scheffer (2012) with permission.

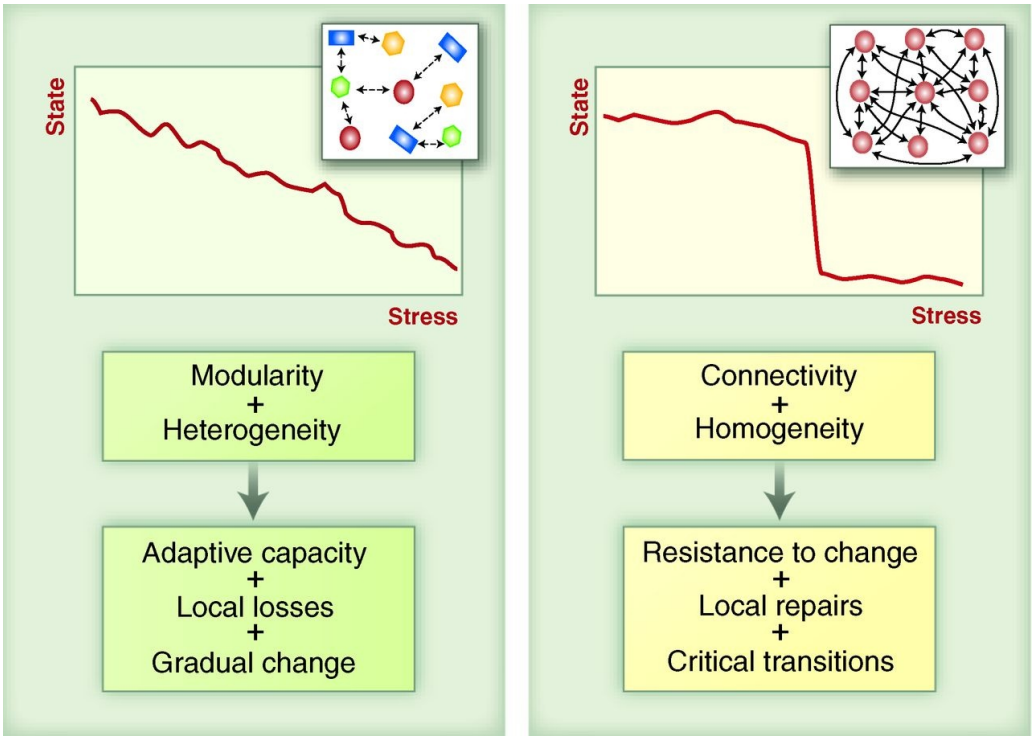

Fig. 3.7. The differences in system connectivity and heterogeneity between steady-state change (continual revolt, remember, or remain) and rapid change (critical transitions). Reproduced from Scheffer (2012) with permission.

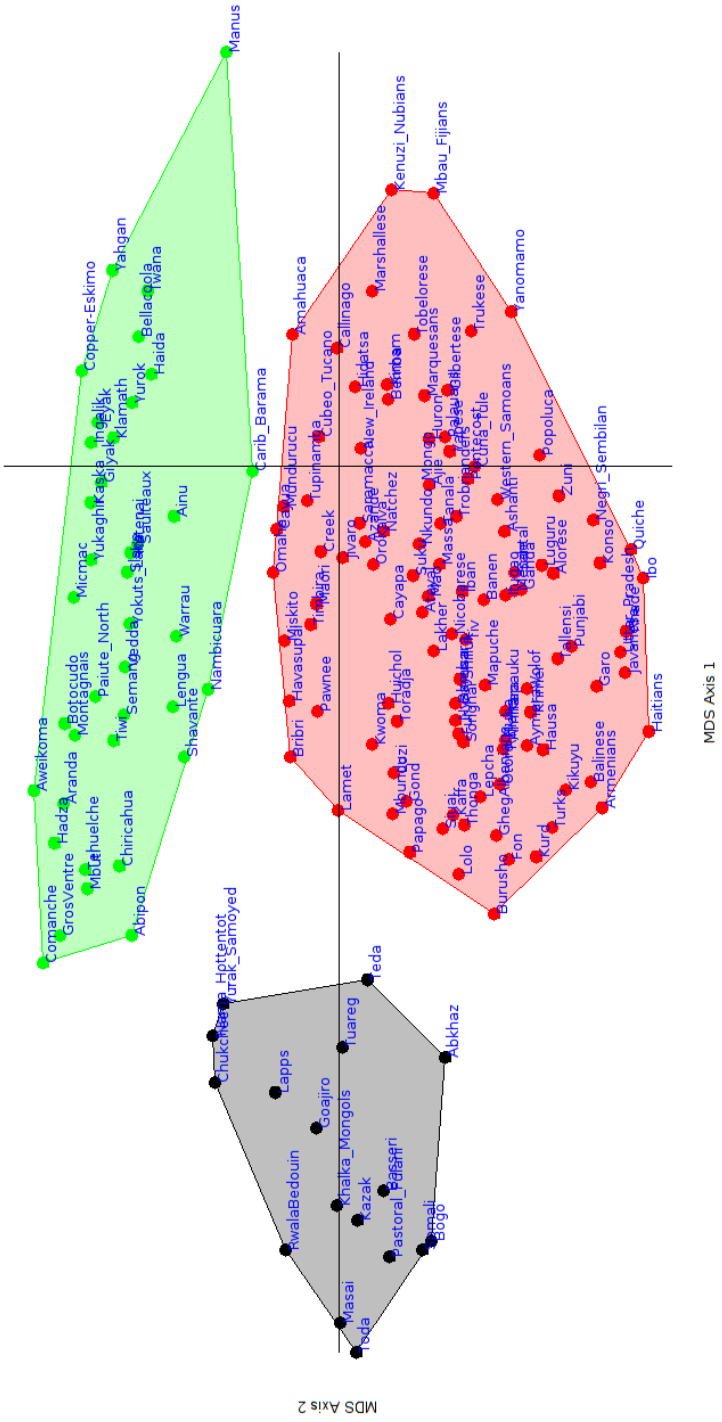

Fig. 3.8. MDS plot of SCCS societes at the macro-scale level of analysis, colored by the results of a 3-cluster K-Medoids clustering routine. Colored areas are convex hulls.

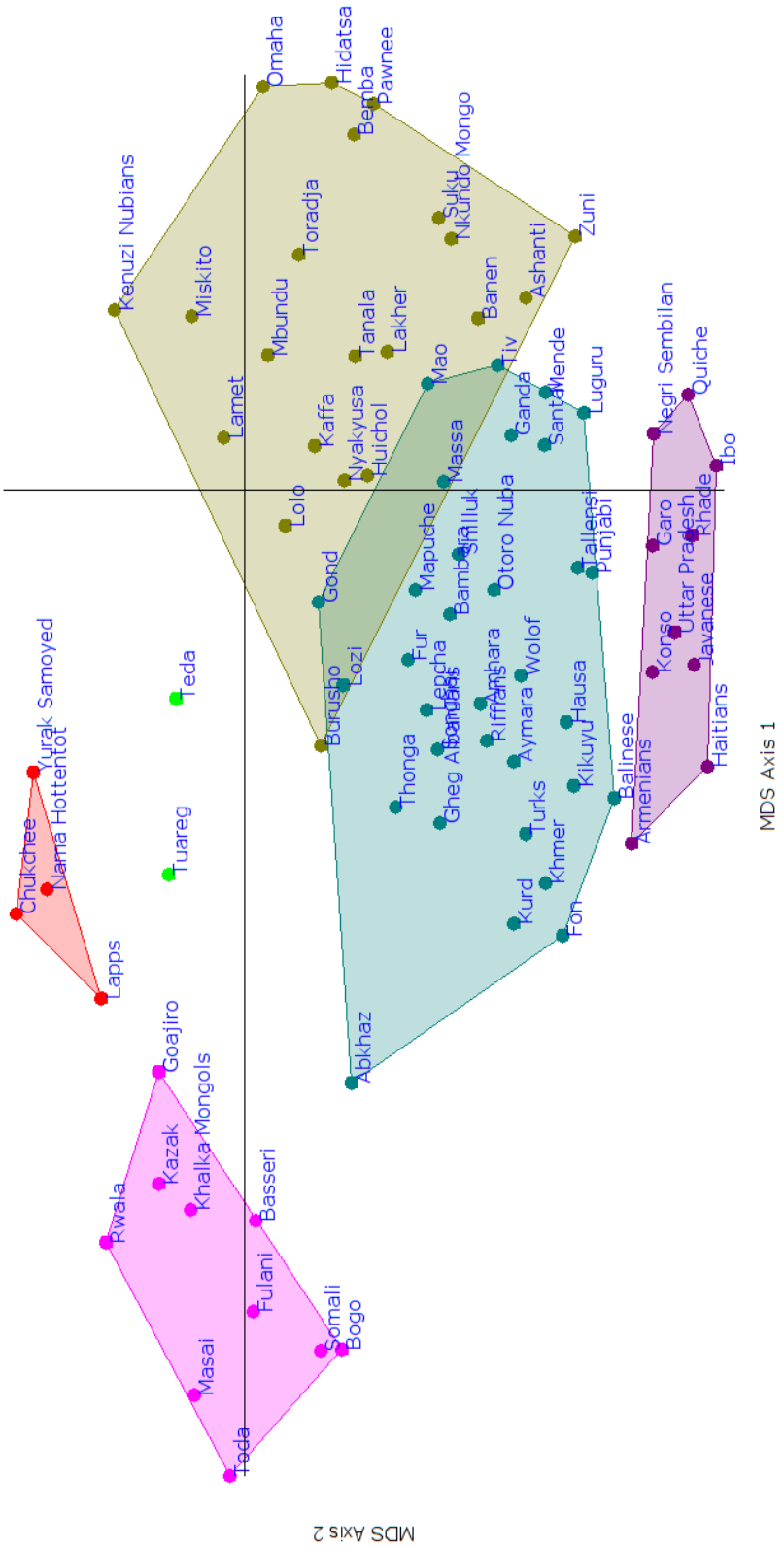

Fig. 3.9. MDS plot of the SCCS societies included in the smaller-scale analysis of agricultural and pastoral groups, colored by a 5-cluster K-Medoids solution. Colored areas are convex hulls.

4. MODELING SOCIAL AND NATURAL PROCESSES

4.1. Modeling Social and Natural Processes

The simulation modeling approach described in this research is not meant to "reconstruct the past" by building a model of "the" Neolithic socio-natural system of Wadi Ziqlab, but rather to create a framework from which to scientifically examine a series of potential PPN social-ecological systems, and the degree to which they may become at-risk for a critical transition over the long-term. This is accomplished by creating a robust set of simplified social and natural process models that reasonably simulate the way these processes behave in the real world, and then dynamically and recursively interconnecting them to create a more complex "system" model. The resulting modeling platform is a kind of laboratory within which to run a series of simulation experiments about past socio-natural systems. The "modeling laboratory" used in this research was developed under the MedLanD project, and thus is known as the MedLanD Modeling Laboratory, or MML.

The laboratory can not, and should not encompass "everything" to do with Neolithic lifeways, but rather should be developed to study a particular aspect of the Neolithic socio-natural system that is of particular interest to the researchers (Kohler and van der Leeuw, 2007). In the case of the MML, this goal is the motivations for, and consequences of, Neolithic subsistence land-use over the long term. This section provides a brief overview of the scope of the MML, and a general outline of its workings. The remainder of this chapter will describe the inner workings of the model in greater detail.

4.1.1. Overview of the Mediterranean Modeling Laboratory

The MML is a combination of a DEVS-Suite (Kim et al., 2009) agent-based model of subsistence agropastoralism (referred to as AP-SiM in other MedLanD publications) with a GRASS GIS (GRASS Development Team, 2012) Landscape Dynamics Model (referred to as LandDyn in other MedLanD publications), connected by a third overarching custom software architecture, referred to as the Interaction Module, or IM. The MML simulates non-irrigated subsistence cereal farming and site-tethered pastoralism, and its connection to surface process dynamics (i.e., erosion and deposition, vegetation growth, and soil fertility) at a regional spatial extent and at an annual temporal scale. The IM acts as both an interpreter and a messenger between the social and natural halves of the MML and also serves as a manager for the coupled agent/landscape simulations by explicitly modeling the interactions between AP-Sim and LandDyn. Using the IM to model interactions within a hybrid model also provides

the researcher with the ability to manage a number of disparities between the agent and environment subsystem models that are inherent to this kind of coupled modeling platform, including disparities of timing, structure, scale, and resolution (Mayer and Sarjoughian, 2007).

The agent-based component of the hybrid model (i.e., AP-Sim) is based on ethnographic data for village-based subsistence agropastoralsim in the Mediterranean region (Al-Jaloudy, 2006; Corbeels et al., 2000; Gibbon, 1981; Hirata et al., 1998; Kamp, 2000, 1987; Khresat et al., 2008, 1998a; Kramer, 1982, 1980; Nablusi et al., 1993; Nordblom et al., 1995; Shoup, 1990; Thomson, 1987; Thomson et al., 1986; Thomson and Bahhady, 1983; Watson, 1979). It consists of two agent types: villages and households. Villages represent a collection of households and are responsible for sending information received from the IM to the appropriate households. Household agents represent a family of agropastoralists acting as a cohesive unit. Household agents farm wheat and barley and raise sheep and goats to acquire food, which they require for survival and growth. The number of people represented by a household strongly influences what it can do. The maximum amount of land that can be planted and subsequently harvested is based on the percentage of each household that is available to do work. The desired amount of farmed land is also based on population, since the number of plots to be farmed by a household in a given year is based on the kilocalorie needs of that household and yield expectations based on the average yield of the previous year. The amount of grazed land is dependent on the number of sheep and goats possessed by a household. Households consume most of the farmed wheat and barley directly and use the rest as supplemental fodder for the goats and sheep. Sheep and goats also need to graze wild vegetation

to round out their diet, and they provide households with additional kilocalories derived from meat and milk products. The yearly consumed kilocalorie need of each household is thus translated to a yearly gross farming kilocalorie need as the sum of wheat and barley kilocalories that will be directly consumed with those that will be used as supplemental fodder. Household birth and death rates change based on household need/kilocalorie yield ratios. If a household fails to meet its energy requirements, the probability that a household member will die increases and the probability of a new household member being born decreases. Likewise, if a household exceeds its energy needs, death rates decrease and birth rates increase.

The IM is responsible for all data interchange between the DEVS-Suite-based AP-Sim and GRASS-based LandDyn. When a household agent requires information about a landscape patch, it sends a coordinate to the IM, which then caches all such information requests from agents to request information about each specific coordinate. The output from those queries is processed and sent to the requesting household agent. After agents have formalized their subsistence plans, the IM then relays these decisions as impacts at specific locations, and executes LandDyn scripts that appropriately modify land cover and soil fertility values, calculate the amount of erosion and deposition. This information is then used to update the digital topographic map, as well as the map of soil depths. The newly updated maps of soil fertility, soil depth,land-cover, and topography are all then used by the agents to make new subsistence plans for the next year, creating

a dynamic simulation of the consequences of yearly household-based subsistence decisions in a low-level Mediterranean agropastoral socio-natural system.

4.1.2 Comparison to Other Land-use Simulation Models

The MML is not the only platform for Land-Use Simulation Modeling (LUSM), however, and it is useful to examine the scope and goals of the MML in comparison to some of these other LUSM systems. There are three essential components to any LUSM platform: a social process modeling engine, a natural process modeling engine, and a method of connecting the two.

An increasingly common social modeling engine used in LUSM is Agent-Based Modeling (ABM), and this is what the MML employs. ABM is a general modeling framework (or "mindset", sensu Bonabeau [2002]) that allows for multiple, independent entities that operate according to sets of decision-making logic in response to stimuli. ABM allows for "emergent properties" – phenomena that develop within the system over time and which could not be predicted at the start of the model run based solely on its input components – in the simulation, which cannot be included in other types of simulation modeling. For example, the most common systems modeling cannon – "equation-based modeling" (sometimes referred to as "macroscopic" modeling) – seeks to simulate the general trends of systems via overarching general process models, and thus are limited in their ability to generate complex emergent phenomena[55] (Bonabeau, 2002; Van Dyke Parunak et al., 1998).

The scale of ABM model complexity differs greatly between the various LUSM systems. Many of the most socially-complex LUSM's (e.g., the "ENKIMDU" project (Altaweel, 2008; Christiansen and Altaweel, 2005; Wilkinson et al., 2007), and the "MASON Afriland" and "MASON Central Asia" projects [(Cioffi-Revilla et al., 2010, 2008, 2007; Rogers et al., 2012)) explicitly track such things as life history (birth, growth, maturity, aging, and death), cultural biases (individual preferences), personal relationships (marriages, father or motherhood, membership in social groups), movements, and life requirements of individual human (and also sometimes animal) agents. These projects are more heavily focused on social dynamics over natural dynamics, and so have heavily parameterized their social modeling engines. Other LUSM platforms are more heavily focused on the natural aspects of the system, and so opt for extremely simplified social ABM implementations (e.g. the very rudimentary social aspects of artifact deposition in "CHILD" project (Clevis et al., 2006; Gasparini et al., 2006; Tucker et al., 2001), and the more complex social interactions in the "CybErosion" project [Wainwright, 2008]). Still other LUSM's have attempted to create both complex social models and complex natural models (e.g. the "Village

55 But emergent properties can and do occur in these types of models.

Ecodynamics" project (Kohler et al., 2007; Kohler and Varien, 2012; Varien et al., 2007)). In all of these cases computational complexity comes at a price; all of these models are computationally intensive, take weeks or months to complete a single modeling cycle, and produced complicated results that are often difficult to interpret. A few LUSM projects have struck a middle balance, however, opting for a moderate level of both social and natural complexity (e.g., the LUCITA model [Lim et al., 2002], and the "Midwest LUCC" project [Evans and Kelley, 2004]), and the MML takes this route as well. This balance allows for reasonably complex LUSM simulation on standard desktop computers.

ABM model complexity is also related to the specific ABM modeling platform used. Several of the most socially complex simulations use advanced ABM platforms like MASS (Ivanyi et al., 2007) (e.g., ENKIMDU), and MASON (Luke et al., 2005) (e.g., MASON AfriLand and Central Asia) to achieve their complexity, while simpler LUSM platforms opt for simpler ABM engines like Swarm (Swarm Development Group, 1999) (e.g., LUCITA). Using an extant ABM platform offers several advantages, mainly in the reduction of programming efforts, a broad base of existing code, and a wider community of developers and researchers. An existing platform may not provide all the behavior desired or software extensibility required for the particular modeling goals of a LUSM project, however, so several LUSM projects have taken the step of coding their own ABM systems from scratch (e.g., Village Ecodynamics, Midwest LUCC, CybErosion). The MML takes a third route by incorporating an ABM system that is fully open-source and easily modifiable (DEVS-Suite [Kim et al., 2009]). This has allowed the development of custom agent behavior and software connections without the need to program an ABM from scratch.

Another difference between LUSM platforms is the scale of social agency. Some LUSM platforms model land-use decision-making at the level of the individual (e.g., ENKIMDU and CybErosion), allowing individuals to perform actions specific to their age, gender, role in society, or other proclivities. However, most platforms model decision-making at the level of the household, and the MML takes this route as well. This is because the household is the minimal economic unit in subsistence agropastoral economies, and most land-use decisions, labor pooling, and consumption occurs at this level (Barlett, 1980; Wilk and Rathje, 1982). Most platforms, including the MML, are also hierarchical, however, in that there are multiple levels of agency (e.g., households and villages) and certain decisions are only made at one level (e.g., the household) while others can only be made a higher level (e.g., the village). For example, while basic subsistence motivations and decision-making may occur at the household-level, actual allocation of land, mediation of property disputes, and other higher-level decisions are made at the village level.

Not all LUSM simulations are spatially explicit (e.g., HilleRisLambers et al., 2001), but land-use is by its very nature a spatially explicit phenomenon, and so a spatially-explicit modeling platform offers key advantages for LUSM. Most ABM frameworks are inherently spatial (e.g., Argonne National Laboratory,

2012; Wilensky, 1999), but typically only include rudimentary spatial processing capabilities, and so are not suitable for simulating spatial processes at the scale or accuracy needed for robust LUSM. Many agent-based LUSM systems incorporate ABM for the social aspects of the system (i.e., decision-making), but use a cellular model (CM. e.g., the use of raster data containers, "map algebra", and cellular automata) for the physical aspects (i.e., "natural" process) of the system (Parker et al., 2003). CM are spatially explicit by their very nature, so are far better and more efficient simulators of spatially explicit processes than are ABM's. The MML takes this "hybrid" approach, using an ABM for the social component of the modeling laboratory, and a CM for the physical aspects of the modeling laboratory. Typically, such "hybrid" LUSM platforms incorporate custom-built CM spatial modeling engines (e.g., all of the aforementioned projects have built custom spatial modeling engines[56]). Thus, many LUSM projects have had to limit the scope of their spatial engines, mainly due to the complexity of coding a geographical modeling platform from scratch. This takes the form of increased cell resolution in some platforms (e.g., the "Village Ecodynamics" project, which models the landscape at 200m resolution [Kohler et al., 2007]), whereas other platforms are limited in terms of complexity (e.g., allowing only a few layers of spatial data)[57]. The MML, on the other hand, was developed to utilize the powerful open-source GIS software platform GRASS (GRASS Development Team, 2012; Neteler and Mitasova, 2007a) as its spatial engine. Because GRASS has been optimized to efficiently handle massive amounts of cellular data, the MML can operate at much higher spatial resolutions[58] and can include many layers of spatially mapped environmental information. This makes for more complex and rich physical modeling than would otherwise be possible on a basic desktop computer.

In order to properly simulate land-use "dynamics" (inter-system feedback over time) LUSM platforms require a means to connect their social modeling engine with their natural process modeling engine. In other words, the two systems must be bound together so that changes in one are "sensed" by the other. The two systems can be "loosely coupled", "closely coupled", or "fully integrated" (sensu Goodchild et al. [Goodchild et al., 1992]). "Loose coupling" implies manual transmission of data from one module to the next. This is the typical workflow of most un-scripted GIS procedures, for example, and is not suitable for simulating processes that must be repeated many times. "Close coupling" means that individual modules are programed such that the ending of one triggers the start of the other, and feeds its output to it directly, and so on in a

56 Note, however, that the ENKIMDU model incorporated an existing agricultural landscape process model: the USDA's "Soil and Water Assessment Tool", or SWAT (Wilkinson et al., 2007).

57 A special case is that of the CHILD project which has developed a custom spatial data model based on evolving triangulated networks that allow for both very high and very low spatial resolution to coexist in the same data model.

58 Theoretically, sub-meter resolution is be possible in the MML, but for most projects, 5-15 meter resolution provides the best compromise of accuracy to run-time

cyclical manner. “Fully integrated” implies that the entire system is programmed into a single software system. Although full integration typically results in faster model run-times and a more seamless user experience, due to the programing effort needed for full integration, most LUSM platforms are closely coupled modular systems[59] where each part of the model is an independent software entity. While the MML is technically a “closely coupled” system, it employs a third, overarching software “wrapper” that controls module timing and execution, and thus obtains some of the aspects and benefits of a “fully integrated” experience from a modular set of software pieces (e.g., an easy-to-use GUI interface, standardized I/O protocols, integrated command architecture, faster running speeds, etc.).

A final difference between the various LUSM platforms is the temporal scale at which the operate. Some LUSM simulations operate as true “discrete event” simulators, so that both social and natural processes occur at the times and temporal interval that is most natural for them (e.g., the ENKIMDU model), but most use a fixed “base” temporal interval. The specific interval differs between projects; some simulate land-use on a daily basis (e.g., CybErosion), while others on a monthly or seasonal basis (e.g., LUCITA), and still others on a yearly basis (e.g. Village Ecodynamics). Such “fixed temporal base” LUSM platforms use different methods to resolve the effects of the simulated social and natural processes to the base temporal interval. Some amalgamate several “discrete events” that are internally simulated at higher temporal resolution (e.g., Village Ecodynamics), while others calculate the effects of modeled social and natural phenomena as averages or as a single equation parameterized to a certain temporal resolution (e.g., LUCITA). The MML uses an annual “base interval”, and uses a combination of both “discrete event” amalgamation (e.g., for individual farming and grazing plot choices, and for population growth) and time-averaged process equations (e.g., for landscape evolution, and for land-cover change) to achieve that resolution.

4.2. Modeling Agropastoral Subsistence Planning in the MML

At the beginning of each simulation year, households must decide upon a subsistence plan consisting of the total amount of farming and grazing plots that they will need, as well as the total amount of firewood they will need to gather throughout the year.

4.2.1. Choosing the Number of Farmed Plots

To determine the number of wheat plots (N_w) needed in the coming year, households use the following decision rules:

59 But the “Village Ecodynamics” model is a fully integrated systems.

Eq. 4.1. $$N_w = \frac{(P_h \cdot F_w) + (P_h \cdot F_w \cdot p_s)}{\mu_w \cdot E}$$

Where, P_h is the current population of the household, F_w is the total amount of wheat needed for subsistence purposes [kg/pers.] (i.e., the "food wheat" needed per person), p_s is the "seeding proportion" needed needed for reseeding the next years' crop [percentage of crop], μ_w is the average amount [kg/ha] of wheat that was grown on the plots owned by the household in the previous year, and E is unit-less "expectation" scalar that determines how conservative farmers are when predicting the amount of land they will need (as the value of E increases, farmers will try to plant more and more above the minimum needed to survive). Thus, the number of wheat plots is determined as the total amount of wheat needed by the household plus the extra wheat needed as seed crop, all divided by the amount of wheat expected to be produced from a typical plot.

In the model, barley is used only as supplemental fodder for ovicaprids. To determine the number of barley plots (N_b) needed in the coming year, households use the following decision rules:

Eq. 4.2. $$N_b = \frac{(P_h \cdot P_{oc} \cdot DM_{tot} \cdot p_b) + (P_h \cdot P_{oc} \cdot DM_{tot} \cdot p_b \cdot p_s)}{\mu_b \cdot E}$$

Where, P_h is the current population of the household, P_{oc} is the number of ovicaprids per person (determined by the modeler – should be based on the importance of pastoral products in the diet), DM_{tot} is the total amount [kg] of digestible matter needed by the average animal in the herd (the actual amount will vary based on the goat/sheep ratio, breed characteristics, and herd profile, as entered by the modeler), p_b is the proportion of the total diet of a herd animal that will be provided by supplemental barley foddering [percentage], p_s is the same "seeding proportion" used in Equation 4.1, μ_b is the average amount [kg] of barley that was grown on the plots owned by the household in the previous year, and E is the same "expectation" scalar used in Equation 4.1. Thus, the number of barley plots is determined as the total amount of barley needed as supplemental fodder by the herd owned by the household plus the extra barley needed as seed crop, all divided by the amount of barley expected to be produced from a typical plot.

4.2.2. Choosing the Amount of Grazing Land

To determine the number of grazing patches (N_g) needed in the coming year, households use the following decision rules:

Eq.4.3. $$N_g = \frac{(P_h \cdot P_{oc} \cdot DM_{tot}) - (DM_{stub} + (P_h \cdot P_{oc} \cdot DM_{tot} \cdot p_b))}{\mu_g}$$

Where, P_h, P_{oc}, DM_{tot}, and p_b are as in Equation 4.2 above, DM_{stub} is the amount of digestible matter [kg] provided by grazing the stubble of the wheat and barley fields owned by the household, and μ_w is the average amount [kg] of digestible matter that was grazed from all the patches exploited by the household in the previous year. Thus, the number of grazing patches is determined as the total amount of digestible matter needed by the herd minus the amounts of digestible matter obtained from stubble-grazing on wheat/barley fields and that obtained as supplemental barley fodder, all divided by the amount of digestible matter expected to be produced from a typical grazing patch.

4.2.3. Choosing the Amount of Firewood Gathering Patches

The number of firewood gathering plots (N_{fw}) needed in a given year is determined by the following algorithm:

Eq. 4.4. $$N_{fw} = \frac{(P_h \cdot F_{tot}) - F_{clear}}{W_i \cdot RC_m}$$

Where, P_h is the current population of the household, F_{tot} is the total amount [kg] of firewood needed per person per year, F_{clear} is the amount of firewood obtained during any new agricultural field clearances that occurred that year [kg], W_i is the intensity at which people gather wood [kg/m^2], and RC_m is the number of raster cells per square meter (i.e., a conversion factor to scale the impacts to the current raster resolution). Thus, the number of firewood gathering patches is determined as the total amount of firewood needed by the household minus the amount they obtained during field clearances, all divided by the amount of firewood that will be gathered from each firewood gathering patch. It is important to note that firewood gathering differs from other activities in that there is no "average return" from the cells, but instead a "gathering intensity" that is determined by the modeler.

4.2.4. Simulating Farmer/Herder Knowledge Biases

It is important to note that in real life, farmers and herders would not have perfect knowledge of mean return rates from their farming and grazing plots.

Memory biases (Koriat et al., 2000]; e.g., transience, absentmindedness, blocking, misattribution, suggestibility, bias, persistence, etc. [Schacter, 1999), and biases of estimation (e.g., errors of representativeness and availability, insensitivity to sample size and predictability, misconceptions of chance, biases due to retrievability of instances, imaginability, etc. [Tversky and Kahneman, 1974]), are always acting to prevent such perfect knowledge, and the model simulates this by randomly perturbing the actual values of μ_w, μ_b, and μ_g according to a Gaussian function before sending them to the agents to be used in the decision algorithms.

4.3. Modeling the Location of Agropastoral Subsistence Activities in the MML

Once each household has developed its subsistence plan for the year (consisting of the number of plots/patches for each type of subsistence behavior), they then must choose the locations of each of these patches. The model has a very simple "negotiation" algorithm, which sets the order in which land patches are chosen by each house and village. This essentially occurs in a "round-robin" system which loops through the list of households in each village, allowing each household to pick one patch in turn until all households have fulfilled their land requirements. The order of the households is randomized each year, so that one particular household is not always getting the first choice of land patches. This system ensures every household has at least some high-ranked land cells in their possession in any given year[60]. In the case of multiple villages, each the households in each village choose separately from each other, and the household's choices are constrained by the choices of households in villages that chose land prior to them. Like the order of households within villages, the order of villages is also randomized each year so that one village does not always get to choose first.

Land patches are chosen based on their "value" to the households. In general, households seek to minimize walking costs while maximizing subsistence returns when deciding upon the locations of plots, and do so using a land valuation equation specific to a particular subsistence task. Thus in any given year, agent movement is governed by the balance of a unique series cost minimization and benefit maximization decisions, which provides a dynamic and constantly changing pattern of movement over time.

60 This is the default behavior of the model. The modeler can choose not to randomize the order of households each time, and to allow each household to pick all their land patches in one go (not round-robin). Doing so would assume some sort of social hierarchy (chiefly authority, for example) where households of "high status" get to pick first, and so may be appropriate in some modeling scenarios. Neolithic society is widely assumed to be egalitarian (Simmons, 2007), however, so I use the default randomization and round-robin routine in all the models presented in this research.

4.3.1. Choosing the Location of Farm Plots

For farming plots, households want relatively level land that has deep fertile soil, but which is not too far away from the village. Thus, farming value (*FV*) of potential plots are evaluated using the following equation:

Eq. 4.5. $$FV = SV \cdot \left(\frac{(F + F_w) \cdot (SD + SD_w)}{F_w + SD_w} \right) - \left(\left(D_w \cdot \frac{D}{D_{max}} \right) + LC_{dval} \right)$$

Here, *SV* is a slope modification value (0°-10°, *SV*=1; 11°-20°, *SV*=0.75; 21°-60°, *SV*=0.25; 60°-90°, *SV*=0) that makes lower slopes more valuable than higher ones, *F* is the current soil fertility value [percentage] (scaled 0-1), F_w is a weighting factor for soil fertility in the decision algorithm, *SD* is the current soil depth [m] (scaled 0-1), and SD_w is a weighting factor for soil depth in the decision algorithm. The maximum soil depth needed for full yields is 1m (Carter et al., 1985; Christensen and McElyea, 1988; Rhoton and Lindbo, 1997; Sadras and Calvino, 2001; Wong and Asseng, 2007), so for depths greater than 1m, *SD* is set to 1. *D* is the least-cost distance of the current cell from the center of the village, D_w is the least cost distance weight in the decision algorithm, and D_{max} is the maximum calculated least cost distance value on the least cost map. Finally, LC_{dval} is a land-cover "devaluation" coefficient such that degree of devaluation of vegetation other than wheat/barley grassland is set according to a "graphing function" (a sequential series of boolean-separated linear regressions that approximate the results of a more complex regression function) parameterized by breakpoints entered by the modeler. Adjusting LC_{dval} preferences farm plots with certain land-cover values, and essentially sets the fallow-cycle of the system (e.g., forest-fallow, bush-fallow, short-fallow, intensive agriculture, sensu Boserup [1965]). Thus, the left side of the equations estimates the general suitability of a plot of land for farming, and the right side estimates the costs to the agent if they were to farm that plot, and the equation balances to an estimate of the total "value" of a particular plot of land to agents from a particular village. This equation selects for deep fertile plots, but scales the attractiveness of such plots based on their slope, and reduces their value based on their distance from the village along the least-cost route and the amount of vegetation currently on the plot. It is also important to note that in the current simulations, agricultural plots are not tenured. Every year, agents simply farm the "best" (according to Equation 4.3) land parcels available to them, and thus, agents are free to drop a parcel of previously farmed land if they perceive that another parcel of land is better.

4.3.2 Choosing Grazing Patches

Once all of the households have chosen agricultural plots, they must decide on locations for grazing. For pastoralism, slope and soil attributes are unimportant when deciding upon grazing locations, but households do prefer

grazing patches that have abundant fodder but which are not too far from the village (Oba, 2012). Thus, the grazing value (*GV*) of potential grazing patches is evaluated according to the following equation:

Eq. 4.6.
$$GV = \frac{\left(DM_w \cdot DM\right) + \left(D_w \cdot \left(1 - \frac{D}{D_{max}}\right)\right)}{DM_w + D_w}$$

Here, *LC* is current the land-cover value of a particular patch, which is proxy for the amount of available digestible matter (fodder) available in the patch, and *LCw* is the weight of the land-cover value in the decision algorithm. *D* is the least-cost distance of the current cell from the village [sec], *Dw* is the least cost distance weight in the decision algorithm, and *Dmax* is the maximum calculated least cost distance value on the least cost map. In Mediterranean environments, slightly immature grassy open oak and pine woodland produces the largest amount of digestible matter, and digestible matter actually decreases as these woodlands mature into denser oak forests (Al-Jaloudy, 2006). To account for this, any *LC* value above 40 (which corresponds to these open grassy woodlands) are rescaled by a boolean function in descending order (e.g., 41 is changed to 39, 42 to 38, etc.) before being rescaled from 0-1 and entered into the equation. This equation favors patches of land with high fodder production, but scales their attractiveness according to their distance from the village along the route of least accumulated costs. Thus grazing patches that have large amounts of edible vegetation, but which are very far from the village are less attractive to agents than are grazing patches that have less edible vegetation, but which are very close to the village. The actual number of cells chosen depends upon the total number of ovicaprids being herded, and the stocking rates of these animals on the landscape. In our models, the total number of ovicaprids herded is linked to the village population by a ratio of animals to people determined *a priori* by the modeler at the start of each model run. This ratio stays constant during each simulation. Stocking rates are also determined by the modeler at the start of each model run, as is the ratio of goats to sheep (which determine the amount of fodder needed and the total kilocalorie output from the herd, based on its size in any given year).

4.3.3 Choosing Firewood Gathering Patches

Finally, households must meet their requirement for firewood. If households clear a plot of land for farming, they acquire and amount of wood equal to a proportion of the standing biomass of the plot, determined from the land-cover value of that plot at the time of clearance. Any additional firewood needed by the household must be gathered from other parts of the landscape. The wood value (*WV*) of landscape patches is calculated by the following equation:

Eq. 4.7.
$$WV = \frac{LC + \left(D_w \cdot \left(1 - \frac{D}{D_{max}} \right) \right)}{1 + D_w}$$

Here, *LC* is the land-cover of a particular patch, *D* is the least-cost distance of the current cell from the village [sec], *Dw* is the least cost distance weight in the decision algorithm, and *Dmax* is the maximum calculated least cost distance value on the least cost map [sec]. Land-cover values between 9 and 50 are rescaled from 0-1 before being input into the equation. Land-cover values below 9 (which equates to grass and shrubs) are deemed to not produce large enough pieces of woody material to make firewood gathering efficient, and so are set to 0. Typically, D_w should be set higher than 1 ($D_w = 3$ by default) because ethnographic research shows that distance is the primary concern when gathering firewood (Tabuti et al., 2003). Thus, the equation favors firewood gathering on those patches with the most amount of woody material suitable for firewood and are also closest to the village. The amount of wood actually gathered depends on two things: the total amount of wood need per person, and the intensity of wood gathering.

4.4. Modeling Agropastoral Subsistence Returns in the MML

The returns of subsistence activities will depend on the type of activity, the particular characteristics of how the activity is performed, and the conditions of the plot that the activity is performed on. Each activity is parameterized at the start of the modeling run, and the MML calculates the returns of each type of subsistence activity at each cell based on these parameters and the conditions at the cell in a given year. These conditions are formed by both the location of the plot in the natural system (soil depth, erosion rates, climax vegetation type) as well as previous human usages of the plot (reduction of vegetation, reduction of soil fertility).

4.4.1. Calculating Farming Returns

Wheat and barley returns (*WR* and *BR*, respectively) are measured in terms of kilograms of harvested grain, which is calculated according to the following equations:

Eq. 4.8.
$$WR = \frac{\left(PR_w \cdot SV \cdot Max_w \right)}{RC_{ha}}$$

Eq. 4.9.

$$BR = \frac{\left(PR_b \cdot SV \cdot Max_b\right)}{RC_{ha}}$$

Where PR_w and PR_b are the potential wheat and barley production rates of a particular plot (scaled from 0 to 1), Max_w and Max_b are the maximum wheat and barley yields possible under ideal conditions [kg/ha], SV is the slope modification value (as used in Equation 4.5), and RC_{ha} is the number of raster cells per hectare (in the model, the size for an individual farm plot is the same as the starting raster cell resolution). As suggested by Rhoton and Lindbo (1997) and Christensen and McElyea (1988), PR_w and PR_b are calculated as the average of three regressions against precipitation, soil depth, and soil fertility:

Eq. 4.10.

$$PR_w = \frac{\left(\left(\left(0.51 \cdot \ln\left(P\right)\right) + 1.03\right) \cdot \left(\left(0.28 \cdot \ln\left(SD\right)\right) + 0.87\right) \cdot \left(\left(0.19 \cdot \ln\left(F\right)\right) + 1\right)\right)}{3}$$

Eq. 4.11.

$$PR_b = \frac{\left(\left(\left(0.48 \cdot \ln\left(P\right)\right) + 1.51\right) \cdot \left(\left(0.34 \cdot \ln\left(SD\right)\right) + 1.09\right) \cdot \left(\left(0.18 \cdot \ln\left(F\right)\right) + 0.98\right)\right)}{3}$$

Where P is the amount of annual precipitation (in meters), F is the current soil fertility value [percentage] (scaled 0-1), SD is the current soil depth [m] (as in Equation 4.5). The particular regression coefficients in Equations 4.10 and 4.11 derive from data presented by various authors. The regressive relationship between wheat/barley yield and precipitation was determined from data presented by Araus et al. (1997a), (1997b b), Pswarayi (2008), and Merah et al. (2000) (Figure 4.1). The regressive relationship between wheat/barley yields and soil depth was determined from data presented by Wong and Asseng (2007) and Carter et al. (1985) (Figure 4.2), and the relationship derived from these data also generally agrees with those presented by Sadras and Calvino (2001) (although data from Sadras and Calvino were not used to determine the regression). And finally, the regressive relationship between wheat/barley yield and soil fertility was determined from data presented by Barzegar et al. (2002) and Quiroga et al. (2006) (Figure 4.3).

4.4.2. Calculating Grazing Returns

Grazing returns (GR) are measured in kilograms of digestible matter, and are calculated according to a different logic than wheat and barley returns:

Eq. 4.12.
$$GR = \left(\frac{DM}{RC_{ha}} \right) \cdot G_i$$

Where *DM* is the amount of sustainably available "digestible matter" (edible biomxass) in a patch [kg/ha], RC_{ha} is the number of raster cells per hectare (again, grazing patches are constrained to be the size of the current raster resolution), and G_i is a "grazing impact factor" (unit-less multiplier, allowing for "unsustainable" grazing practices). The value of *DM* for each cell is calculated by a "graphing function" (a sequential series of boolean-separated linear regressions that approximate the results of a more complex regression function):

Eq. 4.13.
$$\begin{aligned} &if: && 50 \geq LC \geq 40,\ DM = 800 - (10 \cdot LC), \\ &elif: && 40 > LC \geq 27,\ DM = (27.27 \cdot LC) - 663.64, \\ &elif: && 27 > LC \geq 4,\ DM = (2.27 \cdot LC) + 38.64, \\ &elif: && 4 > LC \geq 1,\ DM = (12.5 \cdot LC), \\ &else: && DM = 0 \end{aligned}$$

Where, *LC* is the land-cover value in the 50-year succession regime of the model (coded 0-50).

4.4.3. Calculating Woodgathering Returns

Because wood is typically gathered at a set density at each patch (Karanth et al., 2006), firewood gathering returns (*FR*) are measured in kilograms of wood, and will be the same at each patch:

Eq. 4.14.
$$FR = W_i \cdot RC_m$$

Where W_i is the intensity at which people gather wood [kg/m^2], and RC_m is the number of raster cells per square meter (i.e., a conversion factor to scale the impacts to the current raster resolution).

4.5. Simulating Soil Fertility and Vegetation Dynamics, and the Direct Impacts of Subsistence Activities in the MML

Subsistence activities have both direct and indirect impacts on the land cells upon which they occur. Although there are many types of direct impacts that occur in the real world (e.g., terrace construction, pit digging, etc.), subsistence activities in the MML can only directly impact land-cover (vegetation) and/or soil fertility.

4.5.1. Modeling Soil Fertility Impacts and Dynamics

Soil fertility is tracked in the MML as percentage values, and fertility impacts and the fertility regain rate are both measured in percentage reduction to fertility. All soils start off in each model run at 100% fertility (see Chapter 5, Section 5.3.3), the rates of reduction and regain are set as constants at the start of the model, and the parameterization of the farming system will then dictate the pattern of fertility dynamics over time.

Farming[61] a plot disrupts the natural connections between vegetation, soil, and nutrient flow that occur in natural vegetative communities, and so decreases the amount of nutrients (fertility) available in the soil by an amount that greatly depends upon the particular environment and the type of agriculture being conducted (Khresat et al., 1998a). Although any amount of annual fertility decrease *could* be modeled, experimental research on historical fields suggests that Mediterranean dry wheat/barely farming reduces the fertility of a plot by 0.5-1 percent each year (Bonet, 2004; Bonet and Pausas, 2007, 2004; Khresat et al., 2008, 1998a).

The percentage of remaining soil fertility in a patch affects the farming returns from that patch (see Section 4.4, above), thus incorporating the feedback effects of soil-fertility change as a kind of indirect human impact. This system is purposefully kept simple in the MML, and thus, by adjusting the depletion and regain percentages, it is possible to model the net effect of many different systems of fertility conservation or depletion that would be too complex to model more specifically.

4.5.2. Modeling Vegetation Impacts and Dynamics

The successive regrowth of vegetation on cleared or grazed plots is a complex process influenced by several variables, including climate, topography, geology, phytogeography, and human and animal land-use, and not least, the nature and after-effects of the initial disturbance (Bazzaz, 1979; Huston and Smith, 1987; Turner et al., 1998). There are many existing succession simulation models (and Keane et al. [2004]; e.g. see Usher [1981]), but most of the existing vegetation succession simulation engines attempt to address this complexity through a corresponding increase in complexity of model code (Gustafson et al., 2000; e.g., Pausas, 1999a). The vegetation succession dynamics engine in the MML, on the other hand, is a simple linear succession scheme – sometimes referred to as a "gap" model (Pausas, 1999b) – that allows disturbed patches to regrow through a series of successive stages of vegetation communities. Although

61 At this point grazing has no directly modeled effect on soil fertility in the MML. Although it is conceivable that grazing may have some negative effect on soil fertility, these would likely be very small and indirect. Grazing does have positive effects on soil fertility, especially from the addition of organic matter and nitrates from dung whilst stubble grazing, but these additions can be modeled by a change in the overall fertility regain rate.

Pausas (1999b) argues that gap models are overly simple for long-term vegetation dynamics simulation, the connection of the MML succession model to the human land-use surface process models adds much of the complexity Pausas argues for, without requiring it to be embedded withing the vegetation model itself. The MML gap model is parameterized to the rates and form of vegetation regrowth noted on cleared fields in the Mediterranean region. Under ideal conditions, a completely cleared patch will regrow to mature oak woodland after fifty years (Bonet, 2004; Bonet and Pausas, 2007, 2004), and the rate of change from one plant community to the next is faster in the earlier stages than at the latter (i.e., a power law) (Casado et al., 1986; Debussche et al., 1996). Thus, model thus has 50 successive stages[62], organized so that the rate of successive vegetation community change slows over time (Table 4.1).

The actual rate of regrowth (V_r) in a patch (and thus the actual timing of the succession) depends upon the soil depth and fertility of that patch, and is calculated by taking the average of two power regressions via the following formula:

Eq. 4.15
$$V_r = \frac{\left((-0.000118528 \cdot F^2) + (0.0215056 \cdot F) + 0.0237987\right) + \left((-0.000118528 \cdot SD^2) + (0.0215056 \cdot SD) + 0.0237987\right)}{2}$$

Where F is the current soil fertility [percentage fertility] of the patch and SD is the current soil depth [m] of the patch. the resulting regrowth rate scales between 0 and 1[63] according to a power law so that regrowth slows exponentially as the average of soil depth and fertility approach 0. The actual rate of regrowth (V_r) is in units of "succession amount per year", so that values of V_r less than one mean that vegetation recuperates at some fraction of the "ideal" possible yearly rate.

Grazing and woodgathering impacts act as a slow attrition of vegetative cover over time. As the returns of grazing are measured in kilograms of vegetation, it is easiest to assess their impact in these same units (i.e., in kilograms of biomass removed). The reduction rate of grazing in a patch varies according the value of G_i in Equation 4.12. In essence, G_i sets the "stocking rate" for the grazing catchment; higher stocking rates mean larger amounts of fodder are extracted from each grazing patch in any given year. All else being equal, this translates to a lower total number of needed patches each year, but also means that the land-cover of grazed patches is reduced by a larger amount each time it is grazed. Firewood collection reduces each patch simply by the value of $W_i \cdot RC_m$

62 But note that not all parts of the landscape are capable of supporting climax Mediterranean forest (value "50" in the 50-year succession scheme). There is a "base" paleovegetation map (see Chapter 5, Section 5.5) that provides the "maximum succession" value for each patch, and the vegetation in that patch can never exceed that limit.

63 If soil depth is greater than 1 meter, the soil depth regression is set equal to 1.

(Section 4.4.3 above), which is already in units of kilograms of biomass per square meter, and, unlike grazing, is the same for every patch in every year.

Agents can both graze a patch, and gather firewood on that same patch in the same year, so the impact of the two activities is cumulative. Once the total amount of reduction to biomass from grazing and woodgathering is calculated, the impacts must be converted from units of biomass [kg/m^2] to an amount of reduction in units of "succession amount per year", (i.e., the same units as V_r from Equation 4.15). This is done according to a graphing function, with equivalency breakpoints parameterized by data on average amounts of above-ground biomass for various vegetation communities in Mediterranean environments (as reported in Table 4.2).

Once the vegetation regrowth rate (V_r) at a particular patch is established, and the actual amount of biomass that was grazed away by ovicaprids and/or removed by woodgathering on the patch has been converted to succession units (V_i), the net change to the vegetation in the patch in that year (V_{net}) can be calculated according to the following formula:

Eq. 4.16
$$V_{net} = V_i + V_r$$

The next year's land-cover map is created by adding the map of V_{net} to the previous year's land-cover map. If human impacts outpace regrowth, then V_{net} will be negative and land-cover will be reduced by V_{net} amount. If the human impacts in a patch are less than the regrowth/regain rate, however, V_{net} will be positive and vegetation will regrow by V_{net} amount, until the maximum succession value for the patch is reached.

Farming, on the other hand, directly replaces native vegetation with "artificial" vegetation. In the case of the MML, the planted crops are wheat or barley, which are annual grasses. Thus, the impact of farming a plot is simulated in the MML by directly changing the vegetation succession value of the plot to that of a pure, dense, grassland, which is "5". Actively farmed plots are inaccessible for grazing or woodgathering[64], but newly released farming plots become available to these activities again, and vegetation dynamics return to the governance of Equations 4.15 and 4.16.

The direct impacts of human land-use also have unintended consequences (indirect impacts), and so a series of feedback connections is built into the MML to account for these. Changes to land-cover will affect the amount of soil erosion or deposition that occurs, and these changes to soil depths will in turn affect the rate at which vegetation regrows and the way agents value and choose parcels. Land-cover affects both the local conditions of soil detachment in a particular patch, and the way water that flows through the watershed.

64 But note that the fodder gained from stubble-grazing and the wood gained from plot clearance *is* accounted for in the overall subsistence plan (see Section 4.2, above).

In order to connect the local "soil detachment protectiveness" of land-cover to the surface process equations (Section 4.7, below), an intermediate measure is required. In the case of hillslope processes, this measure is the "C-factor" of the RUSLE/USPED equations (Equation 4.18, below). C-factor is a unit-less measure of the capabilities of a vegetation community to protect from soil dislodgement and transport; specifically, it is the ratio of observed soil loss under a specific vegetative regime versus that under clean-tilled continuous fallow with all other variables held constant (Wischmeier and Smith, 1978). Thus, "real" local values of C-factor must be determined through empirical field experiments, which is outside the scope of the current research. Fortunately, Wischmeier and Smith (1978), have documented C-factor for a wide variety of land-cover communities under a variety of specific local conditions, and so it is possible to estimate a series of C-factor values for specific vegetation communities in the MML vegetation succession model (Table 4.3). These specific equivalences (i.e., the series of match succession values and C-factors) can then be used as breakpoints in a graphing function to estimate values of C for other succession stages.

The C-factor map thus created is entered directly into the hillslope surface process equation (Equation 4.18, below), and the value of C in a particular cell directly affects the amount of erosion or deposition calculated for that cell. C is not a variable in the other surface process equations (soil diffusion or streams), however, so the effects of vegetation must be accounted for in different ways. In the soil diffusion equation (Equation 4.17), the effect of vegetation is encapsulated in the local environmental modifier term κ. There is no specific environmental term in the stream equation (Equations 4.19 and 4.20), however, and any local aquatic vegetation must be accounted for by the substrate erodibility term K_t.

Vegetation also affects the way water flows through the system by slowing its flow, and thus affecting local infiltration and outflow rates. Because the process equations used in the MML were originally developed as 2-D models for use in predicting erosion/deposition on discrete landscape patches or stream-power over linear stream segments, they require the water influx rate to be calculated externally. Most hydrological models integrate the effects of vegetation on runoff by using cover-specific coefficients that account for vegetation's ability to slow the force of flowing water (e.g., Krysanova et al., 2005). The most suitable measure of this that is used in the MML is the C-factor coefficient, but it cannot be directly. Instead, a map of "flow hindrance" can be created from the map of C-factor by making a linear regression of C-factor to the percentage of water that will leave the cell. The regression is parameterized to so that a C-factor value of 0.005 (mature woodland) will only allow 10% of the water to exit the cell, whereas a C-factor of 0.1 (bare land) will allow 98% of the water to leave the cell. Then the average amount of precipitation (see Chapter 5, Section 5.4), is

multiplied by "flow hindrance" to create a map of "net flow contribution[65]". The MML leverages the hydrological modeling capabilities of the GRASS module "r.watershed"[66], which accepts the map of "net flow contribution" to control the amount of runoff each cell contributes to the overall runoff map. It is this final runoff map that affects both the hillslope process equation (value *A* in Equation 4.18) and the stream equation (value *A* in Equation A.1, which is used to estimate the value *R* in Equation 4.20).

4.6. Modeling Population Dynamics in the MML

Although the MML does not track the life histories of specific individuals, it nevertheless includes a realistic simulation engine of demographic change. The base level of agency is at the household, and so this is also the base demographic unit. Thus, while the MML does not know if *specific* individuals have been born or died in a household, it *does* know how many people are alive in each household in each year. Household population changes according to a probabilistic function that balances the chances of a birth or a death in each year. These rates are determined by the ability of a household to feed all its inhabitants, so first all subsistence yields from household farming and grazing must be tallied and compared to the total caloric need of the household's inhabitants. Yields must be converted to kilocalories for this comparison. Wheat is converted by multiplying the total kilograms produced on all plots farmed by the household by its caloric yield per kilogram. Calculating the caloric yield for pastoralism is more complicated. First, the fodder barley yield, the amount of fodder gained from stubble-grazing wheat and barley straw, and the amount of wild fodder grazed must be summed. The total amount of fodder then determines the actual number of animals that were fed (as opposed to the number of animals that the household *planned* to feed), by dividing it by the fodder need per average animal in herd (which is in turn determined by the herd composition ratio and the fodder requirements for each type of herd animal). Finally, the total number of animals fed is multiplied by the average caloric yield per herd animal to determine the total amount of kilocalories gained from pastoral products[67].

---

65 "Flow contribution" can also be thought of as "rainfall excess", which is the correct hydrological term for the amount of rainfall that flows into the hydrological system (i.e., precipitation minus infiltration).

66 The "r.watershed" module also uses a "multiple flow direction" algorithm that produces much smoother and more realistic pattens of flow convergence and divergence than does a simpler "single flow direction" (also known as a "D-8") algorithm (Wilson, 2012).

67 The caloric need per person, the caloric yield per kilogram of wheat, the fodder requirements of herd animals, and the caloric yield per herd animal type are all defined by the modeler at start of the model run. See Chapter 6 for how these values are determined for Neolithic farmers and their domesticates.

Each household in the village starts the simulation with the same "average" birth and death "percentage probabilities"[68], but then may begin to diverge from each other depending upon the recent history of subsistence success or failure of each household. If the subsistence plan of the household falls short of the household's needs (i.e., below a predetermined "buffer" of the total "by the numbers" household caloric need), the probability of a birth occurrence declines and that of death occurrence increases. If the subsistence plan meets or exceeds the household's needs, then the opposite occurs. The amount of increase or decreased birth or death probability depends upon the degree of over- or under-production, and the maximal rate of probability change allowed per year. Up to 15% over- or under production induces an increase or decrease of half the allowable amount, 15-25% over- or under-production induces an increase or decrease of two thirds the allowable amount, and greater than 25% over- or under-production induces an increase or decrease of the full allowable amount, and birth and death probabilities can increase or decrease up to a predetermined maximum and minimum amount[69]. If the subsistence plan of the household provides just-adequate sustenance in a given year (i.e., *within* the "buffer" of the household caloric need), then the probability of a death or birth occurrence slowly returns to the initial "average".

An actual birth or death only occurs in a given year as a series of "random chance" operations. The total number of "random chances" is equal to the total number of people currently alive within the household. For each "random chance", a random "percentage value" is generated by a random number generator, and compared to the household's current "percentage probability" for births or deaths respectively. If the random "percentage value" is less than or equal to the current birth or death "percentage probability", then a birth or death "occurs". The total number of "births" and "deaths" is then balanced, yielding the actual household population change for that year.

4.7. Modeling Landscape Evolution in the MML

The landscape evolution component of the MML is executed by a single addon script for GRASS, called "*r.landscape.evol.py*"[70]. The operation carried out by the script estimates the amount of elevation change due to erosion or deposition that would occur at each point on a landscape in a given year (i.e., a unique set of climatic, physical, and environmental conditions at an annual scale), and iteratively enacts these elevation changes over time. The script uses different process equations for different landforms, and implements them in a manner that

68 See Chapter 6 for more information about Neolithic birth and death rates.

69 The maximum allowed yearly change to birth and death probabilities, and the total maximum and minimum birth and death probabilities are set by the modeler at the start of the simulation.

70 The *r.landscape.evol.py* GRASS addon script can also be used independently of the other components in the MML.

optimizes the ratio of model run-time to accuracy of erosion/deposition calculations.

4.7.1. Estimating Elevation Changes Due to Soil Creep

The module implements a diffusion equation for areas near drainage divides, a three-dimensional transport-capacity limited implementation of USPED for hillslopes and gully heads, and a transport-capacity limited reach-average shear stress function for channels.

The diffusion equation used by the MML is well-known and simulates "soil creep" – the movement of soil downslope due to the effect of gravity and particle movement from rainsplash, bioturbation, and other local factors – on portions of the landscape where there is not enough accumulated runoff for overland flow (Culling, 1965, 1963, 1960; Heimsath et al., 2002). The diffusion equation estimates the change in elevation (*dz*) directly:

Eq. 4.17 $$dz = \kappa \cdot \sin(\beta)$$

Where, κ [m/1000yr] is the diffusion coefficient – an empirically-derived constant estimating the base-line soil-creep rate for different climate/vegetation regimes (REFS)), and β is the topographic slope [deg]. Thus, the value of *dz* is determined as a localized adjustment of κ, as scaled by the steepness of the local topography.

4.7.2. Estimating Transport-Capacity on Hillslopes

Sheetwash and rilling/gullying are both hillslope processes, and erosion/deposition deriving from these processes in the MML are estimated using the Unit Stream Powered Erosion Deposition equation (USPED), derived from concepts described by Kirkby (1971), adapted for two dimensional landscapes by Moore and Burch (1986), and operationalized in a GIS environment by Mitasova et al. (1996a). It is an adaptation of the (Revised) Universal Soil Loss Equation (USLE/RUSLE) to scales larger than a farm field, and for and increased suite of overland flow processes[71] (Degani et al., 1979; Flanagan et al., 2003; Mitasova et

71 The USLE/RUSLE equation was developed as a tool for agricultural scientists to estimate the amount of erosion that would occur on a particular farm plot, given certain input conditions (Renard et al., 1997, 1991; Wischmeier, 1976; Wischmeier et al., 1971; Wischmeier and Smith, 1978). The *LS* factor of the USLE/RUSLE equation is essentially a way to estimate the erosive power (velocity) of running water across the farmplot, and is a combination of the ratio of the actual field length to the USLE experimental plot length (a constant) and a polynomial regression of the average slope across the entire plot. Although it is frequently used at landscape-scales, *LS* becomes increasingly meaningless as the scale of analysis increases. Substituting upslope accumulated area per contour width times the sine of slope for *LS* provides a valid way to include information about the erosive power of flowing water at these

al., 2001, 1996b; Renard et al., 1997, 1991; Singh and Phadke, 2006; Warren et al., 2005; Wischmeier et al., 1971; Wischmeier, 1976; Wischmeier and Smith, 1978). Although Moore and Burch (1986) referred to this approach as Unit *Stream* Power Erosion/Deposition, this name is somewhat misleading in the context implemented here, as the algorithm focuses on hillslopes, small watersheds, and small channels (i.e., rills and gullies). rather than streams, and is, in fact, *less* applicable to larger streams and rivers (Warren et al., 2005).

The USPED equation estimates the transport capacity (q_s) of flowing water at the cell, which is implemented in the MML as:

Eq. 4.18 $$q_s = R \cdot K \cdot C \cdot A^m \cdot \sin(\beta)^n$$

Where R is the rainfall intensity factor for the region [(MJ·mm)/(ha·hr·yr)] , and is computed by an equation that combines monthly precipitation amounts (Renard et al., 1997; Renard and Freimund, 1994). Values of R vary from 0 with no theoretical upper limit (although a practical upper range could be said to be between 20 and 30 with values much above 30 highly unlikely under terrestrial conditions). K is a soil erosion resistance factor [(ton·ha·hr)/(ha·MJ·mm)] based on the percent of sand, silt, clay, and organic matter in the soil. K is scaled from 0 to 1 (i.e., "not erodible" to "highly erodible"). C is a unit-less vegetation erosion protection factor based on the overall ability of different vegetation to hinder raindrops and surface flow, and to bind soil in place. C, like K, is also scaled from 0 to 1[72]. A is the upslope contributing area (flow accumulation per unit cell resolution) and β is again the topographic slope of the cell. The exponents m and n are empirically derived and vary depending upon the process being modeled[73].

Implementing the USPED algorithm in a GRASS script combines GIS modules for calculating slope, aspect, and upslope accumulated area using map algebra. Input data for the script includes a raster DEM of initial surface topography, soil erodibility (K-factor as a constant for uniform soil or a raster map for variable soil), vegetation cover (C-factor as a constant or raster map), and rainfall intensity (R-factor as a constant only). An underlying bedrock topography DEM is also input to provide a limit on the total depth of unconsolidated sediment that can be eroded[74].

---

larger scales.

72 R, K, and C in Equation 4.18 are the K-factor, C-factor, and R-factor of the USLE/RUSLE, which have been calculated empirically for a variety of settings in the Mediterranean (Boellstorff and Benito, 2005; Essa, 2004; Hammad et al., 2004; Martínez-Casasnovas and Sánchez-Bosch, 2000; Renard et al., 1997; Renard and Freimund, 1994; Wischmeier and Smith, 1978). See Section 4.5.2, above, for more information about how C-factor is derived.

73 For sheetwash (flow accumulation large enough for diffuse laminar flow of water), $m = n = 1$, whereas for rill/gully flow (flow accumulation large enough for concentrated turbulent flow of water), $m = 1.6$ and $n = 1.3$ (Mitasova et al., 2001).

4.7.3. Estimating Transport-Capacity in Streams

For flow in channels, the MML estimates transport capacity as a function of shear stress acting upon the channel bottom (Foster et al., 1972; Howard and Kerby, 1983):

Eq. 4.19 $$q_s = S_e \cdot K_t \cdot (\tau)^a$$

Where S_e is the annual number of storm events, K_t is a unitless transport capacity coefficient relating to the typical size of clasts in the channel (ranging from 0.001 to 0.000001, but typically 0.00001 for gravely, sandy-bottom streams), τ is the shear stress [Pa = kg/m^2], and a is and empirically derived exponent related to the type of transport in the channel (typically 1.5 for bedload, and 2.5 for suspended load).

Shear-stress is calculated according to the standard "reach-average" formula:

Eq. 4.20 $$\tau = g_w \cdot \tan(\beta) \cdot R$$

Where g_w is the hydrostatic pressure of water equal to $g \cdot p_w$ (g is the gravitational acceleration constant [9.81 m/s^2], and p_w is the density of water [10000 kg/m^3]), β is the topographic slope [deg], and R [m] is the hydraulic radius of the channel. In a GIS with perfectly square cells, R is best estimated simply as the channel depth (h) [m] (See Appendix A, Section A.1 for the method of calculating h).

4.7.4. Estimating Erosion/Deposition Potential from Transport-Capacity

Both USPED and the reach-average shear stress equation only estimate the transport-capacity (q_s) of flowing water at each cell. In order to determine the net elevation change (dz) predicted by these methods, the MML first must compute erosion/deposition potential (ED_p) at each cell. To do so, it assumes that the system is operating at full transport capacity, and that the divergence of q_s across the cells of a DEM in the downstream direction provides ED_p directly. In a GIS, this is done by finding the divergence in both the x and y directions (i.e., the two cardinal grid directions of a rectangular raster griding system), and summing to find the divergence in the most downstream direction (Mitasova et al., 1996a, 1996b; Warren et al., 2005):

---

74 Bedrock topography is created by the *r.soildepth.py* script, which implements soil-depth modeling as described in Chapter 5, Section 5.3.1. In *r.landscape.evol.py*, when bedrock is reached, it is assumed that no discernible erosion will occur in the time spans being modeled, so soil erodibility is set to zero.

Eq. 5.21 $$ED_p = \frac{\delta q_s \cdot \cos(\alpha)}{\delta x} + \frac{\delta q_s \cdot \sin(\alpha)}{\delta y}$$

Where q_s is the transport capacity as calculated by USPED or the reach-average shear stress equation, and α [deg] is the topographic aspect of a cell.

4.7.5. Converting Erosion/Deposition Potential to Net Elevation Change

Transport capacity, and thus ED_p, is calculated in units of weight per unit area per year ([T/ha.yr] for USPED, and [kg/m^2.yr] for the reach-average shear stress equation). However, in order to iteratively model erosion and deposition across a landscape over time, the calculated values of erosion and deposition must be re-expressed as depth of sediment per cell [m]. This is done by multiplying ED_p by its areal units (hectares for USPED, square meters per cell for reach-average shear-stress equation), and dividing by the unit density of the soil (p) [m^3] times the cell resolution (res) [m^2]:

Eq. 4.22 $$dz = \frac{ED_p \cdot u_a}{p \cdot r}$$

Soil density is approximated using the method outlined by Rawls (1983) combining the percentages of sand, silt, clay and organic matter. Like K-factor, soil density can be entered as a single value or a map of spatially varying values[75]. Although soil density is a spatially variable phenomenon,

4.7.6. Implementing Landscape Evolution

Landscape evolution is change in topography over time. The MML uses the estimated net elevation change (dz) in each year to represent these changes. But before implementing them, the we must know which process equation should be used to model net elevation change for each cell of the DEM. In other words, we must know which surface processes govern landscape evolution on each of the different landforms of the input landscape. Processes are not discrete, however, and there is a natural progression from diffusive soil creep (governed by raindrop force and gravity) to hillslope processes such as overland flow and rilling/gullying (governed by the strength of accumulated flow) to stream processes (governed by the strength of accumulated flow and turbulence). It is important to choose the optimal locations on the terrain for the transition between

75 Although *r.landscape.evol.py* has been programmed to accept a spatially varying soil density map, and such data is available for the Ziqlab Region (e.g., the SOTER soils data, see Chapter 5), the interface module of the MML has been programmed can only accept a single numerical value. Thus, I use a single soil density value of 1.2184, generated from empirical data by for Terra Rossa soils reported by Onori et. al (2006).

surface process models to ensure smooth transition in estimated net elevation change from one landform to the next. Although transition points vary with overall watershed geometry, area, and topographic relief, and also change during the course of a hydrologic event (e.g., as a function of rainfall intensity and duration during a storm), their general locations can be estimated in a GIS on the basis of upslope accumulated area (A) and topographic slope curvature (see Appendix A, Section A.2).

Once the location of flow process transition boundaries is determined, it is possible to use this geometry to paste together the *dz* maps produced by each process equation in a geomorphologically appropriate "global *dz*" map[76]. Although the process outlined in Section 4.7.2 above ensures that the MML uses realistic transition points between the different process equations, when the final "global *dz*" map is assembled, small linear aberrations in *dz* will be present across process transitions because it is still a "hard" boundary. Furthermore, larger aberrations in *dz* can occur at other points in the landscape when a process equation receives input conditions outside its underlying assumptions, or input numerical data which exceed its mathematical limits. While careful tuning of the equations and smoothing of the input DEM help to reduce the frequency and severity of such aberrations, they nevertheless still occur occasionally due to the abstraction required in the creation of digital topographic models. This is combated by an adaptive "soft-knee" limiter (a type of low-pass smoothing algorithm), that is calibrated to remove abnormal spikes or linear artifacts in the "global *dz*" map, while minimally affecting other areas (see Appendix A, Section A.3). The smoothed "global *dz*" map is then can be added to (for deposition) or subtracted from (for erosion) the initial DEM, to create a new DEM after a cycle of land-use and landscape change. This process is iterated at each cycle of the MML to simulate decades to millennia of landscape evolution.

4.8. Chapter Summary

This chapter has described the general scope and has detailed certain aspects of the inner workings of the Mediterranean Modeling Laboratory. The MML has been designed to study the types of agropastoral socio-natural systems that existed during the Neolithic period in the Mediterranean region, and thus the

76 It is important to note that this procedure must occur *after* the output of all the process equations are standardized to the same units of elevation change (*dz*) [m]. It would be extremely problematic to calculate the divergence of q_s across process boundaries because 1) each equation produces very different value of q_s for the same input conditions, 2) this is especially difficult across very large flow thresholds, such as between channels and adjacent slopes because of very high differentials between q_s as calculated down the slope bordering a channel and q_s calculated in the downstream direction within a channel, and 3) USPED and the reach-average shear-stress equation create output in different measurement units, so standardization would have to occur before calculation of flow divergence anyway, and 4) the diffusion equation produces *dz* directly, so this could not be included in the patched q_s map before calculation of divergence anyway.

MML provides a virtual space within which to conduct and empiric and replicable set of modeling experiments into the long-term effect of potential Neolithic subsistence systems. The character of the social and natural process equations described in this chapter reflect that purpose. Furthermore, the MML is designed specifically to study the long term consequences of subsistence land-use decision-making withing this type of socio-natural system. Therefore, the social modeling engine of the MML focuses on this aspect of Neolithic social systems, and purposefully chooses not to focus on other social aspects. This is also reflected in the scale of the social model (households versus individuals), which better reflects the social level at which most land-use decisions are made. The natural models are also designed with human land-use in mind, and the MML focuses on those aspects of the natural system that would be affected by, and would in turn affect human land-use decisions. Finally, the MML has been designed with multiple interconnections between social and natural phenomena, so that all events have repercussions, and these repercussions can drive the evolution of emergent socio-natural phenomena that could not be studied in any other way.

Table 4.1. Table of vegetation succession stages in the MML vegetation dynamics model, and their corresponding vegetation communities.

Land-cover Type	**Succession Stage (yrs)**	**Land-cover Type**	**Succession Stage (yrs)**
Bare land	0	Moderately dense maquis and small trees	26
Very sparse grassland	1	Maquis and small trees	27
Sparse grassland	2	Sparse young woodland and maquis	28
Moderately sparse grassland	3	Moderately sparse young woodland and maquis	29
Moderate grassland	4	Young woodland and maquis	30
Grassland	5	Young open woodland and sparse maquis	31
Grassland with very sparse shrubs	6	Mostly young open woodland and very sparse maquis	32
Grass and sparse shrubs	7	Mostly young open woodland	33
Grass and moderately sparse shrubs	8	Young open woodland	34
Grass and shrubs	9	Young open woodland	35
Shrubs and grass	10	Young open woodland	36
Shrubs and moderately sparse grass	11	Moderate open woodland	37
Shrubs and sparse grass	12	Moderate open woodland	38
Shrubs and very sparse grass	13	Moderate open woodland	39
Shrubs	14	Maturing and moderate open	40

		woodland	
Shrubs and developing maquis	15	Maturing and moderate open woodland	41
Developing maquis	16	Maturing and moderate open woodland	42
Developing maquis	17	Maturing open woodland	43
Maquis	18	Maturing open woodland	44
Maquis	19	Maturing open woodland	45
Moderately dense maquis	20	Maturing open woodland	46
Moderately dense maquis	21	Maturing open woodland	47
Dense maquis	22	Maturing open woodland	48
Dense maquis	23	Maturing open woodland	49
Dense maquis and sparse small trees	24	Fully matured woodland	50
Dense maquis and small trees	25		

Table 4.2. Table of equivalences showing between MML vegetation community/succession value and above-ground biomass (kg/m2). These equivalent values are used as breakpoints in the graphing function that converts between the two. Biomass values are determined from the averages of values reported by three independent studies in the Mediterranean region: De Jong et al. (2003), Rapp et al. (1999), and Terradas (1992).

Land-cover Type	**Succession Stage (yrs)**	**Biomass Value (kg/m2)**			
		De Jong et al. 2003	*Rapp et al. 1999*	*Terradas 1992*	Average
Grass with sparse shrubs	7	*0.095*	*	*0.1*	0.10
Maquis	18	*0.729*	*	*0.6*	0.66
Young Open Woodland	35	*0.67*	*0.75*	*0.8*	0.74
Mature Woodland	50	*1.689*	*1.66*	*2.5*	1.95

Table 4.3. Table of equivalences between MML vegetation community types/succession stages and C-factor values.

Land-cover Description	**Succession Stage (yrs)**	**C-Factor Value**

Bare land	0	0.1
Sparse grassland	2	0.08
Grass with sparse shrubs	7	0.05
Shrubs and sparse grass	12	0.03
Maquis	18	0.01
Moderately open woodland	37	0.008
Fully matured woodland	50	0.005

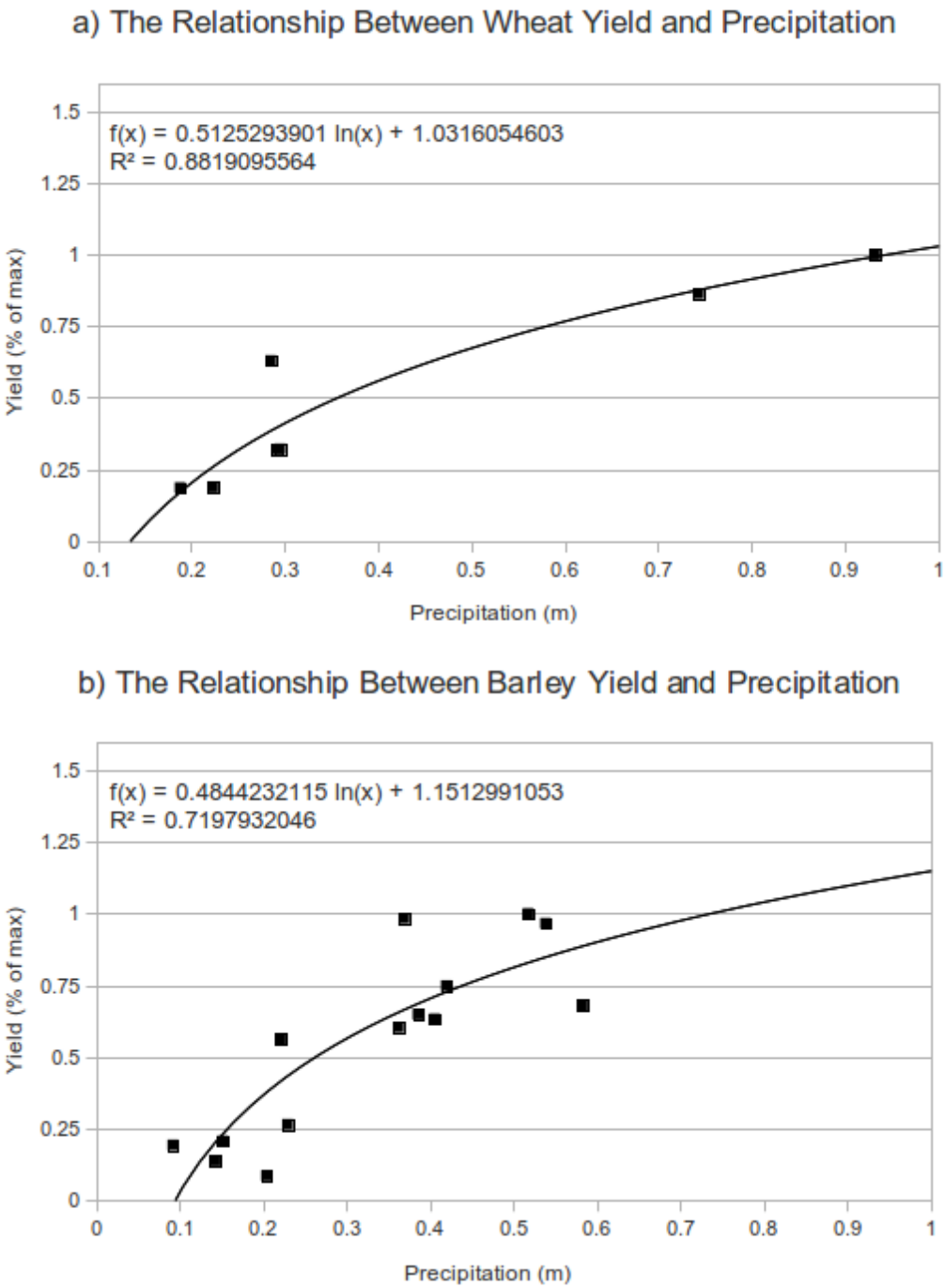

Fig. 4.1. The regressive relationship between precipitation and a) wheat yield, and b) barley yield. Data for these plots comes from Araus et al. (1997a, 1997b), Pswarayi (2008), and Merah et al. (2000).

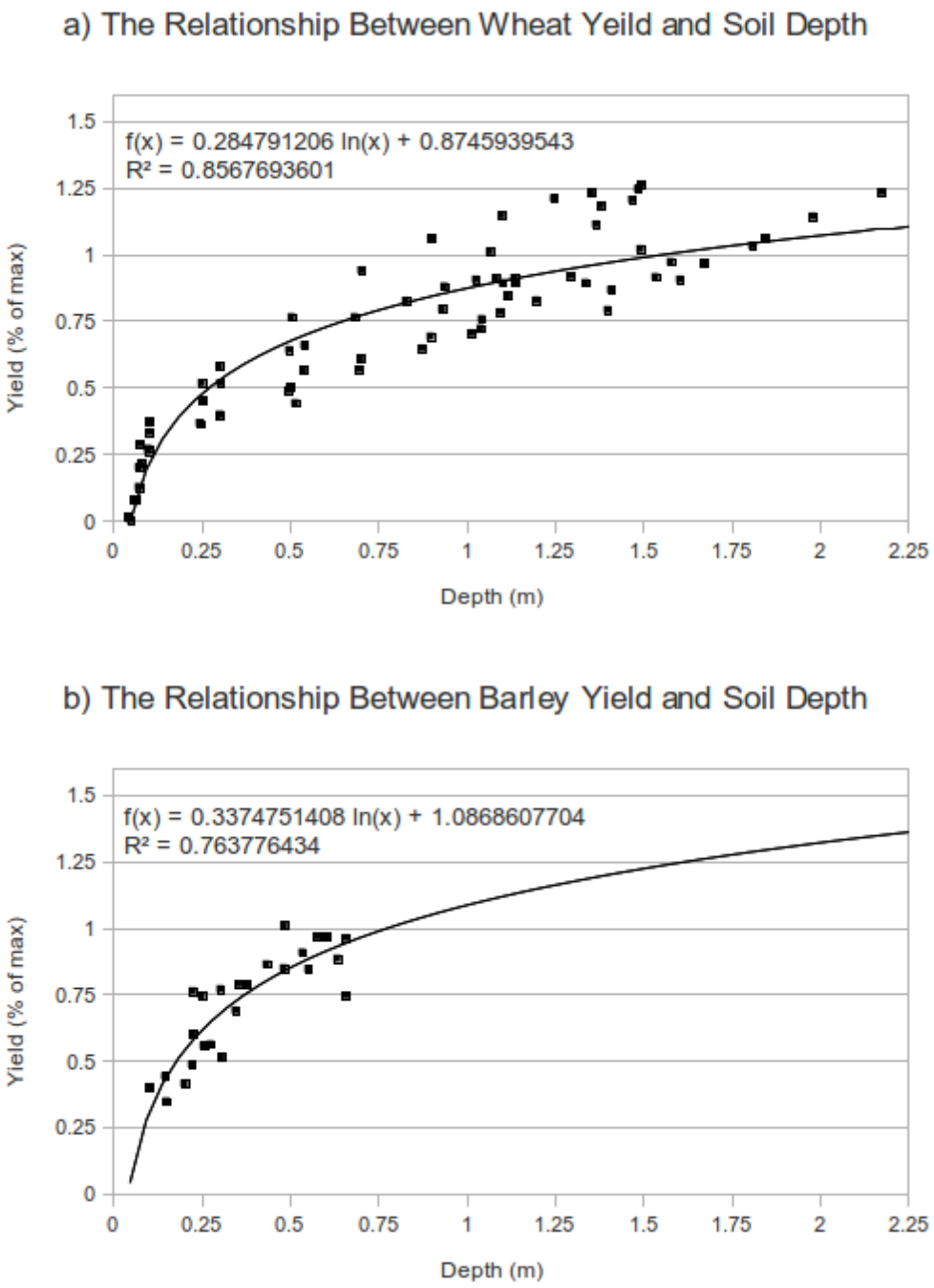

Fig. 4.2. The regressive relationship between soil depth and a) wheat yields, and b) barley yields. The data for these regressions comes from Wong and Asseng (2007) for wheat, and Carter et al. (1985) for barley.

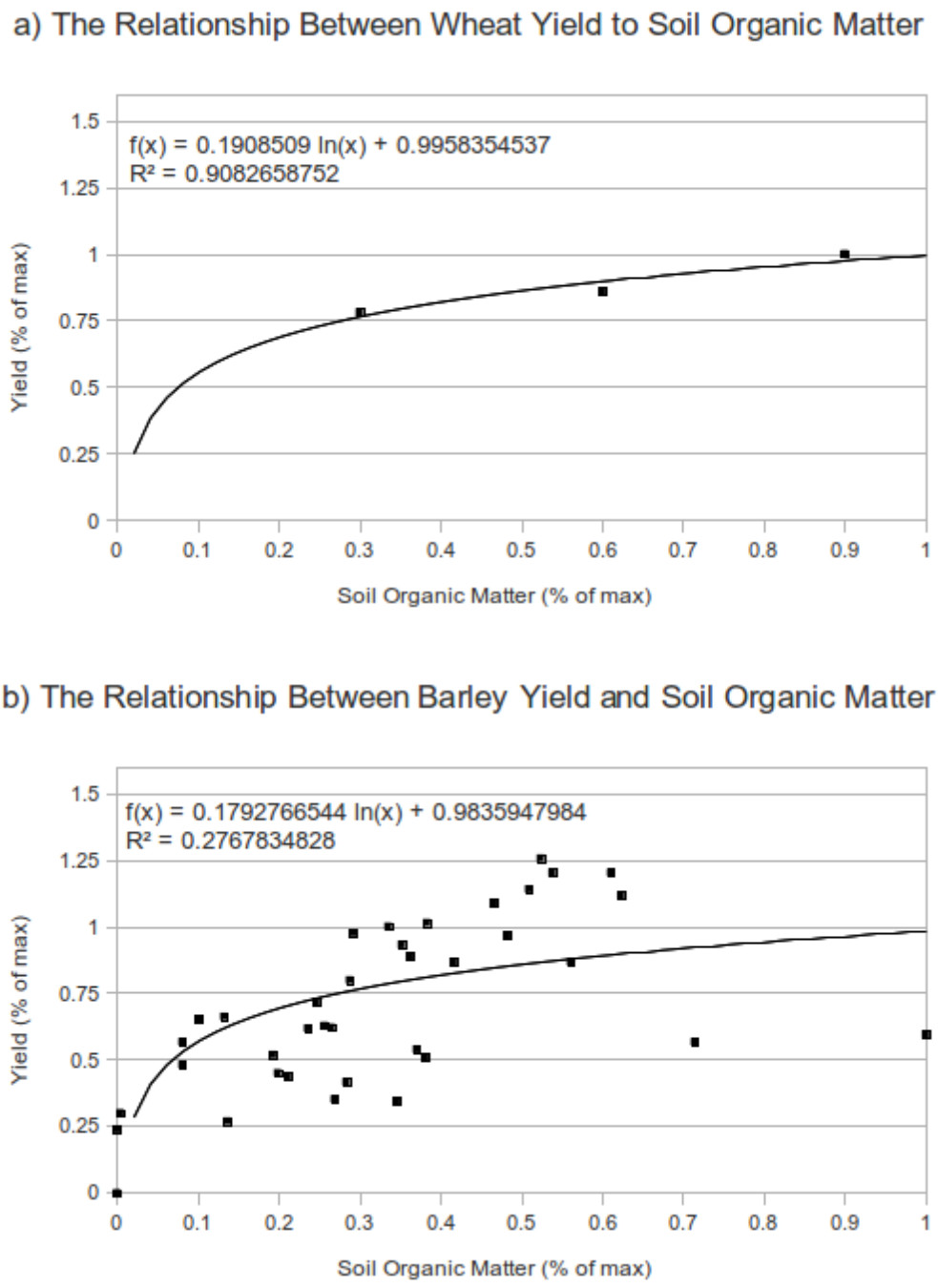

Fig. 4.3. The regressive relationship between soil organic matter (fertility) and a) wheat yield, and b) barley yield. The data for these regressions comes from Barzegar et al. (2002) for wheat, and Quiroga et al. (2006) for barley.

5. PALEOENVIRONMENTAL RECONSTRUCTION

5.1. Chapter Introduction

The modern environment is a product of thousands of years of complex human-environment interaction under changing climatic regimes. Thus it is inappropriate simply to use modern conditions as a direct analog for the environment in which Neolithic people lived. However, by using basic uniformitarian principles, it is possible to create a model of what the Neolithic environment might have been like. This procedure requires both purely inductive techniques (e.g., direct interpolation from proxy records), purely deductive techniques (e.g., modeled reconstructions based only on an understanding of environmental processes), and techniques that are both inductive and deductive (e.g., model-based reconstructions that also require some empirical input).

In its broadest sense, the "environment" can be construed to be everything external to a human agent. This vague notion is unhelpful for the kind of reconstruction needed for socio-natural simulation modeling. Thus, it is important to constrain the concept of "environment" only to those variables that have direct feedback within the simulated socio-natural system. In the simulation approach used in this study, I constrain the environment to 1) topography (the physical shape of the landscape), 2) soil (their depth, resistivity to erosion, and their fertility), 3) climate (macropatterning of temperature and precipitation), and 4) vegetation (the spatial and temporal patterning of plant communities).

Each of these variables needs to be reconstructed before dynamic simulation of Neolithic socio-natural systems is possible. It should be noted that the resulting reconstructions are "snapshots" – reconstructions of the landscape at specific points in time – and are thus static interpretations based the available proxy data and processual models I have chosen to use. However, these reconstructions serve as the starting point and backdrop for dynamic simulation and, thus, will have a large impact on the simulation results. This chapter details the processes I use to reconstruct these environmental variables as they might have been during the LPPNB/PPNC and the Yarmoukian, and provides an assessment of the reliability of the final reconstructions.

5.2. Reconstruction of Ancient Topography

The forces of erosion, deposition, and even tectonism can act on timescales short enough to have caused significant alteration of the physical geometry of the landscape over the Holocene. Thus, the topographic relief of region today is often quite different than it was in the not-too-distant past. A reconstruction of the Neolithic topography is therefore a vital first step in the modeling approach used in this study because it is important that agents in a

model of Neolithic land-use base their land-use decision on Neolithic topography, and not on the topography of today. Without a time-machine, it is impossible to recreate large areas of the Neolithic topography exactly; we can, however, identify remnants of Neolithic topography and areas that have changed since the Neolithic, and use this information to approximate the lay of the land as it was during the Neolithic period.

5.2.1. Landscape Evolution Research in Wadi Ziqlab

The construction of an explicit GIS-based reconstruction of an ancient landscape must be grounded in intimate knowledge of the landscape history of the region being reconstructed. Wadi Ziqlab is an ideal location for this, as the region has been the focus of several geoarchaeological research projects over the last several decades, including new research conducted by the author. The following subsections summarize the findings of previous and new geoarchaeological research, and provide a synthesis of Late Quaternary landscape evolution in the region.

5.2.1.1 Previous Landscape Evolution Studies in Wadi Ziqlab

In 1986-87, The Wadi Ziqlab Project began a systematic series of subsurface testing of alluvial terraces in the main Ziqlab drainage system (see Chapter 2). The LN sites of Tabaqat al-Bûma and al-Aqaba were discovered during this trenching procedure, and it was discovered that both sites were almost completely obscured from the surface by thick layers of overlaying colluvial deposits. Following the discovery of the two sites, Field and Banning (Field, 1994; Field and Banning, 1998) began geoarchaeological research into the interplay between geomorphology and archaeology in Wadi Ziqlab. The thrust of their research was to better understand the colluvial forces that buried Tabaqat al-Bûma and al-Aqaba, with an eye towards predictive modeling of buried Neolithic site locations. Their research thus focused on classifying the types of mass-wasting occurring in the Wadi, understanding the frequency and locations of wasting events, and interpreting the effects of colluvial processes on preserved archaeological material in the Wadi. In addition to examination of remnants of historic and ancient mass-wasting events, they were also able to study 290 new mass-wasting events that occurred in the Wadi during the winter of 1992—an especially wet year.

Field and Banning's research concludes that translational earth flows and rotational earth slumps are the main forms of mass-wasting in the Wadi, and that the frequency and severity of these events increases dramatically during especially wet winters—an observation corroborated by Farhan (1986) and El-Naqa (2001). They found that slumps tend to occur high on Wadi slopes near their rims and the Terra Rossa soils of the plateau. Some slumps do, however, also

form in “hollows” (incipient gully heads) where surface flow becomes concentrated. The slumps remain largely intact as they move rotationally along an arced surface of detachment, creating a characteristic crescent shaped “terrace” at their tops. The slumps also retain the internal bedding and sedimentary features of the original landforms from which they detached.

They found that earth flows, on the other hand, are mainly located in “hollows” or on the steeper mid-portions of the Wadi's slopes. Some 60% of these flows did not reach the Wadi bottom, and the 40% that did were the most fluid (i.e., had the highest internal water contents). The flows often carried displaced material 300 m or more, but were not particularly high-energy events. Flows had different levels of bedding and clast inclusions, which related to variations in flow turbidity, viscosity, and parent material, but many were so fine-grained that they resembled annual slope wash deposits. According to Field and Banning, it therefore appears like that it is these intermittent earth flows, rather than annual slope wash (or rotational slumping), that are the main depositional process responsible for burying the Neolithic sites located on remnant Wadi terraces. This is particularly important because it is likely that Neolithic sites were located preferentially on these terraces close to the valley slopes, and so tend to be covered more deeply than one would expect if only alluvial processes were at work (Banning et al., 1994).

Another team of researchers from Yarmouk University carried out a geoarchaeological study in Wadi Abu Ziad (the next drainage south of Wadi Ziqlab) during the storm events of 1992 (Al-Shreideh, 1992). This study mapped the relationship between hydrographic features and archaeological sites in the Wadi. Although the study mainly focuses on the changes in outflow of the perennial springs in the Wadi during storm events, it also describes the effects of flooding in the Wadi's washes, and documented bank erosion of some of the lower fluvial terraces in the Wadi. The study is important because it provides evidence that fluvial erosion is, and has been, a very important factor in reshaping the morphology of the wadi-bottoms in the Ziqlab region.

In the 2000's, Maher (2011, 2005, 2000; Maher and Banning, 2001) conducted new geoarchaeological work in the region, including a broad geoarchaeological survey of Wadi Ziqlab, Wadi Tayyiba, and Wadi Abu Ziad, and a detailed stratigraphic study of Wadi Ziqlab. Maher’s work, although mainly focused on the Epipaleolithic occupation of wadis, was formulated to better understand landscape change in the region, and so is a particularly helpful source of information for paleotopographical modeling in the region. Among the most helpful resources created during her work are geomorphological maps of the main Ziqlab drainage channel, geological cross sections of the Wadi at various points, stream-profiles diagrams of the main channel and major tributaries, and a collection of detailed stratigraphic drawings for several locations along the Wadi. This work also helped to define the relationship of the modern and ancient springs (identified from tufa deposits), the location and severity of headward incision of the channel during the Holocene, the location and general chronology of the

major fluvial and colluvial terraces, and also discovered several new archaeological sites from different periods. She identifies three major ancient river terraces, which, although not continuous, are found along the entire length of the Wadi: 1) a highly eroded, but generally contiguous upper terrace generally occurring 10-30 m above the Wadi channel, 2) a broad, flat, variably-eroded middle terrace that is 5-10 m above the Wadi channel and, and 3) a lower terrace that is only 1-3 m above the modern Wadi channel. Although Maher was *not* able to map the terraces over the whole region or to directly date their formation (e.g., by OSL), she *was* able to define a series of associations between archaeological sites from different periods and each of the terraces. The oldest materials recovered from the upper terrace are Middle Paleolithic[77], the oldest materials in the middle terrace date to the Epipaleolithic[78], and the lower terraces contain only secondarily-deposited Roman/Byzantine and modern artifacts.

Maher identifies four "knick points" in the main and tributary channels of Wadi Ziqlab where headward erosion has created steep drop-offs[79]. These knick points are very important for paleotopographic reconstruction in the region as they mark points of change in the relationship (and distance) between the Wadi channel and the remnant terraces. The highest knick point is found on only one of the two tributary forks of the Wadi at 750-800 masl, and is well within the upland region in the East. The second-highest knick point is found on both of the major forks at around 200-450 masl, and marks the boundary between the the gentle valley profile of the uplands, and the more incised profile of the lowlands. The final two knick points occur close together in the lower western end of the Wadi – very near two of the Neolithic sites – at 50-100 and 50-125 masl. These knick points likely correlate to the well-known series of four knick points that are found in many of tributary wadis of the Jordan Valley (on both its eastern and western flanks), which are known to occur at more or less the same elevation above sea level as those identified by Maher (Horowitz, 2001). Horowitz believes that the knick points formed during interpluvial periods that, though generally drier, were times when most of the precipitation fell in short thunderstorm bursts, which caused massive runoff and flooding and drastically increased rates of erosion. The sequence of knick points exists due to the interaction of the timing of these interpluvial periods and the rate of tectonic uplift of the highlands. The oldest two knick points (the two at that occur at the highest current elevations) formed around 2.31 mya and 1.75 mya respectively, and thus are quite ancient geomorphological features in the region. The lower two knick points date to 280 kya and 40 kya respectively, and thus were also already present during the Neolithic. Based on the difference in elevation between wadi outlets and the

77 These were surface-finds recovered during pedestrian survey.

78 The Epipaleolithic material is found in a buried red paleosol that is always overlain by an erosional unconformity, which itself is almost always overlain by Neolithic or Late Neolithic material in colluvial deposits.

79 These knickpoints are so steep that they form waterfalls in the portions of the Wadi that have perennial stream flow

lower knick point, Horowitz calculates a current uplift rate of 450 mm per thousand years, suggesting that the these lower knick points have been very active over the Holocene, and remain so today (see also Section 5.2.1.2, below).

Maher studied 15 exposed profiles in the Wadi to better understand its depositional history. The Terminal Pleistocene was apparently a period of fluvial terrace aggradation with stable surfaces evidenced by advanced pedogenesis. Most of the Epipaleolithic sites discovered in the Wadi are found in this paleosol, which is strongly correlated with the basal layers of the middle terrace. The following period was one of intense erosion, perhaps related to the dryer and more seasonally variable conditions of the Younger Dryas. A post-Epipaleolithic unconformity, present most prominently on the middle terraces, most likely dates to this period, which, as there are no remains of Natufian through PPNA sites preserved in the Wadi, likely lasted until the last phases of the PPNA or the earliest phases of the EPPNB. The unconformity is overlain in some places by a thinner layer of alluvium, characterized by smaller clast sizes than the earlier alluvial layers of the Terminal Pleistocene deposits. This thin layer is likely the only Early Holocene deposit in the Wadi, and consists of reworked material eroded from upstream terraces. In other areas, the unconformity is directly overlain by a massive grey colluvial layer. The earliest PPNB material in the Wadi – the basal levels at PPNB Tell Rakkan – rests directly upon the unconformity, and dates to the late MPPNB (see Chapter 2). All *in situ* PPNB and LN material in the Wadi is found fully within the grey colluvium, or in intrusive pits dug into the red colluvium. Thus, it is likely that the colluviation described by Field and Banning (1998) began in the MPPNB, and the Neolithic was a period of net colluvial aggradation on the middle terraces (although it seems that there were at least a few periods of alluvial erosion in the channel). The remainder of the Holocene saw alternating cycles of minor erosion and deposition, and witnessed the formation of the lower terrace in the current Wadi-bottom. Finally, although she did not conduct in-depth stratigraphic study of outcrops in Wadi Tayyiba or in Wadi Abu Ziad, Maher reports that due to differences in morphology, catchment size, and the history of human occupation, the depositional sequences in the three wadis are not the same. Thus the sequence of events documented in Wadi Ziqlab is not necessarily mirrored in the other two wadis.

5.2.1.2. New Geomorphological Fieldwork

In the summers of 2006, 2008 and 2009, I carried out additional geoarchaeological and geomporphological fieldwork in the Wadis Ziqlab, Tayyiba, and Abu Ziad (Figure 5.1). The purpose of the new field work was to expand upon the previous known information (see Section 5.2.1.1, above), to better understand landscape formation in Wadi Tayyiba and Wadi Abu Ziad, to identify and obtain OSL[80] and ^{13}C dating samples from different landforms in all

80 It should be noted that although several OSL samples were taken from various landforms and stratigraphic profiles in all three wadis, due to an issue with the OSL laboratory to which they

three wadis, to better understand the scale and morphology of remnant Neolithic landforms (see Figure 5.1 and 5.2, below), to better understand the patterning of soils and soil-depth in the region (see Section 2.3, below), and to obtain GPS ground control points with which to incorporate this data into a GIS (see Figure 5.2, below). Fieldwork focused on the middle and western portions of the Wadis in the regions that would have been utilized by the Neolithic inhabitants of the region, but portions of the upper (eastern) portion of Wadi Ziqlab were also studied. Three types of research were carried out: 1) systematic pedestrian and vehicular survey of portions of the wadi bottoms, hillslopes, and terraces (and GPS data collection), 2) targeted survey/mapping and GPS data collection at specific locations and landforms, and 3) stratigraphic analysis and OSL/^{13}C sample collection at known and new sedimentary profiles in each Wadi. Fieldwork was accompanied and expanded by intensive stereoscopic analysis of high-resolution (10-25 cm) declassified CORONA satellite imagery from the 1960's[81]. Higher resolution aerial photographs from the 1970's and 1980's and GeoEye (Google Earth) imagery from the 2000's supplemented the CORONA imagery where available.

Detailed results of this work are presented in Appendix B, but the most important data gained from this new research concern the extent of middle terrace remnants and soil depths on remnant landforms in all three wadis. A detailed map of middle terrace remnants was produced by digitization over high resolution imagery informed by field data collected during survey (Figure 5.2). The other important

5.2.2. Considerations for Paleotopographic Reconstruction in Wadi Ziqlab

The method of paleotopographic reconstruction to be used in the Ziqlab region must be able to deal to with several issues pertaining to the scope of this project. The first is the overall scale of the reconstruction. Although all the Neolithic sites are fairly tightly clustered in the middle and lower portions of the Wadi, the surface process model of the MML (see Chapter 4) requires the boundaries of the input DEM to be delineated by real drainage divides. Hydrological analysis in a GIS shows that Wadi Ziqlab stretches over 30 km from its headwaters to its confluence with the Jordan river in the West, narrowing from almost 7 km to less than 2 km in width along this traverse, and drains an area of almost 110 km^2. Adjacent to north is Wadi Tayyiba, which is nearly as long as Ziqlab, but considerably narrower along its entire length. Tayyiba tapers from slightly more than 3 km in its eastern headwaters to less than 1 km near its outlet

were initially sent, none of the samples have been dated at the time of writing

81 CORONA imagery served as the main remotely-sourced imagery source because it documented the area before many of the modern human alterations (e.g., road-building, agricultural terrace bulldozing) occurred.

into the Jordan Valley, and drains an area of only 56 km^2. To the south of Ziqlab, Wadi Abu Ziad is smaller still. At about 13 km in length, it is much shorter than both the other wadis and quickly tapers from a width of about 3.5 km in the upper reaches of its catchment to a width of less than 1 km at its outlet, draining an area slightly larger than 28 km^2. Preliminary site-catchment analysis using least-cost modeling shows that it is highly likely that Neolithic herders would have used grazing land in all three wadis (Ullah, 2011). Together, these three catchments drain an area of nearly 218 km^2 (Figure 5.1), and the Neolithic topography must be reconstructed across this entire area.

The second issue pertains to the degree of post-Neolithic landscape evolution that has occurred in the region. Fieldwork confirms that landform most positively identified with the Neolithic occupation of Wadi Ziqlab is the middle terrace, but the main topographic changes that have occurred since the Neolithic are extensive bank erosion of this terrace and mass-wasting of slope sediments onto it (see Sections 5.2.1.1 and 5.2.1.2, above). GIS-aided mapping of the extent of the middle terrace in all three Wadis shows that large stretches exist where the middle terrace is entirely absent (Figure 5.2). This is due to channel incision and lateral erosion, localized rilling on the terraces themselves, gully intrusion from adjacent hillslopes, and the expansion of tributary wadis in all parts of the drainage system. Furthermore, the surface topography of the remaining terraces remnants has been significantly steepened by Late Holocene colluviation, which has completely covered and obscured any smaller terrace remnants located at the foot of slopes. The method of paleotopographic reconstruction should be able to account for these types of landscape changes, and should also be adaptable enough to accommodate changes in the relationship between the current channel and the middle terraces over the entire length of the each of the wadis.

The third issue is the relationship of the scale of remnant landforms in the region with the scale of the digital terrain data used in this project. High-resolution topographic data (1m or greater), such as LIDAR or DEM extraction from high-resolution stereo imagery such as Quickbird or IKONOS, are desirable for detailed digitization of remnant landform geometry, but are unsuitable for use as a base for paleotopographic reconstruction for several reasons. Firstly, many of these data sources are prohibitively expensive, secondly, their extreme detail means that many modern alterations to the landscape (such as agricultural terraces and road cuts) and other artifacts (such as buildings and trees) obscure the basic topographic trends, and finally, such data are typically of restricted spatial extent. For much of the world – including the Wadi Ziqlab region – the best source of freely available, wide coverage digital elevation data is the 30 m-resolution ASTER GDEM2. This lower resolution is actually *better* for paleotopographic modeling, because many of the modern alterations and artifacts (such as trees and buildings) visible in the high-resolution data are absent or reduced in the GDEM2 due to spatial averaging. The GDEM2 has relatively low inherent spatial error[82],

82 The average vertical RMS error of the GDEM2 is 8.36 m, and the average horizontal RMS error is 0.104 arc-seconds (~ 3.21 m) in the EW direction and -0.175 arc-seconds (~ -5.40 m)

and is created from atmospherically corrected and calibrated stereo ASTER imagery with wide spatial coverage appropriate for watershed-scale paleotopographic reconstruction.

5.2.3. Existing Methods of Paleotopographic Reconstruction

There are three existing approaches to paleotopographic approximation. The most common technique is simple stratigraphic correlation using either basic analytical techniques like the type-fossil approach or simple sedimentary analysis, graphic or logical techniques such as the Harris Matrix, or even by using more advanced techniques such as absolute dating via OSL, C13 or other methods. This technique has the benefit of relative simplicity, but produces only a heuristic picture of ancient landscapes – typically in the form of graphical correlation of stratigraphic units.

Another method extends the level of detail and the usefulness of the basic stratigraphic correlation technique for use in spatial studies via interpolation methods in a GIS. Interpolation is a predictive technique that uses one of a suite of mathematical functions to approximate the value of unknown points based on the values of known nearby data points. When employed in a GIS framework, it is possible to use interpolation to "fill the gaps" between observed stratigraphic sections, thereby creating a continuous "trend surface" DEM of the "top" of the buried layer from a series of spatially segregated stratigraphic sections. Interpolation benefits from an abundance of known data points, so the most successful reconstructions derive from many sources of stratigraphic data, including natural sections, excavation units, geophysical survey, and augers (Chapman et al., 2009; Contreras, 2009; García Puchol et al., 2008; e.g., Lilburne et al., 1998; Prochnow et al., 2007). The technique can produce very detailed renderings of buried, missing, or otherwise obscured strata or paleosurfaces, but it is important to note that most studies that use this technique are focused on predicting the lay of buried surfaces or soil horizons on a single landform (or at most, a small collection of related landforms) in depositional contexts. Another drawback of this technique is that it is designed for the reconstruction of buried remnant patches of ancient surfaces, and thus is best suited for use in depositional environments, such as river valleys, deltas, and alluvial fans. As the spatial scale of interest increases—and in more erosive contexts—it becomes increasingly difficult to accumulate a sufficient quantity of stratigraphic observations of a particular buried stratigraphic layer (or correlated layers) to make good quality interpolation feasible.

A third technique uses interpolation in a broader, less constricted manner, and relies less on detailed stratigraphy and more on basic geomorphology. As outlined by Arrowsmith et al. (2006), the method requires detailed geomorphological mapping of the study region, so that landforms can be coded

in the NS direction (Tachikawa et al., 2011).

according to a chronosequence of depositional and erosive events, which are correlated to the archaeological sequence in the study area. Mapping can be accomplished via a combination of fieldwork and stereoscopic analysis of high-resolution aerial photographs or other remotely sensed data (e.g., LIDAR, Quickbird, SPOT, ASTER), and the map should delineate the major landforms at the highest resolution possible. The geomorphological chronosequence can be correlated to the archaeological time-line of the region via a combination of absolute dating methods (e.g., direct OSL or radiometric dating of sedimentary layers) and relative dating methods (e.g., the "type fossil" and other stratigraphic correlation techniques). The goals is to identify all landforms that have not experienced significant change since a particular archaeological period, and differentiate them from those parts of the landscape that have changed in the intervening millennia. These delineations are then digitized in a GIS, and used to extract the elevation data of the relatively unchanged portions of the landscape from a DEM of the modern surface. That information is then used to interpolate an approximation of the topography in the other areas. Because of its reliance on interpolation from portions of the current land surface, this technique is better suited for those regions that have experienced net erosion in the millennia succeeding the study period – such as downcutting alluvial systems or hillslopes that have experienced mass-wasting – where many remnant landforms remain unburied or at least relatively unaffected by subsequent deposition.

5.2.4. A New Method for Reconstructing Paleotopography

Each of three existing methods of paleotopographic conditions satisfy some of the necessary conditions and requirements for landscape reconstruction in this project, but none of them satisfy all. Thus, I have developed a new method that borrows appropriate techniques from each of the existing methods, but introduces some new techniques to fully satisfy the requirements of paleotopographic reconstruction in the project area.

The first step in the new process is to use high-resolution stereoscopic imagery (CORONA, aerials, Google Earth Geo Eye) to create a digitized map of remnant portions of the middle terrace and the locations of knick points, narrows, and other flow-regime changes. These higher resolution data may not align absolutely with the GDEM2 data, however, so direct translation of the digitized area is not possible. This is because the median size of middle terrace remnants in the Tayyiba, Ziqlab, and Abu Ziad drainages is about 7, 5, and 2 GDEM2 raster cells, respectively (Table 5.1 and Figure 5.2). This small number of raster cells means that the geometry of many of the remnant terraces will be poorly delineated at the native 30m GDEM2 resolution, and small translational errors in terrace digitization could lead to the inclusion of GDEM2 cells not belonging to the landforms digitized from higher resolution imagery. Therefore, the digitized terrace outlines are only used as a "guide" for an automated identification of the area below the terrace edges, which are then removed and interpolated over, as in

the third procedure in Section 5.2.3 above. The automated procedure thus relies solely on the GDEM2 topographic data, and so avoids the introduction of translational errors between data-sources or resolution-induced sampling errors.

Resolution errors are further combated by decreasing raster cell size with a Regularized Spline-Tension (RST) interpolation from the native 30 m of the input GDEM2 to a 10 m resolution in the output raster[83]. RST interpolation connects input data points with all other points via "spline" functions, which can be "tuned" by manipulation of "smoothing" and "tension" parameters (Mitasova and Mitas, 1993; Neteler and Mitasova, 2007b). The smoothing parameter affects how closely the splines must pass by data points, whereas the tension parameter affects the overall "stiffness" of the splines themselves. Reducing the raster cell size during the interpolation allows for smoother, more detailed, topographic modeling than is possible at its native 30 meter resolution, but it is important to remember that such interpolation cannot "add" data not collected at the original resolution; that is, the extra detail added by interpolation is only a model, informed by the data that was originally collected by the sensor at its native resolution, and carried out according to the parameters of the RST run (i.e., the "tension" and "smoothing" values) (Mitasova and Mitas, 1993). The approximating properties of RST interpolation are actually beneficial for certain aspects of paleotopographic approximation, and so RST is an integral component of the reconstruction in its own right. For example, by setting the tension and smoothing parameters to increase spline stiffness and decrease the influence of individual points in the local neighborhood in the RST interpolation results in a new DEM of the project region that has gentler slopes and softer topographic breaks, which better approximates the original geometry of the wadi slopes and remnant alluvial terraces before the increased colluvial activity of the Late Holocene.

The remainder of the automated procedure involves a combination of hydrological modeling and cost-surface approximation techniques to delineate areas of the landscape that are most likely to be related to recent/current fluvial activity, or which are likely to be newer than the time-period in question. The first step is to understand current fluvial activity in the wadi system, and is accomplished via GIS-based hydrological modeling. I advocate for a hydrological modeling engine that uses a multidirectional flow-routing algorithm (MFD) to estimate the flow of water across the landscape[84] (Neteler and Mitasova, 2007b).

---

83 A resolution of 10m was chosen as a compromise between precision and model run-time. Although it is important to have a raster resolution that is high-enough to reasonably replicate the scale at which most fluvial process occur (i.e., the width of gullies or streams), increasing resolution exponentially increases the number of cells, and thus the number of calculations that must be done every simulation cycle. A 10m cell resolution allows for a reasonable increase in the resolution of modeled fluvial process, while only increasing the size of the base DEM to about 5 million raster cells. This translates to a 3-4 minute run-time per simulation cycle – an acceptable compromise. RST interpolation is implemented in GRASS via the v.surf.rst module.

84 Multidirectional flow routing is implemented in GRASS via the r.watershed module.

MFD routes a proportion of the outflow from a cell to all downslope cells – scaled according to the degree of elevation difference – and thus produces more accurate/realistic modeling of flow lines than does a simpler "D-8" algorithm that can only route flow to the single-most downslope cell. MFD results in a realistic map of the accumulated flow in all parts of the landscape (Figure 5.3).

The main regions of current or recent fluvial activity are typically 1) gullies and washes, 2) the active channels of small tributary wadis, 3) the active channel and active floodplain/terraces of the main wadi itself. In most of these landforms the modeled flow patterns produced by the MFD routine are typically diffuse; that is, these landforms are generally defined by the presence of active flow across their entire surfaces. Thus, the isopleth that delineates all flow accumulation values higher than a particular threshold for that landform[85] also delineates the geometry of these landforms themselves, and so these landforms can be "automatically" digitized via a boolean map algebra statement. In the main wadi drainages, however, the nature of flowing water is to "concentrate" in the central channel, and this is reflected in the results of the MFD flow-modeling routine. In these areas, the focused flow means that the thresholding approach tends to only define the active channel itself, and cannot define the boundaries of the active floodplain or any alluvial terraces that are newer than the period in question, so an additional step is required to "automatically" digitize these landforms. This "next step" takes the form of a cost-surface approximation procedure that is based on the topographic relationship of floodplains and terrace risers to the active channel. Floodplains are typically flat (or slightly "backwards" sloping), and are separated from the active channel by levies or risers. Relict alluvial terraces are typically remnants of such floodplains that are now left stranded above the current active plain by subsequent channel incision. Thus, assuming a locally uniform amount of incision, all correlated relict terraces and floodplains in a particular portion of the drainage network should be found at the same height above the active channel. Directly measuring height-above-channel in a GIS is difficult, but can be approximated by the "accumulation" of slope over horizontal distance as one travels perpendicularly away from the active channel. This is achieved in a GIS by using the channel line as derived from the MFD hydrological model as a series of starting points for a "walking cost" approximation routine that calculates the cost of travel from the starting point(s) to all other points on the landscape along the route of least resistance. Costs are calculated from an input map of the cost it takes to traverse each cell. In this case, the "cost" of traversing a cell is the linear distance of the cell from the active channel, multiplied by the topographic slope of that same cell[86]. A threshold/cutoff can then determined on this output "cost-surface" map

85 The different thresholds in modeled flow accumulation for each of the specific landforms must be determined by "trial and error" experimentation for a given area under a given type of environment and climate.

86 Note that in future approximations, a better measure of cost for this application is the accumulated gain in elevation as each cell is traversed. A map of local elevation gain at each cell can be calculated as the cell-resolution times the tangent of slope.

approximately delineates all cells below a certain height above the channel, and the isopleth thus formed can be extracted via a boolean map algebra equation. Again, trial and error experimentation is required to obtain a reasonable result; the thresholding cost-value will be different for different drainages in different environments and climates, and will also change according to the position of the particular wadi segment in the drainage network.

5.2.5. Neolithic Paleotopographic Reconstruction of the Ziqlab Area

Using the techniques described in section 5.2.4 above, and knowledge of the locations of various narrows, widenings, knick points, wadi confluences, the outlet points for the three wadis (see Appendx B), and those terraces that have known Neolithic material from Section 5.2.1 (Figure 5.2), I was able to delineate those portions of each wadi that are likely newer than the Neolithic (Figure 5.4). Once these areas were identified, digitized, and removed from the base GDEM2, RST interpolation was used to create a new "paleoDEM" (Figure 5.5).

It is useful to compare the original GDEM2 topography with the simulated paleotopography. Figure 5.5 shows side-by-side 3-D views of the original GDEM2 and the interpolated "PaleoDEM". The first thing of note is that the interpolation routine smoothed the topography in the plateau region and in the wadi bottoms. Much of the "roughness" in the GDEM2 likely stems from trees and human structures, so the smoothing affect likely helps to remove these types of modern artifacts from being included in the digital topography. Some of the GDEM2 roughness may also be due to erosion scars in these landforms, which tend to cause "lumpy" terrain. Again, the interpolation routine removes these features, which is appropriate for the purposes of the reconstruction. It is also clear that the interpolation flattened the bottom of the Wadi significantly, and the incision below the Tell Rakkan knickpoint is less intense than on the GDEM2. Figure 5.6 shows another set of 3-D views of the PaleoDEM, this time colored by the amount of elevation change from the GDEM2. This is a useful heuristic to help confirm the nature of the paleotopographic reconstruction on the different landforms in the project region. Using this heuristic image, we can confirm that the wadi-bottoms have indeed been filled in, and that the sections below the knickpoints have been filled in more (up to about 30 m in some places) than those above the knickpoints. The general smoothing effect in the plateau region seems to be from both the flattening of "lumps" as well as the filling in of "pits". There also seems to be a small degree of spatial patterning in the location of these artifacts, with "lumps" being located preferentially in the interior of the plateaus, and "pits" being located preferentially near gully incisions. This patterning lends credence to the assertion that the "lumps" are likely houses, trees, or other protrusive human-made features, and that the "pits" are likely erosion scars.

We can also see that the interpolation has extensively reshaped the slopes as well. The colluvial deposits of the later Holocene have been removed at the foot of slopes, returning them to morphologies more similar to those of Neolithic

landscapes. The upper slopes have also been modified, and material has been removed from the plateau edges. While the removal of material in these areas seems counter to our goal of paleotopographic reconstruction (i.e., we ought to be *adding* material in these areas, rather than removing it), this procedure does shape the morphology of these features in a way that is similar to their supposed Neolithic form before substantial removal of material by colluviation and mass-wasting (i.e., softer slope breaks at the edges of the plateau, and gentler slopes overall).

5.3. Reconstructing Ancient Soils

There are three properties of soils that are important in the MML: 1) their depths, 2) their resistivity to erosion, and 3) their fertility. Because all three of these properties may have changed considerably over time, it is imperative to the success of the modeling endeavors undertaken in this research that the conditions of these soil properties be reconstructed as they might have been at the start of the LPPNB.

5.3.1. Sources of Soil Data in the Region

The earliest soils research carried out in Wadi Ziqlab was a rough summary of soil and bedrock types in the Wadi carried out in the late 1960's by Fisher et al. (1966), and was based largely on aerial photographic data with minimal ground truthing. This research produced the only high-resolution soil (Figure 5.7) and bedrock (Figure 5.8) maps currently available, but unfortunately they only cover the main Ziqlab drainage itself. The highest resolution full-coverage geological map of the region is a 1:200,000 map from the Israeli Geological Survey (Sneh et al., 1998), and the highest resolution full-coverage soils map of the region is the 1:500,000 revised Soils and Terrain (SOTER) map from the International Soil Reference and Information Centre (Batjes et al., 2003). Although these maps are admittedly coarse, they nevertheless remain the only source of digitized full-coverage spatial soils and bedrock data available for the project region, and so, supplemented by field work conducted by Maher (2011, 2005) and by the author (see Section 5.2.1, above), form the starting point for the GIS-based paleosoil reconstructions described in this section.

5.3.2. Modeling the Depth of Soils Across the Landscape

Due to extensive soil loss in many areas, and the accumulation of colluvial sediment minimally affected by pedogenesis in others, modern soil depths bear little resemblance to those of the early or middle Holocene. Modeling the depth of soils (i.e., depth from surface to bedrock) on the landscape is important both for surface-process simulation and for simulating agricultural output and vegetation

regrowth. Many factors affect the depth of sediment in any location in any given time, such as climatic conditions, vegetative cover, the position of the landform in the landscape, and the overall age of the landform/landscape in general. The two main processes that change soil depth are sediment transport (erosion/deposition) and regolith production (subsurface weathering). Despite a significant amount of research into the relationship of environment, surface processes, and bedrock weathering rates (Braun et al., 2001; Burke et al., 2007; Dietrich et al., 2003; Heimsath et al., 2002, 2001, 2000, 1999, e.g., 1997; McBratney et al., 2003; Minasny and McBratney, 1999, 2006), there exists no clear consensus for a single algorithm or procedure for predicting soil thicknesses across an entire landscape. The situation is further complicated by the fact that soil depths are the product of many interacting physical, chemical, and biological processes, and so the depth profile of each landscape is sure to be different, if not completely unique. Regardless of these complexities, a variety of approaches have been taken: from simulated landscape evolution over thousands of years (Minasny and McBratney, 2006) to basic extrapolation from existing soil profiles (Förster and Wunderlich, 2009). I employ a technique that is intermediate between these two extremes—implemented in a script for GRASS ("*r.soildepth.py*")—to create "soil depth" maps across varying topography. The method encapsulated in the script takes advantage of the known relationship between various derivatives of topography (slope and curvature) and local soil depths. The basic relationship is non-linear (Heimsath et al., 2002), but can be simplified to the following general rules[87]: 1) All else being equal, soils tend to be shallower in areas of high slope, and deeper in areas of low slope, and 2) All else being equal, soil depths tend to be shallower in areas of high topographic convexity, and deeper in areas of high topographic concavity. The method I have developed uses these topographic rules to first construct a map of idealized soil depth "rates" across the landscape, which is then rescaled according to the known minimum and maximum soil depths in the study region (See Appendix A, Section A.4 for how soil depth "rates" are calculated).

5.3.2.1. Modeling Soil Depths in Wadi Ziqlab

During the geoarchaeological fieldwork described in section 5.2.1.2 above, I examined remnants of undisturbed Terra Rossa soils in the uplands of the Ziqlab catchment near the hilltop town of Tubna, reworked Terra Rossa soils on the agricultural plateau below the town of Dayr Abu Said, and several soils on the terraces in Wadi Ziqlab itself. The best intact Terra Rossa soils are found only in the upland areas under forested conditions. Mild to moderately reworked Terra Rossas are found in most other areas of the uplands and the lower plateau, where agriculture, forest clearance, and intensive grazing have significantly altered the land cover. Soils on these remnant landforms were observed to be between 0 and ~20 m in depth. The modeled Neolithic paleotopography (created as described in

87 It should be noted that these rules, and this method of soil-depth estimation, are meant for landscapes dominated by fluvial and/or colluvial processes. This method is not appropriate for use in landscapes dominated by other processes (e.g., arctic tundra, dunes, glaciated slopes).

Section 5.2, above) served as the base input to the soil depth estimation function. Without access to any real empirical information on the particular baseline relationships between slope, curvature, and soil depths of all parts of Neolithic Wadi Ziqlab, I calibrated the soil-depth approximation function to those remnant landforms I observed during fieldwork.

Figure 5.9 shows the resulting Neolithic soil depth map derived from these initial conditions. We can see that the deepest soils are in the Wadi-bottoms and flat plateau region, and the shallowest soils on the hillslopes. This pattern aligns with our understanding of the way soil depth patterns across the landscape, and provides a reasonable soil-base for the start of the LPPNB. The one abnormal pattern present in the model is that Wadi-bottoms and the flat plateau areas appear to have similar depth profiles. This is due to the inability for the soil-depth estimations routine to differentiate between flat areas at the bottom of a basin (e.g. the Wadi-bottoms) that would receive a large amount of sediment input, and those in elevated locations (e.g., up on the plateaus) that wouldn't receive much sediment input at all. The presence of deeper-than-normal soils on the plateau region is not overly vexing, however, as these very flat areas are likely not very susceptible to erosion anyway, and clearly retain a significant proportion of their ancient Terra Rossa soils even to this day (Chapter 3).

5.3.3. Modeling Soil Erodibility

Other than their depths, the other two soil properties having an effect in the models are their resistivity to erosion and their fertility. In the MML, soil resistivity to erosion is measured as the K-factor used in the well-known RUSLE equation, and measured in units of volume of erosion per unit erosive force (see Chapter 4). Measuring K-factor directly is difficult and costly, so it is usually estimated from measurable soil properties. The method most commonly used today is to use a lookup table, such as the one provided by Stewart et al. (1975), which is the method I use in this research. This method requires the soils to be first classified according to the USDA standard soil texture, which can be calculated by the USDA's online Soil Texture Calculator software (USDA, 2012) from standard soil-texture data (percent sand, silt, clay, and organic matter in the matrix).

Because soil texture and K-factor vary spatially, it is very important that the soil data be spatially explicit (i.e., GIS-compatible). The scale of the data is also important. Although very spatially detailed soil data with many subdivisions of soil types (e.g., Fisher et al., 1966) would seem to be preferable, it is counter-intuitively inappropriate to use these high-resolution data when modeling the spatial patterning of soils in the past. This is because the finer-scale patterning of soils likely has more to do with localized (and perhaps anthropogenic) erosion of ancient soils and subsequent formation of a variety of (often anthropogenic)

younger soils on redeposited material over the intervening millennia[88]. Many of the finer subdivisions of soil-types may thus be "artificial" in that they did not exist in the early Holocene, so using spatially coarser data with fewer subdivisions of types results in a more generalized K-factor map that avoids the error of creating soil variations that did not exist in the past.

The SOTER soils geodatabase (Batjes et al., 2003) best meets these criteria, and so serves as the input soil data source used in the models presented in this research. The SOTER soil data is encoded as discrete vector polygons, attached to a database with detailed soils information, including all the textural data needed to define the USDA soil texture category. I recoded the polygons according to K-factor value determined from the lookup table in Stewart et al. (1975), and then converted the map to raster format. Because of the way the original data were encoded, the boundaries between soil units are unrealistically sharp. This is problematic, as sharp boundaries will cause the landscape evolution equations (Chapter 4) to become unbalanced during calculation of flow divergence, which tends to result in the calculation of unnaturally large amounts of erosion or deposition "spikes" in these areas. Furthermore, the coarseness of the input data (SOTER is 1:500,000) means that the geometry of these borders is also unrealistic, consisting of several long straight lines connected by sharp angles. Both of these issues can be ameliorated through a multi-stage smoothing process. First, several decreasing scales of modal moving-window filters are applied to the map, which smooths the sharp angles of the borders into gently arcing curves. The sharpness of the borders is then blurred by applying a moving-window mean-smoother with a large cell neighborhood. The resultant soil borders are unrealistically smooth with very simple geometries. In the "real world", soil borders are typically complex and are often convoluted or "fuzzy" (Burrough, 1989; Burrough et al., 1992). Realistic "fuzzy" border geometry is modeled by introducing stochastic "jittering" in the border regions[89]. The resulting borders are more complex and realistic than those of the input data, allowing a more naturalistic transition between one soil unit and the next without inducing artificial "boundary effects" in the landscape evolution equations (Figure 5.10).

5.3.4. Modeling Soil Fertility

The fertility of agricultural soils has a large impact on agricultural yields (see Chapter 4). Thus, it is important to model the spatial pattering of variation in fertility of the soils present in the Ziqlab region. The modern inhabitants of the

88 Empiric research indicates that this seems to be true in northwest Jordan (Khresat et al., 1998b).

89 This is achieved by first temporarily transforming the raster soil to a vector points map with each raster cell assigned to a unique point. The geometry of this temporary vector points map is then "perturbed" by adding a Gaussian random value to the X and Y coordinates of each point (in this case with μ of 0 and θ of 80 m). The "perturbed" map is then translated back to raster format, and a medium-sized median moving-window filter is applied.

Ziqlab region exhibit clear preferences for doing agriculture on specific soils; they prefer to plant non-irrigated cereal crops on the reworked Terra Rossa soils of the western plateau, and on the brown stony soils of the lowest terraces in the wadi bottoms. But non-irrigated cereal crops are also planted on all other the soils of in the region, including the colluvial soils and rendzinas of the limestone slopes. However, it is unclear if these modern preferences relate only to the fertility of these soils, and not with their other characteristics such as ease of plowing, amount of field stones, or proximity to modern villages and roads. The SOTER data, and the data collected by Fisher et al. (1966) suggest that modern soils in the Ziqlab region do contain differing amounts organic carbon and nitrogen, the two hallmarks of soil fertility for plant growth. However, a study of different soils in Northern Jordan suggests that most modern soils actually contain a similar – and low – amount of organic matter, ranging between 0.5% and 1.1% (Khresat et al., 1998a, 1998b). Furthermore, a comparative study of soils in the Ajloun region (a few kilometers south-east of Wadi Ziqlab) shows that soil organic material decreased by 30% after 50 years of continuous rainfed annual wheat and barley cultivation compared to a neighboring plot that retained the native pine/oak forest cover over the same period (Khresat et al., 2008). Although there was no significant difference in Potassium and Nitrogen content between the two soils, the farmed plot did show significant increases in soil bulk density and and soil pH, and significant decreases in cation exchange capacity. In general, the cultivated soils were found to be significantly depleted of nutrients after 50 years of continuous cropping[90]. These contrasting reports further confuse the matter, but would seem to suggest that differences in soil fertility are largely anthropogenic. In any case, it is highly unlikely that modern patterns of farming soil fertility decline exactly match those that may have been induced by the Wadi's Neolithic inhabitants, who lived in different locations, had vastly different farming technology than do today's occupants (e.g., no plows, fertilizers, or other modern conveniences), and who farmed very different varieties of wheat, barley, and pulses. Furthermore, many of these modern soils were likely not present in the Wadi at all during the Neolithic, especially the colluvial soils that now cover much of the ancient river terraces where Neolithic farmers would likely have planted their crops.

So, like soil texture, modeling the spatial patterning of ancient soil fertility is complicated by the fact that modern patterns of soils—and thus fertility—are unlikely to be similar to those of the distant past. Thus we are faced with two complications: 1) high-resolution modern soil maps are inappropriate because many modern soils likely did not exist in the Neolithic, or had very different spatial pattering, and 2) modern soils likely have drastically lower amounts of organic carbon and nitrogen than did ancient soils. In light of these complications, the best solution is to assume that all soils in the Neolithic were at 100% of their respective fertility, and this is approach that I have used in the models presented in this research.

90 This is supported by an earlier study in the area around Irbid (also very close to Ziqlab) by the same research team (Khresat et al., 1998a).

5.4. Paleoclimate Reconstruction

Climate variables—especially temperature and precipitation—play an important role in both natural processes (affecting things such as erosion rates and vegetation growth rates) and social processes (affecting things such as farming retunrs and grazing patch rejuvenation). Climate is essentially a "moving average" of weather conditions that represents the "typical" weather of a region, and its changes over time. It is important for the research presented here to reconstruct climatic conditions as they were during the Neolithic, rather than today, for use as input into the social and natural systems models used in the MML.

5.4.1. Methods of paleoclimatological modeling

There are several methods for estimating climatological conditions in the past, but they can be broken down into two general types (Bradley, 1999): 1) estimates derived from proxy records, and 2) estimates based on atmospheric physics. Proxy records include things such as pollen cores, ice cores, glacial varve records, cave speleothems, tree ring sequences, and deep-sea cores, all of which provide indirect evidence for past climatic conditions in their catchment zones (such as the composition of gases trapped in ice bubbles, the thickness and chemical composition of tree-rings, and the species composition and abundance in pollen cores or diatomaceous sediment samples).

Proxy records are widely used to gain a general understanding of how climate changed in the past, but there are some problems with using them to reconstruct the climate of a particular location (Bradley, 1999; Campin et al., 1999; Mcshane, 2011; Wilson et al., 2005). Firstly, because many proxy records are composed of material drawn from very large catchments (especially deep sea cores and pollen records), they are highly subject to problems of scale. That is, it becomes difficult to understand the meaning of particular changes in the proxy (e.g., species abundance), when the size of the catchment becomes very large. Secondly, proxy records suffer from locational biases. Such records are only preserved in very specific locations, where all the necessary conditions for the production and preservation of the record exist. For example, pollen records require a moist anoxic environment in order to be preserved, and so can only be found in places like fens, bogs, and lakes. This locational bias means that most of the time, the nearest proxy record is at quite a distance from the location of a particular archaeological site or study area, and so may not perfectly reflect the climatic conditions of that site. Thirdly, the temporal resolution and temporal accuracy of the resultant climate reconstruction depends on the temporal resolution and temporal accuracy of the proxy record. If the proxy record is coarse (such as pollen records recovered from disjointed layers or features at and archaeological site), or if the dating method used to chronologically order the data

is coarse or contains high inherent error (such as radiocarbon for certain periods and materials), then the climate reconstruction based on these data will be correspondingly coarse or inaccurate as well. Fourthly, many proxy records, especially those based on plant or animal remains, can be affected by non-climatic processes, including human alteration of the environment (e.g., by intentional burning or clearance). Finally, although it is arguable that reference to multiple proxies should be used to provide a more robust and fine-grained picture of past climate, many of the existing records are incompatible due to methodological differences (e.g., in classification of species, in dating methods, in sampling strategy), and so cannot be combined or even directly compared in a meaningful way. These issues make it quite difficult (but not impossible) to use proxy records directly in the type of socio-natural systems modeling of the MML. These proxy records nevertheless provide historical data that may be directly related to climatic conditions, and so are useful to use as comparative "checks" on the accuracy of other methods of paleoclimatological estimation. Many of the extant proxy records in the Southern Levant can be found in Robinson et al. (2006).

Simulation modeling based on atmospheric physics is an alternative and widely accepted method for estimating past climatic conditions. There are a several different specific methods of paleoclimatic simulation, however, and each has its own merits and difficulties. Most methods fall into a general category of models that are known as General Circulation Models (GCM's), spatially explicit models that simulate the circulation of ocean and atmospheric currents in order to estimate global- or continental-scale past climate conditions[91]. One downside of GCM models is that their global or continental scope make them computationally very intensive, and so typically they are run at very coarse spatial and temporal scales. "Fine" resolution GCM climate models have cell-sizes of 10 km or more, which makes it difficult to estimate the climate in a particular location. While this particular issue does *not* in itself preclude the use of climatological values retrodicted ("hindcasted") by a GCM paleoclimatological model in the MML, it is a symptom of another issue with GCM modeling that *does* have ramifications for its use in the MML. GCM models are based solely on an understanding of broad-scale climate, and so do not, and cannot, include local information, even if there are well known localized variables that influence climatic conditions in that location (Otto-Bliesner and Schulz, 2009).

91 Briefly, GCM modeling is based on a knowledge of global/regional/historic processes that influence climate, such as Milenkovitch Cycles (eccentricity, axial tilt, and precession of Earth's orbit), major volcanic eruptions and meteor impacts, the concentration of greenhouse gases and airborne particular matter in the atmosphere over time, the spatial and temporal pattern of sea temperature and ocean levels, and the spatial and temporal patterning of major ocean and wind currents. See Donner and Schubert (2011) for an excellent and thorough review of the history of development of GCM modeling, and a complete description of how GCM modeling works.

5.4.2. The Archaeoclimatology Macrophysical Climate Model

Fortunately, there is an approach to paleoclimatological modeling that does incorporate localized variables, and also allows truly fine-scale spatial and temporal paleoclimatological retrodiction. The method (known as the Archaeoclimatology Macrophysical Climate Model, or AMCM [Bryson and Bryson, 1996; Bryson and McEnaney-DeWall, 2007]; Ruter et al., 2004) retrodicts climatic variables at the locations of modern weather stations that have the standard 30-year-average climate data (i.e., the span from 1961 to 1990, as recorded by the World Meteorological Organization [World Meteorological Organization and National Climatic Data Center (U.S.), 1998]). The AMCM redtrodicts climate by deriving the relationship between local 30-year-average weather conditions and a GCM model. The procedure creates a multiple regression equation between local weather variables (e.g., mean annual precipitation) and influential climate phenomena (e.g., the location of the jet stream) that can be fine-tuned by the modeler. The model then uses this regression to retrodict the past climate at the location of the weather history[92]. The AMCM can redrodict monthly rainfall totals, monthly mean, min, and max temperature, monthly number of rain days, monthly snow fall, monthly evaporation, monthly days below 0° C, and monthly days above 40° C at 100-year intervals to 40,000 years BP, as long as these variables are present in the input data for a particular weather station.

The data recorded by the two World Meteorological Organization weather stations in or near the Wadi Ziqlab region are in the town of At-Tayyiba, situated in the western plateau zone bordering the Jordan Valley, and at the Irbid nursery, in the eastern upland area. The climatic variables recorded by these two stations include monthly amount of precipitation, the monthly mean temperature, the number of rain days per month, the amount of evaporation per month, and the monthly days below 0° C or above 40° C, and so these are also the types of data output from the AMCM in the location of these two stations. Rather than choose the AMCM model output of only one of the weather-station locations to represent the entirety of the project area, I average the output for the two stations, and use the resulting mean values.

Figure 5.11 and 5.12 show the resulting temperature and precipitation histories as modeled for the Wadi Ziqlab region over the Holocene, with the LPPNB/PPNC and the Yarmoukian periods highlighted. Some interesting trends are noticeable in the model output: Summer temperatures and summer evaporation rates are actually slightly lower today than they were in the Neolithic, but summer temperatures are not significantly different between the LPPNB/PPNC and the Yarmoukian. Winter temperatures (and evaporation rates) are significantly warmer today than they were in the Neolithic, and winters were

92 It is important to note that climate change in the modern era has been shown to be the product of both natural and social processes (Griggs and Noguer, 2002; Pachauri, 2007; Solomon, 2007), and AMCM also accounts for the human contribution to atmospheric dust and greenhouse gasses in the post-industrial period.

slightly warmer in the Yarmoukian than in the LPPNB/PPNC. Precipitation amounts are likewise much lower today than they were in the Neolithic, and in general were slightly lower in the Yarmoukian than they were in the LPPNB/PPNC. Interestingly, it seems that this is because of both reduced storm frequency as well as reduced precipitation per storm event (a trend continuing until the modern day). The LPPNB/PPNC is characterized by a brief, but dramatic upswing in precipitation, which had decreased very rapidly at the end of the preceding MPPNB. By the end of the LPPNB/PPNC, precipitation amounts had dropped back to the same levels as the end of the MPPNB. The Yarmoukian is also characterized by a brief upswing in precipitation, albeit much smaller than that of the LPPNB, but precipitation generally declined over the period, and continued to do so until it stabilized in the late Holocene (with brief periods of stability in the Wadi Rabah/Early Chalcolithic, and at a few other times). The number of rain days per year also briefly surged in the LPPNB/PPNC (following a sharp decline in the MPPNB), but then generally declined over the Yarmoukian and subsequent periods.

It is also useful to understand how the seasonality of rainfall changed over time, and one way to do so is to examine the average amount of precipitation that fell each month (Figure 5.13). It is interesting to note that the LPPNB/PPNC and Yarmoukian are characterized by *both* a general decrease in annual precipitation, *and* significant fluctuation in the seasonality of rainfall. For example, one interesting trend is the rapid reduction of March rainfall that began in the middle of the MPPNB. Although declining, March remains the month with the heaviest rainfall throughout all phases of the Neolithic; but, by the Bronze age, March rainfall is no more significant than that of January or February. As with the trend in annual precipitation, the LPPNB/PPNC is characterized by a brief, but dramatic upswing in March precipitation, which had decreased very rapidly at the end of the preceding MPPNB. This pattern is repeated in January rainfall to a somewhat lesser degree, and again in February to an even lesser degree. It becomes clear that the brief resurgence of higher annual precipitation in the middle of the Yarmoukian is due to an increase in March precipitation in those years, which is *not* mirrored by an increase in January and February rainfall. One other interesting pattern is the *increase* in May precipitation starting at the beginning of the LPPNB, and continuing through the Yarmoukian, Wadi Rabah/Early Chalcolithic, until eventually declining again in the middle of the Bronze Age. The precipitation rates in all other months remain relatively stable over the middle and late Holocene.

5.4.3. Conversion to MML climatological input

The particular climate variables that are required by the MML include the annual amount of precipitation, the number of storm events per year, the average length of a storm event, the average precipitation per storm event, and the R-factor (a measure of rainfall "intensiveness"). We must calculate these values

from the AMCM output data: The amount of annual rainfall is simply the total of each month's precipitation. If we assume that each rainy day equals one storm, we can use that number to estimate the annual number of storms. We can then estimate the amount of precipitation per storm by dividing the total annual precipitation by the annual number of storms. Estimating R-factor is more difficult because R-factor is actually a measure of raindrop force over time, which is information not collected by most weather stations (nor can it be directly retrodicted by the AMCM). R-factor can, however, be estimated from the AMCM output by first calculating the Modified Fournier Index (MFI, a measure of the temporal periodicity of rain events) from the monthly rainfall totals in a given year, and then deriving the R-factor from the MFI value via a regression function developed by Renard and Friemund (1994).

Estimating the average length of a storm event is also problematic. Like R-factor, it is not recorded in the original climate data, and thus also not output by the AMCM. Unlike R-factor, however, it cannot be estimated from any of the other AMCM output. Research has shown that the average length of storms in northern Jordan in the modern era is about 8 hours, with a standard deviation of about ±4 hours (Hammad et al., 2006; Volohonsky et al., 1983). We cannot use these modern data directly, however, because it is clear that modern conditions do not match those in the past (see Section 5.4.2, above). This discrepancy not only stems from a higher number of storms (rainy days) during the Neolithic, but also in a larger amount of rainfall per storm event, so it is highly likely that storms during the Neolithic were longer than those of today. In the absence of a more robust method for estimating the length of storms during the Neolithic period, I use the upper end of the 1σ confidence interval for modern storm-duration times, which yields an estimate of 12 hours for the average length of Neolithic storms.

Although the MML is capable of accepting dynamic climatic variables (i.e., a list of different climatic variables for each model-year), I have chosen to use mean values for the time period being modeled (the LPPNB/PPNC). Although the climate was indeed variable within this period (as noted in Section 5.4.2, above), I have chosen to hold the climate as a constant in order to better understand the impacts of human component of the Neolithic socio-natural system. Although the specific patterning of *intra*-period climatic variability (e.g., yearly changes in climatic conditions from the beginning of the LPPNB to its end) might indeed have played a part in the instigation for the post-PPNB dispersal, it is likely that average *inter*-period variability (i.e., differences in the average climate between the LPPNB/PPNC and the Yarmoukian) will capture much of that motivation. Table 5.2 summarizes the input MML climate values for the LPPNB/PPNC and for the Yarmoukian as converted from the AMCM output.

5.4.4. Conversion to full-coverage climate maps

The AMCM output from multiple weather stations can be converted to full-coverage raster maps of each climate variable using a method developed by

Hill et al. (2008) that extrapolates the data from each weather station point to other points on the landscape via multiple regression against various topographic features (such as elevation, aspect, slope, distance to coast, etc.). The method must be calibrated to the climatic characteristics for the particular region, however, and so requires a fair amount of analyst expertise. Hill et al. (2008) perfected the process using the Southern Levant, however, and created maps for each AMCM output variables at 100-year intervals for the last 40,000 years at 90 meter resolution. Although these maps are *not* used directly by the MML, they are used to develop the paleovegetation maps that *are* used as input (see Section 5.5, below).

5.5. Paleovegetation Reconstruction

Due to millennia of intensive human land-use and climate change, modern patterns of vegetation in the study region are very different from those of the past (Fall et al., 2002). It is therefore inappropriate to use modern vegetation patterns (such as those derived from classification of multispectral satellite imagery) as input into MML simulations of Neolithic subsistence, and so we must turn to Predictive Vegetation Modeling (PVM, sometime also referred to as Species Distribution Modeling). The essence of PVM is to "decode" the complex interactions of many environmental, ecological, and geological (and sometimes also social) phenomena that interact to determine the spatial patterning of vegetation at local, regional, or even global scales.

5.5.1. Methods of paleovegetation modeling

The first attempts at large-scale PVM began in the late 19th century, with "snapshot" models that predicted the global spatial patterning of climax vegetation communities based on manual mathematical calculations that formalized early modeler's assumptions about the dependence of vegetation on climatic variables (Miller et al., 2007). In the modern era, more complex PVM algorithms have been used. The most common method involves the creation of Generalized Linear Models (GLM's), which are regression models between spatial patterning of vegetation and various predictor variables) (e.g., Davis and Goetz, 1990; Kupfer and Farris, 2007; Miller and Franklin, 2002). GLM models require many assumptions to be made about the linearity of the relationships between many independent variables and, therefore, most GLM vegetation models are provided with the caveat that they are very site-specific (i.e., not applicable to large regions) (Davis and Goetz, 1990). Several methods have been suggested for overcoming such site-specificity, but the most commonly used techniques boil down into two categories: more advanced "weighted regression" techniques, and decision-rule techniques[93]. Weighted regression models (such as Bayesian Estimators and Geographically Weighted Regression) essentially allow

93 See Soto-Berelov (2011) for a more exhaustive list of modern PVM techniques.

for the importance of specific predictor variables in the regression to change in different sub-regions based on prior knowledge (e.g., Kupfer and Farris, 2007), whereas rule-based methods (such as Classification Tree analysis) are hierarchical, non-linear methods of predicting spatial variability that rank predictors and sort them according to the linkages of a boolean decision "tree", ultimately predicting the type of vegetation in a patch by the final "branch" of the tree that is reached in that area (e.g., Miller and Franklin, 2002). Both methods result in significant improvement over the GLM methods (Kupfer and Farris, 2007; Miller and Franklin, 2002) but, in order to achieve this increased accuracy, both types of models must be highly parameterized with intimate knowledge of the many ecological relationships between the species being modeled and the predictor variables used in the modeling routine, making them quite complicated for use in paleovegetation reconstruction on a large scale.

Maximum Entropy (MAXENT) modeling – a type of unsupervised computer-learning technique – was adapted for use in PVM by Phillips et al. (2006) specifically as a way to overcome the need for prior intimate knowledge of the interrelationships needed by GWR and CT models[94]. The MAXENT method is conducted within a GIS-compatible open source software tool (MaxEnt 3.3 [Phillips et al., 2010]), and requires input of "presence only" data for different vegetation types at specific locations (such as that collected along vehicular or pedestrian transects during survey), and raster maps of environmental predictor variables. These predictor variables include geographic variables such as slope, aspect, elevation, soil type, and distance to nearest coastline, and climatic variables such as solar insolation, evapotranspiration rate, seasonal precipitation, and seasonal temperature. The MAXENT routine creates a unique set of rules governing the interaction of these variables at each input site for each known vegetation class, and then uses these rules to predict the probability of the existence of that vegetation class at all other points on the landscape. This automation makes MAXENT especially suited for retrodicting the spatial patterning of vegetation in the deep past, because it can be used directly with the climate raster map produced from the output of the AMCM model runs.

5.5.2. Paleovegetation modeling in the Southern Levant

Soto-Berelov (2011) used this approach (i.e. MAXENT modeling with paleoclimate maps derived from AMCM data) to model the spatial patterning of vegetation over the Holocene for the entire southern Levant (Figure 5.14). Soto-Berelov compiled an exhaustive database of historical vegetation transects across the length and breadth of Israel, Palestine, and Jordan, carefully verified and extended by new field work, to serve as the vegetation presence input for a MAXENT PVM classification routine of the region. She refined the MAXENT classification by comparing its output under modern climatic conditions to those

94 But it is not the only machine-learning method developed to do so. See Soto-Berelov (2011, table 5.1) for other machine-learning techniques that have been applied to PVM.

of other PVM techniques and with existing vegetation maps created from classified remotely-sensed imagery. Then, substituting the paleoclimate maps created by Hill et al. (2008), she was able to use the refined MAXENT classification rules to predict the spread of several types of climax vegetation communities at 1 km resolution at 500-year intervals from 12,000 BP to the present day. Soto-Berelov checked the accuracy of the produced PVM maps against available proxy records, and by internal accuracy assessment using typical "training set"/"testing set" data separation techniques commonly used in most types of classification analysis. It is important to note that her PVM maps predict the climax vegetation that would likely have have been present at each 1 km cell *without* human interference (i.e., based solely on natural predictor variables). These climax models are ideal for use in MML modeling experiments, as they can serve both as "initial" conditions (i.e., the pattern of vegetation before intensification of Neolithic land-use at the beginning of the LPPNB), and as "boundary" conditions that constrain the upper-limit of the vegetation regrowth to the environmentally-appropriate succession level predicted by the MAXENT model for each cell at each time period. Thus, I use Soto-Berelov's paleovegetation model for 9000 BP as the initial conditions for the LPPNB/PPNC MML simulations, and as the basis for the climax vegetation conditions in throughout the period. Her paleovegetation model for 8500 BP (i.e., the Yarmoukian) is used to understand the extent of anthropogenic vegetation change after 700 simulated years of LPPNB/PPNC land-use (i.e., her 8500 BP model represents the pattern of vegetation that would have existed at the end of the LPPNB/PPNC had there been no human impacts).

5.5.3. Conversion to MML vegetation input

Soto-Berlov's models cannot be used directly in the MML because she uses a different vegetation classification scheme (i.e., she is interested in climax vegetation communities across many plant geographic zones, and not succession within one zone), and must be reclassified to fit the succession scheme used in the MML, and Table 5.3 shows the equivalence rules used to complete this reclassification. Once the PVM maps are reclassified, they must be brought to the proper resolution (i.e., from 1 km to 10 m), their geometry must be refined to remove sharp angles, and the boundaries between plant communities must be softened to prevent destabilization of the landscape evolution routine in those areas. This is done in much the same was as with the SOTER soils data (Section 5.3.3, above), except that the final median-smoother window is not applied. This allows the perturbed border areas are allowed to remain "patchy", which more realistically simulates the way vegetation transitions across ecozones (Figure 5.15).

5.6. Chapter Summary

In this chapter, I have reviewed previous geoarchaeological work in the Wadi Ziqlab region, and have reported the results of the new work that I carried out for this project. This work makes clear the point that the Early/Middle Holocene environment of the Wadi was quite different than it is today, and underscores the need for explicit paleoenvironmental reconstruction before simulation modeling of Neolithic land-use is possible. Following this, I described the way in which the findings of the geoarchaeological fieldwork inform a GIS-based reconstruction of the physical environment during the Neolithic period. I discussed the methods I used to digitally model past environmental conditions, and I have analyzed the resultant reconstructions of Neolithic topography, soils, climate, and vegetation. I also discussed the implications of specific details of the reconstructions, and how the reconstructions themselves will serve as input to the landscape/land-use simulations reported on in subsequent chapters.

Table 5.1. Areal (ha) statistics for middle terrace remnants in all three of the Wadis of the project area.

Statistic	**Wadi Tayyiba**	**Wadi Ziqlab**	**Wadi Abu Ziad**
n	35	65	27
Mean	1.28	0.85	1.04
Median	0.60	0.43	0.20
Mode	0.22	0.18	0.06
Std Dev	2.72	1.59	2.14

Min	0.10	0.05	0.01
1st Quartile	0.28	0.22	0.10
3rd Quartile	1.15	0.89	0.95
Max	16.23	11.85	10.02

Table 5.2. Climate variables as input to the MML for the LPPNB/PPNC and Yarmoukian periods. Values extrapolated from the averaged AMCM output for the Tayyiba and Irbid Nursery weather stations, and then time averaged across the length of each time period.

Climate Variable	LPPNB/PPNC Averages	Yarmoukian Averages
Storm length (h):	12	12
R-factor:	8.78	6.78
Precipitation per rain even (mm):	10.13	9.62
Number of rain days:	99	94
Annual Precipitation (mm):	995	895

Table 5.3. Table of equivalences used to convert the MAXENT climax vegetation types to stages in the vegetation succession order used in the MML.

MAXENT land-cover Category (from Soto-Berelov, 2011)	MML land-cover Category
Evergreen oak maquis and forest, Transition deciduous - evergreen oak forest, Deciduous oak maquis and forest, Pine forest, Open forests of Juniper, Open forests of Pistacia atlantica, Open forests of carob and pistachio, open forests of juniper, oak, pistachio, Mediterranean non forest	Mature Woodlands (succession value 50)
Semi steppe batha, Transition Shrub steppe-semi steppe batha	Immature Woodlands (succession value 36)
Transition Shrub steppe-Desert vegetation, Transition Shrub steppe-Desert savannoid	Shrub Maquis (succession value 19)
Shrub steppe	Shrubs (succession value 14)
Mediterranean savannoid, Hydrophitic/Mediterranean savannoid	Grasslands (succession value 5)
Desert vegetation, Desert savannoid, Halophytic, Sand dune, Sudanian, Hydrophitic/Tropical Sudanian, Halophytic/Tropical Sudanian, Halophytic/Hydrophitic	Sparse Grassland (succession value 3)

Fig. 5.1. Outline of the project area on GeoEye imagery.

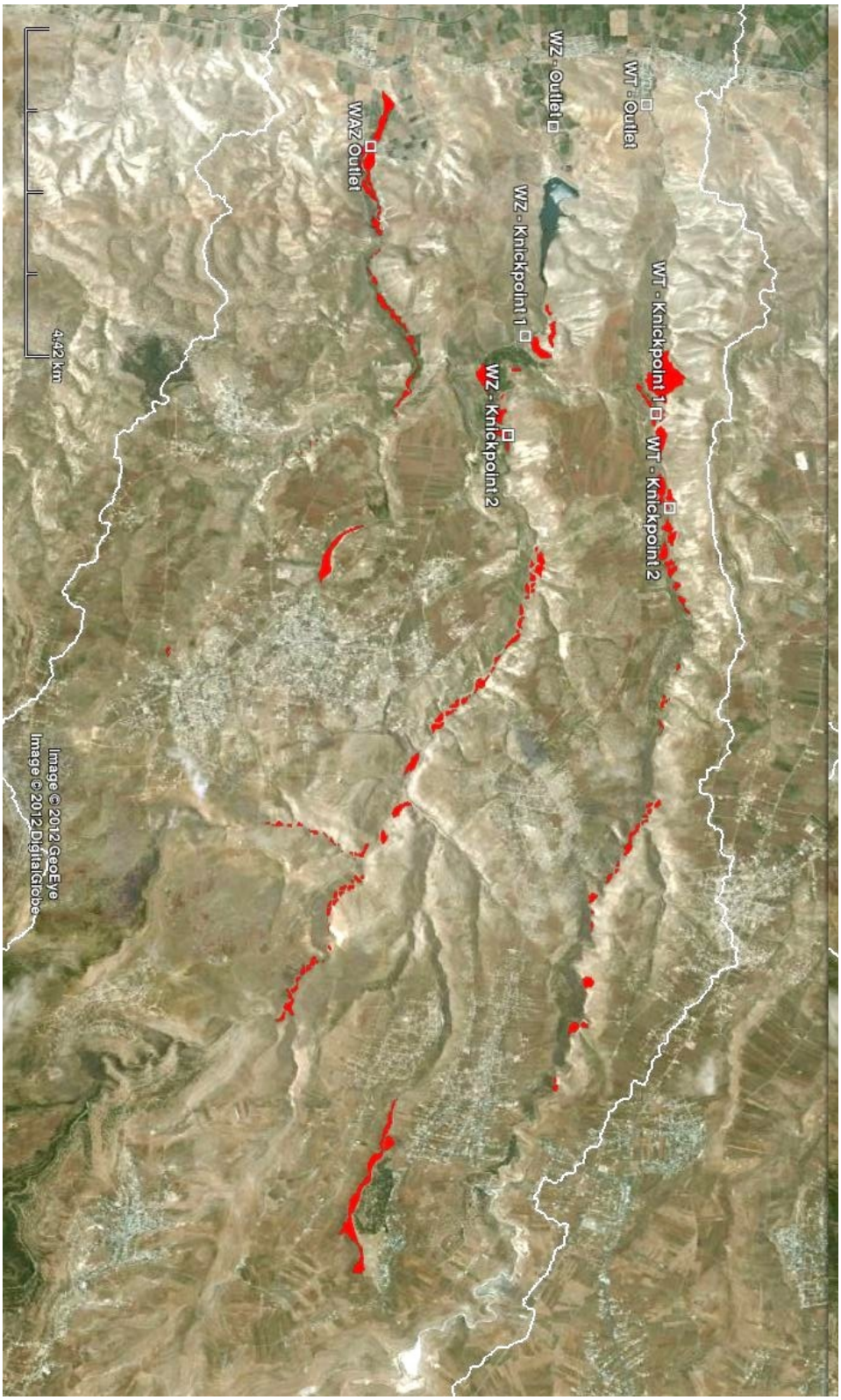

Fig. 5.2. GeoEye imagery of the project areas with the knick points and wadi outlets marked, and the middle terrace remnants outlined in red,

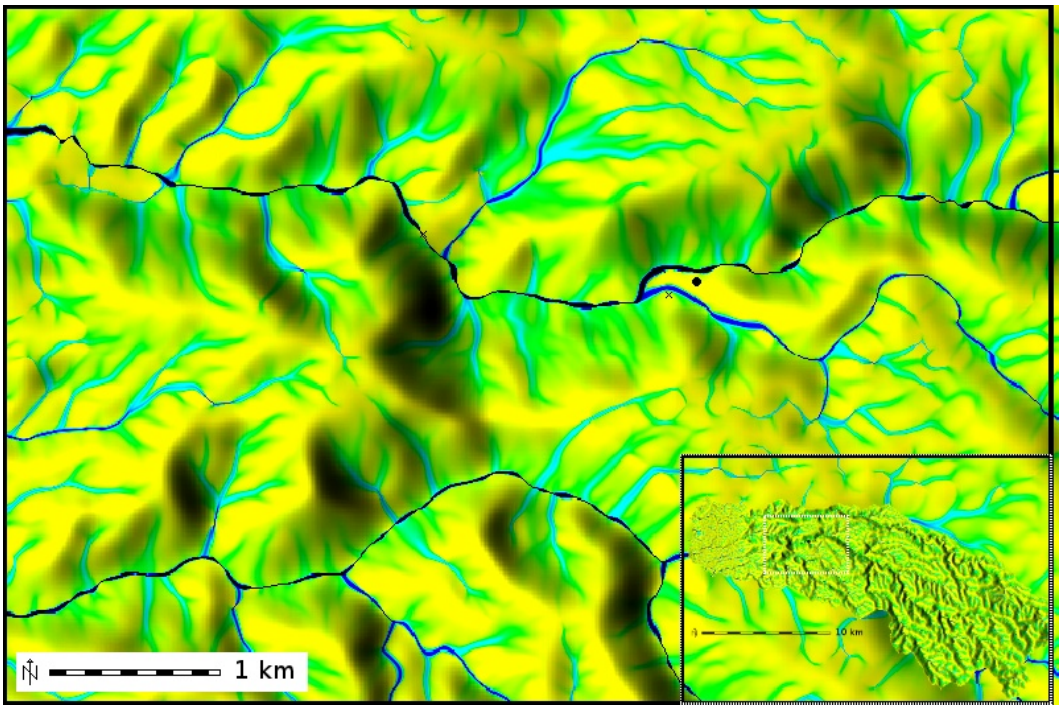

Fig. 5.3. Detail of the flow accumulation map near Tell Rakkan. Inset shows the whole project area.

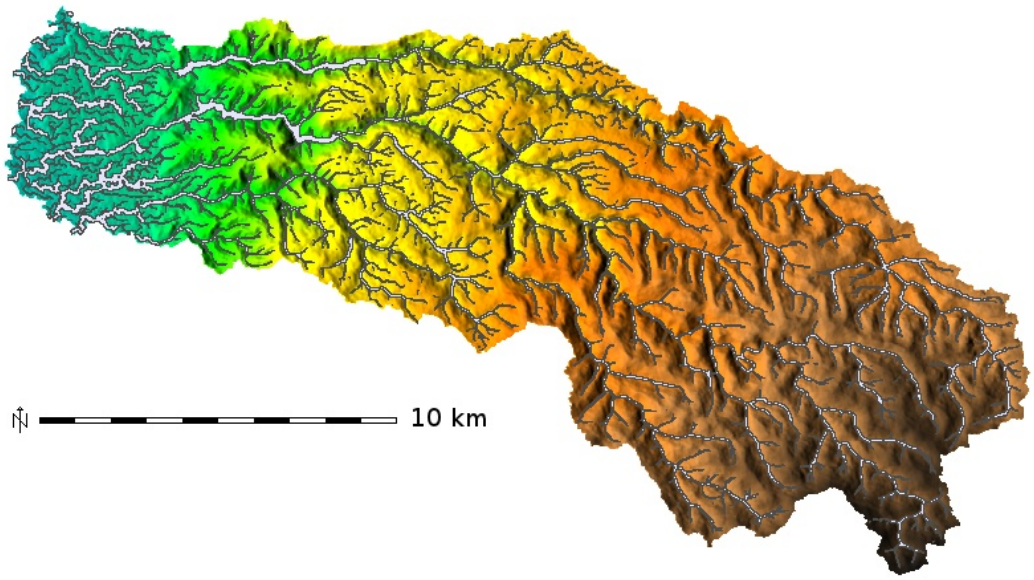

Fig. 5.4. Map of the portions of the project area detected by the automated detection routine. The elevation data within the boundaries defined by the routine is ignored during the interpolation of the "PaleoDEM".

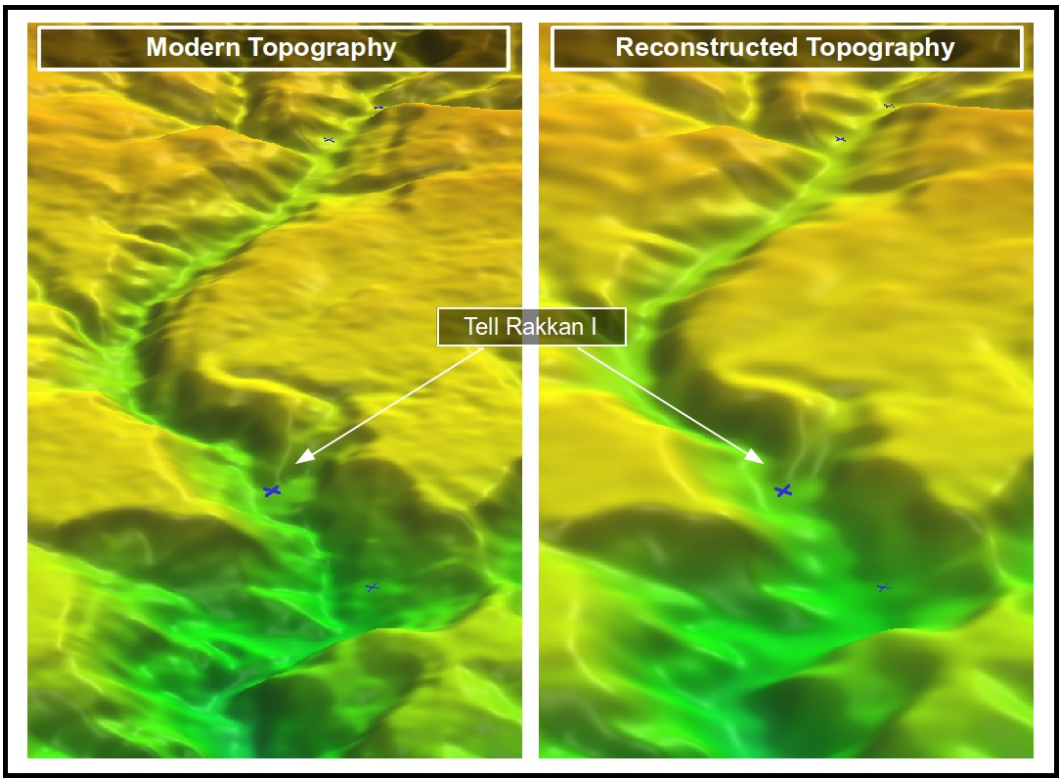

Fig. 5.5. 3-D perspective views of the modern DEM (left) and the interpolated "PaleoDEM" (right). The large blue X marks the location of Tell Rakkan, and the smaller blue X's mark the location of the other LN sites.

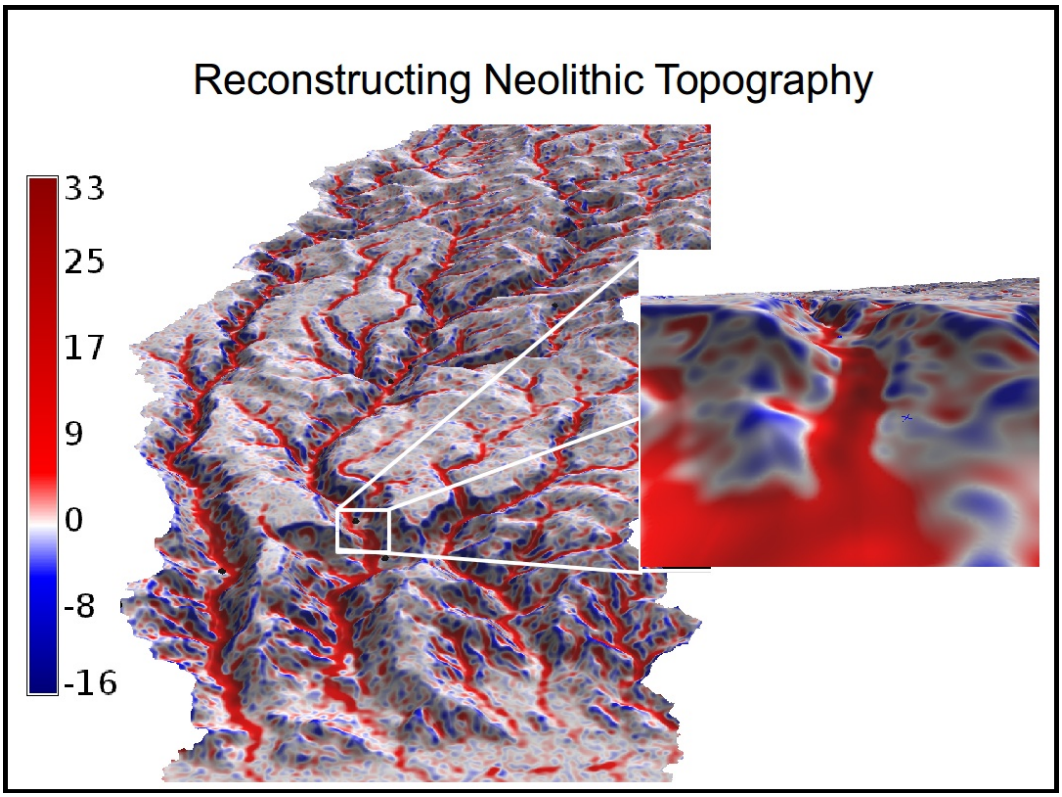

Fig. 5.6. 3-D perspective view of the project area, colored by the difference in elevation between the Modern DEM and the "PaleoDEM". Red indicates areas of raised elevation in the interpolated "PaleoDEM", and blue indicates areas of lowered elevation. Inset shows a close up of the pattern near Tell Rakkan.

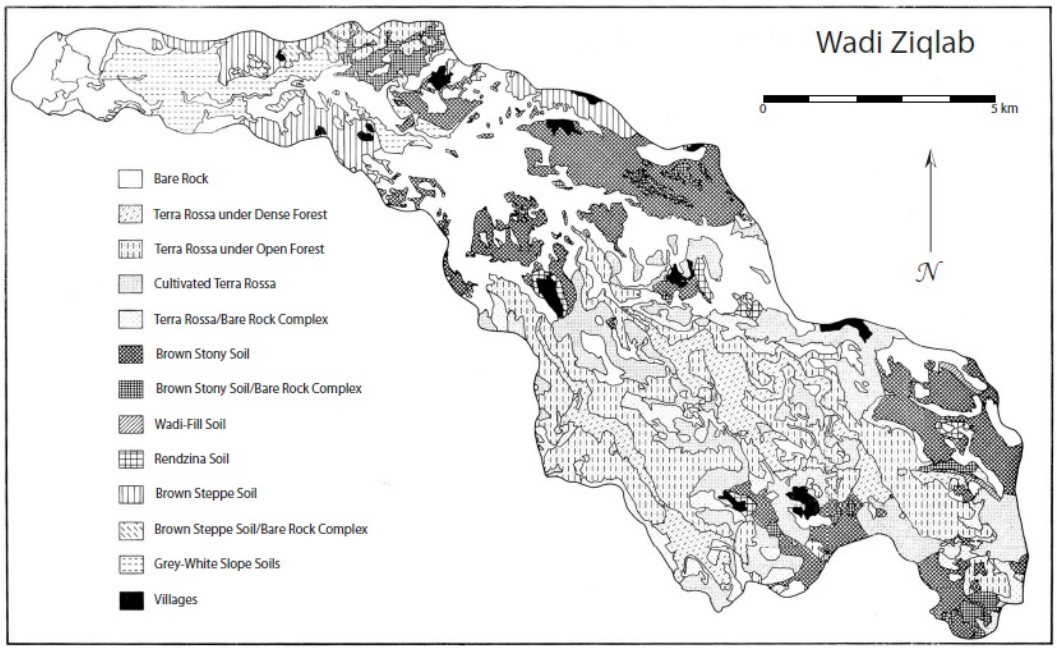

Fig. 5.7. The Fisher et al. (1964) soils map of Wadi Ziqlab.

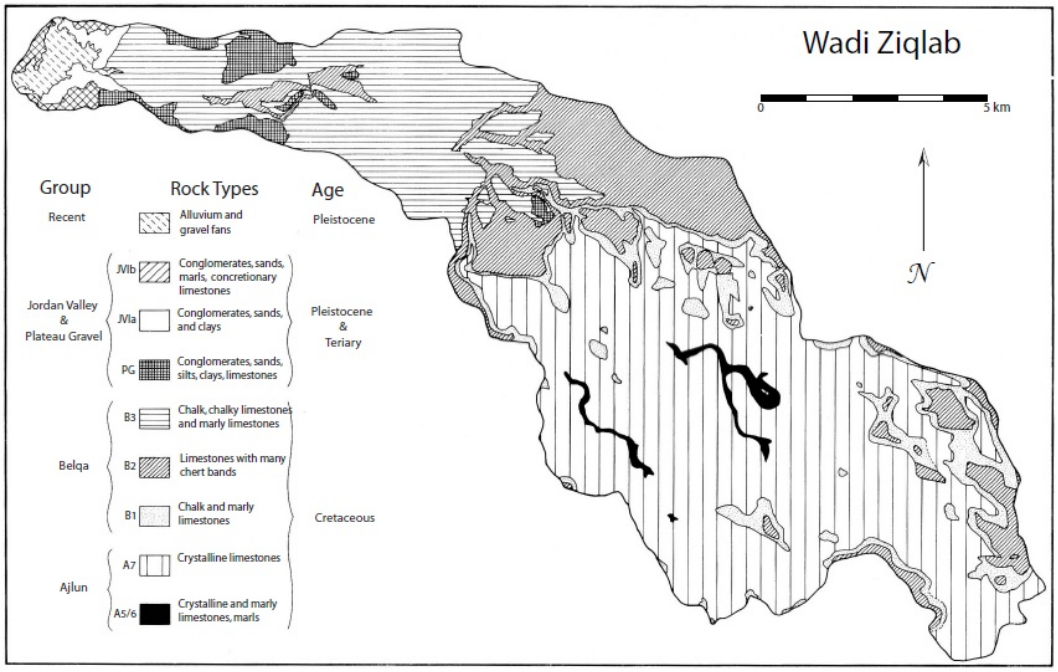

Fig. 5.8. The Fisher et al. (1964) bedrock geology map of Wadi Ziqlab.

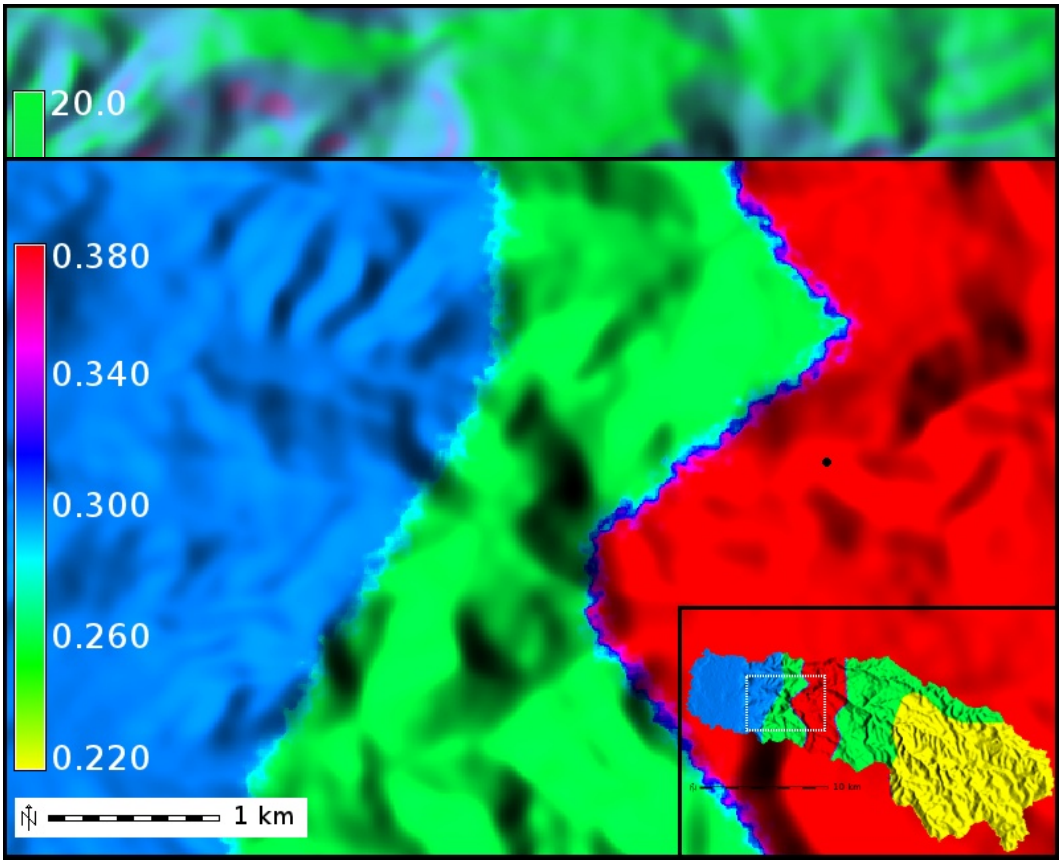

Fig. 5.10.Detail of the K-factor map in the vicinity of Tell Rakkan. Inset shows the entire project area.

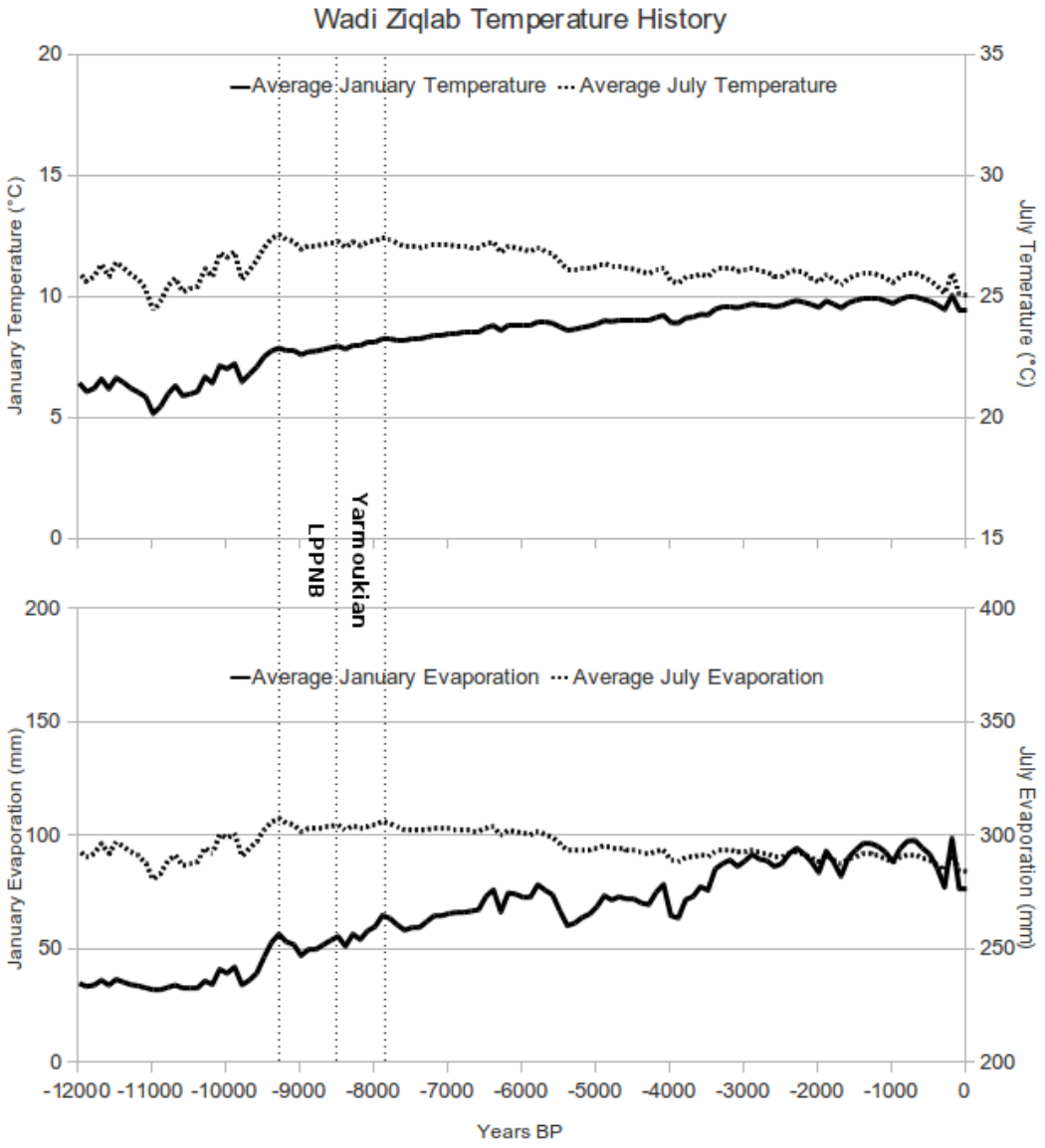

Fig. 5.11. Holocene temperature history for the Wadi Ziqlab region, as modeled by the AMCM. All dates are in calendar years before present.

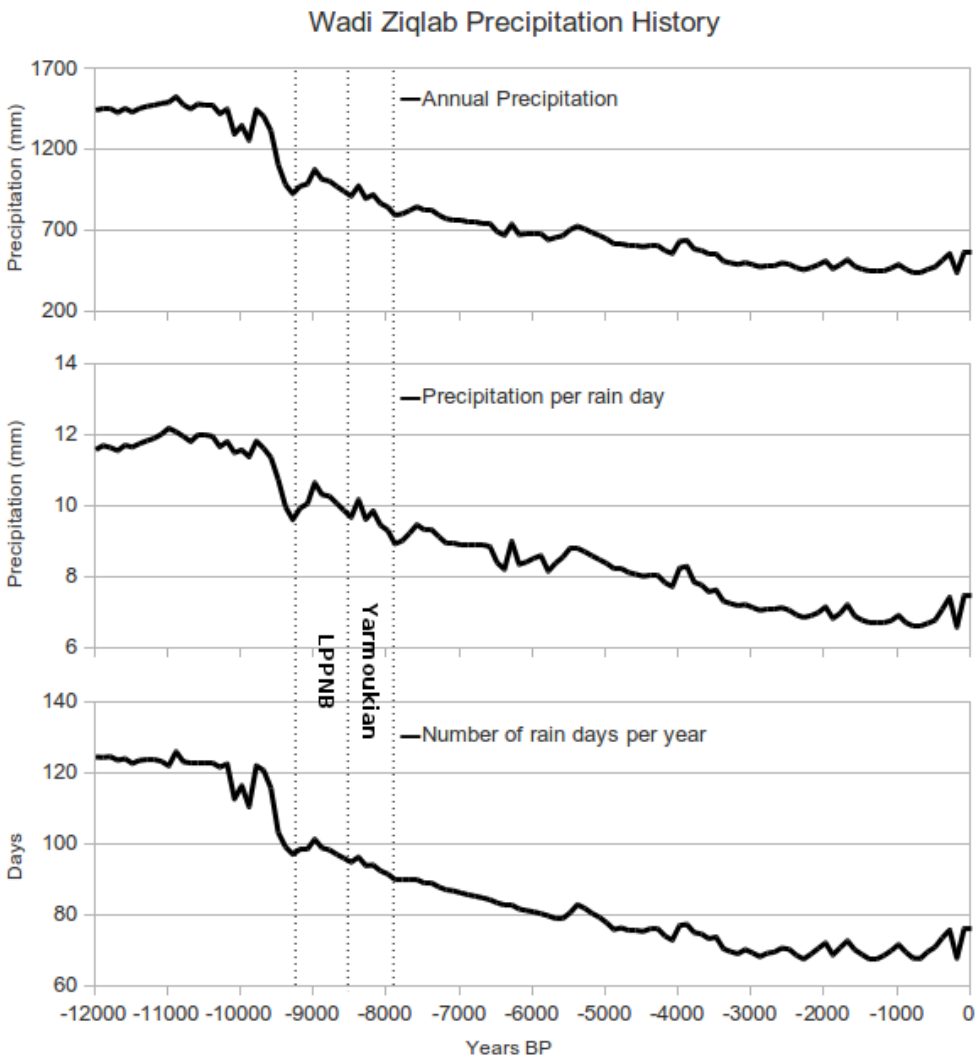

Fig. 5.12. Holocene precipitation history for the Wadi Ziqlab region as modeled by the AMCM. All dates are in calendar years before present.

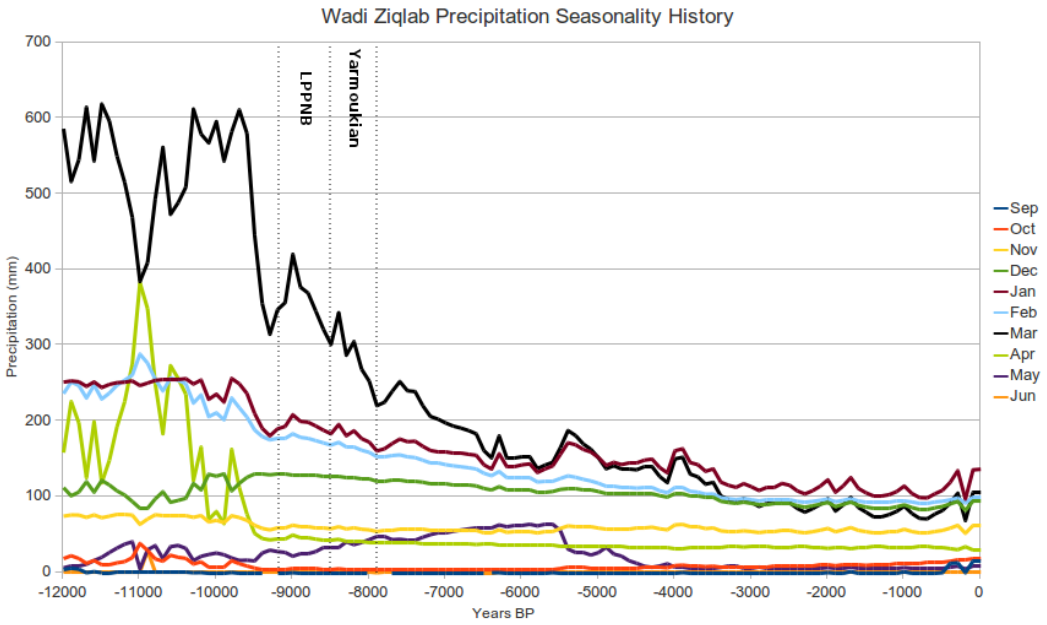

Fig. 5.13. Holocene precipitation variability history for the Wadi Ziqlab region as modeled by the AMCM. All dates are in calendar years before present.

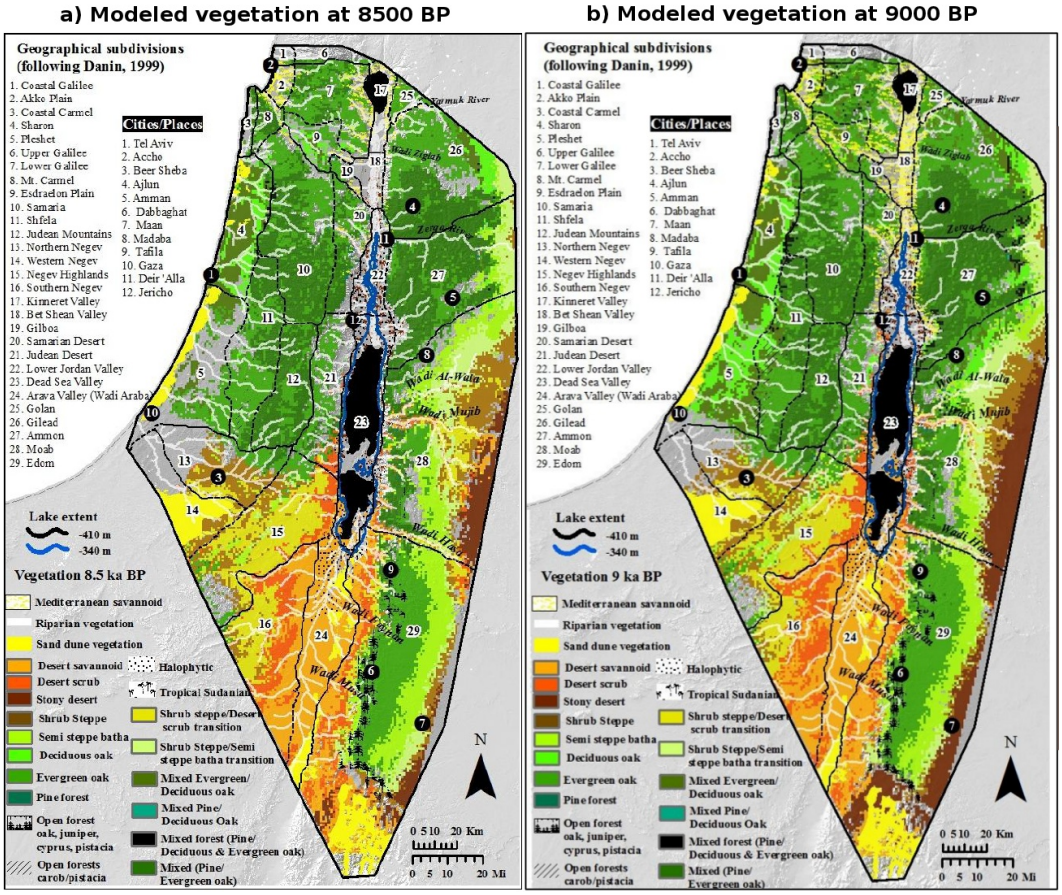

Fig. 5.14. Vegetation maps of the southern Levant as created by the MAXENT PVM for the year 8500 BP (left) and 7500 BP (right). After Soto-Berelov (2011).

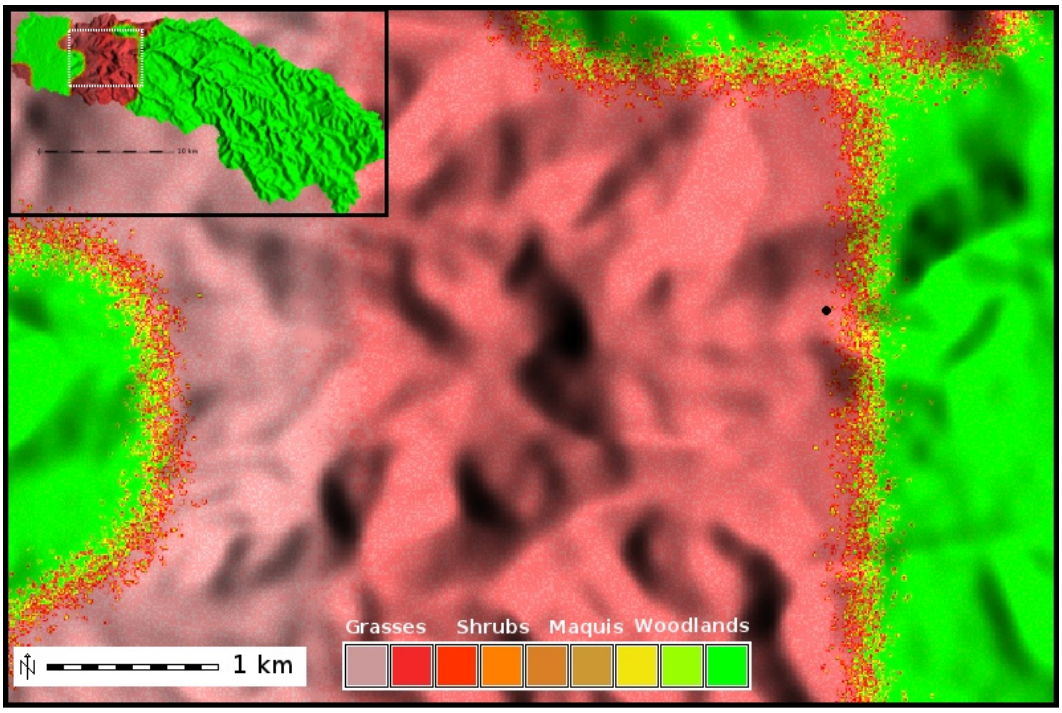

Fig. 5.15. Detail of the input LPPNB/PPNC vegetation map in the vicinity of Tell Rakkan. This map derives from the MAXENT PVM output for the year 8500 BP (Figure 5.11-a), and was converted to the MML input format according to the conversion rules defined in Table 5.3. Inset shows the entire project area.

6. MODELING THE PPN-LN TRANSITION IN WADI ZIQLAB

6.1 Chapter Introduction

This chapter describes the way I use the MML to better understand the conditions that led to the PPN/LN transition. First, I draw upon the archaeological data presented in Chapter 2 and the CAS approach to the transition outlined in Chapter 3 to define three general types of subsistence systems that could have been in operation in PPNB Wadi Ziqlab. I then flesh out these subsistence strategies by drawing upon the archaeological data from the PPNB (Chapter 2), and ethnographic data (introduced in this chapter). These data are used to parametrize the MML (as described in Chapter 4) for each of the three subsistence systems. Finally, I devise a series modeling experiments to systematically vary a small number of key aspects of each potential PPNB subsistence system to better understand the long-term dynamics of different aspects of subsistence, and to better understand the implications of subsistence choices on long-term resilience and vulnerability.

6.2. Composing PPN Land-Use Modeling Experiments

The goal of the MML modeling experiments conducted in this research is to better understand the sequence of events that led to a major social transition visible in the archaeological record, but before any such experiments can be conducted, the economic and social aspects of the MML must be parameterized to reflect Neolithic lifeways[95]. But what is the best way to do that? The fragmentary nature of the archaeological record—especially that of Tell Rakkan I—precludes direct parameterization of the model from archaeological data alone. Furthermore, the current picture of life in Neolithic Levant suggests that there were a variety of agropastoral subsistence systems simultaneously in existence across the region and over time (Asouti, 2006; Asouti and Fuller, 2012; Conolly et al., 2011; Rollefson, 2004; Zeder, 2008), so we also cannot use a better preserved/studied PPN site in the region (such as 'Ain Ghazal) as a direct analog for the PPN lifeway of Tell Rakkan I. The same issue arises for ethnographic data; we cannot pick just one ethnographically known group to be used as an analog for PPN subsistence at Tell Rakkan I.

We must nevertheless use data from modern and ancient peoples who live(d) in similar environments to Wadi Ziqlab and practice(d) a similar lifeway to that which we believe was practiced by Neolithic people in the Wadi. But how do we choose which values to use, and from which particular modern or ancient

95 The environmental and physical aspects of the MML must also be parameterized to the the natural conditions of the Neolithic period, but I have already discussed how this was accomplished in Chapter 5.

society and/or geographic area to choose them from, without falling into the trap of strict ethnographic analogy (i.e., as originally conceived of by Gould [1978] and others)? It is precisely this conundrum that the simulation modeling approach is designed to address. Since we cannot know "the" lifeway of the Neolithic inhabitants of Wadi Ziqlab, several plausible scenarios for subsistence at Tell Rakkan I must be constructed, simulated, and compared to archaeological reality.

In the research presented here, this is achieved through the following process: First, basic numerical data on subsistence-based agropastoralism in Mediterranean environments are collected from as wide a variety of ethnographic datasets as possible. Then, these data are collated, and the spread and central tenancies of each parameter are tabulated and collected into a central database. Finally, the aspects of the system that are most likely related to the cause of the PPN/LN transition are identified and a series of simulation experiments are designed in which these aspects are varied systematically across a reasonable parameter-sweep. It is important to note that although this process may utilize aspects of ethnographic data, it is nevertheless a scientific approach to the study of past lifeways, and not an analogical one (Wylie, 1985).

6.2.1. Parameterizing Neolithic Subsistence Behavior

Of the discrete subsistence systems identified in the analyses presented in Section 6.2, PPN economies in the Wadi Ziqlab region are most likely to have been within the "subsistence pastoralism", "mixed agropastoralism", or "intensive agriculture" adaptive basins, so it is necessary to conduct modeling experiments for each of these three subsistence types. To do so, I have compiled a database of plausible values for the basic socio-economic/socio-ecological underpinnings Neolithic subsistence. These data derive from an extensive literature review of ethnographic, archaeological, and agronomic research relating to traditional small-scale subsistence systems based on sheep/goat pastoralism, and wheat/barley agricultural with ancient or primitive/heirloom breeds/cultivars in Mediterranean environments. Although quite a bit of diversity exists within the database, I have chosen to hold the basic components of each of the three possible Neolithic subsistence systems (agriculture, agropastoralism, and pastoralism) constant, and only vary a few key components of the systems that relate directly to the amount of time people spend engaging in pastoralism versus farming. Thus, the three modeled subsistence systems differ only in the ratio of reliance on (and thus effort expended to produce) animal products versus cereal crops. "Agriculturalists" must obtain 80% of their diet from cereals and 20% from animal products, "agropastoralists" require a 50% mix of cereals and animal products, and "pastoralists" need to obtain 80% of their diet from animal products, and only 20% from cereals. The other components of the subsistence system do not change between models, and are based on averages calculated from the compiled ethnographic database. They are reported in Table 6.1, and it is also important to note that individuals in all three subsistence systems are assumed to

require an average of 2500 "agropastoral kilocalories" per day in order to remain healthy[96]. Production in each of the three modeled subsistence strategies is therefore tuned to this goal.

These strategies are implemented in the MML by adjusting the yearly per capita kilocalorie goals for both agricultural and pastoral subsistence activities to match the ratios reported above. P_{oc} (the number of ovicaprids per person) in equations 4.2 and 4.3 (Chapter 4), must also be adjusted to meet these goals (see Table 6.2). Both of these factors affect the yearly land-use plans created by the agents by changing the ratio of the amount of land planned for use growing wheat and barley versus that planned for grazing. They are set at the start of a model run, and remain constant throughout the length of the run.

6.2.2. Parameterizing Neolithic Wood Gathering Behavior

Because the effects of firewood and structural timber gathering are important aspects of one of the hypotheses being tested, proper parametrization of this behavior is essential. Ethnographic data suggests that small scale subsistence agropastoralists consume 1600-4300 kg of firewood per person per annum (Bhatt and Sachan, 2004; Fleuret and Fleuret, 1978; Fox, 1984; Karanth et al., 2006; Naughton-Treves et al., 2007; Reddy, 1981), and that they gather wood at an intensity of between 0.06 and 0.09 kg/m^2 (Karanth et al., 2006). The rates of use and gathering intensity depend upon the actual use and style of domestic hearths, cooking methods, winter temperatures and house types, and the general character of the vegetation in near the village. In the models presented here, I use a wood need of 2000 kg/pers. per year, and a gathering intensity of 0.08 kg/m^2, which is consistent with the firewood needs of the inhabitants of an agricultural village like PPNB Tell Rakkan (e.g. domestic cooking and heating with occasional plaster-making [Asouti and Austin, 2005]).

6.2.3. Parameterizing Neolithic Population Dynamics

Based on an archaeological estimates of the size of Tell Rakkan I (Banning and Najjar, 1999; Banning, 2001, and also see the discussion o Tell Rakkan I in Chapter 3), I chose to begin the simulation experiments with an initial population of 60 people evenly divided into 10 households[97]. Households will grow or die off over time according to the basic demographic model outlined in

96 Greer and Thorbecke (1986) report a "food poverty line" of about 2250 daily calories for subsistence agropastoralists in Kenya. Hartter and Boston (2008, 2007). They and Thomson et al. (1986) report a daily caloric intake of about 3500 calories for subsistence agropastoralists in Uganda and northwest Syria, respectively, and that these calories come almost completely from agropastoral products. The PPN inhabitants of Wadi Ziqlab consumed a significant quantity of wild resources, and although the exact proportion of the PPN diet derived from agropastoral products is unknown, I assume a 70/30 split between agropastoral and wild resources, thus producing a 2500 daily agropastoral caloric need.

Chapter 4. Human population dynamics are extremely important drivers of change in socio-natural systems, however, so it is important to parameterize the demographic model to plausibly simulate Neolithic population dynamics. Archaeologists have estimated the total population growth rates of prehistoric agricultural groups to be between 0.05% and 0.1% (Bocquet-Appel, 2002).[98] There is general agreement that subsistence-based agriculturalists have an average birth rate of 6.6% (Bentley, 2003), but little consensus has been reached regarding death rates. In order to derive some estimate of plausible Neolithic death rates, a member of the MedLanD team conducted ABM experiments of demographic growth (Bergin et al., 2012). These experiments used the accepted birth rate as a given constant, and iteratively stepped through various death rates until the rate of overall population growth was within the limits of the archaeologically known rates. The research indicated that death rates of 5.2% and 5.7% represent the extremes of the accepted continuum of hypothetical prehistoric agricultural population rates (Cowgill, 1975), and these values are used as the "base" rates in the experiments discussed here.

6.2.4. Constructing Simulation Experiments for the PPN/LN Transition

Drawing on the three hypotheses for the instigation of the PPN/LN transition I laid out in Chapter 2, I have devised a series of modeling experiments that systematically test the social and environmental effects of three key socio-ecological aspects in each of the three potential Neolithic subsistence systems: the way people choose plots, the density at which people stock their herd animals, and the amount to which farming practices reduce soil fertility. The specifics of the experiments are summarized in Table 6.2, but can be summarized into four types of "subsistence mindsets" per subsistence strategy: 1) "good lazy", 2) "good hardworking", 3) "greedy lazy", and 4) "greedy hardworking". "Good" subsistence mindsets work to have a minimal impact on soil fertility under continuous usage (e.g., they partially replenish soil fertility with manure, compost, or engage in other fertility-enhancing practices). "Good" mindsets also want to achieve herding goals in the most minimally invasive way possible, and so stock herd animals at low densities (e.g., they choose to use a relatively larger grazing catchment for a particular number of herd animals). "Greedy" mindsets

97 I chose to start the simulation with an initial population that was well below the estimated maximum population that could have been housed at the site in order to allow the population to increase to meet any natural "equilibrium" that might exist, and to avoid artificially large initial impacts derived from beginning with an impossibly large population. I should also be noted that while Byrd and Banning (1988) estimate PPNB houses to hold only 3-4 people, Banning (2003) also points out that "houses" do not necessarily equal "households" in the PPN. Therefore I chose to use an initial household size of 6 people, which derives from ethnographic data reported by Hillman (1973) and Kramer (1982, 1980).

98 Although research by Eshed et al. (2004) using skeletal material from the Levantine PPN suggest a higher population growth rate of 0.5% to1% in that period, issues with the severe sample bias within the exisiting PPN skeletal collection raise serious doubts about the accuracy of this estimate.

are less concerned about maintaining soil fertility, and undertake farming practices that can lead to a decline in fertility under continuous usage (e.g., they implement no proactive fertility conservation practices). "Greedy" mindsets also want to get the most out of their grazing lands as possible, and so stock herd animals at a higher density (e.g., they used a smaller grazing catchment for the same number of animals). "Lazy" mindsets want to obtain their agricultural products with the least amount of work possible, and so prefer to use farm plots that have already been cleared or are covered with easily-removed vegetation, even if these plots are of relatively lower quality than nearby wooded plots (i.e., they don't want to expend the effort of cutting down trees). "Hardworking" mindsets, on the other hand, want to produce as much food per farm plot as possible, and so would rather choose the best possible farm plots regardless of the current vegetative cover of the plot (i.e., they do not mind exerting the labor to cut down trees on a plot as long as the potential agricultural returns from the plot are high).

"Good" versus "greedy" mindsets are implemented in the MML by changing the soil fertility impact value according to Table 6.2, adjusting the value of G_i (the "grazing impact factor") in equation 4.12 (Chapter 4) to equal the stocking rates reported in Table 6.2. "Lazy" versus "hardworking" mindsets are implemented in the MML by varying $LCdval$ (the land-cover "devaluation" coefficient) in equation 4.5 (Chapter 4).

6.2.5. Emergence and Experiment Repetition

Emergent phenomenon are an important aspect of complex systems (see discussion in Chapter 3). Even starting from identical initial conditions, no two model-runs will be exactly alike and, in fact, can be very different. The degree to which the same initial conditions may result in vastly different outcomes is a meaningful and very important characteristic of particular complex systems, which relates to the concepts of resilience and vulnerability to critical transitions (see Chapter 3). All else being equal, complex systems that have high capacity for emergence are highly unpredictable, but may also be highly adaptable and resilient. It is therefore essential to have a way to measure (or at least understand) the "emergence potential" of each the different simulated PPNB subsistence systems discussed above. The only way to achieve this is to repeat each of the individual simulation experiments multiple times and to visualize and measure the variability between each repeated run, and that is the approach I have taken in this research[99]. Not all experiments result in significant variability between repeated

99 Note that this reason is different from, but not necessarily contradictory to, the often-cited argument for repetition of model-runs in simulation studies, which is that aggregate statistics compiled across all repeated runs provide a confidence-interval on the general trend of a simulation run (i.e., aggregation controls for random model errors or stochastic variability) (see Galán et al., 2009). In the case of complex phenomena, aggregation will actually obscure

runs (i.e., not all systems will have a high potential for emergence), however, and due to the amount of time and computer-power required to complete model-runs, I chose to focus my available computing power on experiments that seemed to have a high capacity for emergence after two consecutive runs[100]. Thus, while all experiments were repeated at least twice, experiments that showed divergence were repeated up to five times[101]. Although I believe this was a reasonable compromise for the current research, future research will follow a protocol of fewer experiment variants with more repetitions per variant.

6.3. Chapter Summary

In this chapter, I have shown that natural divisions *do* occur in human subsistence behavior, and that it is possible to define discrete subsistence strategies. Furthermore, the existence of these discrete strategies align with the predictions of macroecology, and the concept of "adaptive basins". Of the "adaptive basins" in human subsistence behavior identified in this exercise, those of "agriculturalists", "agropastoralists", and "pastoralists" most closely match the picture of PPNB subsistence that we have formed from the archaeological data from Wadi Ziqlab and other PPNB sites in northern Jordan. I then showed how the MML can be used to simulate these base socio-economic types by parameterizing it with data from research into modern groups engaging in similar subsistence activities. I then derived a series of modeling experiments to be conducted within the MML specifically formulated to assess the three hypotheses for the instigation of the PPN/LN transition that were laid out in Chapter 2. Finally, I discussed the need for multiple runs to better understand the capacity for

---

the dynamics of the system, and will not allow the identification of multiple stable states or other indicators of complexity.

100For example, due to the extra processing time it takes to sort through longer lists of potential farmplots, the "agriculturalist" model runs required 3-4 times longer to complete than the other models (up to 8-10 days for a single "agriculturalist" simulation), which is a not-inconsiderable amount of time.

101This experiment repetition framework was the goal for the research, and simulation experiments were scheduled and carried out according to it. However, as I began to analyze the data, I noticed that several computing and human errors had occurred. For example, if a model was prematurely stopped or paused (which, unfortunately was unavoidable due to electrical work being conducted in the building), it proved to be impossible to restart the simulation at the same system state (due to the nature of the way initial household populations are arranged). This meant that both the temporal dynamics and ultimate outcomes of restarted models were irredeemably affected, and so they could only be effectively compared up to the point of interruption. Also, due to small mistakes in the configuration files, some of the models appeared to have completed successfully, but instead resulted in total die-off of population (e.g., due to a mistakenly imbalanced requirement/production ratio). Thus, some experiments were effectively repeated fewer times than initially thought, and some repetitions were incomplete (due to interruption). Time and computing restrictions have thus far prevented correction to these issues, but the results (presented in the next chapter) are still robust enough for the objectives of this research.

emergence (intuited as divergent model trajectories over time) in each modeled subsistence strategy.

Table 6.1. Table of economic and ecological data used to parameterize the models of PPN subsistence systems.

Data type	Data		Source
Pastoral product yields	*Baladi Goat*	*Awassi Sheep*	
Milk output (kg/yr):	200	60	Degen, 2007
Milk energy (kcal/kg):	753.6	1005.6	Mavrogenis and Papachristoforou, 1988
Percent milk not suckled:	66%	66%	Nablusi et al., 1993; Epstein, 1982
Percent milch animals:	36%	20%	Nyerges, 1980
Milk yields (kcal/yr):	99475.2	39821.76	Calculated from the above
Meat output (kg/animal):	10.09	14.88	Sen et al., 2004
Meat energy (kcal/kg):	1090	2300	USDA, 2011
Percent meat animals:	25%	25%	Nyerges, 1980
Meat yields (kcal/yr):	10998.1	34224	Calculated from the above
Goat:Sheep Ratio:	2	1	Ullah, 2011
Average yield (kcal/yr/animal):	38560.597	16520.352	Calculated from the above
Herd animal attributes	*Baladi Goat*	*Awassi Sheep*	
Body weight (kg):	40	70	Wilson, 1982; Epstein 1982; Degen, 2007
Fodder requirement (kg/yr/head):	584	894.25	Stuth and Sheffield 1991
Percent diet from barley fodder:	10%	10%	Thomson et al., 1986
Wild fodder need (kg/yr/head):	525.6	804.825	Calculated from the above
Barley need (kg/yr/head):	42.05	71.54	Calculated from the above
Agricultural Product Yields	*Barley*	*Wheat*	
Energy yield (kcal/kg):	3000	3540	Smith, 2006; Fairbairn et al., 1999
Maximum possible yields (kg/ha):	2500	3500	Pswarayi et al., 2008; Araus et al., 1998, 2001
Seed reserve:	15%	15%	Hillman, 1973
Required labor (man days/ha/yr):	50	50	Dabasi-Scheng, 1978
Wood gathering			
Wood need (kg/person):	2000		Karanth, 2006
Gathering intensity (kg/m2):	0.08		Karanth, 2006
Labor and planning			
Maximum farming distance (hrs):	3		Estimated from McCall 1985
Maximum grazing distance (hrs):	8		Ullah, 2011
Farm yield expectation scalar:	75%		Estimated from Grisley and Kellogg, 1983
Labor availability (man days/yr):	300		Estimated from McCall 1985
Wood gathering distance weight:	3		Estimated from Karanth, 2006; Hartter and Boston, 2007, 2008

Table 6.2. Table showing the variables used to create the twelve modeling experiments (numbered and labeled) and the specific values of these variables in each modeling experiment.

	1) Good-lazy pastoralists	**2) Good-lazy agropastoralists**	**3) Good-lazy agriculturalists**
Agropastoral ratio:	20/80	50/50	80/20
Ovicaprids per person:	26	17	7
Herd stocking rate:	~0.15 animals/ha	~0.15 animals/ha	~0.15 animals/ha
Farming fertility decline:	1% per yr	1% per yr	1% per yr
Farm plot preference:	Maquis or less	Maquis or less	Maquis or less

	4) Greedy-lazy pastoralists	**5) Greedy-lazy agropastoralists**	**6) Greedy-lazy agriculturalists**
Agropastoral ratio:	20/80	50/50	80/20
Ovicaprids per person:	26	17	7
Herd stocking rate:	~0.3 animals/ha	~0.3 animals/ha	~0.3 animals/ha
Farming fertility decline:	2% per yr	2% per yr	2% per yr
Farm plot preference:	Maquis or less	Maquis or less	Maquis or less

	7) Good-hardworking pastoralists	**8) Good-hardworking agropastoralists**	**9) Good-hardworking agriculturalists**
Agropastoral ratio:	20/80	50/50	80/20
Ovicaprids per person:	26	17	7
Herd stocking rate:	~0.15 animals/ha	~0.15 animals/ha	~0.15 animals/ha
Farming fertility decline:	1% per yr	1% per yr	1% per yr
Farm plot preference:	None	None	None

	10) Greedy-hardworking pastoralists	**11) Greedy-hardworking agropastoralists**	**12) Greedy-hardworking agriculturalists**
Agropastoral ratio:	20/80	50/50	80/20
Ovicaprids per person:	26	17	7
Herd stocking rate:	~0.3 animals/ha	~0.3 animals/ha	~0.3 animals/ha
Farming fertility decline:	2% per yr	2% per yr	2% per yr
Farm plot preference:	None	None	None

Table 6.3. Table of economic and ecological data used to parameterize the models of PPN subsistence systems.

Data type	Data		Source
Pastoral product yields	*Baladi Goat*	*Awassi Sheep*	
Milk output (kg/yr):	200	60	Degen, 2007
Milk energy (kcal/kg):	753.6	1005.6	Mavrogenis and Papachristoforou, 1988
Percent milk not suckled:	66%	66%	Nablusi et al., 1993; Epstein, 1982
Percent milch animals:	36%	20%	Nyerges, 1980
Milk yields (kcal/yr):	99475.2	39821.76	Calculated from the above
Meat output (kg/animal):	10.09	14.88	Sen et al., 2004
Meat energy (kcal/kg):	1090	2300	USDA, 2011
Percent meat animals:	25%	25%	Nyerges, 1980
Meat yields (kcal/yr):	10998.1	34224	Calculated from the above
Goat:Sheep Ratio:	2	1	Ullah, 2011
Average yield (kcal/yr/animal):	38560.597	16520.352	Calculated from the above
Herd animal attributes	*Baladi Goat*	*Awassi Sheep*	
Body weight (kg):	40	70	Wilson, 1982; Epstein 1982; Degen, 2007
Fodder requirement (kg/yr/head):	584	894.25	Stuth and Sheffield 1991
Percent diet from barley fodder:	10%	10%	Thomson et al., 1986
Wild fodder need (kg/yr/head):	525.6	804.825	Calculated from the above
Barley need (kg/yr/head):	42.05	71.54	Calculated from the above
Agricultural Product Yields	*Barley*	*Wheat*	
Energy yield (kcal/kg):	3000	3540	Smith, 2006; Fairbairn et al., 1999
Maximum possible yields (kg/ha):	2500	3500	Pswarayi et al., 2008; Araus et al., 1998, 2001
Seed reserve:	15%	15%	Hillman, 1973
Required labor (man days/ha/yr):	50	50	Dabasi-Scheng, 1978
Wood gathering			
Wood need (kg/person):	2000		Karanth, 2006
Gathering intensity (kg/m2):	0.08		Karanth, 2006
Labor and planning			
Maximum farming distance (hrs):	3		Estimated from McCall 1985
Maximum grazing distance (hrs):	8		Ullah, 2011
Farm yield expectation scalar:	75%		Estimated from Grisley and Kellogg, 1983
Labor availability (man days/yr):	300		Estimated from McCall 1985
Wood gathering distance weight:	3		Estimated from Karanth, 2006; Hartter and Boston, 2007, 2008

Table 6.4. Table showing the variables used to create the twelve modeling experiments (numbered and labeled) and the specific values of these variables in each modeling experiment.

	1) Good-lazy pastoralists	**2) Good-lazy agropastoralists**	**3) Good-lazy agriculturalists**
Agropastoral ratio:	20/80	50/50	80/20
Ovicaprids per person:	26	17	7
Herd stocking rate:	~0.15 animals/ha	~0.15 animals/ha	~0.15 animals/ha
Farming fertility decline:	1% per yr	1% per yr	1% per yr
Farm plot preference:	Maquis or less	Maquis or less	Maquis or less

	4) Greedy-lazy pastoralists	**5) Greedy-lazy agropastoralists**	**6) Greedy-lazy agriculturalists**
Agropastoral ratio:	20/80	50/50	80/20
Ovicaprids per person:	26	17	7
Herd stocking rate:	~0.3 animals/ha	~0.3 animals/ha	~0.3 animals/ha
Farming fertility decline:	2% per yr	2% per yr	2% per yr
Farm plot preference:	Maquis or less	Maquis or less	Maquis or less

	7) Good-hardworking pastoralists	**8) Good-hardworking agropastoralists**	**9) Good-hardworking agriculturalists**
Agropastoral ratio:	20/80	50/50	80/20
Ovicaprids per person:	26	17	7
Herd stocking rate:	~0.15 animals/ha	~0.15 animals/ha	~0.15 animals/ha
Farming fertility decline:	1% per yr	1% per yr	1% per yr
Farm plot preference:	None	None	None

	10) Greedy-hardworking pastoralists	**11) Greedy-hardworking agropastoralists**	**12) Greedy-hardworking agriculturalists**
Agropastoral ratio:	20/80	50/50	80/20
Ovicaprids per person:	26	17	7
Herd stocking rate:	~0.3 animals/ha	~0.3 animals/ha	~0.3 animals/ha
Farming fertility decline:	2% per yr	2% per yr	2% per yr
Farm plot preference:	None	None	None

7. RESULTS AND DISCUSSION

7.1 Chapter Introduction

In this chapter, I present the results of the modeling experiments described in the previous Chapter. The four simulation experiment types were conducted with each of the three potential PPNB subsistence strategies, for a total of twelve independent simulation experiments. Each experiment was run for 700 annual cycles (i.e., the length of the PPNB/C) with reconstructed PPNB/C climate, environment, and topography (see Chapter 5). The MML produces a prodigious amount of output data, including basic statistics for each modeled year about village and household population, yearly erosion/deposition, amount (area) of each vegetation type, soil fertility, and soil depth. These statistics provide the data with which to compare the different modeling experiments, and have been analyzed in various ways by previous MedLanD research to examine the effects of population, site location, and climate on the amount of human-caused environmental degradation, among other things (Barton et al., 2012, 2010a, 2010b; Ullah and Bergin, 2012). I use some of those same analytical techniques, but introduce some new methods of analysis as well. I focus on diachronic trends in human population, land-cover/vegetation, soil properties, and erosion and deposition rates, and then discuss the dynamics of the relationships between these different human and natural components, and pay particular attention to the evidence for potential "early-warning" indicators of critical transitions (e.g., differences in resilience, multiple stable states, and stochasticity in time-series patterning, Chapter 3, Figures 3.6 and 3.7) (Scheffer, 2010; Scheffer et al., 2012, 2009), for panarchical feedback relationships between scales/components of the Neolithic SES (e.g., "Remember", "Revolt", "Disinterest", Chapter 3, Figures 3.2 and 3.3), and for general differences between experiments relating to subsistence strategies (agriculture, agropastoralism, and pastoralism) and mindsets ("good", "greedy", "hardworking", "lazy").

Throughout this Chapter, I will refer to the specific modeling experiments by the names laid out in Table 6.2 (Chapter 6). Furthermore, I have retained a consistent color scheme throughout all plots and figures, so that specific model runs will be plotted with the same color on plots where individual runs are shown (e.g., "Run 1" will be blue on each plot, "Run 2" will be red on each plot, and so on for all repeated runs of each model variant) and specific experiments will be plotted with the same color on plots were all experiment runs are condensed into a single line (e.g., "greedy-hardworking pastoralism" will always be green).

7.2. Population

The number of people supported by a subsistence system and how population changes over time are proxies for a variety of other aspects of the system, such as overall system-potential, system-stability, system-emergence potential, and system-resilience. Furthermore, as a proxy, demography is relatively intuitive and familiar to archaeologists, so it is thus useful to begin my investigation of the experiment results with an examination of the temporal patterning in village population over the 700 years of each model run.[102]

7.2.1. Average Population Levels

Population time-series are plotted for all runs of all models in Figure 7.1. Several interesting patterns are apparent in these time-series, but the initial observation is that after a variable initial "ramp up" period that occurs at the instantiation of every model-run when agents are loosed upon a "virgin" landscape[103], each of the three subsistence strategies result in markedly different population levels over time. Table 7.1 summarizes the "ramp up" time, and the average[104] and standard deviation of "post ramp-up" population levels achieved for each experiment. These values represent the rounded averages across all repeated runs.

Several interesting trends are visible in the data presented in Table 7.1. First, the three subsistence types result in markedly different ranges of average population. Further, agropastoral and pastoral subsistence produce internally similar average populations, respectively, regardless of mindset ("good/greedy", "lazy/hardworking"). This is not true for the agricultural models, where both "good" model variants had similar average populations, which were different and much lower than that of the "greedy" model variants. Finally, although there is clear separation and standardization between subsistence strategies in terms of average population, there is considerably more variability and overlap between them when the standard deviation in populations are examined. However, there seems be a pattern of greater overlap between various mindsets of pastoralism and agropastoralism than there is between those of agriculture an agropastoralism.

In general, agriculture produces larger standard deviations than pastoralism, suggesting that absolute variation in population is larger in the agricultural models but it is very interesting that "good" agropastoralism has the

---

102 In this section, I am only examining the patterning of the total village population, and not the populations of each individual household. Calculating household population over time in the version of the MML used in this research is very difficult. The newer version of the MML has been improved to facilitate this.

103 This typically results in a dramatic initial increase in population, reaching a first "peak" before falling to some sort of equilibrium or to random or repeated fluctuation.

104 For models that had more than one stable state (see below), average population sizes were also recorded for each state (indicated in Table 7.1 by a slash).

smallest standard deviation of all experiments, but that "greedy" agropastoralism has the largest. This indicates that agropastoralism may be very sensitive to land-use mindset.

Finally, looking at the length of the "ramp up" periods for each model, it seems that it takes longer for agricultural models to achieve their first stable population (200 years or more), a little less long for agropastoralists (75-175 years), and much shorter for pastoralists (0-50 years). Remembering that each model was initiated with 60 individuals and comparing this to the average post-"ramp up" populations achieved in all experiments, the length of the "ramp up" period clearly relates to the disparity between the initial population and the "equilibrium" population reached over time. As the "ramp up" period is not typical, and thus is discarded from many statistical comparisons, this creates some disparity between experiments in useable run-time. In future modeling experiments, it will likely be better to allow the models to "burn in" until the "ramp up" period is over, and then to begin the model clock.

While these summary statistics provide some interesting initial observations, they mask a great deal of temporal pattering and variability. That variation is interesting, and will be further investigated below.

7.2.2. Population Stability

Looking at the population time-series in Figure 7.1, four general categories of temporal patterning can be discerned: 1) "Metastable" trajectories that achieve a dynamic equilibrium around a single stable state over time, 2) "Multi-stable" trajectories that have two alternative stable states over time, 2) "Unstable" trajectories that regularly or stochastically fluctuate over time, and 4) trajectories that begin as "Metastable" or "Multi-stable", but which trend to "Unstable" over time. Using these four categories, Table 7.2 summarizes the general population stability patterning for each of the 12 modeling experiments. Interestingly, there is a clear association of "Metastablity" with agriculture, and "Multi-Stability" with pastoralism. Agropastoralism, however, can lead to ether "Metastability" or to instability, depending upon subsistence mindset. The presence of "Multi-Stable" population trajectories in the experiment results is especially interesting in relation to the idea of multiple stable states and hysteresis between them. The presence of hysteresis is important in relation to the concpet of critical transition, so a measure of cyclicty within modeled population trajectories is important, and that will be investigated next.

7.2.3. Population Cyclicity

Looking again at the general population time-series diagrams in Figure 7.1, it is also apparent that several trajectories appear to be oscillating at regular intervals (i.e., they are hysteretic). Periodicity (or "Cycle Width", to use the term

coined in Chapter 3) in time-series data can be assessed through a procedure known as Lag-1 Autocorrelation, which can give an empirical assessment of the presence and character of hysteresis within model output. Lag-1 Autocorrelation works by making two identical copies of a time-series, and then comparing each with each other (by calculating a correlation coefficient) while iteratively "lagging" one copy in single time-step increments. This produces a plot of correlation coefficient at different "lags", or "cycle widths", measured in years. I conducted Lag-1 Autocorrelation on the population time-series for all runs of each of the 12 models. These analyses were only conducted for the post-"Ramp up" portions of the time-series, and this is reflected in the length of the resulting autocorrelation plots shown in Figure 7.2. These plots also show a 95% confidence interval, produced by autocorrelation of a "white noise" (random) time-series of equal length. If the correlation coefficient exceeds this confidence interval at a particular lag time, then that time period can be considered a significant scale of repeated oscillation in the time-series trajectory.

The different post-"ramp up" cycle-widths of the experiments revealed by autocorrelation provides an interesting comparison with the stability patterns noted in section 7.2.2, above. Cycle-width patterning across all the experiments exhibits a few similarities with the patterns of metastability/ multi-stability/instability, but reveals a few key differences as well. Interestingly, all experiments were highly autocorrelated at very short lags (up to about 25-50 years), indicating the presence of very short-term oscillation in population in all subsistence variants. Secondly, all agricultural subsistence variants, and the "good" variants of agropastoralism seem to exhibit high small-scale cyclicity (about 50 years or so), in that they have a patterned series of regularly spaced lags exhibiting moderate autocorrelation. The fact that these lags are evenly arranged (i.e., they repeat like a sine-wave) means that the same very strong small-scale cycle-width of about 50 years is being "discovered" by the autocorrelation routine each time the lag-size reaches a multiple of this increment. This is clearly related to the "Metastability" of these runs, where they achieve a relatively short-term oscillation around a stable dynamic equilibrium. The remaining variants of agropastoralism, and both "greedy" variants of pastoralism exhibit two strong scales of cyclicty: one short (less than about 50 years), and another long (250-300 years), although some of the models also seem to exhibit a weaker medium-length scale of cyclicity (about 150 years). These models also differ slightly in the strength of the longer-cycle autocorrelation. This is clearly related to the tendency of these subsistence variants to produce unstable population trajectories, which vary widely over time. It is interesting to note that this variation seems to be quite regular at small time-scales, and potentially also again at a larger time-scale. This may suggest that the variation is not random, and may be a sign of a cyclical set of feedbacks. In this sense, these "unstable" population trajectories might be better understood as "highly dynamic equilibria". Finally, "good" pastoralism exhibits a wide variety of autocorrelation between repeated runs. Some runs result in a very large, continuous range of significant autocorrelation (from 1 year up to about 300 years), other runs result in only short or very short-term periods (up to

only about 30 years), and still other runs have medium-term autocorrelation (up to about 100 years). This is clearly related to the exact timing of hysteresis ("flipping") between alternative stable states, which is not consistent between runs (i.e., the "flip" can occur at any point in a model run). These trends are very interesting, but more statistically rigorous methods of inter-run comparison are needed in order to confirm these patterns.

7.2.4. Inter-Run Variability in Population Trends

A relatively simple statistical method to assess inter-run variability is to calculate the coefficient of variation in absolute population between model runs at each model-year for each experiment[105], and then to calculate the average and standard deviation of yearly coefficient of variation over all 700 years. These are figures are shown as a bar chart (with standard deviation) for each experiment in Figure 7.3. On this figure, low average coefficients of variation indicate minimal inter-run variation over time, whereas high coefficients of variation indicate large inter-run differences. Figure 7.3 shows that a clear separation exists between four subsistence strategies that result in highly variable populations over time (all pastoral variants, and "greedy" agropastoral variants) and four minimally variable subsistence strategies (all the agricultural subsistence variants, and "good" agropastoral variants). plot these as individual time-series for each experiment. I should note that for experiments with only 2-3 runs, coefficient of variation (or any other such comparative statistic) is not very meaningful, and so some of these results should be regarded cautiously. However, the patterns that result are still heuristically useful, so the patterns reported here are still interesting.

There are clearly more nuances to these trends, so it is useful to visualize the yearly inter-run coefficients of variation as a time-series plot for each experiment (Figure 7.4). Three general trends are apparent in these plots (summarized in Table 7.4): 1) a general decrease in variability over time, 2) a general increase in variability over time, and 3) fluctuating levels of variability over time. In general agriculture and "good" agropastoralism result in less variability over time, pastoralism results in more variability over time, and "greedy" agropastoralism fluctuates over time. These trends are enlightening, but how do they relate to the patterns in cyclicity revealed by the Lag-1 Autocorrelation procedure conducted in Section 7.2.3, above?

This can be discovered by the creation of a Mantel Correlogram for each experiment. The Correlogram is created through a similar Lag-1 procedure to the autocorrelation routine described in Section 7.2.3, but instead each individual time-series from each repeated run is lagged against all other time-series in the set, and a global cross-correlation coefficient is calculated for each lag-time. If the cross-correlation coefficient at a particular lag is high, then that is cycle-width

105Note that these comparisons are also done post-"ramp up". Also note because only one successfully completed run exists for "good-harworking" agropastoralism, it could not be included in this, or other analyses that compare multiple runs.

that is shared across all repeated runs, regardless of the specific timing of the oscillations in each repeated run (i.e., the exact years in which the time-series plot "peaks" in any individual run). The resulting Correlograms plot as a single line for each of the 12 experiments, and are shown in Figure 7.5. The results, summarized in Table 7.4, generally mirror those created from visual assessment of the amalgamated autocorrelation routines for each experiment (Table 7.2), and confirm the separation of three general groups of population variability over time, which are: 1) low variability at all lags (agriculture and "good" agropastoralism), 2) variability increasing with lag-time ("good" pastoralism), and 3) variability high at medium time-scales and low at long time-scales ("greedy" agropastoralism and "greedy" pastoralism).

7.3. Vegetation Dynamics

Vegetation is a good proxy for system potential (especially related to the grazing potential of the system) and for the amount of interconnection between the human and natural components of the SES. Vegetation is highly dynamic in both the spatial and temporal dimensions, so both dimensions must be analyzed.

7.3.1. Spatial Pattering of Vegetation

The human effect on the spatial dimensions of land-cover is measured in multiple ways. First, the year-700[106] land-cover maps (Figure 7.6 shows a sample map for each of the 12 experiments) can be visually compared. The spatial pattering in the final vegetation maps provides a heuristic understanding of the locations of human subsistence activities, and provides some insights into what is driving the differences between experiments. Each of the twelve models affected the local environment differently, and resulted in a variety of "zones of impact" around Tell Rakkan I. The size of the "zone of impact" is certainly related to both the overall population being supported and the general amount of land required for the type of subsistence being practiced, so the two major patterns are unsurprising: 1) agriculturalists clearly require the largest farming catchments, pastoralists the smallest, and agropastoralists an intermediary-sized catchment, 2) "greedy" model variants require larger catchments than their respective "good" variants. However, it is somewhat surprising that"lazy" subsistence variants do not require significantly larger catchments than their respective "hardworking" variants. This is contrary to the expectation that the preference for already-cleared farmplots by "lazy" farmers would lead to *smaller* farming catchments in "lazy" models. This reversed pattern is partially explained by the availability of "natural" grass- and shrubland (i.e., where grass or shrubs is the climax vegetation class) to Tell Rakkan I, afforded by the site's location at the border of the grassland/

106In cases where experiments resulted in massive depopulation by the end of the simulation period, it is more useful to compare the vegetation maps from the year of the highest achieved population.

woodland ecozone transition. Even so, one would still expect "lazy" models to result in smaller agricultural catchment, however, so there must be an additional factor affecting catchment size between the model types. One possibility is that constant cropping of the closest farmpatches in "lazy" models quickly depletes these patches of their fertility and/or quickly reduces soil depths in these areas, leading to reduced returns and the need for a larger agricultural catchment over time. It is important to realize that "Lazy" models need not lead to greater fertility or soil-depth depletion over the entire length of the simulation or across their entire catchments in order to have this effect; they need only induce depletion more quickly and only to the closest farmplots. This possibility will be explored further in Section 7.3.2, below.

7.3.2. Temporal Patterning of Vegetation

While the maps of peak-population land-cover provide a good proxy for the "zone of impact" around Tell Rakkan (i.e., the sum of the agricultural and pastoral catchments) for each of the modeled subsistence strategies, they do not reveal how these impacts accrued or changed over time. The MML outputs a land-cover statistics file that records the amount of area given over to each of the 50 land-cover classes in every year of a simulation run. These data can be analyzed in a variety of ways, but the simplest is to calculate the coefficient of variation in the spatial extent of each land-cover class over time (i.e., across all 700 years) for all simulation runs, which can then be averaged for each experiment and plotted together (Figure 7.7) so that the temporal variability of each land-cover class for every experiment can be directly compared. Plots of this nature have been used in previous MedLanD research (Barton et al., 2012, 2010b; Ullah and Bergin, 2012), and the method of interpreting them has been described in depth in those publications. In general, gazing and woodgathering tend to produce plots that show increased variability of maquis and young woodlands than would have occurred in the absence of humans. This is due to the "top-down" impact of these activities, manifesting in a slow attrition to climax vegetation, which tends to increase biodiveristy in grazing catchments, as long as the catchments are not over-grazed (Barton et al., 2010b; Perevolotsky and Seligman, 1998). Farming, on the other hand, tends to produce plots that show massive increases in the amount of grasslands. This is due to the "bottom-up" impact of farming, which "instantaneously" changes the land-cover of a patch to grassland, typically leading to reduced biodiversity in agricultural catchments (Barton et al., 2010b). These "vegetation variability" plots thus can show the relative importance of farm-plot clearance, ovicaprid grazing, and firewood gathering in affecting land-cover change between the experiments. That is, the balance of "top down" to "bottom up" disturbances will create a unique curve in the plot of vegetation-type variability, and the form of this curve (size, shape, number and location of peaks) can be used to interpret the specific combination of disturbance types in a given subsistence model.

Looking at the variability plots for each of the twelve models (Figure 7.7), several patterns are apparent. First, “good” model variants produced the expected pattern that the agriculturalist models should produce a vegetation variability curve skewed to the left (i.e., “bottom up”), pastoralist models should produce a variability curve generally skewed to the right (i.e., “top down”), and that agropastoralists should have a non-skewed curve (i.e., “top down” and “bottom up” balancing to mainly disturb secondary succession vegetation communities). Second, “greedy” model variants produced much more land-cover variability in general than did “good” model variants. However, rather than a simple amplification of the variability patterns produced by “good” land-use, “greedy” land-use resulted in fundamentally different variability. Chiefly, being “greedy” resulted in a large increase in “top down” effects for all models. Some of this is certainly due to the greater yearly impact to vegetation in grazed plots caused by a higher ovicaprid stocking rate, and also due to increased firewood gathering due to generally larger populations in these models. But in fact, it is the “greedy” agriculturalist models in which the largest increase in a right-skewness manifests. This is counterintuitive to the expectations that it is grazing and woodgathering that cause right-skewed curves, as these models were among those with the lowest amount of grazing. They did have the largest populations, so woodgathering was likely very intense. These subsistence regimes also resulted in very large farming catchments, so field clearance and regrowth dynamics on the edges of this catchment may also be driving much of this right-skewed variation. This last idea is supported by the additional observation that being “greedy” also seemed to add additional left-skew to all subsistence models. This is likely due to increased rotation in the fallow-cycle because of heavier yearly fertility loss in these models. Finally, although there were some minor differences between “lazy” and “hardworking” model variants, being “lazy” did not lead to markedly different variability patterns, which is again counter to expectations.

Another way to look at vegetation variability over time is to calculate a measure of biodiversity at each time step, and to construct a time-series plots of biodiversity for each model run. I measured biodiversity using Simpson's Index of Diversity (frequently referred to as “Simpson's D”), which is a simple and widely-used measure of ecosystem diversity calculated as the proportion of each individual species in relation to the total number of species present in the ecosystem. Simpson's Index of Diversity is measured on a scale of 0-1, where 0 is no diversity (all individuals in ecosystem are from one species), and 1 is maximum diversity (all species represented in equal quantities). In order to use this index, I considered each of the 50 succession stages as individual “species”, and used the areal coverage (square meters) of each vegetation type in any given year as a measure of the “number of individuals” present in the ecosystem.

The resultant biodiversity time-series plots for all experiment runs are shown in Figure 7.8. Several interesting patterns are visible in these plots. Firstly, all types of human land-use resulted in increased biodiversity, but some land-use strategies had a larger affect on biodiversity than others. “Greedy”

agropastoralists and pastoralists had similar amounts of temporal variability (stochasticity) in biodiversity, and more variability than the other models. All pastoralist models, and the "greedy" agropastoral models had similarly elevated amounts of between-run variability. "Greedy" variants of the agropastoral and pastoral models produced similar patterns of biodiversity over time, and both produced generally higher amounts of biodiversity than their "good"counterparts. Interestingly, and opposite to the above trend, the "greedy" agriculturalists produced *less* biodiversity than their "good" counterparts over time. However, both "greedy" agriculturalist models had an initial "spike" in biodiversity, in which the maximum possible biodiversity was almost achieved. These spikes co-occur with the timing of the initial population growth "ramp ups", but were were relatively short-lived. It seems clear that this initial surge, and subsequent decline in biodiversity is related to both the right-skewness of the temporal vegetation curves, and the total eradication of forests by the end of these experiments. Furthermore, these plots indicate that these impacts occurred early in the simulation, and may have been created some sort of boundary condition (i.e., the population outgrew the available land). Biodiversity did eventually stabilize in these models, however, supporting the idea that once this boundary condition was met, some kind of carrying capacity had been reached. These lines *are* very slightly negatively sloped, however, indicating that biodiversity is still reducing over time in these subsistence strategies.

In order to further investigate this issue, and also in hopes of revealing other nuances of temporal pattering in vegetation in the other experiments, I also created vegetation "wavelet diagrams" for all runs of each experiment. A wavelet diagram is rasterization of a statistical matrix, in which numbers are replaced by a color ramp. In this case, the matrix was composed of the spatial extent (measured in number of cells) of each of the 50 vegetation classes at all years of the model. The x-dimension of the matrix represents each of the 50 land-cover classes (with succession stage increasing to the right), and the y-dimension represents time (with time progressing "down" from the top). The resulting wavelet diagram offers a simple visual representation of the timing of change across all vegetation classes at once, and so is a powerful heuristic device for discovering subtle patterns not easily-noticeable with other techniques.

Example wavelet diagrams from individual runs of each of the twelve experiments are shown in Figure 7.9. Investigation of the wavelet diagrams show several interesting patterns. First, a clear differentiation is noticeble between "good" and "greedy" variants for all subsistence types. All "greedy" variants show a marked increase in variability of land-cover class 36 (immature woodland), which seems to mark a boundary condition that these experiments achieve after the first 50 to 200 years of the simulation. It is likely, then, that *all* "greedy" are using the entire catchment (i.e., to the edges of the DEM) at some point in time. What is especially interesting is the different way in which these models respond to this boundary condition. The "greedy" agricultural models result in total deforestation within the first few years of reaching the boundary

condition, suggesting that it acts more like a "brick wall" for a highly agricultural subsistence base. The pastoral and agropastoral models experience temporary deforestation, which then oscillates over time as the forest regrows and then is cleared again. Furthermore, for pastoralists, this oscillation appears fairly regular, but for agropastoralists, it is more random. In general, all of these "greedy" strategies lead to a reduction in the number of vegetation communities present on the landscape over time. As the number of land-cover types decreases, humans must rely on a less diverse palette of vegetation for grazing and woodgathering, which suggests that the level of connectedness of the pastoral-ecology component system increases as the number of vegetation communities decreases.

There is some equally interesting patterning among the wavelet diagrams of the "good" subsistence strategies as well. First, there is a clear difference between the wavelet patterns of "good" agriculture, and those for "good" agropastoralism and pastoralism. The main difference between these two groups is in the amount of impact to the spatial extent of grasslands and shrubs: the later group has a relatively small effect, while the former has a relatively large. This corresponds to expectations about the "top down" nature of grazing impacts versus the "bottom up" nature of farming impacts. Second, "good" pastoralism exhibits clearly visible oscillation in vegetation extent at fairly large timescales, suggesting some large-scale cyclicity in ecosystem change. Finally all "good" variants exhibit small, but interesting "squiggles" of variability in the woodland range. These "squiggles" occur at slightly different times in each model, but always appear to "clear up" over time. It is unclear what is causing these, but they may indicate some finer-scale interactions or pattens related to the base succession cap of vegetation in the region.

7.3.3. land-cover Dynamics and Population Stability Patterns

How does all of this temporal and spatial patterning of land-cover relate to the four patterns of population identified in Section 7.2.2, above? I investigated this by subjecting the temporal vegetation matrices (i.e., the same matrices used to construct the wavelet diagrams) to a Principle Components Analysis (PCA), which redistributes the variability present in the data set along a series of decreasingly important axises, or "components". "Scree" plots, which show the percentage of the variability accounted for by each component, indicate that almost all (>98%) the variability present in all input data sets lies within the first two components for all model variants. Thus, the spatial patterning of input cases (which are model-years) in the 2-D space created by using the first two components as axises in a bivariate plot should accurately capture the patterning of temporal variability in vegetation. That is, years with similar vegetation profiles should plot close together on the PCA plot, and years that have significantly different vegetation should plot far apart. Four distinct patterns appear in the resultant plots, which match exactly the population stability patterns

summarized in Table 7.3: “Metastable”, “Multi-Stable”, “Unstable”, and “Metastable trending to Unstable”.

Figures 7.10 through 7.13 show example Principle Component plots for “Metastable”, “Multi-stable”, “Unstable”, and “Metastable trending to Unstable” experiments. These plots show Component 1 along the y-axis, and Component 2 along the x-axis. The loadings for each vegetation classes across each axis are also shown in these figures, which helps to explain the visual patterning. “Metastable” experiments (Figure 7.10) exhibit a “clump and tail” pattern on the PCA plots. The “tail” relates to the “ramp up” period where vegetation is being actively, and directionally altered from year to year, and the “clump” relates to the stable vegetation state that is achieved once these models reach metastability around a dynamic equilibrium. It is of note that the “clumps” are highly spatially autocorrelated on the PCA plots, indicating that once metastability is reached, vegetation only varies within a small range. The loadings plots indicate that most of the change occurring during the “ramp up” period is in the woodland vegetation classes, and that most change occurring once metastability is achieved is in the grassland through maquis vegetation range.

“Multistable” experiments (Figure 7.11) exhibit a “bimodal” pattern on the PCA plots, where most input years are clustered into two distinct clusters. This clearly indicates that there are two alternative stable vegetation states in these models. There is also a “tail” that relates to the “ramp up” period in these models, but perhaps more interesting is the presence a several “outlier” years that occur, widely-interspersed, in the zone between the two clumps. The loadings plots indicate that the cluster separation is mainly related to dynamics in the middle range of woodland vegetation, which, coincidentally, is also the most productive range of vegetation in terms of edible biomass for ovicaprid grazing. Thus, it appears likely that ovicaprid grazing is the main driving factor for hysteresis between the two alternative stable states in the model. The presence of only a very dispersed set of points in the space between the two clusters indicates that the “flip” between these alternative states occurs very rapidly, over the space of only a few years. Finally, the variation *within* each cluster (i.e., *within* each alternative stable vegetation state) seems to be driven mostly by dynamics at the top range of woodland vegetation, and to a lesser degree, by dynamics in the grass and shrublands.

“Unstable” models (Figure 7.12) exhibit a “meandering” or “random-linear” pattern, where consecutive years seem to be mildly autocorrelated, but that there is no distinct clustering over time. That is, the vegetation state “wanders” randomly over time, sometimes “doubling back” to a state it once occupied, but not with any regularity. The PCA loadings are less meaningful in this case, but they seem to indicate that vegetation variability over time is driven by dynamics in the “maqui/immature woodland” zone, and at the “mature woodland”. This may be due to the competing needs of plot-clearance for “bottom up” farming, and the preferences of “top down” grazing in this “greedy-harworking” agropastoralists experiment.

Finally, “Metastable trending to unstable” experiments exhibit a PCA plot pattern that has both the “tail and clump” of the “Metastable” experiments, and the “meandering” pattern of the “Unstable” experiments. The “clump” is much less autocorrelated than in the “Metastable” PCA plots, and seems to show a pattern of increasing variation within the clump over time. This is interesting because it would seem that the metastability achieved in the first years of these experiments is not completely stable, and that internal dynamics in this supposedly “stable” vegetation state seem to be self-amplifying, until they reach the point where the entire system leaves the stable states, and enters into random, unstable movement through the vegetation spectrum over time. Again, the PCA loadings plots for this type of experiment must be interpreted with much caution, but it again seems that this patterning is being driven by two sets of dynamics at the top and middle end of the vegetation succession scheme.

7.3.4. Land-Cover Dynamics and Alternative Stable States

What is driving the hysteresis in the three models that resulted in more than one stable population state (“good-hardworking pastoralists”, “good-lazy pastoralists”, and “greedy-lazy pastoralists”)? It is difficult to draw a direct causal link, but it is logical that some inherent cyclicty or other patterned variation in land-cover dynamics may play a large role in controlling this hysteresis. As a starting point, it is interesting to visually compare land-cover maps from each stable state for the three hysteretic models (an example comparison is seen in Figure 7.14). Most strikingly, the size difference between the zone of impact for high-population stable states and those for low-population stable states is not very large in any of the three model runs. This suggests that the land-cover dynamics of only a relatively small portion of the landscape is largely responsible for determining the system-states of a particular subsistence strategy at any given time. These small regions seem to occur at the edges of the pastoral catchments, and so may thus be the “critical impact zones” that are most responsible for controlling/triggering the (critical) transition between stable states. The vegetation-cover range in the pastoral “critical impact zones” are those in the middle-range of woodland, which are, again, those that produce the most edible biomass for ovicaprid grazing. This corresponds to the insights gained from the PCA analysis of the temporal patterning in vegetation for “Multi-Stable” models described in Section 7.3.3, above. There also is an extension of farming land in the “high” state, and we will investigate soil fertility and depth dynamics below to see if these may also contribute to hysteresis.

Finally, some additional insights may be gained by examine the temporal dynamics in vegetation of hysteretic models as captured by the same type of “wavelet” diagrams described in Section 7.3.2, above. Figure 7.15 shows wavlet diagrams for all five runs of a highly hysteretic experiment (“good-lazy” pastoralism). Alternative vegetation states are clearly visible on these diagrams, and their timing corresponds to that in the population time-series data. What is

especially interesting is that occasional "blips" – brief switches from one state to the other and then back – appear on some of these plots (indicated in Figure 7.15 by black arrows). Scheffer (2012, 2009) predicts the presence of such "blips" as "early warning" signs of critical transitions.

7.4. Landscape Evolution Dynamics

The spatial and temporal patterning of human-caused erosion can be considered a different, yet related, proxy for the location and temporal patterning of the connections between humans and landscapes than that of vegetation. An examination of these patterns elucidates and extends the insights gained in Section 7.3, above.

7.4.1. Landscape Evolution Control Model and Sensitivity Analysis

The human contribution to erosion and deposition in each experiment is derived through the use of a control model carried out in *r.landscape.evol.py* using the same climatic, environmental, and topographic contexts as the other experiments, but with no human land-use (i.e., land-cover remained static) across the entire 700 years of the LPPNB. This control model provides a base-line from which to compare the human contribution to erosion and deposition cause by the different land-use choices in the twelve simulation experiments.

Other types of control models can be conducted in an iterative manner, altering an input variable in known increments. This is typically referred to as "Sensitivity Analysis", and is done in order to provide a comparative framework for experiment interpretation. In the current round of experiments, the impact of human alteration of vegetation to rates of erosion and deposition over time is of special interest, as other potentially influential variables (such as climate change) were held constant. Thus, I conducted a short-term (100-year) Sensitivity Analysis into the effects of land-cover on erosion and deposition. I ran several small control models in *r.landscape.evol.py* with the same topographic and hydrological parameters used in all of the experiments, but input a series of static and homogeneous vegetation maps for each control model. The results are plotted as time-series of median erosion and deposition in Figure 7.16, which show the temporal trend in erosion/deposition under different homogeneous vegetation regimes. The overall impact of vegetation on erosion/deposition patterns as expected (i.e., erosion/deposition increases as land-cover becomes more substantial and protective), but an interesting phase-change appears in erosion rates between the "shrubs" and "maquis" land-cover types. land-cover of "shrubs" is substantially less protective than that of "maquis" or better, so this distinction can be expected to produce interesting patterns of differential erosion in experiments that produce vegetation mosaicked among these two general groups of vegetation classes. Furthermore, when the variation in erosion rates over time

are calculated and plotted for each of these control models (Figure 7.17), an very strong exponential relationship between erosion temporal variation and land-cover is found to exist. That is, the less-protective the land-cover, the more likely it is that erosion will continually increase over time. Thus, experiments that reduce the amount of forest and maquis are more likely to experience continued and increasingly high amounts of erosion over time.

7.4.2. Overall Human Affect on Sediment Balance

A good first analysis of the general impact of each of the 12 subsistence varieties on landscape evolution over the LPPNB is to calculate the human impact on overall sediment balance after 700 years. This is done by first creating a "cumulative net elevation-change map" for each experiment run by subtracting the year-700 elevation from the year-0 elevation, and then summing the values of all cells in the resultant map. If erosion and deposition were perfectly balanced, the sum would be 0. If the sum is negative, then erosion outpaced deposition, and vice versa if the sum is positive. When this is completed for all runs, and the average sediment balance calculated across repeated runs for each of the 12 experiments, it seems that any type of human land-use balances to net erosion after 700 years (Table 7.5, top). However, it appears that the absolute amount of erosion is greater in the agricultural models than the other two subsistence suites, and also greater in the agropastoral models than in the pastoral ones.

Boxplots created by averaging summary statistics from the cumulative net elevation change maps of all repeated runs of each experiment (Figure 7.18) further illustrate the trend towards net erosion in all twelve models, but also show that there is quite a bit of variability in the absolute range of erosion/deposition between the different models. In general, however, the inter-quartile range is larger for the "greedy" models than for their respective "good" variants, and larger for agriculture than for either of the other subsistence strategies.

A more nuanced picture appears when the overall sediment balance of the control model is subtracted from these, leaving behind only the human contribution to the net sediment balance from each of the types of subsistence (Table 7.5, bottom). It is now possible to separate the models into two new groups: 1) those that lead to more erosion than would naturally occur in the absence of humans (agriculture and "greedy" agropastoralism), and 2) those that lead to less net erosion and deposition than would naturally occur (pastoralism and "good" agropastoralism). It is extremely interesting that these divisions match those in average variation in population over time (Figure 7.3). It is also worth noting that "greedy" models lead to generally more erosion than their respective "good" counterparts, and the same is true between "lazy/hardworking" model pairs.

7.4.3. Spatial Patterning of Landscape Evolution

Visual examination of the 700-year cumulative erosion/deposition maps created in the above analysis allows a general heuristic understanding of the differences in the spatial patterning in erosion/deposition between experiments, but the extent of human impacts on these maps is often unclear. Using map algebra, the 700-year cumulative net elevation-change values from the control model can be subtracted from these maps, leaving only the net contribution to elevation change caused by human activity. Differences in the spatial patterning of human-caused erosion and deposition between models allows insight into the portions of the landscape that are affected by the different types of human land-use.

Figure 7.19 shows an example "human-caused" net elevation-change map for each of the 12 experiments. The spatial patterning in these maps shows general alignment with the spatial patterning of the vegetation maps (Figure 7.6). The general pattern shared by all subsistence strategies is for increased erosion in the farming catchment. This is clearly due the removal of more protective types of land-cover, and the maintenance of an artificial grassland on these areas from year to year, which is within the range of elevated erosion rates discovered by the sensitivity experiments. This helps to explain why the amount of area subjected to increased erosion rates scales with the degree of agriculture in the subsistence system (i.e., is largest in the agriculturalist models, second largest in the agropastoral models, and smallest in the pastoralist models). It may also explain why the "greedy" models also had more extensive eroded areas than the "good" models: these models seemed to have had more land under cultivation in any given year, and so experienced wider-scale erosion.

Using map algebra, it is possible to calculate the standard deviation in net elevation change at each cell between the repeated runs. In the output map, areas with high standard deviations are those that have widely different values of net elevation change after 700 years. Thus, this map both summarizes the general variability in net elevation-change due to divergent model-run trajectories in each experiment, and identifies highly variable areas. These highly variable areas are those areas of the landscape where the amount of human-induced erosion or deposition is unpredictable, and thus are quite sensitive to the emergence potential in the model.

The spatial patterning of the inter-run variability in the location of erosion and deposition in the twelve models (Figure 7.20) shows that the most variable regions of the landscape are at the outside edges of the agricultural and pastoral catchments, respectively. This is particularly interesting in comparison with the patterning in vegetation dynamics in section 7.3 above, which indicated that dynamics/variability in these areas is also responsible for controlling/ triggering the timing and nature of the transition between stable states in models that have multiple stable states. This all suggests that under certain subsistence regimes, these areas may be key locations in the ecological "memory" (i.e., "ecological

inheritance") of the system, where random effects may "take root", self-amplify, and produce path-dependent trajectories that may lead to hysteresis.

There are some other interesting patterning visible in these data as well. First, erosion/deposition on agricultural land seems to be more variable than on pastoral land. Second, variability on pastoral land is higher in those models that had a larger pastoral component (i.e., agropastoralism, and pastoralism). Thirdly, variability was more widespread in the "greedy" models than in the good models. And fourthly, variability was only slightly more widespread in the "lazy" models than in the "hardworking" models. One final observation of note is that in models that resulted in "Unstable" or "Trending to Unstable" population time-series (both forms of "greedy" agropastoralism, and "greedy-lazy" pastoralism) the pastoral catchment is very large, and seems to exhibit interesting and highly variable sensitivity between model runs, suggesting that the instability in these models derives from the increased effect of stochasticity in larger pastoral catchments.

7.4.4. Temporal Patterning of Landscape Evolution

Previous MedLanD research has identified several important indicators in the temporal patterns of erosion and deposition output by the MML (Barton et al., 2010b). Temporal patterning of human impact to erosion and deposition rates is most efficiently achieved by subtracting the median erosion/deposition values of the control model from those of each modeling run in a spreadsheet *post facto*[107]. These values are iteratively summed to calculate the cumulative median human-caused erosion and deposition, which can then be plotted as time-series and visually compared. The cumulative amount of human-caused deposition and erosion is a good gauge for the overall environmental impact of different subsistence practices over time. Experiments are compared by plotting these statistics on the same axes, and also be comparing the total cumulative erosion and deposition after 700 years (Figures 7.20 and 7.21, for deposition and erosion, respectively). It is important to note that because this the net *human* impact to erosion/deposition, it is possible to achieve negative values, which indicate that *less* erosion or deposition occurred in the simulation than would have happened with no human land-use.

The resulting time-series curves show another aspect of the different ways each of the models affect erosion and deposition. Although the main pattern in these data shows that all "good" had significantly less impact on erosion/deposition than did their "greedy" counterparts, there are some other

107Tests undertaken by MedLanD project staff in preparation for the analyses presented in Barton et al. (2010b) showed that there was no statistical difference between "human contribution" values produced by *post facto* subtraction of yearly median control model values in a spreadsheet and "human contribution" values generated directly from maps made by subtracting control model erosion/deposition maps from experiment erosion/deposition maps in a GIS. The huge increase in calculation time needed to accomplish the latter is thus unwarranted.

interesting patterns that are worthy of discussion. Because climatic variables are held constant in these simulations, changes to erosion and deposition rates are intrinsically tied to changes in the land-cover of the project area. Clearly, the large expansion of artificial grassland (wheat and barley fields) in the agricultural models lead to greatly increased erosion, and reduced deposition. Even the "good" agricultural models result in very high amounts of erosion and deposition, which is not at all clear in the other measures examined above.

Pastoralism seems to result in the lowest human contribution to erosion in both the "good" and "greedy" model-suites, and in fact results in *less* erosion than would have occurred without human land-use (and quite high levels of increase deposition). Agropastoralism shows a similar, although less drastic pattern. This is particularly interesting in the light of the temporal vegetation patterns (Figure 7.9), which indicates that, at least in the "greedy" variants of these models, significant deforestation occurs periodically throughout the simulation, which would be expected to lead to increased erosion rates. One possible reason for this counterintuitive result may be due to the fact that grazing tends to create a "patchy" landscape, rather than a uniformly cleared one. This increased heterogeneity of vegetation (i.e., "mosaicking") may provide a series of vegetated "check dams", which may sufficiently reduce the stream power of flowing water and thus lead to lower-than-expected erosion.

Finally, "greedy-hardworking" pastoralism seems to result in a unique pattern of erosion, where it initially was very less than would be with out human land-use, but eventually began to drop rapidly back towards the level of the control model, and, in some model-runs, dropped so far as to be more than would have occurred naturally. This model also showed the highest inter-run variability, which is interesting because it was also the run with the least stable population over time.

The shape of these curves is illustrative of amount of connectedness between parts of the system, in that increases in average human-caused cumulative erosion and deposition are due to human manipulation of land-cover. Thus, increasing connectedness between humans and vegetation should be visible on the time-series plots as continual increase in average human-caused cumulative erosion and deposition over time. This is, in fact, the exact pattern that occurs for all agriculturalist models. Interestingly, it seems that being "lazy" greatly affects the rate of increase (and overall amount) of human-caused erosion and deposition, and therefore system connectedness. Neutrality or reduction in erosion, on the other hand, is indicative of increased biodiversity, and thus decreased connectedness, and this is what we see in the agropastoral and pastoral models.

7.5. Soil Dynamics

In the model, soil fertility and depth are the variables that control vegetation regrowth and farming yields, so it is very important to understand

spatial and temporal patterning in soil dynamics, and how these relate to the patterns noted in the other analyses.

7.5.1. Temporal Variability in Soil Depth

Figure 7.23 show time-series graphs of the net human effect on average soil depths for each model. These statistics were calculated by subtracting the yearly average soil depth in the control model (i.e., with no human land-use) from the yearly average soil depth of each model (i.e., with different types of human land-use). In these graphs, positive numbers mean that human land-use resulted in generally deeper soils than would have naturally occurred, while negative numbers mean the human land-use resulted in generally shallower soils than would have naturally occurred. The patterns of human effect on soil depths unsurprisingly track very well with those erosion and deposition (see Section 7.4, above).

Notably, all agriculturalists models resulted in net reduction in soil depths over time, at much larger scales than any of the agropastoralists or pastoralists models. Furthermore, soils continued to get shallower over time in these models, at very steady rates. The "greedy" model variants had a much greater impact on soil depths than did the "good" model variants. Where measurable, all four model variants had very low inter-run variability (although, again, these results should be regarded cautiously for those experiments with only 2-3 runs).

All four agropastoral models initially resulted in generally deeper soils, but the rate of soil depth increase was not steady in any of these models. For both "good" model variants, the time-series appears as a gentle curve such that net human effect on soil depth would eventually become negative after another hundred years or so. Where measurable, inter-run variability was low for both "good" agropastoral model variants. For both "greedy" model variants, the time-series graphs are curves with peaks at about 350. Although quite variable between runs, net human impact on soil depth becomes negative (net shallower soils) at 400 to 650 years for the "hardworking" variant, or at 550 to 650 years for the "lazy" variant (and one "lazy" model-run had not yet crossed the origin at year 700). Furthermore, both "greedy" agropastoral models resulted in a large amount of inter-run variability, and it is especially interesting that the inter-run variability of the "greedy-lazy" model seems to increase dramatically over time.

The difference between the "good" and "greedy" pastoralists models is similar to that of the agropastoralists models, except that "good" pastoralism seems to result in continued net increase of soil depth over time. The "good" pastoralist models also had very low inter-run variability (although one run of the "good-hardworking" model variant did diverge from the general trend after about 450 years). The "greedy" pastoral models resulted in soil depth impact patterns very similar to the "greedy" agropastoral models except that neither had crossed the origin (i.e., transferred to a net reduction to soil depth) by the end of the

simulation (although they clearly would have done so after another 100 to 200 years), and the "peak" amount of human-caused increased soil depth was higher in the pastoral models than in the agropastoral models. Inter-run variability was higher in the "greedy-hardworking" pastoral model, and although run-divergence appeared to have occurred early in this model variant—the first divergence occurred at 200 years—the last divergence did not occur until at about 450 years. In contrast, the "greedy-lazy" pastoral model retained low inter-run variability until about 450 years, when two runs simultaneously and quickly diverged to a much lower state (i.e., there was a rapid net human-caused decrease to soil levels). This largely mirrors the changes in population that occurred in these models.

The temporal pattering in inter-run variation in human effect on soil-depth for each of the experiments provides some additional insights to these observations. Because of the presence of both positive and negative values (i.e., that some experiments resulted in deeper soils than would occur naturally), coefficient of variation cannot be calculated, so standard deviation is used instead. In the resultant time-series plots (Figure 7.24), several trends are discovered. First, as expected, "good" model variants have lower overall inter-run variation than "greedy" models. "Greedy" pastoralism and agropastoralism exhibit increasingly divergent human effect on soil-depth over time, and interestingly, so too does "good" pastoralism. Finally, "greedy" agriculture exhibits initially very high divergence up to about 250 years, followed by a drastic reduction in inter-run variability, which then eventually very slowly rises again over the last 150 years of the simulation. This pattern may be "real", but also may be due to simple stochastic differences between the two runs that created an erroneous "spike in standard deviation. This pattern might disappear if more than two runs could have been conducted.

7.5.2. Spatial Patterning in Soil Depth

The temporal pattering in human-effect on soil-depth does not provide any indications about differential human-effects on different parts of the landscape. To investigate if human activity affected soil differently on different landforms in each model, I first created maps of the average human effect on soil-depth across all runs of each experiment. I then used the same landscape parsing rules used to determine process breakpoints procedure described in Appendix A, Section A.2 to create a map of four major landforms (see Figure A.3): 1) ridges, 2) upper slopes, 3) mid-slopes and gullies, and 4) channels. I then extracted the average human effect on soil-depth for these four landform types in all 12 experiments. These data are summarized in Figures 7.25 and 7.26. Several interesting things are apparent. Firstly, all variants of every subsistence type reduced soil depths on the upper slopes, but the actual amount that they did so varied widely. "Greedy" agriculture had a much large impact on upper-slope soil-depths than any other subsistence variant. Secondly pastoralism, agropastoralism, and "good"

agriculture all actually led to *deeper* soils on "ridges" (which also includes other flat areas, like plateaus and large terraces) than would have occurred with no land-use, but "greedy" agriculture led to *shallower* soil-depths in these same areas. Finally, any agricultural land-use also led to shallower-than-natural soil-depths on midslopes and in channels, but pastoral and agropastoral land-use did not.

I repeated this procedure, but broke the landscape apart by groupings of low-slope (< 10º), medium-slope (10º - 20º), and high-slope (> 20º). Low-slope regions are more preferred farming locations by agents in the MML, medium-slope areas are farmable, but not preferred, and high-slope areas are not farmable (and so may be preferred as grazing territory). Figures 7.27 and 7.28 show the average human effect on soil-depths in each of these slope-zones for each of the 12 models. Agriculture decreases soil-depths in all slope-zones, but "greedy" agriculture does so to a much higher degree than "good" agriculture. Pastoralism and agropastoralism all increase soil-depths in low-slope areas, but decrease it in high-slope areas, and variably affect the medium slope-zones. This data indicates that grazing on the steeper areas increases erosion there, but that the loosed sediment does not travel far (i.e., it is deposited at the base of the slope). It also indicates that farming, especially "greedy" farming greatly increases erosion on farmed fields, and may lead to serious reduction in soil-depth of these fields over time.

7.5.3. Temporal Patterning in Soil Fertility

Soil fertility is another good proxy for system potential, and is an especially good proxy for the health of the agricultural component of the system. Soil fertility statistics are recorded for every year, and average soil fertility can be plotted as a time-series in much the same way as population and erosion/deposition. The times-series plots of fertility for all 12 models (Figure 7.29) show some differences between experiments, but the main observation is that soil fertility varied only over a very narrow range of values in all of the model-runs: no model resulted in soil fertility values averaging less than 98% of full fertility in any given year. This is likely because farm plots were not tenured in any of the models, and so the farmplot choice logic in the model (see Chapter 4) allowed agents to establish an efficient bi- or tri-annual fallow-rotation cycle that prevented significant reduction to soil fertility over time. This is significant because it means that no experiments reached a point where agricultural land was a limited resource (i.e., when an extensive land-use system would no longer be tenable).

The second thing of note is that the time-series patterns for fertility track very well with those for population for all models. This is unsurprising, considering that soil fertility is a major component of grain yield, and that population levels are tied to the amount of grain that can be grown (see Chapter 4). Thus all of the differences between the models noted for population (see section 7.2, above) hold true for soil fertility (i.e., those model that resulted in

larger village populations also had an overall larger impact to soil fertility). Finally, it seems that "lazy" models experienced a slightly more rapid decline in soil fertility at the start of the simulation than did their "hardworking" counterparts. This supports the idea that "lazy" models more quickly reduced the yield-potential of the close by fields, and so eventually needed larger farming catchments than those in the "hardworking" model variants.

Finally, it is possible to calculate the coefficient of variation at all model-years across the repeated runs for each experiments, and to create time-series plots of these values (Figure 7.30). These plots show the patterning in emergence, or between-run deviation, over time. Two significant trends can be seen: 1) all "good" model variants have steady, and low, coefficients of variation over time, and 2) all "greedy" model variants have higher, and more variable coefficients over time. This means that being greedy significantly affects predictability, and triggers emergence/divergence in soil-fertility dynamics. Finally, even though all "greedy" variants maintain highly dynamic patterns in inter-run fertility variability through time, "greedy" pastoralism exhibits a clear trend towards increasingly higher values of inter-run variation, "greedy" agriculture shows a clear trend of *decreasing* values of inter-run variation over time, and "greedy" agropastoralism maintains a relatively even spread of variation values over time. This is interesting, as it suggests that the agricultural returns of even "greedy" agriculture is become more predictable (i.e., less emergent) over time, whereas those of "greedy" pastoralism are becoming less predictable (i.e., more emergent).

7.6. Discussion

Some common trends occur in the analysis presented in the preceding sections, and there are several important insights that can be made from these observations. In this section, I will discuss what these results mean for important questions of stability, predictability, emergence, stress, resilience, and critical transitions in low-level food-producing SES. The modeling experiments presented here show that fairly small differences in subsistence behavior/choices can lead to very divergent patterns of population dynamics and environmental impacts. Small differences in the stocking density of animals, the impact to fertility of the farming practices, or the preference for already cleared fields have very large impacts on the size of the ecological footprint, temporal trends in system stability over the long-term, and the degree to which emergent phenomena can drive begin to self-amplify and affect directionality in these trends.

The analyses of these experiments make it clear that the main limiting factor on population growth in the MML is uncertainty in subsistence yields from year to year. Agents are only trying to meet their basic needs (i.e., they are "satisficing"), and so the more accurately agents can predict the number of farming and grazing plots they will need in a given year, the higher the chance that they will receive a sufficient subsistence return. Most of the models reach one or more stable states, and it so is clear that agent population in each of these stable

states is being limited/regulated by a sort of dynamic "carrying-capacity" threshold, inherent to each suite of subsistence choices. Stability is achieved once population sizes reach this threshold, because a large enough number of sub-optimal farming and/or grazing patches are utilized so that significant discrepancy between the returns from the planned subsistence activities and the actual subsistence need of the agents begins to occur. After this point, stochasticity in subsistence returns couples with lag-times between poor-return/high-return years and decreased/increase population growth rates to induce a cyclical "dynamic equilibrium" sinusoidally hovering near a long-term population mean.

This is not to say that the "stable" systems identified in the simulation experiments are "balanced" in the very long term. These stable systems have very large maximum potential, and so have larger ecological footprints, and more drastic effects on biodiversity, soil, and erosion and deposition rates. These stable systems seem to be reasonably path-dependent, and all indicators point to a general reduction in system resilience and an increase in system connectedness over time. "Greediness" exacerbates this, and several of the "greedy" models completely exhausted woodland resources at a very early point in the simulations. Further, "greedy" models tended to reduce soils in agricultural land. The accumulated impacts of these models fundamentally changes the ecological portions of the SES, likely making it impossible to easily switch to another style of food production. All of this suggests that they are at great risk for a major critical transition. While no such critical transitions were observed for these subsistence systems, I should reiterate that the current round of experiments was conducted under stable environmental conditions. I wonder if these systems would remain as stable in the face of rapid climate change?

Some of the modeling experiments did show evidence for multiple stable states within a single subsistence strategy. It seems that the accumulation of many relatively small reductions in the amount of high-quality farming and grazing patches—especially those at the far edges of the site's catchment—over several decades that eventually surpasses a "tipping point", and the population crashes in to an alternative, lower stable state. At this point, another "dynamic equilibrium" takes hold, and subsistence occurs within a much smaller site catchment, allowing the previously depleted patches at the far edges of the old catchment to regain their quality. Once these patches have regenerated past another "tipping point", they again become attractive, and come to be used again. The expansion of into these lands yields more resources, and the population can return to the original, higher, stable state.

This clearly meets the criteria for "critical transitions" as described in Chapter 3. What is most interesting about the timing of these critical transitions is that they do not necessarily occur at the same times or intervals in different runs of the same model. This means that it would be almost impossible for an agent to predict when one of these critical transitions may occur, or even if one will occur at all. Unpredictability is a hallmark of complexity, and it is clear that these critical transitions are complex phenomena. The "level" (e.g., equilibrium

population) of each of the alternative stable states is basically the same between runs, however, suggesting that the states themselves are well defined "natural" attractors.

In unstable systems, subsistence choices—and the impacts that occur from them—balance the system towards uncertainty. That isn't to say that there is not a "preferred" system state (for example, the unstable "greedy-lazy" agropastoralist model tended to achieve an "equilibrium" population of about 200 people), but that remaining at that state is difficult for long periods of time, and so unstable models are characterized by periodic crashes in system state. The accrual of deleterious impacts occurs at a faster rate, and so the one fully unstable model in the current experiments ("greedy-lazy" pastoralism) had one of the shortest cycle widths of any of the twelve models. Unlike multistable models, the "crashes" in the unstable models do not meet the criteria for "critical transitions" (even though they occur just as rapidly) in that the system does not remain at the lowered system state for a lengthy period of time; rather, it begins to recovers almost immediately. Unstable models are also characterized by very high amounts of inter-run variability, which means that they are highly unpredictable systems. The "crashes" in system-state do not occur on a regular interval, and are spaced very differently in each of the five model-runs, so it is highly unlikely that agents operating within them would be able to predict them. Instability does not equate to lower system resilience, however; on the contrary, unstable models were characterized by fairly high system resilience. In fact, the "instability" of these models may be linked to their ability to quickly adapt to changing conditions (i.e., to their resilience).

Perhaps most interestingly, some models were initially stable in the early years of the simulation, but trended towards instability in the latter years. This illustrates that the specific type or nature of "stability" or "multistablity" in a regional SES is not an immutable characteristic, but can change over time. It is particularly interesting that in these models, the trend towards instability was an emergent property of the system (i.e., instability was *not* induced by external perturbation from climate, war, etc.). Further, the advent of instability seems to have been coincident with a general increase in system potential and decrease in system resilience over time, but that system potential was extremely variable (varying from very high to very low in different model-runs). In general, the transition from stability to instability also accompanied a rapid and extreme increase in divergence between model runs, indicating that the system switched from being fairly predictable to being wildly unpredictable.

How do these trends relate to the amount of stress that individuals would encounter under the various modeled subsistence regimes? Resource scarcity or unpredictability is a major source of stress in low-level food-producing SES, and is likely the major stressor driving change in these modeling experiments. Looking at the patterning in population, vegetation, and soil over time, several subsistence strategies that have correlated frequent high amplitude surges and declines in these measures. These strategies can be understood to be experiencing

a recurring resource imbalance, and thus are more likely to experience resource stress, than those with lower amplitudes or less frequent surges (i.e., stability over time). By this measure, agriculture and "good" agropastoralism would seem to have the lowest levels of this type of resource stress, "greedy" agropastoralism the highest levels of resource stress, with pastoralism intermediate between these. Also, all else being equal, a "greedy" subsistence mindset always produces more resource stress than a "good" mindset.

Another source of resource-related stress derives from inequalities that arise between households in sedentary agricultural societies due to small-scale resource variability (Kelly, 1991). This stress typically manifests in high levels of inter-household competition over a limited set of resources, and would be visible archaeologically as large differences in maximum populations between households in a single community. Although this phenomenon could be directly measured in the output data of newer versions of the MML (i.e., by graphically comparing household "life histories", or population trends, over time) it is not possible with the version used in this research. However, based on the patterning I have seen in vegetation and soil properties, I would expect "greedy" mindsets to produce more of this kind of stress as well, but this is a topic that would be interesting to explore in future modeling experiments with newer versions of the MML.

Other types of more socially-derived stresses exist in real agropastoral SES, but because the social modeling engine of the MML is highly simplified, these types of stress have no effect in the current experiments. However, the general amount of social stress that may result from each of the 12 land-use mindsets can only be inferred through overall population size and stability over time. The relationship between population size and social stress has been established by Johnson (1982), in his investigation of "scalar stress" among low-level food producers. As the overall population of a community increases, scalar communication stress also increases, potentially affecting social cohesion and igniting social strife (Johnson, 1982). Thus, subsistence strategies that allow for very high populations, can be also be understood to result in higher levels of social stress, which can be a source of instability if not mitigated by special social institutions (Kuijt, 2000b). By this measure, four agricultural subsistence variants would lead to much greater levels of scalar stress than would the pastoral and agropastoral subsistence variants, and agropastoralsim would lead to higher levels of scalar stress than pastoralism.

A final, less well-understood source of stress is uncertainty due to emergence. This produces stress by making the outcome of actions highly unpredictable, so that conducting the same action (e.g., farming) in the same set of circumstance (e.g., same field or on the same landform), there is little confidence in obtaining the same result each time. Pastoralism and "greedy" agropastoralism were the most emergent of the modeled subsistence strategies, and so would lead to the highest amounts of emergent stress, whereas agriculture and "good" agropastoralism would not. However, the existence of a very stable

“equilibrium” across all repeated model-runs in these subsistence variants would make long-term social planning possible, potentially leading to an increase in social complexity, and a concurrent rise in social stresses.

Thus, these three sets of stressors are interconnected, so that change in one affects the others. They would have acted in opposite ways on the LPPNB SES, in a sort of dynamic “push-pull” system that could induce change or promote stability. Stress from resource imbalance and emergence would tend to favor an increasing reliance on agriculture, which these modeling experiments show is a stable, predictable subsistence system. However, a greater reliance on agriculture seems to lead to higher populations, introducing more social stress which may push people towards an increased reliance on pastoralism. The other solution would be to mitigate these social stresses in a different way, such as by creating new and potentially complex social institutions.

7.7. Summary

Based on the results of the analyses above, I estimated the generalized amounts of system potential, resilience, and connectedness for each of the twelve models, which are summarized in Table 7.7. It seems that these experiments show two major subsistence attractors with different characteristics. Under the modeled conditions (stable Mediterranean climate), agriculture provides a quite stable subsistence base that allows for relatively high populations and increasing predictability over time. It seems to be relatively immune to fluctuations deriving from subsistence mindset, although there is some indication that territorial "packing" may occur a result of mindsets that encourage less sustainable resource use. In the case of such packing, certain types of vegetation may become locally depleted, leading to a reduction in system resilience over time. Nevertheless, a subsistence system based mainly on agriculture seems to be the "best" solution if a large, relatively stable population base is the measure of success. This is quite interesting in relation to the "mega-site" phenomenon of the LPPNB. Using those same measures, pastoralism is a much less attractive, although not altogether unattractive, option.

Secondly, it seems that the addition of domestic animals to the subsistence base has divergent effects, depending upon the ratio of agriculture to pastoralism. The inclusion of domestic animals seems to further-stabilize the resource base if the ratio is small. By the time agriculture and pastoralism become equally important to the resource base, an additional source of instability is introduced. Equally-mixed agropastoralism in stable Mediterranean ecosystems is thus the most sensitive of the three simulated subsistence strategies to differences in subsistence mindset. Under conservationist mindsets, agropastoralism can be extremely stable and predictable, while being capable of supporting a relatively large population base. Interestingly, reducing conservationist ethics, and minimizing field-clearance labor makes it wildly unpredictable, and unstable over time. This is very interesting in the light of the ethnographic research conducted

in Chapter 3, which also suggested that certain forms of agropastoralism were inherently unstable.

Finally, under the modeled conditions, pastoralism can support much fewer people, and tends to result in a kind of "hysteresis" between two alternative stable population levels at medium to long-term cycle-widths. Pastoralism is thus less predictable than agriculture over the long-term in stable Mediterranean ecosystems, but is still fairly predictable at small or medium time-scales. Pastoralism is also fairly immune to perturbation due to subsistence mindset, although it seems to be sensitive to mindsets that encourage a combination of less sustainable resource use and minimization of field-clearing labor.

Table 7.1. Table of population sizes for each model run and stability measurements for population time-series output of the twelve models.

"Ramp-up" time (years)				
		Agriculturalists	Agropastoralists	Pastoralists
Hard-working	Good	150	75	n/a
	Greedy	225	150	n/a
Lazy	Good	200	175	n/a
	Greedy	225	75	50

Average "Equilibrium" Population Level				
		Agriculturalists	Agropastoralists	Pastoralists
Hard-working	Good	543	202	88 (70/125)
	Greedy	787	184	112 (70/130)
Lazy	Good	539	202	90 (70/125)
	Greedy	775	183	118

"Equilibrium" Population Level, Stdev				
		Agriculturalists	Agropastoralists	Pastoralists
Hard-working	Good	29	10	23
	Greedy	39	45	25
Lazy	Good	29	10	20
	Greedy	34	38	25

Table 7.2.Summary of demographic stability patterns for all experiments

Overall Population Stability (between all runs)				
		Agriculturalists	*Agropastoralists*	*Pastoralists*
Hard-working	*Good*	Metastable	Metastable	Multi-stable
	Greedy	Metastable	Trending to Unstable	Multi-stable
Lazy	*Good*	Metastable	Metastable	Multi-stable
	Greedy	Metastable	Unstable	Trending to Unstable

Table 7.3. Table summarizing general trends in post-"ramp up" population oscillation cycle-widths in individual runs (autocorrelation) for each experiment type. Correlations calculated by lag-1 procedure (see Figure 7.2).

Autocorrelation Time Spans (all runs)

		Agriculturalists	Agropastoralists	Pastoralists
Hard-working	Good	Short with some medium time scales	Short with some medium time scales	Variable between runs
	Greedy	Short with some medium time scales	Short, medium, and long time scales	Short and long time scales
Lazy	Good	Short with some medium time scales	Short with some medium time scales	Variable between runs
	Greedy	Short with some medium time scales	Short and long time scales	Short and long time scales

Autocorrelation Cycle Width Strength

		Agriculturalists	Agropastoralists	Pastoralists
Hard-working	Good	Very strong for short, weaker for medium	Very strong for short, weaker for medium	strong or weak
	Greedy	Very strong for short, weaker for medium	strong, weak, strong	strong, strong
Lazy	Good	Very strong for short, weaker for medium	Very strong for short, weaker for medium	strong or weak
	Greedy	Very strong for short, weaker for medium	strong, weak, strong	strong, weak

Table 7.4. Table summarizing trends in variation between experiment-runs over time for each experiment.

Long-term Population Variability Trends (inter-run)

		Agriculturalists	Agropastoralists	Pastoralists
Hard-working	Good	Decrease	N/A	Increase
	Greedy	Decrease	Fluctuates	Increase
Lazy	Good	Decrease	Decrease	Increase
	Greedy	Decrease	Fluctuates	Increase

Table 7.5.Table summarizing general trends in population oscillation cycle-widths common to all runs (cross-correlation) of each experiment type. Correlations calculated by lag-1 procedure (see Figure 7.2).

Cross-Correlation Cycle Width (between all runs)

		Agriculturalists	Agropastoralists	Pastoralists
Hard-working	Good	all	N/A	short through medium
	Greedy	all	short, medium, long	short, long
Lazy	Good	all	all	short through medium
	Greedy	all	Short, long	short, long

Cross-Correlation Cycle Width Strength (between all runs)

		Agriculturalists	Agropastoralists	Pastoralists
Hard-working	Good	always strong	N/A	continuously declining
	Greedy	always strong	strong, medium, weak	strong, strong
Lazy	Good	always strong	always strong	continuously declining
	Greedy	always strong	strong, medium	strong, medium

Table 7.6. Table of sediment balances (sum of cumulative erosion and deposition) after 700 years for all twelve models.

Raw Net Sediment Balance (m^3)

		Agriculturalists	*Agropastoralists*	*Pastoralists*
Hard-working	*Good*	-218184	-202447	-200788
	Greedy	-363398	-203437	-199836
Lazy	*Good*	-217343	-202639	-200295
	Greedy	-357215	-204203	-201552

Change in Sediment Balance due to Human land-use (m^3)

		Agriculturalists	*Agropastoralists*	*Pastoralists*
Hard-working	*Good*	-15376	362	2020
	Greedy	-160590	-628	2972
Lazy	*Good*	-14535	170	2514
	Greedy	-154406	-1395	1256

Table 7.7. Table summarizing the amount of system potential, resilience, and connectedness in each of the twelve modeling experiments, based on the measures presented in this chapter.

System Potential

		Agriculturalists	*Agropastoralists*	*Pastoralists*
Hard-working	*Good*	Medium-High	Medium	Low
	Greedy	High	Medium	Low
Lazy	*Good*	Medium-High	Medium	Low
	Greedy	High	Medium	Low

System Resilience

		Agriculturalists	*Agropastoralists*	*Pastoralists*
Hard-working	*Good*	Low	Low	High
	Greedy	Low	High	High
Lazy	*Good*	Low	Low	High
	Greedy	Low	High	High

System Connectedness

		Agriculturalists	*Agropastoralists*	*Pastoralists*
Hard-working	*Good*	High	Medium	Low
	Greedy	High	Medium-Low	Medium-Low
Lazy	*Good*	High	Medium	Low
	Greedy	High	Medium-Low	Medium-Low

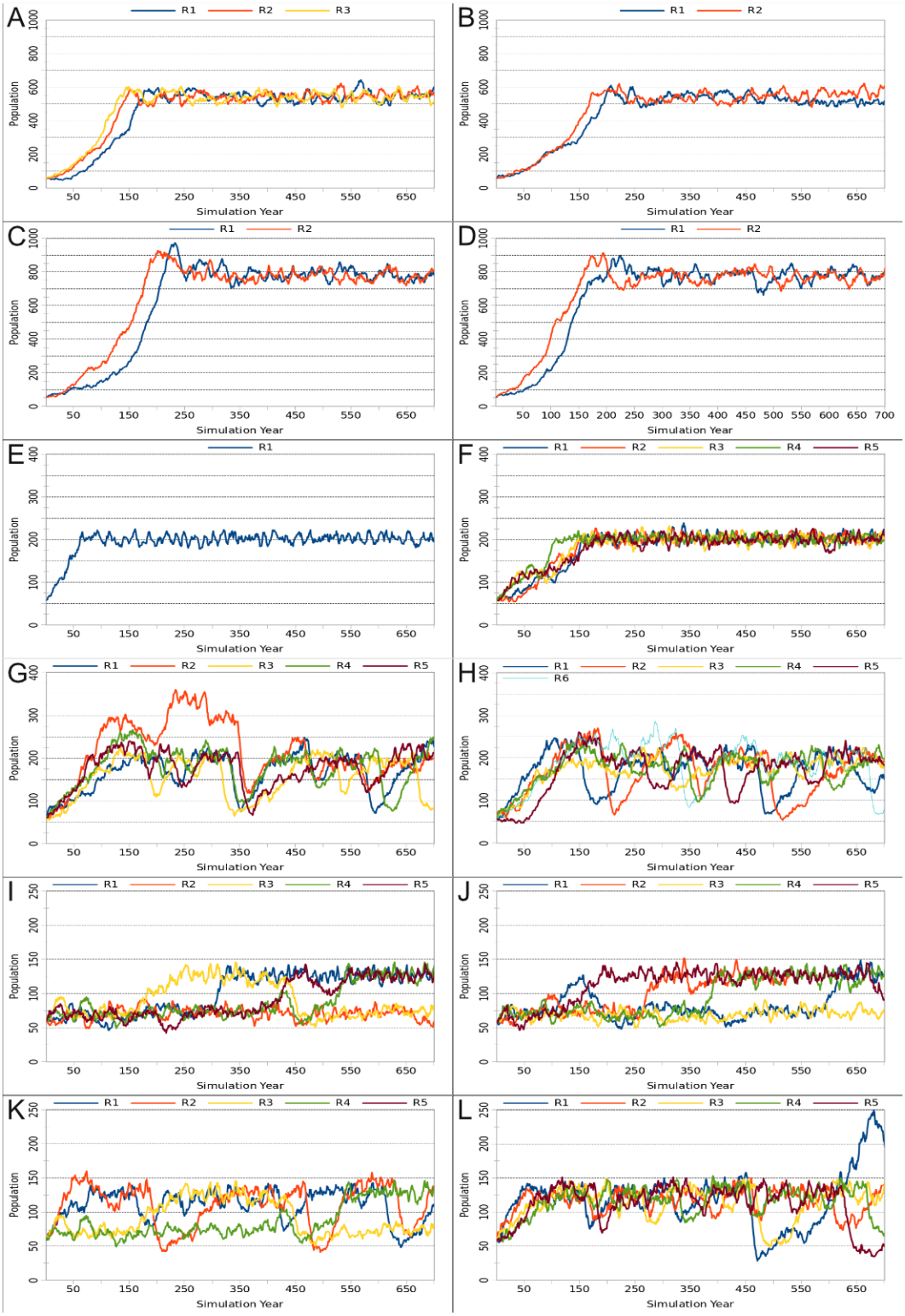

Fig. 7.1.Population time-series plots for all runs of all models. A–B : Good Hardworking and Lazy Agriculture, C–D: Greedy Hardworking and Lazy Agriculture, E–F: Good Hardworking and Lazy Agropastoralism, G–H: Greedy Hardworking and Lazy Agropastoralism, I–J: Good Hardworking and Lazy Pastoralism, K–L: Greedy Hardworking and Lazy Pastoralism.

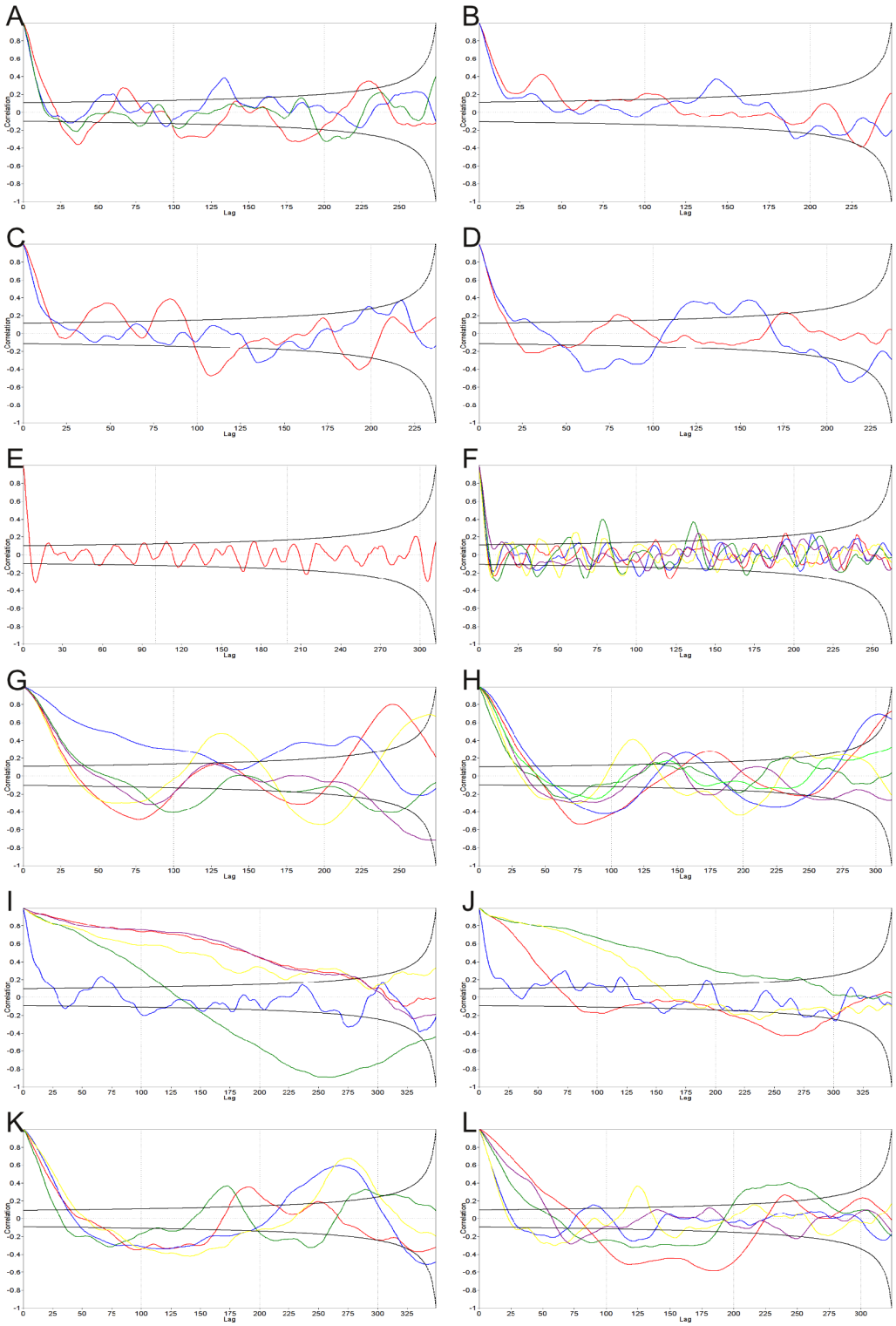

Fig. 7.2. Lag-1 autocorrelation plots of post-”ramp up” population time-series for all runs of all models. A–B : Good Hardworking and Lazy Agriculture, C–D: Greedy Hardworking and Lazy Agriculture, E–F: Good Hardworking and Lazy Agropastoralism, G–H: Greedy Hardworking and Lazy Agropastoralism, I–J: Good Hardworking and Lazy Pastoralism, K–L: Greedy Hardworking and Lazy Pastoralism.

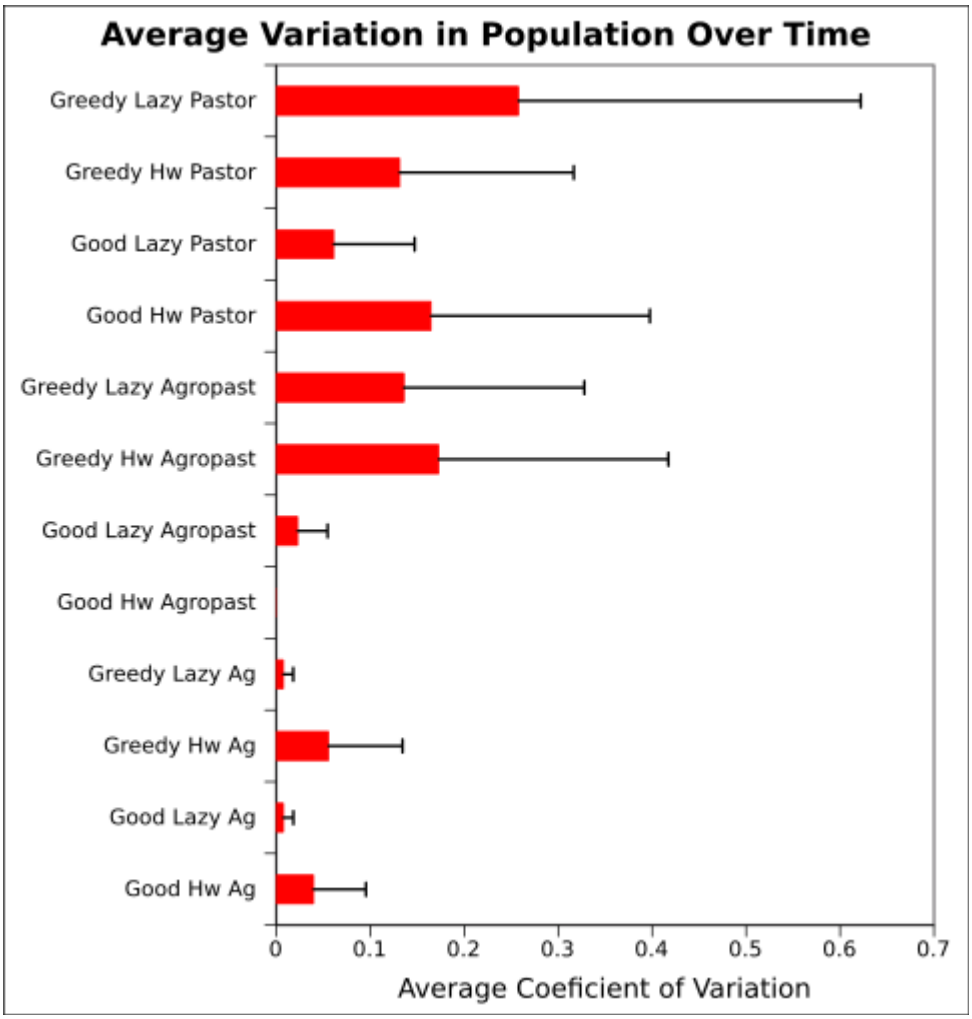

Fig. 7.3. Average inter-run variability in population size across all post-"ramp up" years for each of the 12 experiments. Error bars show the standard deviation (in the positive direction only).

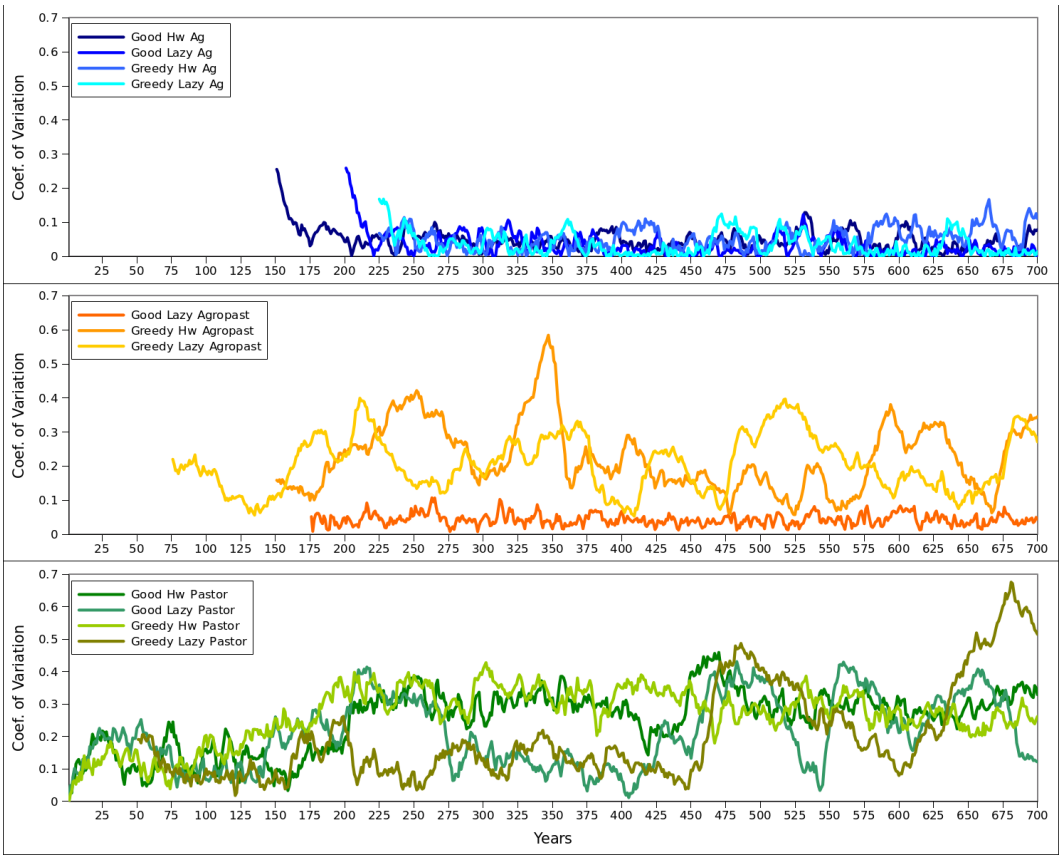

Fig. 7.4. Time-series plots of the variation in post-"ramp up" populations between repeated runs of all agricultural experiments (top, blue lines), agropastoral experiments (middle, orange lines), and pastoral experiments (bottom, green lines). Units are standardized as coefficient of variation.

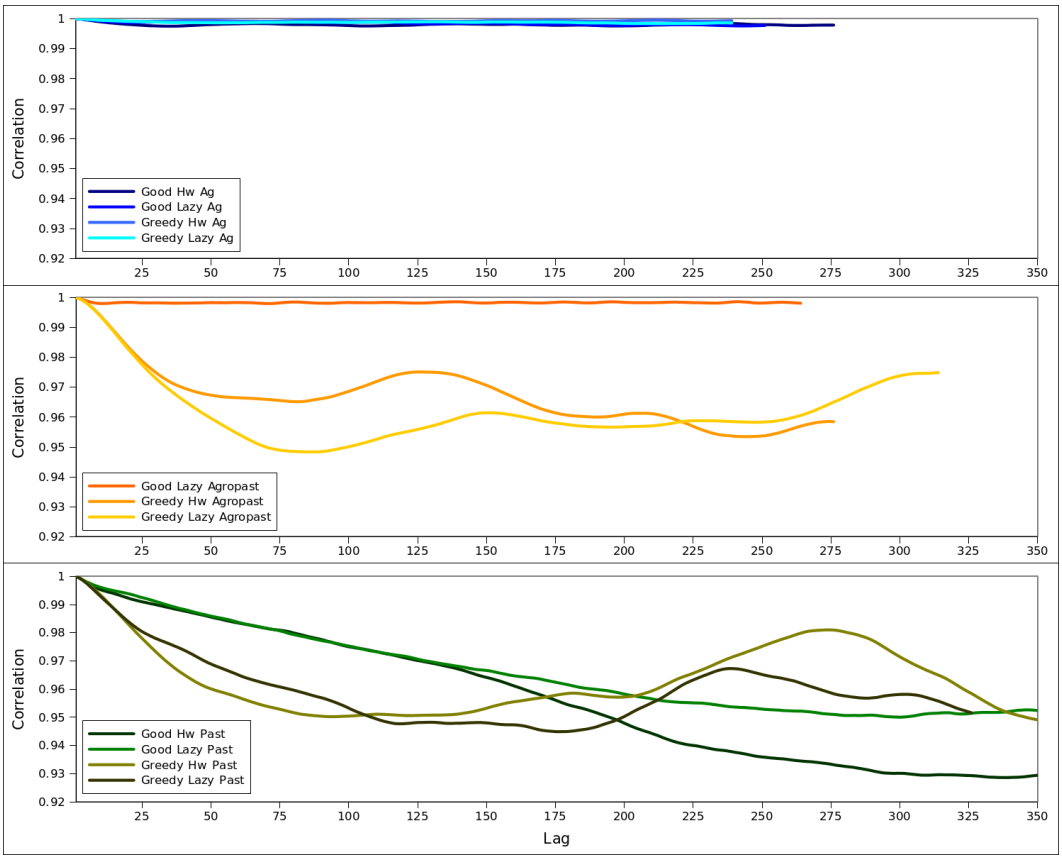

Fig. 7.5. Mantel correlograms showing the "lag-1" cross-correlation results for all post-"ramp-up" population time-series between all runs of each agricultural experiment (top, blue lines), agropastoral experiment (middle, orange lines), and pastoral experiment (bottom, green lines). "Peaks" in a correlogram show scales of cyclicity shared by all runs of a particular experiment. X-axis then denotes the "cycle width" in years.

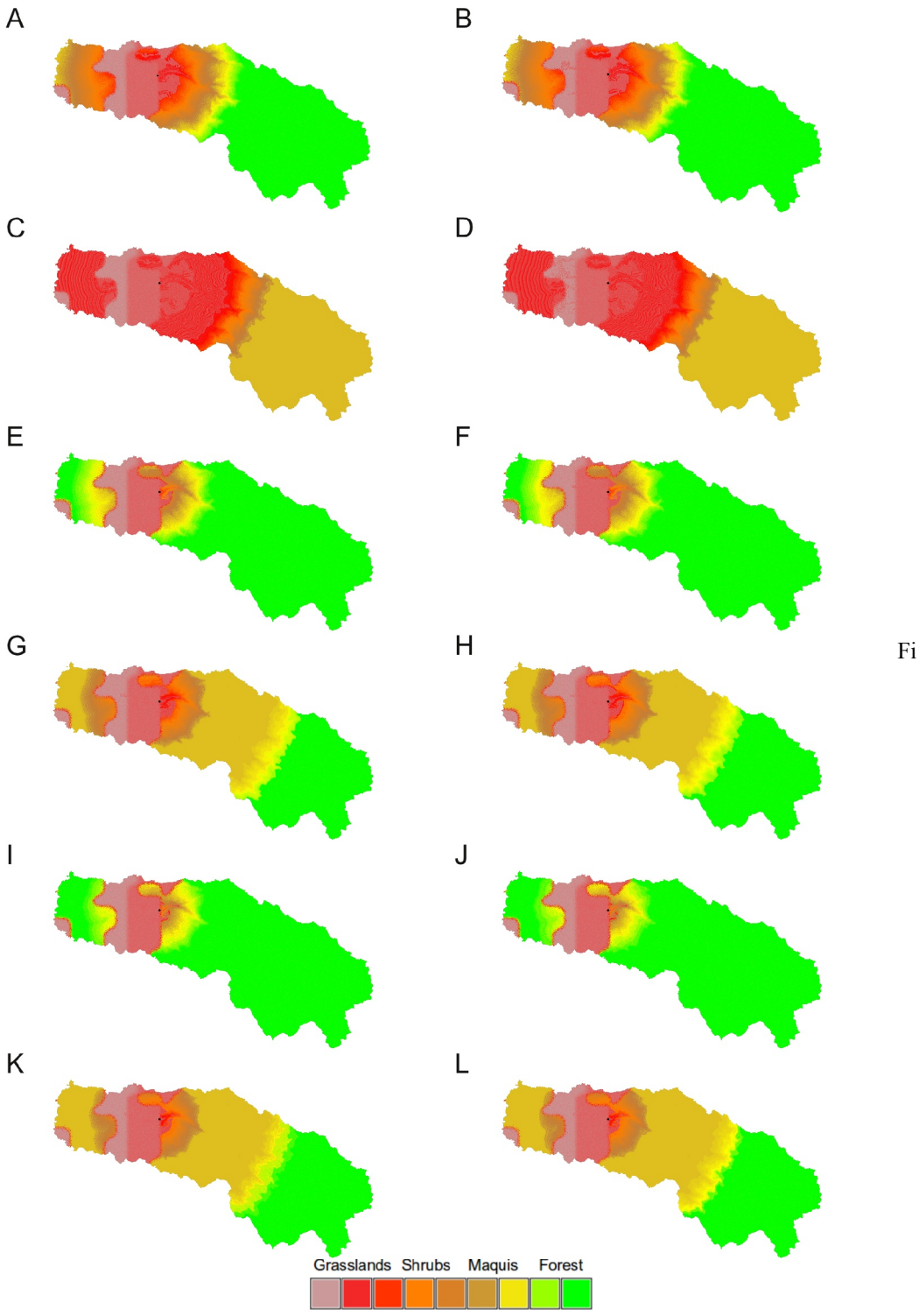

Fi

g. 7.6. Example “high population” land-cover maps for all runs of all models. A–B : Good Hardworking and Lazy Agriculture, C–D: Greedy Hardworking and Lazy Agriculture, E–F: Good Hardworking and Lazy Agropastoralism, G–H: Greedy Hardworking and Lazy Agropastoralism, I–J: Good Hardworking and Lazy Pastoralism, K–L: Greedy Hardworking and Lazy Pastoralism. Black dot shows the location of Tell Rakkan I.

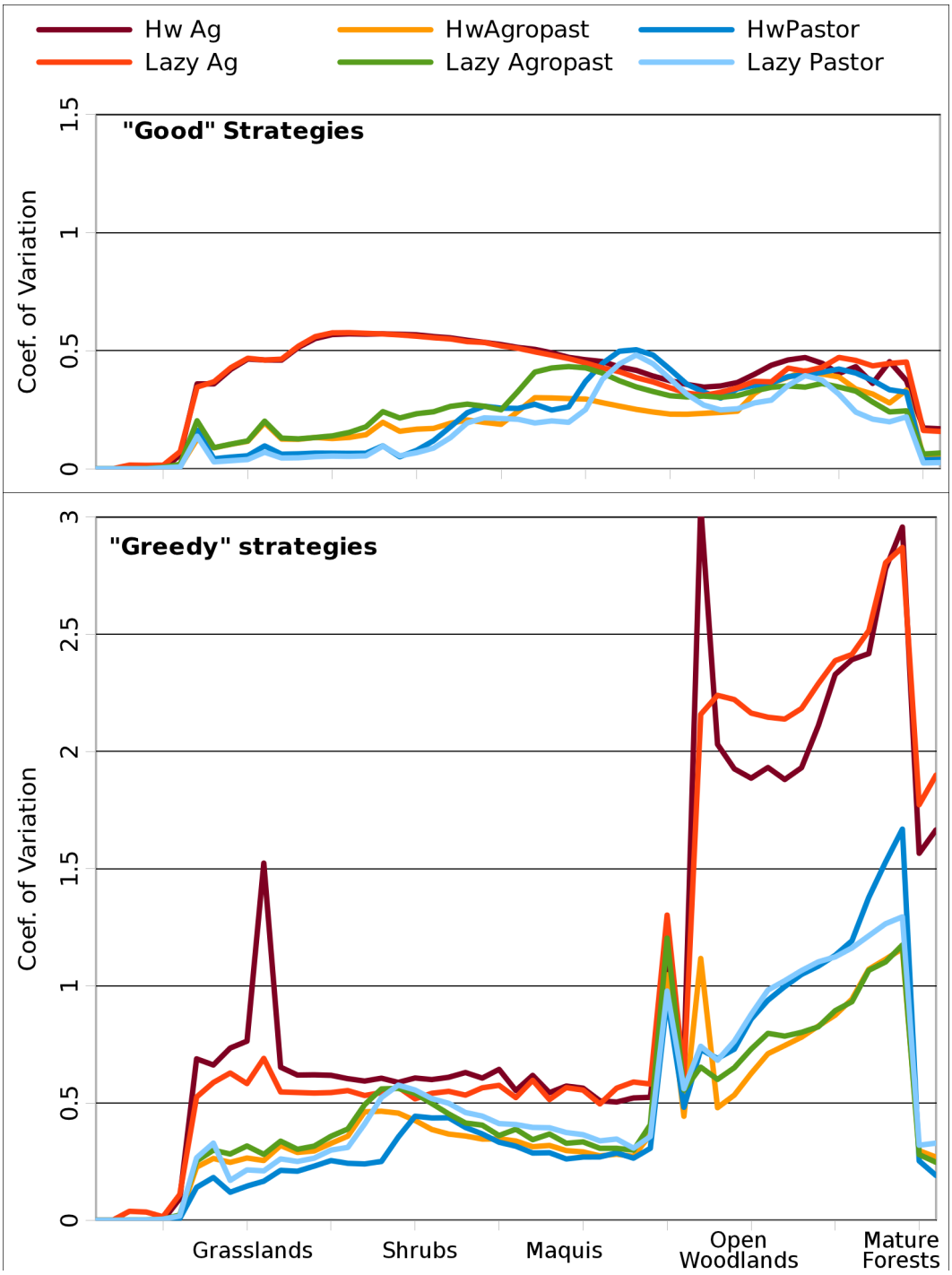

Fig. 7.7. Temporal variation "curves" in land-cover types over 700 years for each of the 12 modeled subsistence strategies. Coefficient of variation calculated for each vegetation class based on its spatial extent across all of the 700 years

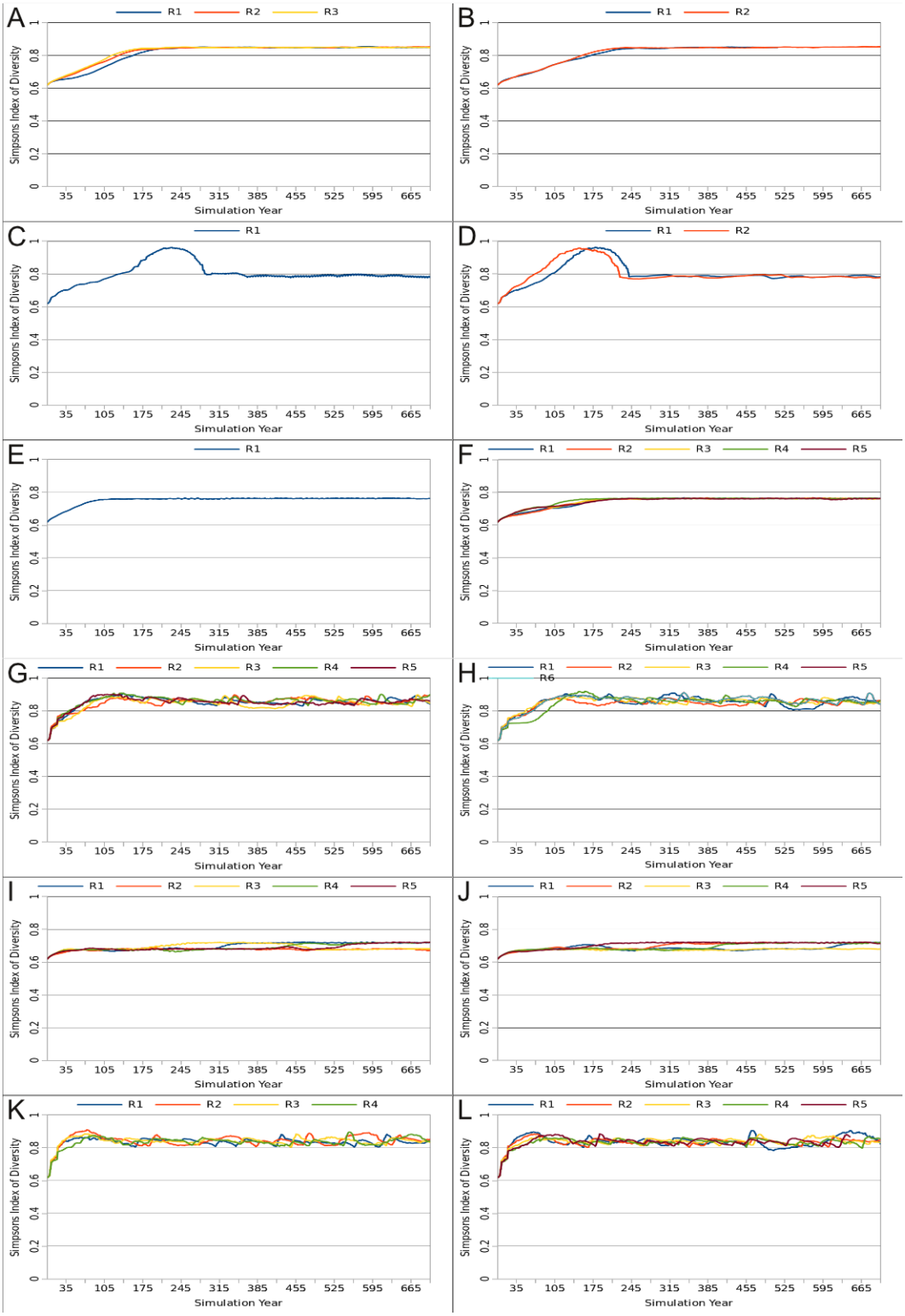

Fig. 7.8.Biodiversity (Simpsons D) time-series for all runs of all models. A–B : Good Hardworking and Lazy Agriculture, C–D: Greedy Hardworking and Lazy Agriculture, E–F: Good Hardworking and Lazy Agropastoralism, G–H: Greedy Hardworking and Lazy Agropastoralism, I–J: Good Hardworking and Lazy Pastoralism, K–L: Greedy Hardworking and Lazy Pastoralism.

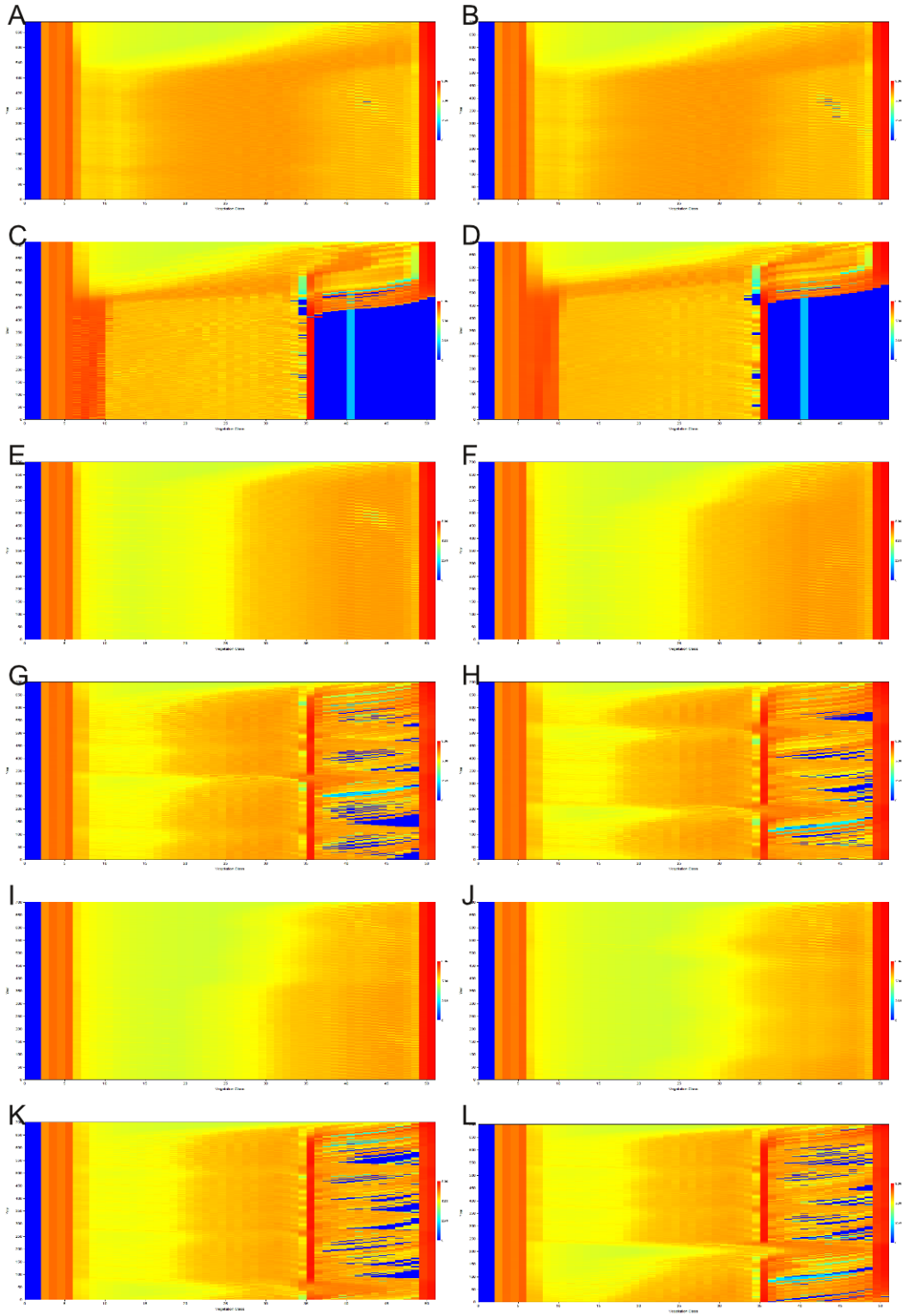

Fig. 7.9. “Wavelet” plots showing vegetation trends for all runs of all models. A–B : Good Hardworking and Lazy Agriculture, C–D: Greedy Hardworking and Lazy Agriculture, E–F: Good Hardworking and Lazy Agropastoralism, G–H: Greedy Hardworking and Lazy Agropastoralism, I–J: Good Hardworking and Lazy Pastoralism, K–L: Greedy Hardworking and Lazy Pastoralism.

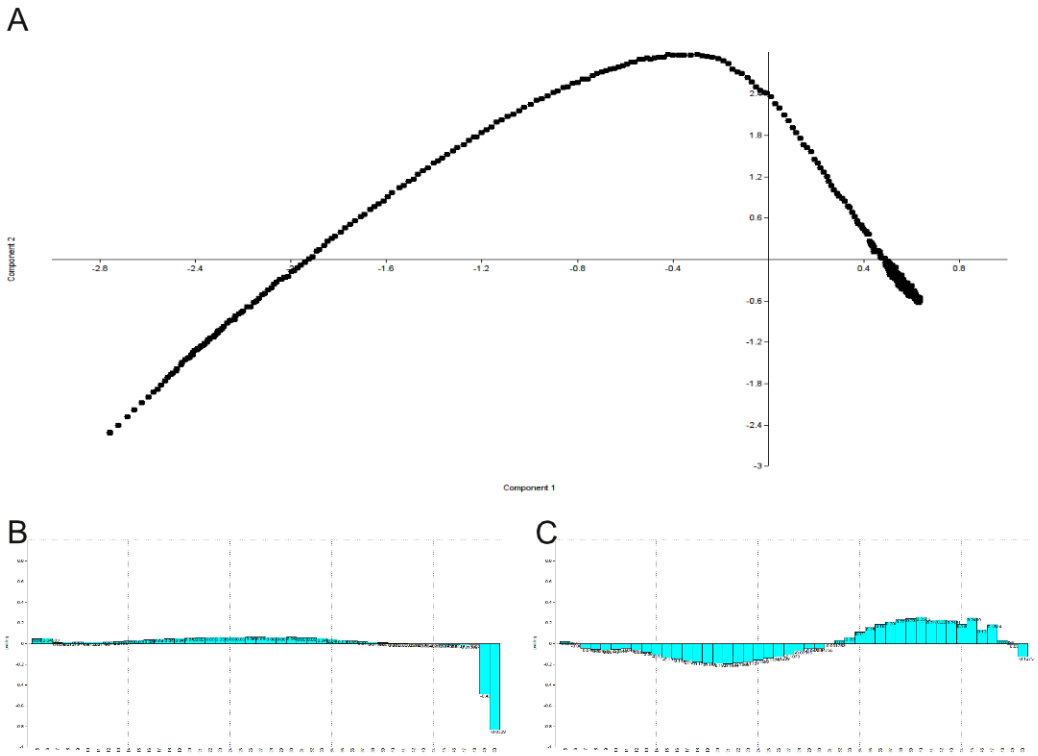

Fig. 7.10. A) Principle components analysis of the temporal and patterning of vegetation variation for an example "metastable" experiment run. Each dot represents an individual year of the experiment. B) The loadings for each vegetation class along principle component 1 (y-axis in PC plot). C) The loadings for each vegetation class along principle component 2 (x-axis in PC plot).

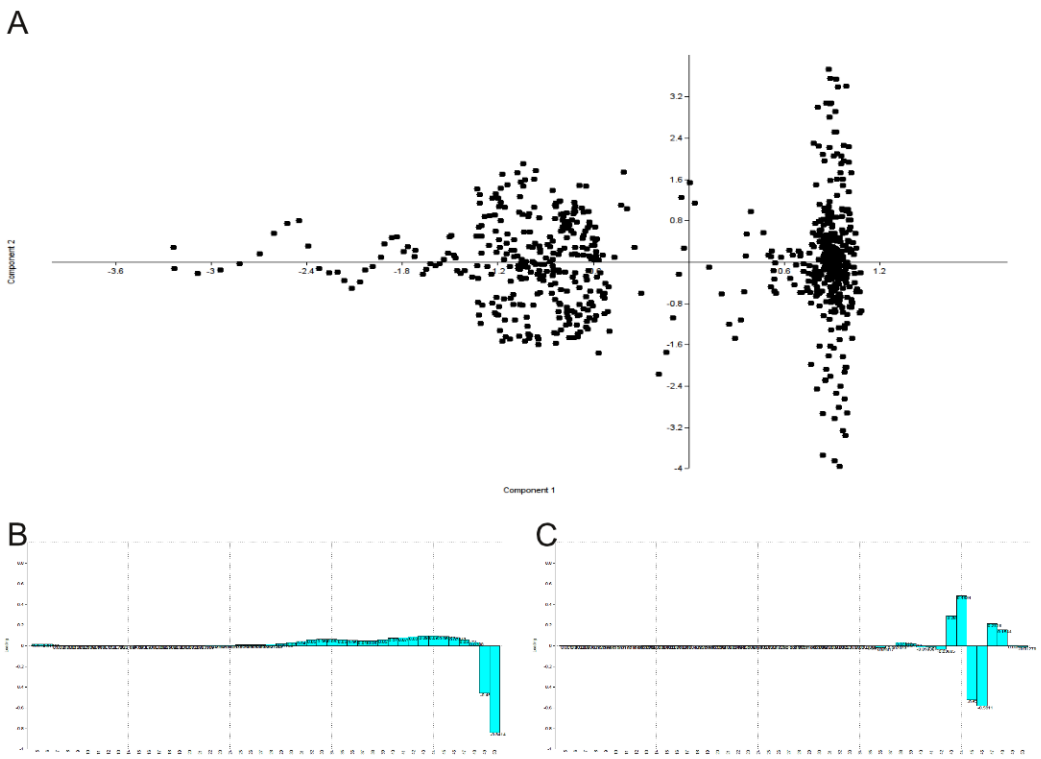

Fig. 7.11. A) Principle components analysis of the temporal and patterning of vegetation variation for an example "multi-stable" experiment run. Each dot represents an individual year of the experiment. B) The loadings for each vegetation class along principle component 1 (y-axis in PC plot). C) The loadings for each vegetation class along principle component 2 (x-axis in PC plot).

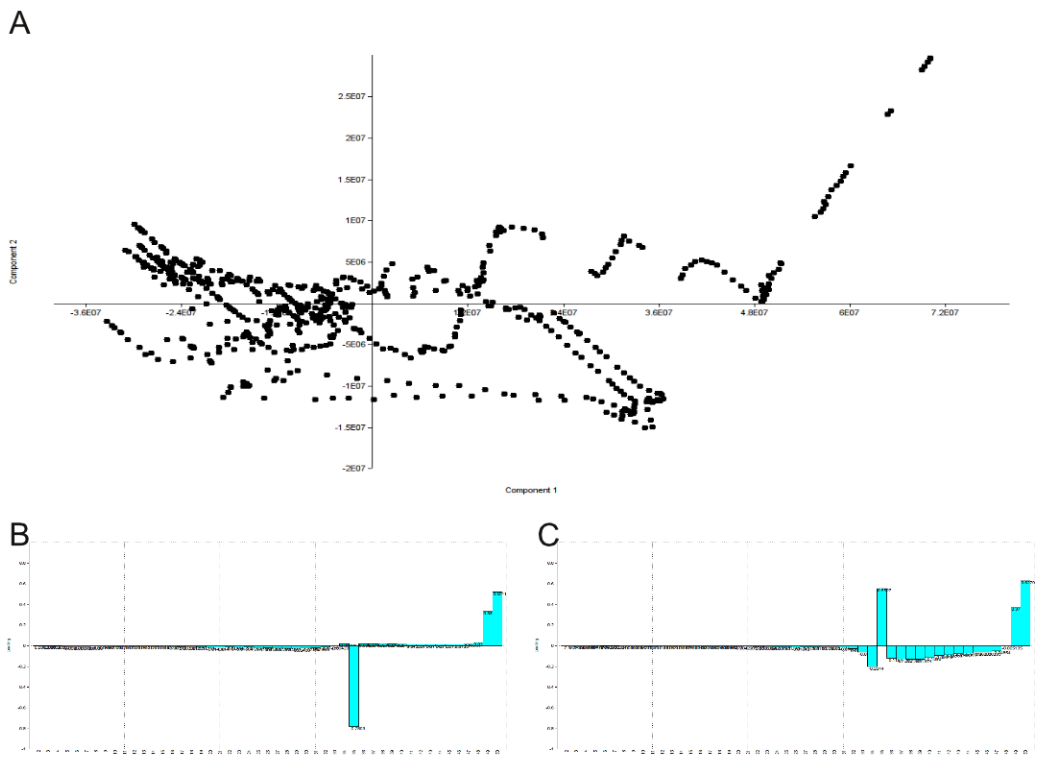

Fig. 7.12. A) Principle components analysis of the temporal and patterning of vegetation variation for an example "unstable" experiment run. Each dot represents an individual year of the experiment. B) The loadings for each vegetation class along principle component 1 (y-axis in PC plot). C) The loadings for each vegetation class along principle component 2 (x-axis in PC plot).

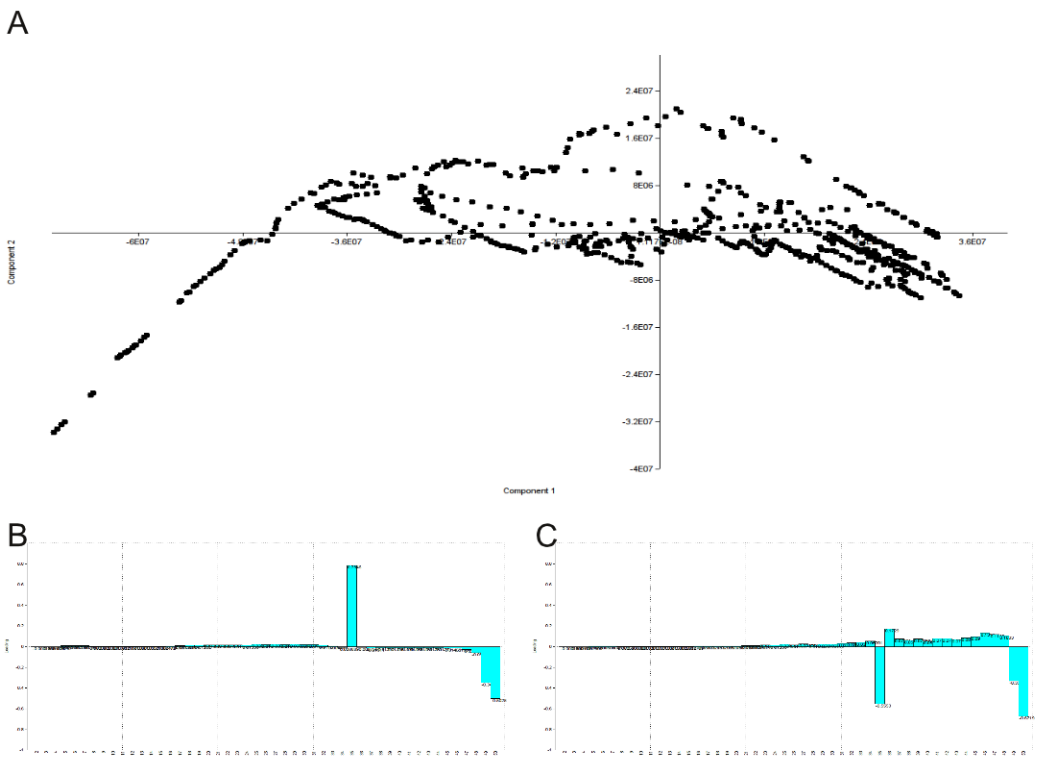

Fig. 7.13. A) Principle components analysis of the temporal and patterning of vegetation variation for an example "stable trending to unstable" experiment run. Each dot represents an individual year of the experiment. B) The loadings for each vegetation class along principle component 1 (y-axis in PC plot). C) The loadings for each vegetation class along principle component 2 (x-axis in PC plot).

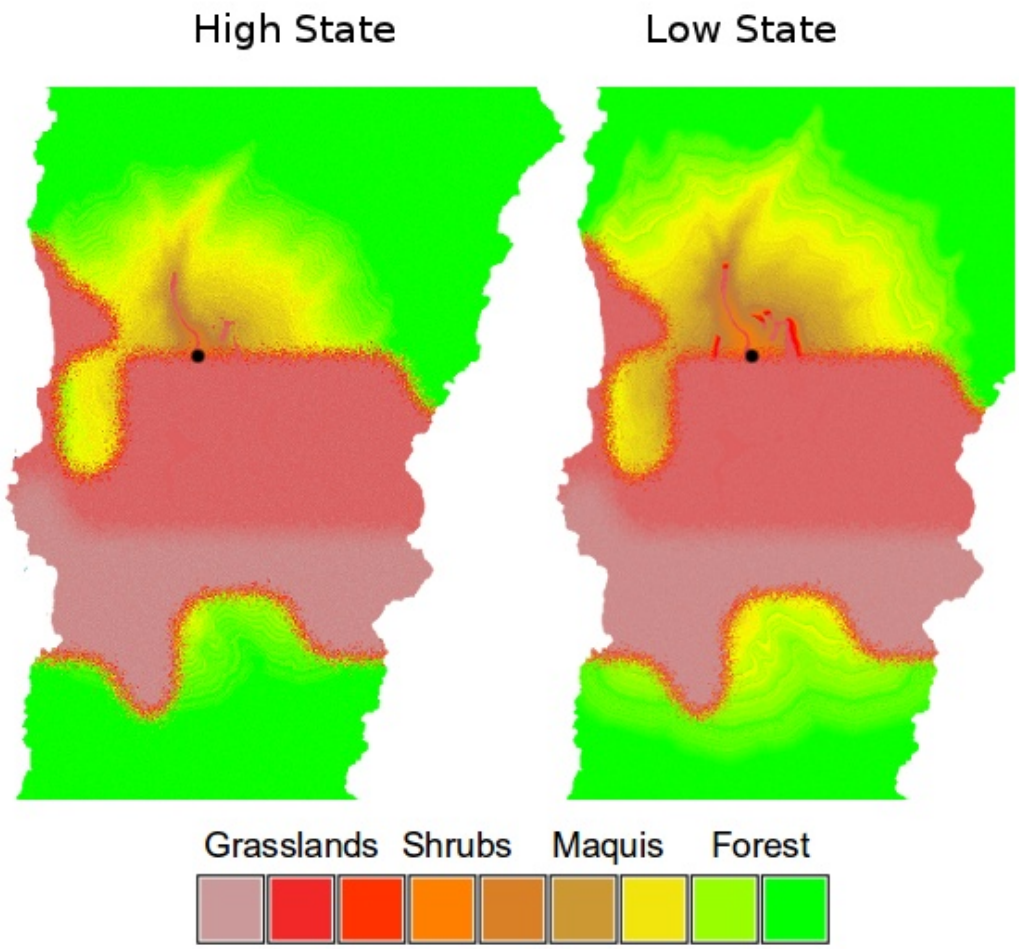

Fig. 7.14. Comparison of the land-cover maps from a high population stable state (left) and a low population stable state (right) for the "good-lazy" pastoralist model. Black dot shows the location of Tell Rakkan I.

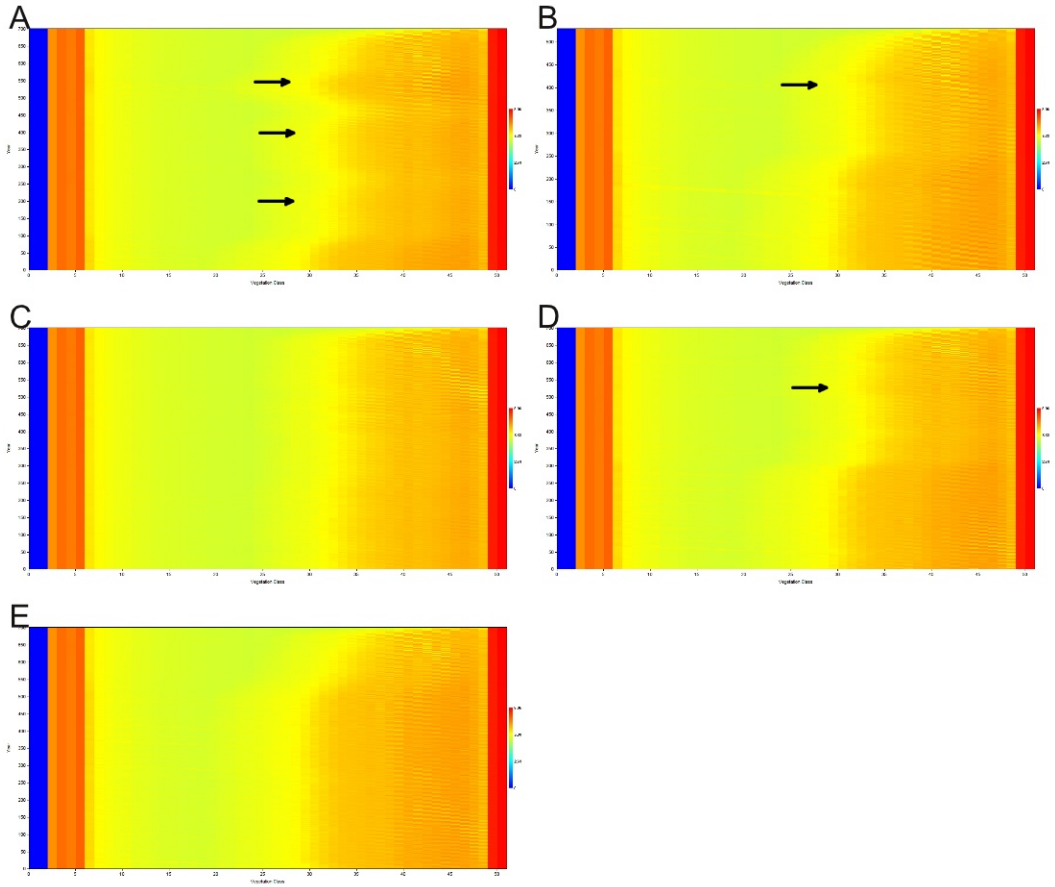

Fig. 7.15. “Wavelet” plots for all five runs of the “good-lazy” pastoralism experiment showing the temporal patterning of vegetation change in each run. Runs are in numerical order from top left, and the black arrows point to brief “phase switches” that may be indicators of an imminent critical transition.

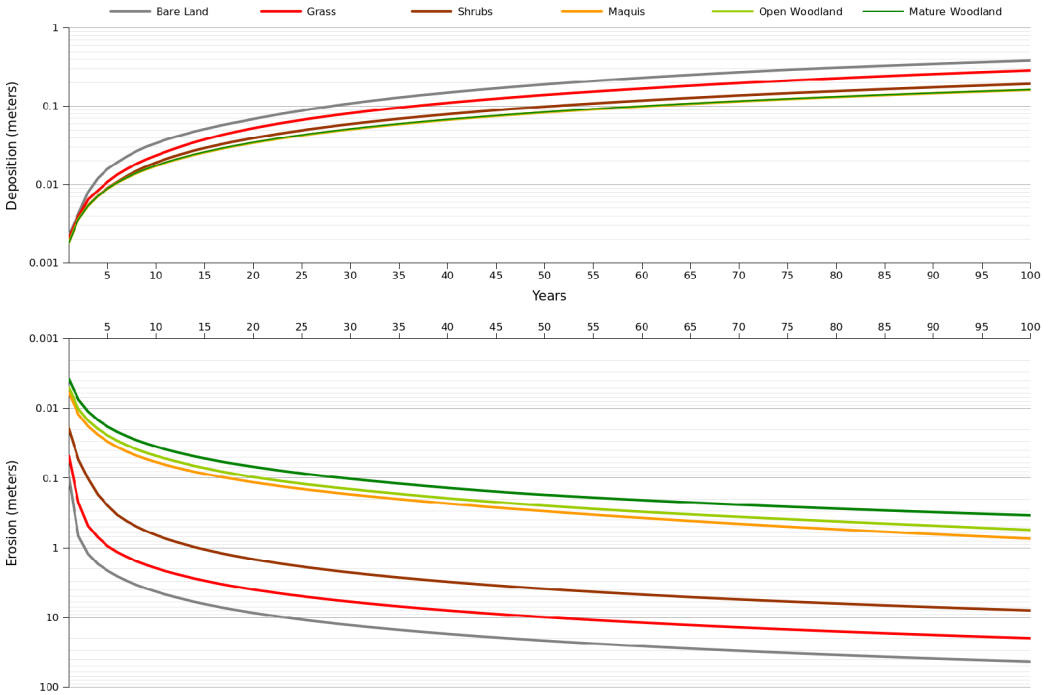

Fig. 7.16. Time-series trends for a series of short-term landscape evolution control models under different, but spatially homogeneous vegetation regimes.

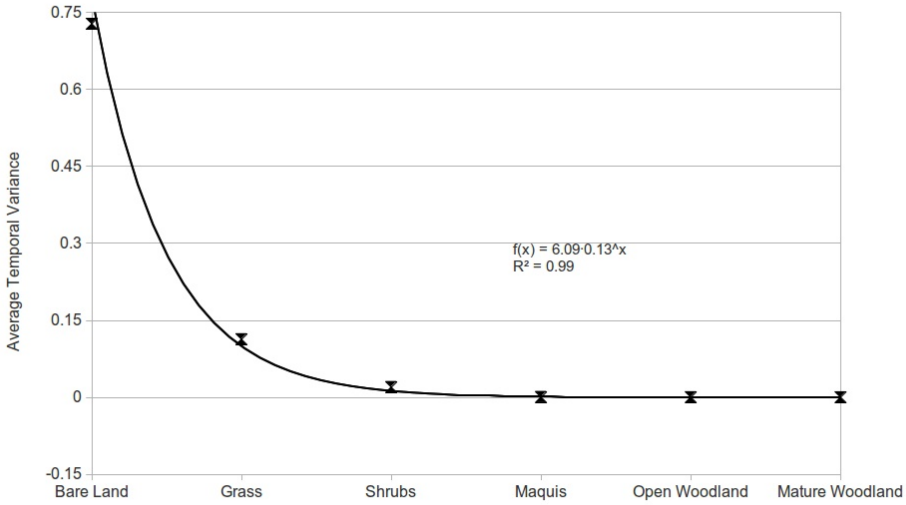

Fig. 7.17. Average (of all raster cells) temporal variance in net elevation change for each of the short -term homogeneous vegetation landscape evolution model runs.

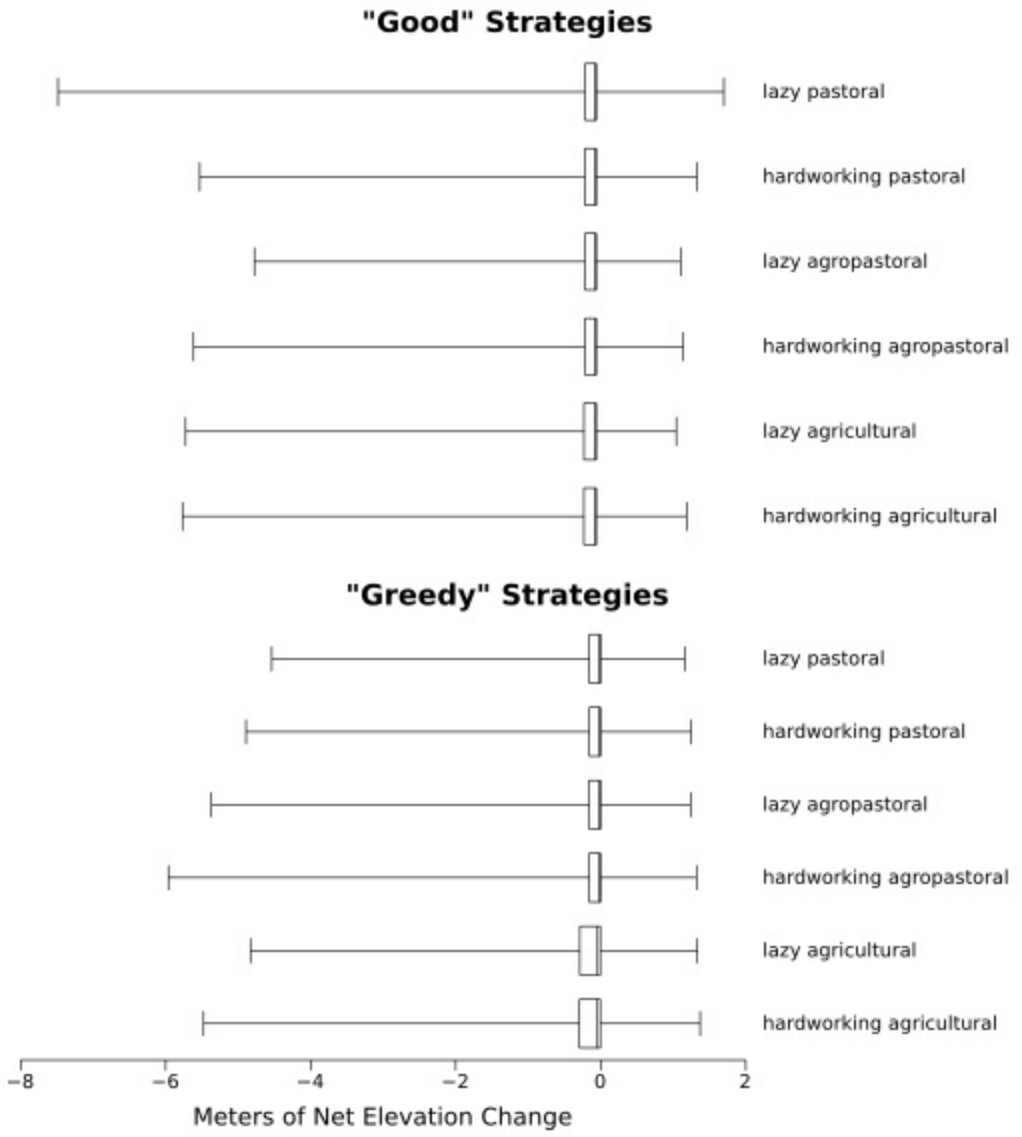

Fig. 7.18. Box-plots summarizing the range of cumulative net elevation change values after 700 years in the 12 modeling experiments.

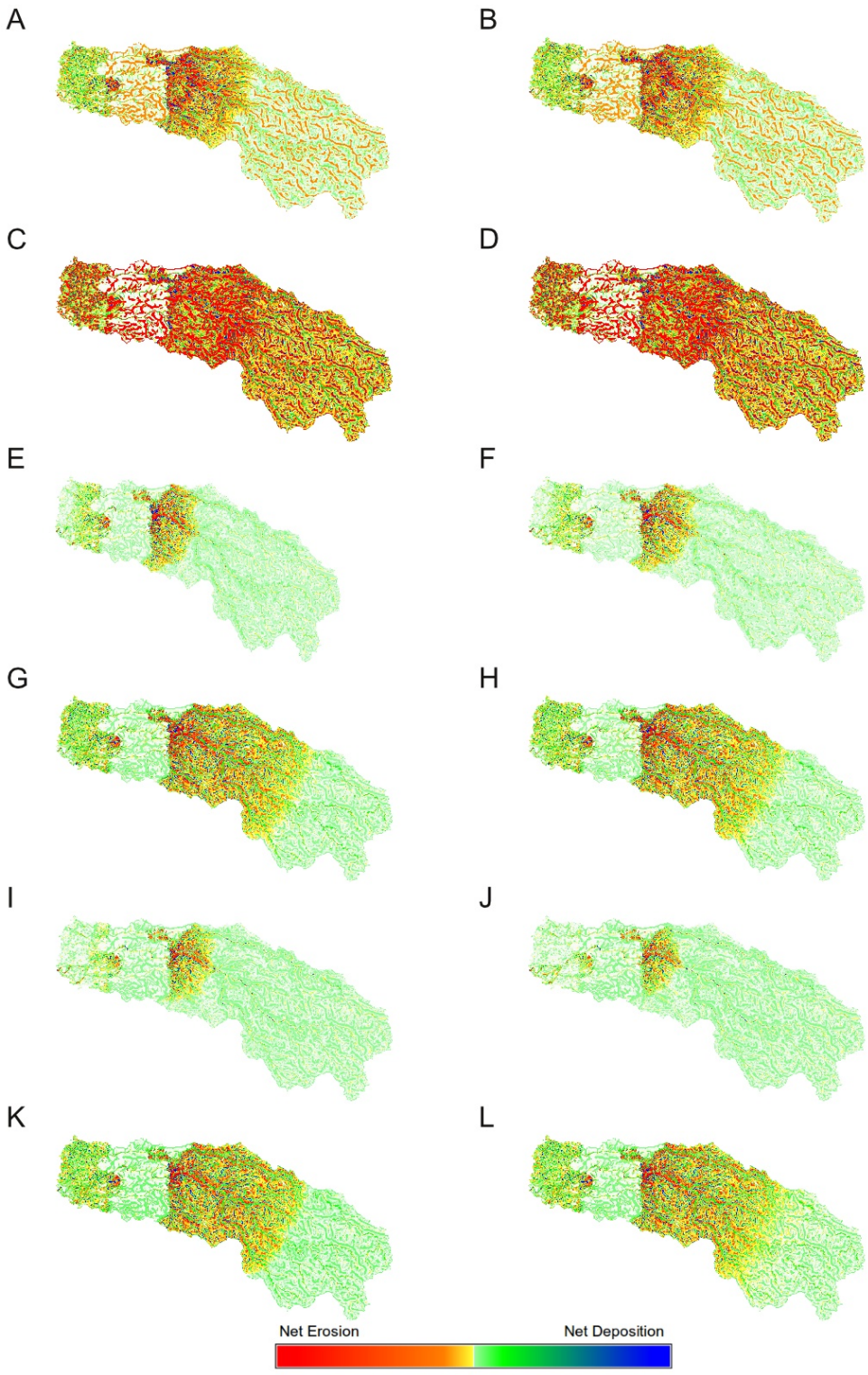

Fig. 7.19. Cumulative human-caused elevation change maps for all runs of all models. A–B : Good Hardworking and Lazy Agriculture, C–D: Greedy Hardworking and Lazy Agriculture, E–F: Good Hardworking and Lazy Agropastoralism, G–H: Greedy Hardworking and Lazy Agropastoralism, I–J: Good Hardworking and Lazy Pastoralism, K–L: Greedy Hardworking and Lazy Pastoralism.

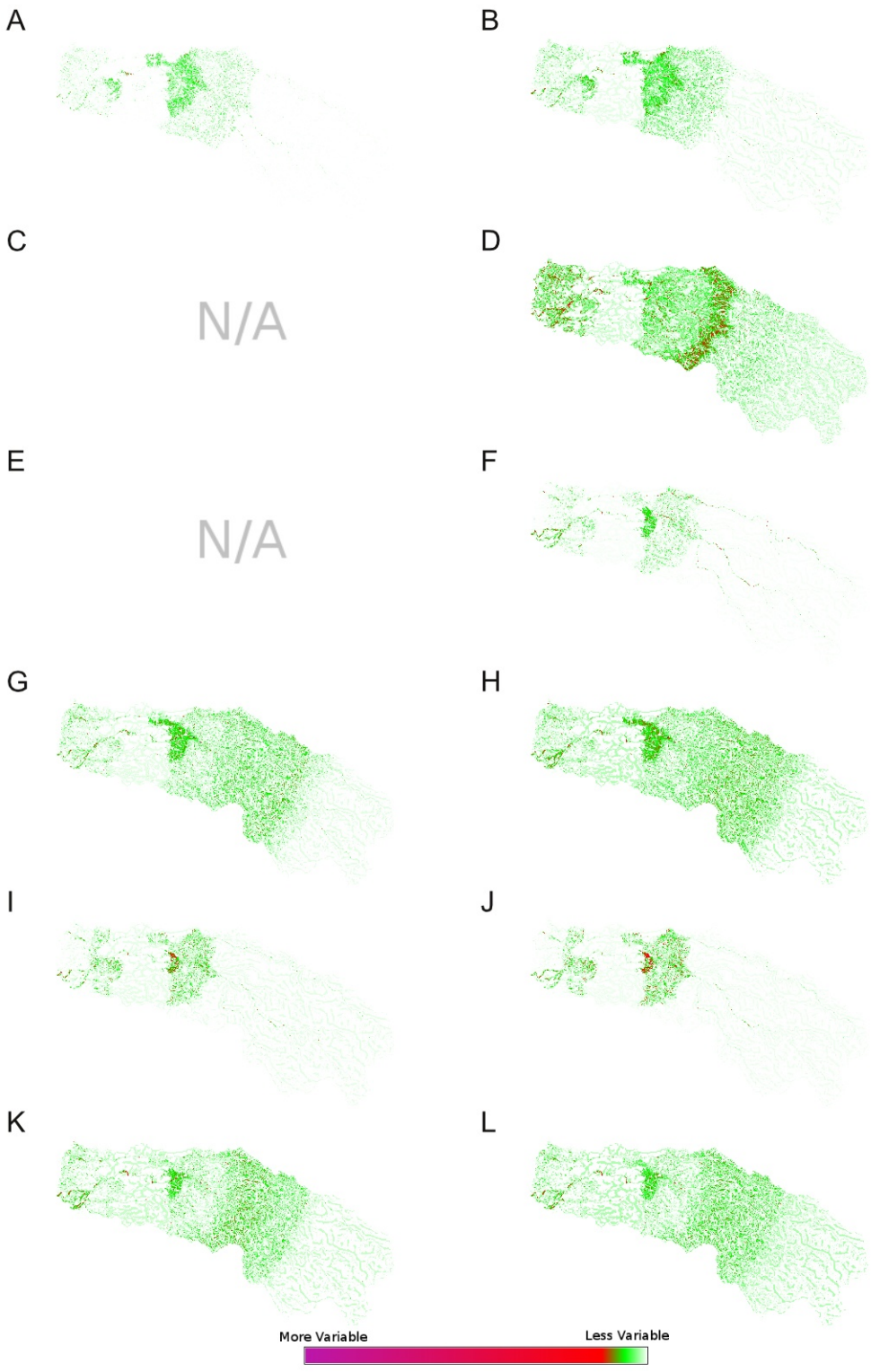

Fig. 7.20. Maps of inter-run variance in cumulative elevation change for all models. A–B : Good Hardworking and Lazy Agriculture, C–D: Greedy Hardworking and Lazy Agriculture, E–F: Good Hardworking and Lazy Agropastoralism, G–H: Greedy Hardworking and Lazy Agropastoralism, I–J: Good Hardworking and Lazy Pastoralism, K–L: Greedy Hardworking and Lazy Pastoralism.

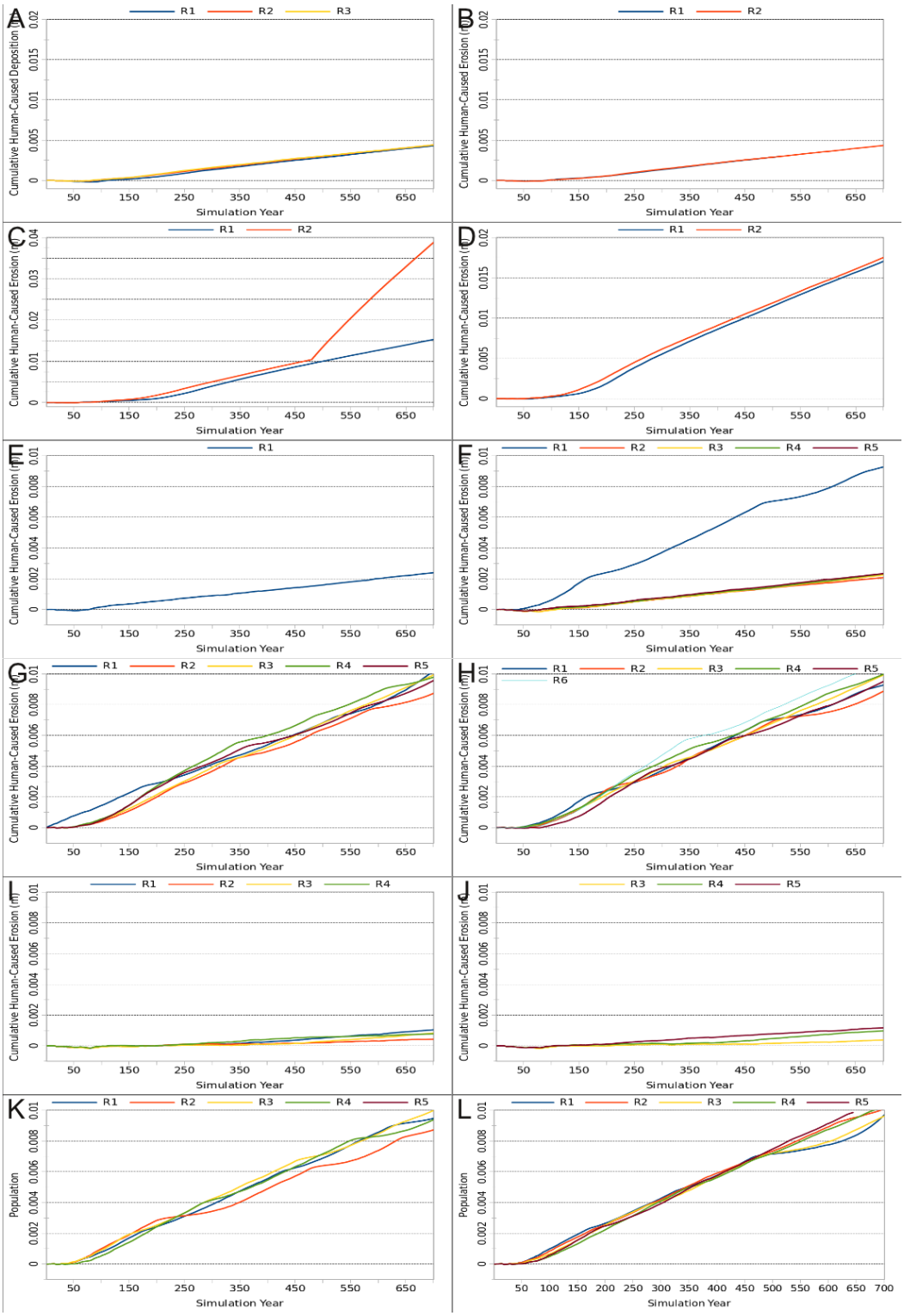

Fig. 7.21. Time-series of cumulative human-caused deposition for all runs of all models. A–B : Good Hardworking and Lazy Agriculture, C–D: Greedy Hardworking and Lazy Agriculture, E–F: Good Hardworking and Lazy Agropastoralism, G–H: Greedy Hardworking and Lazy Agropastoralism, I–J: Good Hardworking and Lazy Pastoralism, K–L: Greedy Hardworking and Lazy Pastoralism.

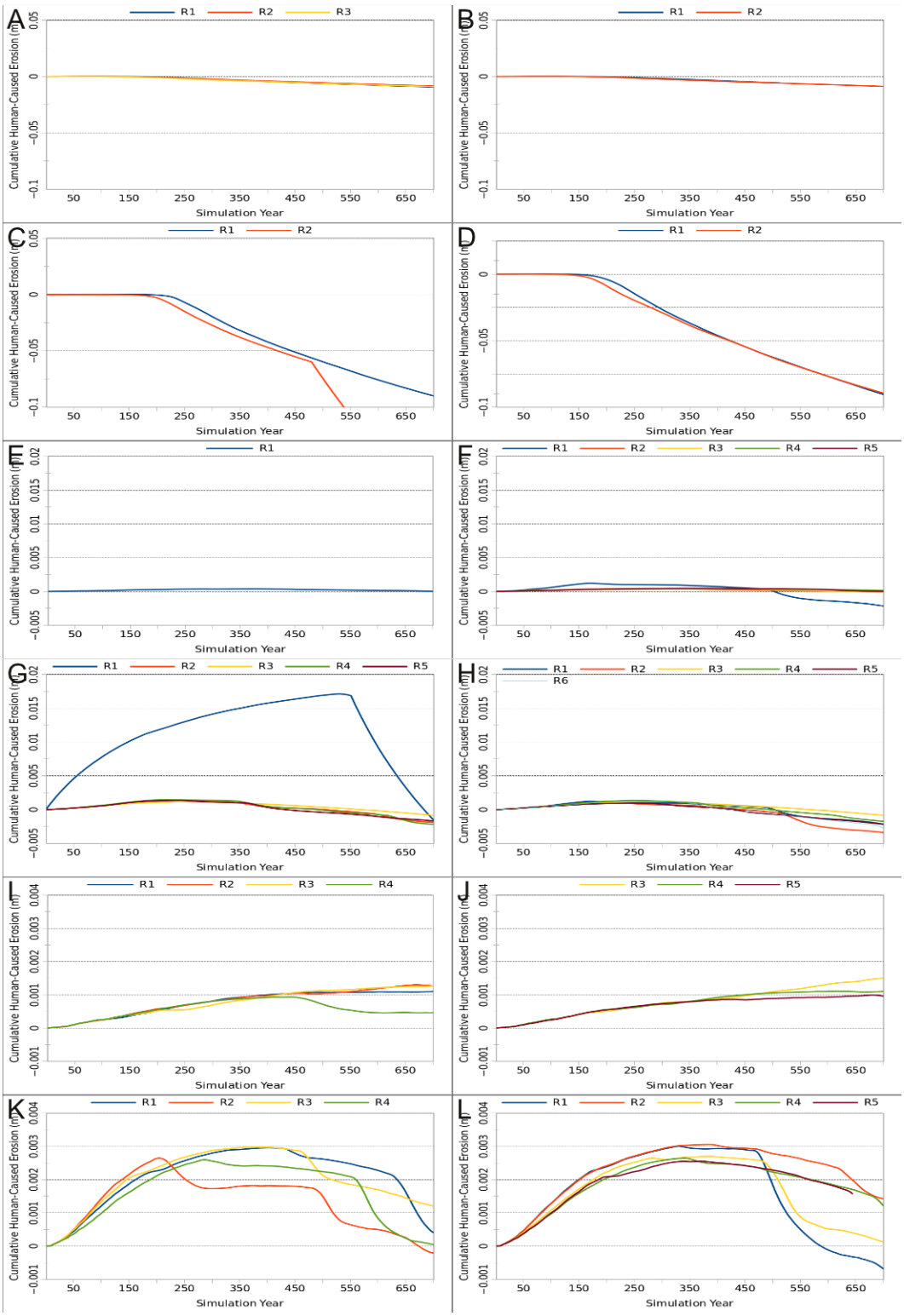

Fig. 7.22. Time-series of cumulative human-caused erosion for all runs of all models. A–B : Good Hardworking and Lazy Agriculture, C–D: Greedy Hardworking and Lazy Agriculture, E–F: Good Hardworking and Lazy Agropastoralism, G–H: Greedy Hardworking and Lazy Agropastoralism, I–J: Good Hardworking and Lazy Pastoralism, K–L: Greedy Hardworking and Lazy Pastoralism.

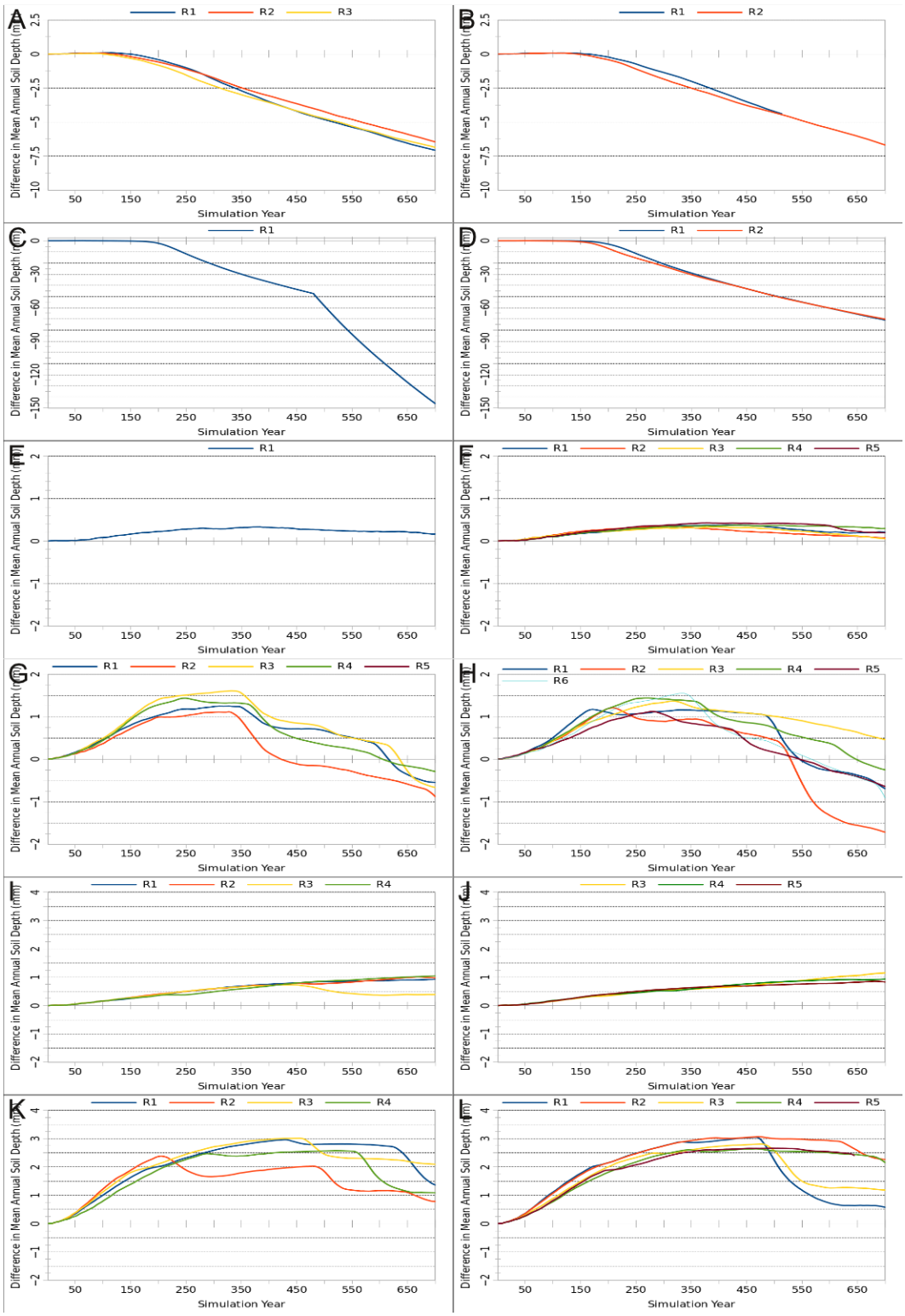

Fig. 7.23. Time-series of human effect on soil depth for all runs of all models. A–B : Good Hardworking and Lazy Agriculture, C–D: Greedy Hardworking and Lazy Agriculture, E–F: Good Hardworking and Lazy Agropastoralism, G–H: Greedy Hardworking and Lazy Agropastoralism, I–J: Good Hardworking and Lazy Pastoralism, K–L: Greedy Hardworking and Lazy Pastoralism.

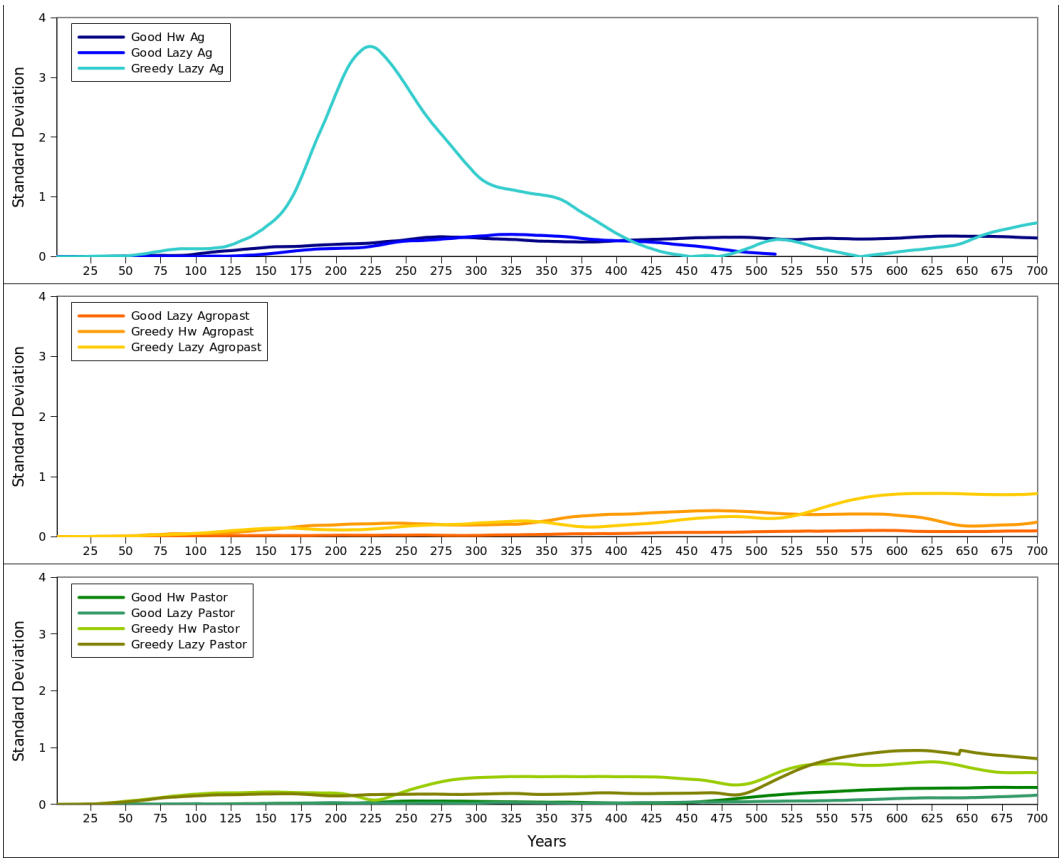

Fig. 7.24. Time-series plots of the variation in human-caused change to soil-depths across all runs of each of the experiments. Note that units are in standard deviations, and so are not standardized between each experiment. Nevertheless, important differences in temporal pattering is apparent.

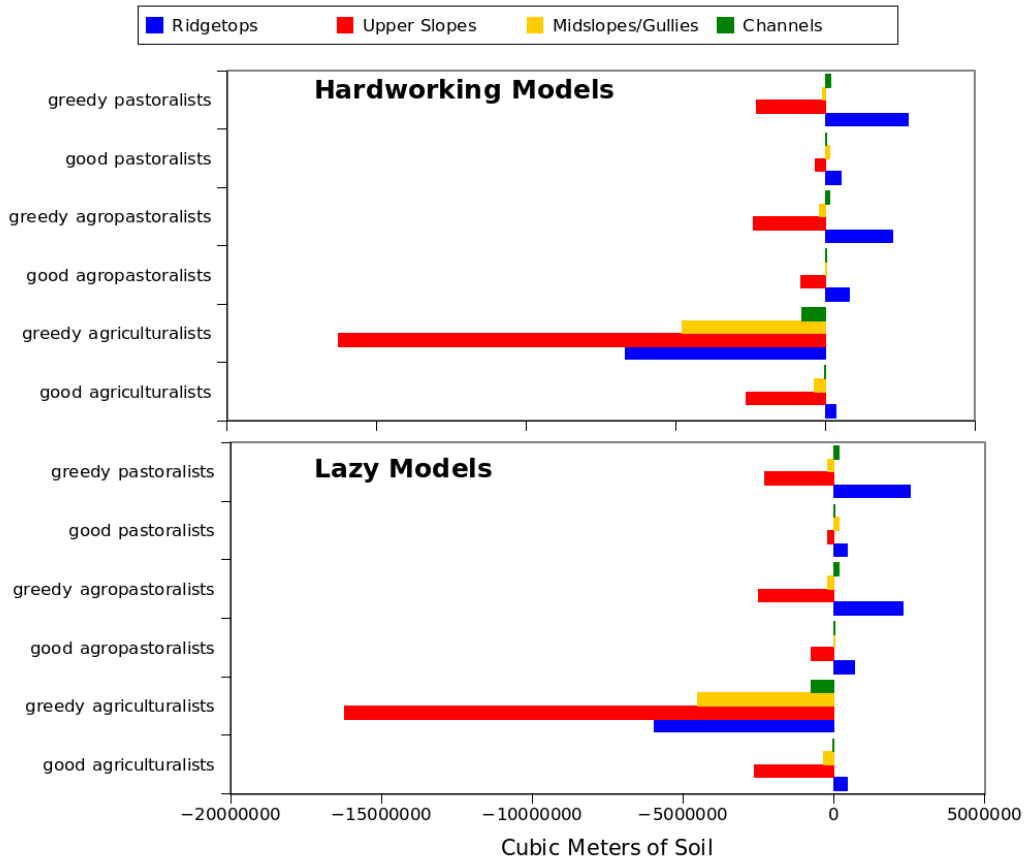

Fig. 7.25. Cumulative effect of humans on soil-depth for different landforms, broken down by experiment.

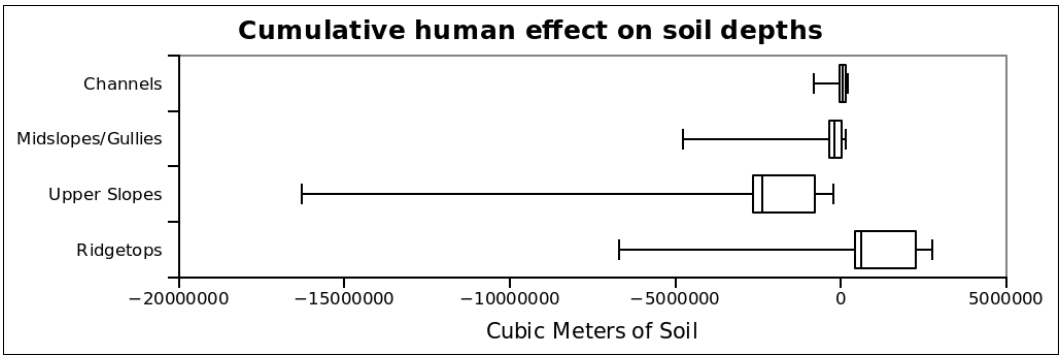

Fig. 7.26. Cumulative effect of humans on soil-depth for different landforms, box-plots of averages across all experiments.

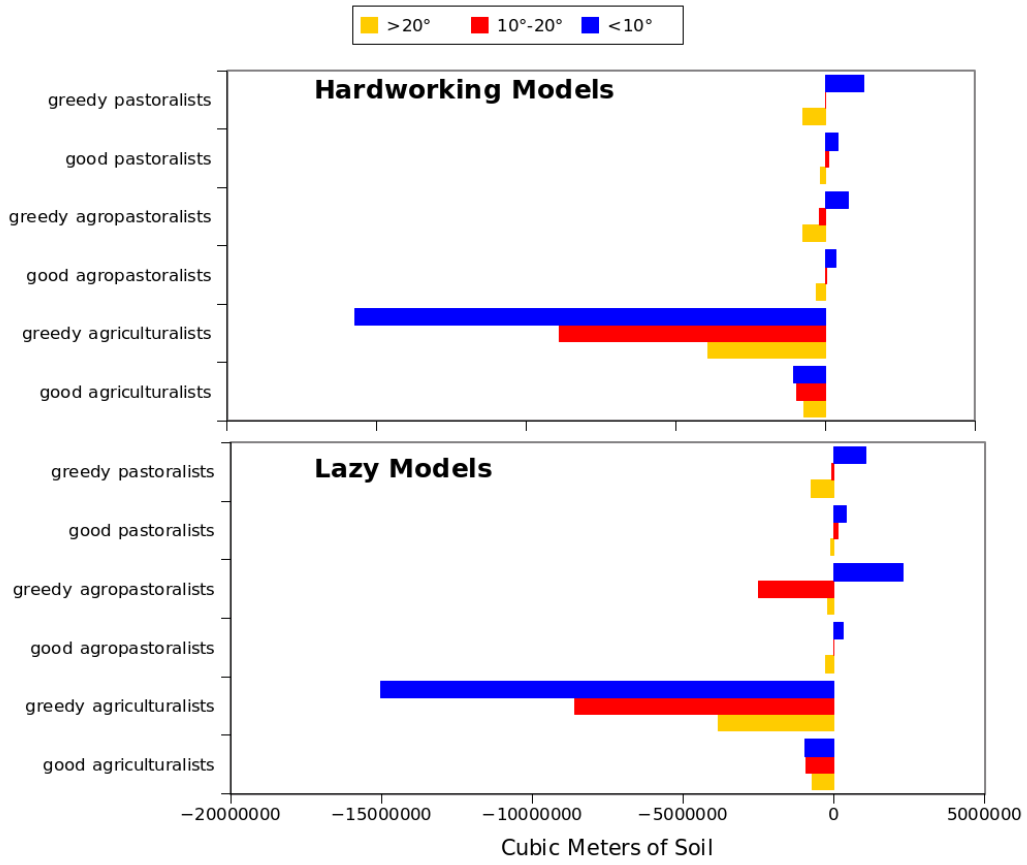

Fig. 7.27. Cumulative effect of humans on soil-depth for different slopes, broken down by experiment.

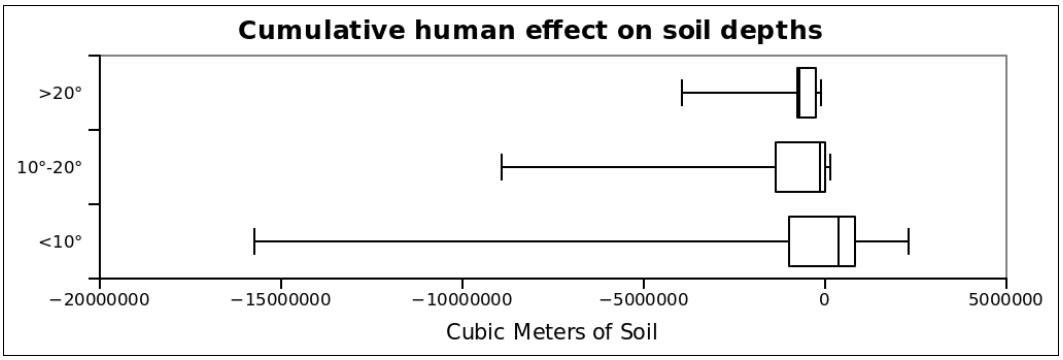

Fig. 7.28. Cumulative effect of humans on soil-depth for different landforms, box-plots of averages across all experiments.

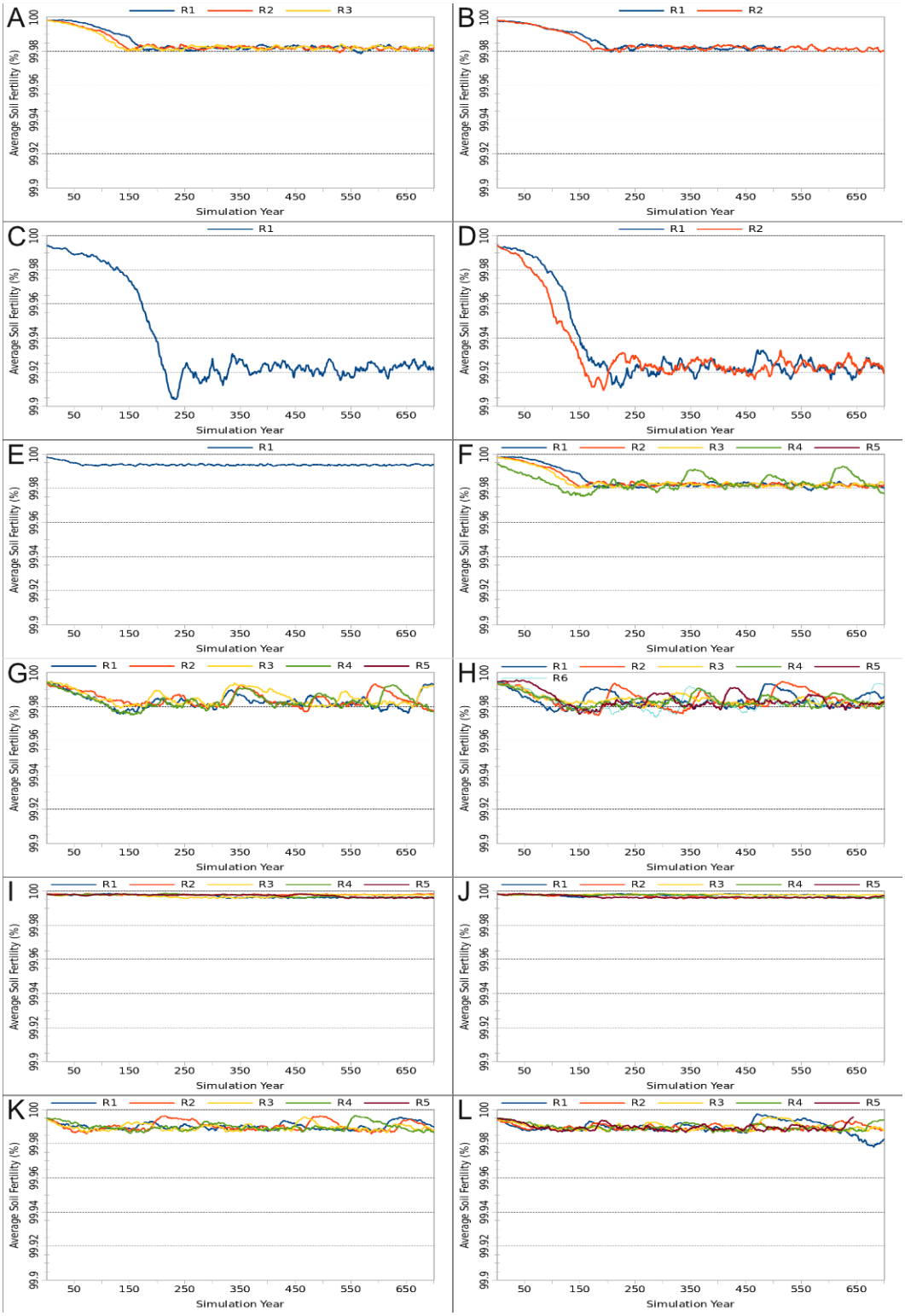

Fig. 7.29. Time-series of soil fertility for all runs of all models. A–B : Good Hardworking and Lazy Agriculture, C–D: Greedy Hardworking and Lazy Agriculture, E–F: Good Hardworking and Lazy Agropastoralism, G–H: Greedy Hardworking and Lazy Agropastoralism, I–J: Good Hardworking and Lazy Pastoralism, K–L: Greedy Hardworking and Lazy Pastoralism.

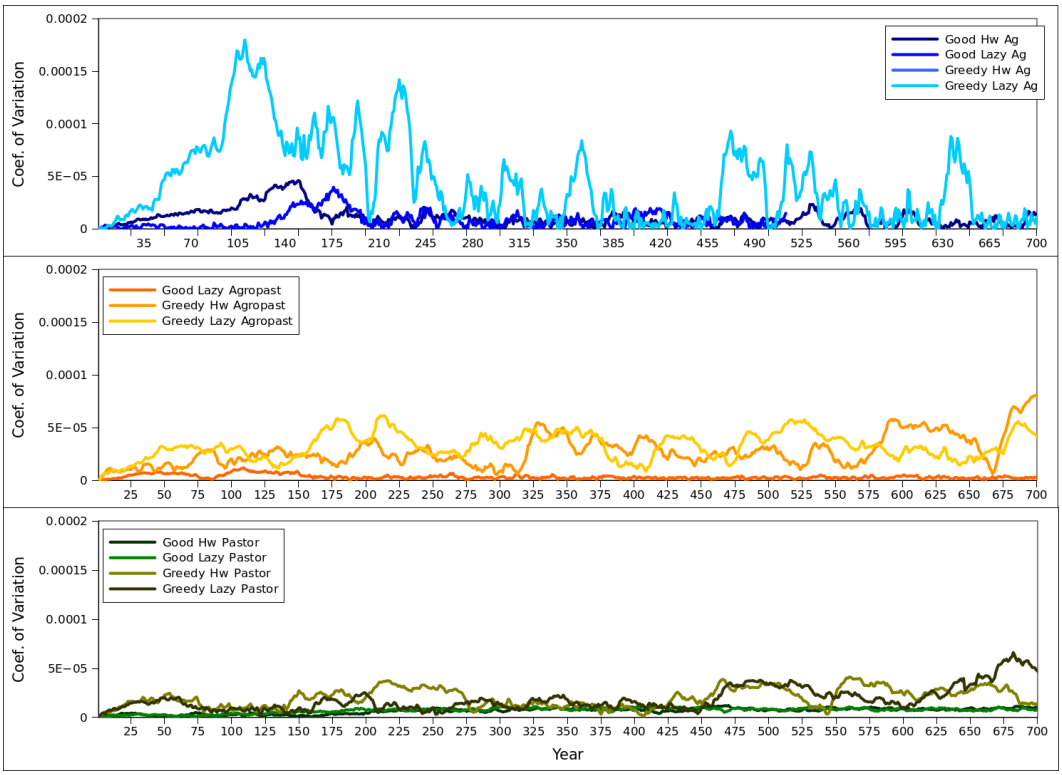

Fig. 7.30. Time-series plots of the variation in soil fertility between repeated runs of all agricultural experiments (top, blue lines), agropastoral experiments (middle, orange lines), and pastoral experiments (bottom, green lines). Units are standardized as coefficient of variation.

8. CONCLUSION

8.1. Implications for the PPN-LN Transition

What implications do the outcome of these simulations have for our understanding of the cause of the PPN-LN transition in general, and in Wadi Ziqlab in specific? First, and most importantly to the theme of this research project, the simulation approach has allowed for a much more nuanced picture of the dynamic relationship between PPNB people and their environment. A variety of complex phenomenon and emergent properties are apparent in the output of the twelve simulations, and relatively minor differences between some of the modeled subsistence systems led to vastly different outcomes. The simulations highlight the roles of resilience, connectedness, and system potential in regional panarchies, and documents how they interconnect with stability and unpredictability in the different potential Neolithic SES. These dynamics are missing from the oversimplified narratives of past investigations, which makes it clear that narrative explanation is an inadequate means of explanation for the nature and timing of transitional events in complex systems. It should also be noted that none of the twelve models led to total catastrophe (ie., the whole population dying out), supporting the idea that traditional ideas about societal "collapse" need to be rethought.

8.1.1. Implications for the PPN-LN Transition in Wadi Ziqlab

It is not important, however, if any of the twelve models perfectly mimicked the character of the actual PPN SES of Wadi Ziqlab, but rather that they were realistic representations of SES's that *could* have existed in the region. The archaeological proxies of the level of system potential from Wadi Ziqlab best fit with the patterns of system potential produced by the pastoral and agropastoral simulation models. In particular, these models produce population sizes that are within the range of those estimated for Tell Rakkan I (less than 300 people), whereas the agriculturalist models all result in much higher "equilibrium" populations. This suggests that the Neolithic economy of PPNB Tell Rakkan I was not yet overly reliant on agriculture, but does not preclude the possibility that the MML is simply not sophisticated enough to accurately represent the number of people that could be supported by a dominantly agricultural economy. Further, the archaeological data relating to subsistence practices in the LPPNB in general (and to a lesser degree, that from Tell Rakkan I in specific) suggests that agriculture *was* important, however, and was becoming more important over time. Moreover, there is no evidence at Tell Rakkan I to suggest that pastoralism was the dominant subsistence activity (scant faunal remains, no documented animal enclosures, etc.). Given the size of the site and the relative permanence of the (albeit small amount) architecture documented in the limited excavations of the

site, it is most likely that the inhabitants of Tell Rakkan I practices a subsistence economy similar to those of the agropastoral simulation models.

If this is true, some general conclusions about the nature of the LPPNP regional SES can be drawn from the results of the simulation experiments (see Chapter 7). First, the small differences in herd animal stocking rates and in farming impact between the four agropastoral models yielded wide differences in system potential, system resilience, system connectedness, cyclicity, divergence, stability, predictability, and the amount of cumulative human impacts over time. Thus, while agropastoralism can be a highly stable, predictable subsistence system in some circumstances, it can be a wildly unstable and potentially vulnerable subsistence system in others. Although agents in the MML could not adapt their land-use decision-making criteria, real people can and do. Thus, it stands to reason that minor adjustments in subsistence choices could have had large effects on the PPN SES centered at Tell Rakkan I. Further, if the inhabitants wanted to increase predictability, stability, and system output (potential, in the form of increased grain yields, higher population, etc.), they could have consciously made decisions that led to these outcomes, such as increasing reliance on agriculture over time. However, in doing so, they would have given up some of the resilience inherent to smaller-scale mixed systems. This would have been exacerbated over time as the cumulative effects of human land-use fundamentally altered the potential for them to revert to a more pastoral way of life, and could potentially have put them at greater risk for a critical transition.

So, was the PPN-LN transition in Wadi Ziqlab a critical transition? The evidence from the simulation models do not prove it to have been such, but offer tantalizing clues that suggest that it could have been. If it was a critical transition, then the small-scale LN subsistence system could be understood as the smaller-scale alternative stable state in a hysteretic cycle of a more general suite of Neolithic SES.

8.1.2. Implications for the PPN-LN Transition in General

Although situated in Wadi Ziqlab, the results of this simulation experiment nevertheless have some implications for the nature of the PPN-LN transition in other parts of the Southern Levant, and in the "megasites" of the Jordanian Highlands in particular. The very large populations assumed to have been housed in the megasites could clearly only be supported by a dominantly agricultural subsistence system. These high populations could only be supported by massive catchments, however, and the two simulations with the largest populations were utilizing the entire Wadi Ziqlab watershed by the end of the PPNB—a situation not even matched by the modern usage of the Wadi! These systems were very stable throughout the length of the simulations, but this stability and large system potential came at the cost of increasing connectedness and rigidity over time. In short, these highly agricultural systems began to lack resilience, and so seem to be at ever-greater risk of falling, or being pushed into a

critical transition by a variety of internal and external factors over time. What is most interesting is that although these systems are very stable and predictable in the short-term, the cost of this stability is increased risk of catastrophic failure in the long-term. The experiments conducted in this research did not result in a critical transitions for agriculturalists, so it is not possible to estimate what the characteristics of a purely agricultural alternative stable state might be, but it seems likely that it could be one of the other major "attractors" in human subsistence variability identified in Chapter 3 (e.g., agropastoralism, intensive agriculture, pastoralism, specialized pastoralism, or hunting and gathering).

Another implication of the results of this research is that while rigidity may have made the PPN SES more vulnerable to outside influence (rapid climate change, warfare, etc.), outside influence would not have been a *necessary* trigger for the transition. Further, if a series of Neolithic towns were connected in a regional network, the failure of only one town—whether due to a self-imposed critical transition, or external disturbance—could have affected them all. Any such disturbance would have been exacerbated by the accumulation of 700 years of increasing rigidity and decreasing resilience in the subsistence system of all the large LPPNB towns, and so what started as a single critical failure of one component of the regional system, could initialized a cascade of failure throughout the entire network (See Heckbert et al. [2012] for an example of this in another computational model of ancient SES).

8.2. Future Research Directions

The results of the simulation experiments presented in this dissertation were insightful, but were ultimately limited by the structure of the MML and the scope of the modeling experiments formulated for this research. This research represents the largest-scale use of the MML modeling environment to date, and so has also exposed a number of weaknesses in the modeling infrastructure (e.g., the inability to recover from interrupted runs, internal errors disrupting statistical output, malformatted or cumbersomely-formatted statistical output, human error associated with managing the arrangement of simulation experiments on multiple desktop computers, etc.). Steps are already being taken to mitigate some of these issues, however, so future modeling experiments should be less error-prone.

The current round of modeling experiments were intentionally limited in scope. For example, climate (and consequently vegetation climax limits) and site location were held constant for the entire 700 years of the simulation run. Clearly, these are critical variables for understanding the nature of the PPN-LN transition, and feature prominently in two of the five existing hypotheses for the instigation of the transition (i.e., the "climatic forcing" and "settlement reorganization" hypotheses). The current round of experiments can (and do) inform us of the extent to which to PPNB SES of Wadi Ziqlab *may* have been vulnerable to rapid climate change, but cannot (and do not) reveal the intricacies of the effect of climate change on the different potential Neolithic SES. Likewise, the current

round of experiments can (and do) reveal the limitations and opportunities afforded by the central location of PPNB SES atTell Rakkan I, but cannot (and do not) reveal the potential benefits and costs of the multi-sited LN SES. These are two clear avenues for future research, which I plan to investigate further.

The construction of the MML presented also some important limitations on the scope of the experiments that could be conducted in this research. For example, because the number of households can never change in a simulation, in many of the simulations, they simply grow in size until they no longer represent a realistic "household". This means that analysis of inter-household differences becomes meaningless because the variability in access to land between households is greatly reduced because of averaging effects across the very large catchments they now hold. Thus, it is not possible to analyze the amount of synchronicity in the adaptive cycle of the households, which is a major indicator for the risk of critical transitions. These limitations would be circumvented if households were allowed to fission. Another limitation of the MML is that there are no land-tenure restrictions, so agents are free to exchange farm parcels whenever it seems beneficial to do so. This seems to inevitably lead to a quick "swiddening" style of agriculture, which may be a reasonable model for Neolithic farming, but is clearly not the only style of rain-fed agriculture possible, and also means that, unless the entire catchment is given over to agriculture, agents will always choose to swidden (even with increased preference for non-forested patches). If land access was more restricted (e.g., through, tenure) it is likely that soil fertility levels would be more drastically affected over time, which would likely lead to quite different population dynamics. Furthermore, agent behavior in the MML is only determined by a "satisficing" style of decision making (i.e., while agents do try to minimize costs, they are really only trying to meet their minimum requirements). Different decision strategies (e.g., profit maximizing, pure cost minimizing, etc.) would also likely lead to different outcomes. Finally, agents in the MML are not allowed to modify their basic subsistence goals during the simulation. This necessarily reduces the amount of variability in model runs (which is good for the initial modeling experiment conducted here), but means that an essential component of subsistence dynamics cannot be modeled, and so it is impossible to determine under which conditions agents might switch subsistence strategies (e.g., in a critical transition between agriculture and pastoralism). These issues are slated to be addressed in the next version of the MML, and so future modeling experiments into the PPN-LN transition can capitalize on this improved functionality to investigate the effects of more nuanced and complex agent behavior.

Finally, the experiments conducted in this research reiterated the need for multiple runs. Emergence is a powerful component of complex systems, and many repeated runs are need in order to better understand its influences. Most of the measures of inter-run variability I used in the current research would require at least 5-10 repeats to be statistically robust, so in future research, it will be

prudent to conduct many more repeated runs than the 2-5 repeats of the current research.

8.3. Conclusion

This research has suggested that the PPN-LN transition in Northern Jordan can be explained as a critical transition between fundamentally different states of Neolithic SES. The simulation models used in this research are admittedly simple, and lack sophisticated social components. Nonetheless, it is clear that the Neolithic subsistence and land-use were complex phenomena, and that recursive and dynamic feedback between the human and natural portions of the system produced emergent properties that could not be predicted or planned for by Neolithic peoples. In the simulations, we can see how the everyday decisions of farmers and herders, intent on feeding their families for another year, could manifest in drastic and lasting change in a coupled human and natural system. The simulation approach taken in this research couples with the explanatory power of complexity theory to provide a powerful analytical tool to approach and disentangle previously intransigent archaeological problems. The work presented here had barely scratched the proverbial surface of this technique, and will serve as a launching off point for a much future research.

BIBLIOGRAPHY

Abel, N., Cumming, D.H.M., Anderies, J.M., 2006. Collapse and reorganization in socialecological systems: questions, some ideas, and policy implications. Ecology and Society 11, 17.

Abrantes, F., Voelker, A. (Helga L., Sierro, F.J., Naughton, F., Rodrigues, T., Cacho, I., Ariztegui, D., Brayshaw, D., Sicre, M.-A., Batista, L., 2012. Paleoclimate Variability in the Mediterranean Region, in: P. Lionello (Ed.), The Climate of the Mediterranean Region. Elsevier, Oxford, pp. 1–86.

Adler, P., Raff, D., Lauenroth, W., 2001. The effect of grazing on the spatial heterogeneity of vegetation. Oecologia 128, 465–479.

Al-Jaloudy, M.A., 2006. Country Pasture/Forage Resource Profiles: Jordan [WWW Document]. Food and Agriculture Organization of the United Nations Country Pasture Profiles. URL http://www.fao.org/ag/AGP/agpc/doc/Counprof/Jordan/Jordan.htm#4.%20RUMINANT%20LIVESTOCK%20PRODUCTION%20SYSTEMS (accessed 5.13.10).

Al-Nahar, M., 2010. Tell Abu Suwwan, A Neolithic Site in Jordan: Preliminary Report on the 2005 and 2006 Field Seasons. Bulletin of the American Schools of Oriental Research 1–18.

Al-Shreideh, A.M., 1992. Water Resources and Systems in the Wadi Abu Ziyad basin and their Relationship with Human Settlement: A Hydrological and Archaeological Study (Unpublished MA thesis). Yarmouk University.

Altaweel, M., 2008. Investigating agricultural sustainability and strategies in northern Mesopotamia: results produced using a socio-ecological modeling approach. Journal of Archaeological Science 35, 821–835.

Anderson, P.M., Barnosky, C.W., Bartlein, P.J., Behling, P.J., Brubaker, L., Cushing, E.J., Dodson, J., Dworetsky, B., Guetter, P.J., Harrison, S.P., others, 1988. Climatic changes of the last 18,000 years: Observations and model simulations. Science 241, 1043–1052.

Araus, J.L., Amaro, T., Voltas, J., Nakkoul, H., Nachit, M.M., 1998. Chlorophyll fluorescence as a selection criterion for grain yield in durum wheat under Mediterranean conditions. Field Crops Research 55, 209–223.

Araus, J.L., Amaro, T., Zuhair, Y., Nachit, M.M., 1997a. Effect of leaf structure and water status on carbon isotope discrimination in field-grown durum wheat. Plant Cell Environ 20, 1484–1494.

Araus, J.L., Febrero, A., Buxó, R., Camalich, M.D., Martin, D., Molina, F., RODRIGUEZ-ARIZA, M., Romagosa, I., 1997b. Changes in carbon isotope discrimination in grain cereals from different regions of the western Mediterranean Basin during the past seven millennia. Palaeoenvironmental evidence of a differential change in aridity during the late Holocene. Global Change Biology 3, 107–118.

Araus, J.L., Slafer, G.A., Romagosa, I., Molist, M., 2001. FOCUS: estimated wheat yields during the emergence of agriculture based on the carbon isotope discrimination of grains: evidence from a 10th millennium BP site on the Euphrates. Journal of Archaeological Science 28, 341–350.

Argonne National Laboratory, 2012. Repast Symphony. http://repast.sourceforge.net/.

Arrowsmith, R., DiMaggio, E., Barton, C.M., Sarjoughian, H.S., Fall, P., Falconer, S.E., Ullah, I.I., 2006. Geomorphic mapping and paleoterrain generation for use in modeling Holocene (8,000-1,500 yr) agropastoral land-use and landscape interactions in southeast Spain. Am Geophys Union, San Francisco, CA.

Asouti, E., 2006. Beyond the Pre-Pottery Neolithic B interaction sphere. Journal of World Prehistory 20, 87–126.

Asouti, E., Austin, P., 2005. Reconstructing woodland vegetation and its exploitation by past societies, based on the analysis and interpretation of archaeological wood charcoal macro-remains. Environmental Archaeology 10, 1–18.

Asouti, E., Fuller, D., 2012. From foraging to farming in the southern Levant: the development of Epipalaeolithic and Pre-pottery Neolithic plant management strategies. Vegetation History and Archaeobotany 21, 149–162.

Banning, E.B., 1982. The research design of the Wadi Ziqlab Survey, 1981. American Schools of Oriental Research Newsletter 8, 4–8.

Banning, E.B., 1983. Wadi Ziqlab Survey, in: Keller, D.R., Rupp, D.W. (Eds.), Archaeological Survey in the Mediterranean Area, BAR International Series. British Archaeological Reports, Oxford, pp. 341–344.

Banning, E.B., 1985. Pastoral and Agricultural Land Use in the Wadi Ziqlab, Jordan: An Archaeological and Ecological Survey (Doctoral Thesis). University of Toronto, Toronto.

Banning, E.B., 1992a. Tabaqat al-Buma, Wadi Ziqlab. American Journal of Archaeology 96, 506–507.

Banning, E.B., 1992b. 1992 Excavations at Wadi Ziqlab, al-Kura, Jordan. Canadian Archaeological Association Newsletter 12, 3–4.

Banning, E.B., 1995. Herders or Homesteaders? A Neolithic Farm in Wadi Ziqlab, Jordan. Biblical Archaeologist 58, 2–13.

Banning, E.B., 1996. Highlands and Lowlands: Problems and Survey Frameworks for Rural Archaeology in the Near East. Bulletin of the American Schools of Oriental Research 301, 25–45.

Banning, E.B., 1998. The Neolithic Period: Triumphs of Architecture, Agriculture, and Art. Near Eastern Archaeology 61, 188–237.

Banning, E.B., 1999. Neolithic and Chalcolithic Archaeology in Wadi Ziqlab, Northern Jordan. Occident & Orient 4, 46–48.

Banning, E.B., 2001. Settlement and Economy in Wadi Ziqlab During the Late Neolithic, in: Amr, K. (Ed.), Studies in the History and Archaeology of Jordan VII: Jordan by the Millennia, 7. Department of Antiquities, Amman, pp. 149–156.

Banning, E.B., 2003. Housing Neolithic Farmers. Near Eastern Archaeology 66, 4–21.

Banning, E.B., 2007a. Wadi Rabah and related assemblages in the southern Levant: Interpreting the radiocarbon evidence. Paléorient 33, 77–101.

Banning, E.B., 2007b. Time and Tradition in the Transition from Late Neolithic to Chalcolithic: Summary and Conclusions. paleo 33, 137–142.

Banning, E.B., 2010. Houses, households, and changing society in the Late Neolithic and Chalcolithic of the Southern Levant. Paleorient 36, 46–87.

Banning, E.B., Blackham, M., Lasby, D., 1998. Excavations at WZ 121, A Chalcolithic Site at Tubna, In Wadi Ziqlab. Annual of the Department of Antiquities of Jordan 42, 141–159.

Banning, E.B., Byrd, B.F., 1987. Houses and the Changing Residential Unit: Domestic Architecture at PPNB 'Ain Ghazal, Jordan. Proceedings of the Prehistoric Society 53, 309–325.

Banning, E.B., Dodds, R.R., Field, J., Kuijt, I., McCorriston, J., Siggers, J., Taani, H., Triggs, J., 1992. Tabaqat al Buma: 1990 excavations at a Kebaran and Late Neolithic site in Wadi Ziqlab. Annual of the Department of Antiquities of Jordan 36, 43–69.

Banning, E.B., Dodds, R.R., Field, J., Maltby, S., McCorriston, J., Monckton, S., Rubenstein, R., Sheppard, P.J., 1989. Wadi Ziqlab Project 1987: A Preliminary Report. Annual of the Department of Antiquities of Jordan 33, 43–58.

Banning, E.B., Fawcett, C., 1983. Man-land relationships in the ancient Wadi Ziqlab: report of the 1981 survey. Annual of the Department of Antiquities of Jordan 27, 291–309.

Banning, E.B., Gibbs, K., Gregg, M., Kadowaki, S., Rhodes, S., 2002. Excavations at al-Basatin, Wadi Ziqlab, Jordan. Neolithics 2, 13–14.

Banning, E.B., Gibbs, K., Kadowaki, S., 2003. Excavations at a Late Neolithic site, al-Basatin, in Wadi Ziqlab, Jordan. Annual of the Department of Antiquities of Jordan 47.

Banning, E.B., Gibbs, K., Kadowaki, S., 2011. Changes in material culture at Late Neolithic Tabaqat al Buma, in Wadi Ziqlab, northern Jordan, in: Lovell, J., Yorke, R.M. (Eds.), Culture, Chronology and the Chalcolithic: Theory and Transition., Council for British Research in the Levant Supplementary Series. Oxbow Books, Oxford, pp. 36–60.

Banning, E.B., Maher, L.A., Kadowaki, S., Gibbs, K., 2004. Excavations at a Late Neolithic site in Wadi Ziqlab, Northern Jordan. Antiquity 308.

Banning, E.B., Najjar, M., 1999. Excavations at Tell Rakan I, a Neolithic site in Wadi Ziqlab. Neo-Lithics 99, 1–3.

Banning, E.B., Rahimi, D., Siggers, J., 1994. The Late Neolithic of the Southern Levant: Hiatus, Settlement Shift or Observer Bias? The Perspective from Wadi Ziqlab. Paléorient 20, 151–164.

Banning, E.B., Rahimi, D., Siggers, J., Taani, H., 1996. The 1992 Season of Excavations in Wadi Ziqlab, Jordan. Annual of the Department of Antiquities of Jordan 40, 29–49.

Banning, E.B., Siggers, J., 1997. Technological Strategies at a Late Neolithic Farmstead in Wadi Ziqlab, Jordan, in: Gebel, H.G., Kafafi, Z., Rollefson, G.O. (Eds.), The Prehistory of Jordan II: Perspectives from 1997. Ex Oriente, Berlin.

Barlett, P.F., 1980. Adaptive Strategies in Peasant Agricultural Production. Annual Review of Anthropology 9, 545–573.

Bar, S., Rosenberg, D., 2011. Newly Discovered Yarmukian and Wadi Rabah Sites in the Southern Jordan Valley and The Desert Fringes of Samaria During the 7th and 6th Millennia BC: Preliminary Report. Archaeology, Ethnology and Anthropology of Eurasia 39, 32–39.

Bartolome, J., Franch, J., Plaixats, J., Seligman, N.G., 1998. Diet Selection by Sheep and Goats on Mediterranean Heath-Woodland Range. Journal of Range Management 51, 383–391.

Barton, C.M., Ullah, I.I., Bergin, S., 2010a. Land use, water and Mediterranean landscapes: modelling long-term dynamics of complex socio-ecological systems. Philosophical Transactions of the Royal Society A: Mathematical, Physical and Engineering Sciences 368, 5275 –5297.

Barton, C.M., Ullah, I.I., Bergin, S.M., Mitasova, H., Sarjoughian, H., 2012. Looking for the future in the past: Long-term change in socioecological systems. Ecological Modelling 241, 42–53.

Barton, C.M., Ullah, I.I., Mitasova, H., 2010b. Computational modeling and Neolithic socioecological dynamics: a case study from Southwest Asia. American Antiquity 75, 364–386.

Bar-Yosef, O., 1985. A Cave in the Desert: Nahal Hemar: 9,000-year-old-finds. Israel Museum.

Bar-Yosef, O., 2001. Lithics and the social geographical configurations identifying Neolithic tribes in the Levant. Beyond tools. Redefining PPN Lithic assemblages of the Levant 437–448.

Bar-Yosef, O., 2002. The Natufian culture and the early Neolithic: Social and economic trends in Southwestern Asia. Examining the Farming/Language Dispersal Hypothesis, McDonald Institute Monographs, University of Cambridge, Cambridge 113–126.

Bar-Yosef, O., Alon, D., 1988. Nahal Hemar Cave: the excavations.

Bar-Yosef, O., Meadow, R.H., 1995. The Origins of Agriculture in the Near East, in: Price, T.D., Gebaur, A. (Eds.), Last Hunters-First Farmers: New Perspectives on the Prehistoric Transition to Agriculture. School of American Research Press, Santa Fe, pp. 39–94.

Barzegar, A.R., Yousefi, A., Daryashenas, A., 2002. The effect of addition of different amounts and types of organic materials on soil physical properties and yield of wheat. Plant and soil 247, 295–301.

Batjes, N.H., Rawajfih, Z., Al-Adamat, R., 2003. Soil data derived from SOTER for studies of carbon stocks and change in Jordan. Version (1.0), ISRIC. The Netherlands: World Soil Information.

Bazzaz, F.A., 1979. The Physiological Ecology of Plant Succession. Annual Review of Ecology and Systematics 10, 351–371.

Bejan, A., 2007. The constructal law in nature and society, in: Bejan, A. (Ed.), Constructal Theory of Social Dynamics, International Workshop on the Constructal Theory of Social Dynamics. Springer, New York, pp. 1–34.

Bejan, A., Lorente, S., 2011. The constructal law origin of the logistics S curve. Journal of Applied Physics 110, 024901–024901–4.

Belfer-Cohen, A., Goring-Morris, N., 1997. The articulation of cultural processes and Late Quaternary environmental changes in Cisjordan. paleo 23, 71–93.

Bender, F., 1975. Geology of the Arabian Peninsula: Jordan. United States Government Printing Office.

Bender, F., Khdeir, M.K., 1974. Geology of Jordan. Gebrueder Borntraeger.

Bentley, R.A., 2003. Complex systems and archaeology: empirical and theoretical applications. University of Utah Press, Salt Lake City.

Bentley, R.A., Maschner, H.D.G., 2003. Complex systems and archaeology. University of Utah Press, Salt Lake City.

Berger, J.-F., Guilaine, J., 2009. The 8200 cal BP abrupt environmental change and the Neolithic transition: A Mediterranean perspective. Quaternary International 200, 31–49.

Bergin, S., Ullah, I.I., Barton, C.M., Gravel-Miguel, C., 2012. Human-Environment Interactions in a Changing Environment: A Computational Model of Agropastoral Practices and Landscapes in Neolithic Spain, in: Socio-natural Systems in Pastoral and Agro-pastoral Societies: Archaeological Investigations of Pastoral Landscapes. Presented at the 77th annual meeting of the Society of American Archaeology, Memphis.

Berthold, M.R., Cebron, N., Dill, F., Gabriel, T.R., Kötter, T., Meinl, T., Ohl, P., Sieb, C., Thiel, K., Wiswedel, B., 2008. KNIME: The Konstanz information miner. Data Analysis, Machine Learning and Applications 319–326.

Berthold, M.R., Cebron, N., Dill, F., Gabriel, T.R., Kötter, T., Meinl, T., Ohl, P., Thiel, K., Wiswedel, B., 2009. KNIME-the Konstanz information miner: version 2.0 and beyond. AcM SIGKDD explorations Newsletter 11, 26–31.

Bettinger, R.L., 1987. Archaeological approaches to hunter-gatherers. Annual Review of Anthropology 16, 121–142.

Bhatt, B.P., Sachan, M.S., 2004. Firewood consumption pattern of different tribal communities in Northeast India. Energy Policy 32, 1–6.

Binford, L.R., 1977. Forty-seven trips: A case study in the character of archaeological formation processes, in: Wright, R.V.S. (Ed.), Stone Tools as Cultural Markers. Australian Institute of Aboriginal Studies, Canberra, pp. 24–36.

Binford, L.R., 1977. For theory building in archaeology: essays on faunal remains, aquatic resources, spatial analysis, and systemic modeling. Academic Pr.

Binford, L.R., 1980. Willow Smoke and Dogs' Tails: Hunter-Gatherer Settlement Systems and Archaeological Site Formation. American Antiquity 45, 4–20.

Binford, L.R., 1983. Working at archaeology. Academic Press New York.

Binford, L.R., 2001. Constructing frames of reference: an analytical method for archaeological theory building using ethnographic and environmental data sets. University of California Press, Berkeley.

Blackham, M., 1997. Changing Settlement at Tabaqat al-Buma in Wadi Ziqlab, Jordan: A Stratigraphic Analysis, in: H. G. Gebel, Z.K., Rollefson, G.O. (Eds.), Prehistory of Jordan II: Perspectives from 1997, Studies in Early Near Eastern Production, Subsistent, and Environment 4. Ex Oriente, Berlin, pp. 345–360.

Blackham, M., Fisher, K., Lasby, D., 1997. Excavations at Tell Fendi, a Late Chalcolithic Site in the Jordan Valley, Jordan. Echos Du Monde Classique/Classical Views 41, 1–4.

Bledsoe, B.P., 2002. Stream Erosion Potential and Stormwater Management Strategies. Journal of Water Resources Planning & Management 128, 451.

Bocquet-Appel, J.P., 2002. Paleoanthropological Traces of a Neolithic Demographic Transition. Current Anthropology 43, 637–650.

Boellstorff, D., Benito, G., 2005. Impacts of set-aside policy on the risk of soil erosion in central Spain. Agriculture, Ecosystems and Environment 107, 231–243.

Bonabeau, E., 2002. Agent-based modeling: Methods and techniques for simulating human systems. Proceedings of the National Academy of Sciences 99, 7280–7287.

Bonet, A., 2004. Secondary succession of semi-arid Mediterranean old-fields in south-eastern Spain: insights for conservation and restoration of degraded lands. Journal of Arid Environments 56, 213–233.

Bonet, A., Pausas, J.G., 2004. Species richness and cover along a 60-year chronosequence in old-fields of southeastern Spain. Plant Ecology 174, 257–270.

Bonet, A., Pausas, J.G., 2007. Old Field Dynamics on the Dry Side of the Mediterranean Basin: Patterns and Processes in Semiarid Southeast Spain. Old Fields: Dynamics and Restoration of Abandoned Farmland 247.

Borg, I., Groenen, P.J.F., 2005. Modern multidimensional scaling: Theory and applications. Springer Verlag.

Boserup, E., 1965. The Conditions of Agricultural Growth: The Economics of Agrarian Change Under Population Pressure. George, Allen, and Unwin, London.

Bourgeron, P.S., Humphries, H.C., Riboli-Sasco, L., 2009. Regional analysis of social-ecological systems. Natures Sciences Sociétés Vol. 17, 185–193.

Bradley, R.S., 1999. Paleoclimatology: Reconstructing Climates of the Quaternary. Academic Press.

Braun, J., Heimsath, A.M., Chappell, J., 2001. Sediment transport mechanisms on soil-mantled hillslopes. Geology 29, 683–686.

Brayshaw, D.J., Rambeau, C.M.C., Smith, S.J., 2011. Changes in Mediterranean climate during the Holocene: Insights from global and regional climate modelling. The Holocene 21, 15–31.

Brooks, A., Yellen, J., 1987. The Preservation of Activity Areas in the Archaeological Record: Ethnoarchaeological and Archaeological Work in Northwest Ngamiland, Botswana, in: Kent, S. (Ed.), Method and Theory for Activity Area Research: An Ethnoarchaeological Approach. Columbia University Press, New York, pp. 63–106.

Bryson, R.A., Bryson, R.U., 1996. High resolution simulations of regional Holocene climate: North Africa and the Near East, in: Nüzhet Dalfes, H., Kukla, G. (Eds.), Third MIllennium BC Climate Change and Old World Collapse, Nato ASI Series I: Global Environmental Change. Springer Verlag, Berlin, pp. 565–593.

Bryson, R.A., McEnaney-DeWall, K., 2007. An Introduction to the Archaeoclimatology Macrophsical Climate Model. University of Wisconsin.

Burdon, D.J., Quennell, A.M., 1959. Handbook of the Geology of Jordan. Government of the Hashemite Kingdom of Jordan.

Burke, B.C., Heimsath, A.M., White, A.F., 2007. Coupling chemical weathering with soil production across soil-mantled landscapes. Earth Surface Processes and Landforms 32, 853–873.

Burrough, P.A., 1989. Fuzzy mathematical methods for soil survey and land evaluation. Journal of Soil Science 40, 477–492.

Burrough, P.A., Macmillan, R.A., van DEURSEN, W., 1992. Fuzzy classification methods for determining land suitability from soil profile observations and topography. Journal of Soil Science 43, 193–210.

Butzer, K.W., 1982. Archaeology as human ecology: method and theory for a contextual approach. Cambridge University Press, Cambridge.

Byrd, B.F., 1994. Public and Private, Domestic and Corporate: The Emergence of the Southwest Asian Village. American Antiquity 59, 639–666.

Byrd, B.F., Banning, E.B., 1988. Southern Levantine Pier Houses: Intersite Architectural Patterning during the Pre-Pottery Neolithic B. paleo 14, 65–72.

Campbell, D., 2010. Modelling the Agricultural Impacts of the Earliest Large Villages at the Pre-Pottery Neolithic–Pottery Neolithic Transition, in: Finlayson, B., Warren, G. (Eds.), Landscapes in Transistion. Oxbow Books, Oxford, pp. 173–183.

Campin, J.-M., Fichefet, T., Duplessy, J.-C., 1999. Problems with using radiocarbon to infer ocean ventilation rates for past and present climates. Earth and Planetary Science Letters 165, 17–24.

Carmel, Y., Kadmon, R., 1999. Effects of grazing and topography on long-term vegetation changes in a Mediterranean ecosystem in Israel. Plant Ecology 145, 243–254.

Carter, D.L., Berg, R.D., Sanders, B.J., 1985. The effect of furrow irrigation erosion on crop productivity. Soil Science Society of America Journal 49, 207–211.

Casado, M.A., Miguel, J.M., Sterling, A., Peco, B., Galiano, E.F., Pineda, F.D., 1986. Production and spatial structure of Mediterranean pastures in different stages of ecological succession. Plant Ecology 64, 75–86.

Chapman, H., Adcock, J., Gater, J., 2009. An approach to mapping buried prehistoric palaeosols of the Atlantic seaboard in Northwest Europe using GPR, geoarchaeology and GIS and the implications for heritage management. Journal of Archaeological Science 36, 2308–2313.

Christensen, L.A., McElyea, D.E., 1988. Toward a general method of estimating productivity-soil depth response relationships. Journal of soil and water conservation 43, 199–202.

Christiansen, J.H., Altaweel, M.R., 2005. Understanding Ancient Societies: A New Approach Using Agent-Based Holistic Modeling. Structure and Dynamics 1.

Cioffi-Revilla, C., Luke, S., Parker, D.C., Rogers, J.D., Fitzhugh, W.W., Honeychurch, W., Frohlich, B., Depriest, P., Amartuvshin, C., 2007. Agent-based modeling simulation of social adaptation and long-term change in Inner Asia, in: Advancing Social Simulation: The First World Congress in Social Simulation, Edited by T. Terano and D. Sallach. Tokyo, New York, and Heidelberg: Springer Verlag.

Cioffi-Revilla, C., Rogers, J.D., Latek, M., 2010. The MASON HouseholdsWorld Model of Pastoral Nomad Societies. Simulating Interacting Agents and Social Phenomena 193–204.

Cioffi-Revilla, C., Rogers, J.D., Wilcox, S.P., Alterman, J., 2008. ‘Computing the Steppes: Data Analysis for Agent-Based Modeling of Polities in Inner Asia, in: Annual Conference of the American Political Science Association.

Clare, L., 2010. Pastoral Clashes: Conflict risk and mitigation at the Pottery Neolithic Transition in the Southern Levant. Neo-Lithics 10, 13–31.

Clevis, Q., Tucker, G.E., LOCK, G., Lancaster, S.T., Gasparini, N., Desitter, A., Bras, R.L., 2006. Geoarchaeological simulation of meandering river deposits and settlement distributions: a three-dimensional approach. Geoarchaeology 21, 843–874.

Colledge, S., 2001. Plant exploitation on epipalaeolithic and early neolithic sites in the Levant, BAR International. Oxford.

Colledge, S., Conolly, J., Shennan, S., 2004. Archaeobotanical Evidence for the Spread of Farming in the Eastern Mediterranean. Current Anthropology 45, S35–S58.

Conolly, J., Colledge, S., Dobney, K., Vigne, J.-D., Peters, J., Stopp, B., Manning, K., Shennan, S., 2011. Meta-analysis of zooarchaeological data from SW Asia and SE Europe provides insight into the origins and spread of animal husbandry. Journal of Archaeological Science 38, 538–545.

Contreras, D.A., 2009. Reconstructing landscape at Chavín de Huántar, Perú: A GIS-based approach. Journal of Archaeological Science 36, 1006–1017.

Corbeels, M., Shiferaw, A., Haile, M., 2000. Farmers' knowledge of soil fertility and local management strategies in Tigray, Ethiopia, Managing Africa's Soils. Russell Press, Nottingham.

Cordova, C.E., 2007. Millennial Landscape Change in Jordan: Geoarchaeology and Cultural Ecology. University of Arizona Press.

Cowgill, G.L., 1975. On Causes and Consequences of Ancient and Modern Population Changes. American Anthropologist 77, 505–525.

Culling, W.E.H., 1960. Analytical Theory of Erosion. The Journal of Geology 68, 336–344.

Culling, W.E.H., 1963. Soil Creep and the Development of Hillside Slopes. The Journal of Geology 71, 127–161.

Culling, W.E.H., 1965. Theory of Erosion on Soil-Covered Slopes. The Journal of Geology 73, 230–254.

Dabasi-Scheng, L., 1978. Economic aspects of shifting cultivation, in: FAO/SIDA Regional Seminar on Shifting Cultivation and Soil Conservation in Africa, Ibadan (Nigeria), 2-21 Jul 1973. Presented at the FAO/SIDA Regional Seminar on Shifting Cultivation and Soil Conservation in Africa, FAO, Ibadan, pp. 78–99.

David, P.A., 1988. Path-dependence: putting the past into the future of economics, Institute for mathematical studies in the social sciences Technical Report. Stanford University.

David, P.A., 1993. Path-dependence and predictability in dynamic systems with local network externalities: a paradigm for historical economics, in: Technology and the Wealth of Nations. Pinter, London, pp. 208–231.

David, P.A., 2001. Path dependence, its critics and the quest for "historical economics", in: Garrouste, P., Ioannides, S. (Eds.), Evolution and Path Dependence in Economic Ideas: Past and Present. Edward Elgar Publishing , Inc., Northhampton, pp. 15–40.

David, P.A., 2007. Path dependence: a foundational concept for historical social science. Cliometrica 1, 91–114.

Davies, C.P., Fall, P.L., 2001. Modern pollen precipitation from an elevational transect in central Jordan and its relationship to vegetation. Journal of Biogeography 28, 1195–1210.

Davis, F., Goetz, S., 1990. Modeling vegetation pattern using digital terrain data. Landscape Ecology 4, 69–80.

Davis, J., Simmons, A.H., Mandel, R.D., Rollefson, G., Kafafi, Z., 1990. A postulated Early Holocene summer precipitation episode in the Levant: Effects on Neolithic adaptations. Presented at the 55th annual meeting of the Society for American Arcaheology, Las Vegas.

Day, R.L., Laland, K.N., Odling-Smee, F.J., 2003. Rethinking adaptation: the niche-construction perspective. Perspectives in Biology and Medicine 46, 80–95.

Deal, M., 1985. Household Pottery Disposal in the Maya Highlands: An Ethnoarchaeological Interpretation. Journal of Anthropological Archaeology 4, 243–291.

Debussche, M., Escarré, J., Lepart, J., Houssard, C., Lavorel, S., 1996. Changes in Mediterranean plant succession: old-fields revisited. Journal of Vegetation Science 7, 519–526.

Degani, A., Lewis, L.A., Downing, B.B., 1979. Interactive Computer Simulation of the Spatial Process of Soil Erosion. Professional Geographer 31, 184–190.

Degen, A.A., 2007. Sheep and goat milk in pastoral societies. Small Ruminant Research 68, 7–19.

De Jong, S.M., Pebesma, E.J., Lacaze, B., 2003. Above-ground biomass assessment of Mediterranean forests using airborne imaging spectrometry: the DAIS Peyne experiment. International Journal of Remote Sensing 24, 1505–1520.

Dietrich, W.E., Bellugi, D.G., Sklar, L.S., Stock, J.D., Heimsath, A.M., Roering, J.J., 2003. Geomorphic transport laws for predicting landscape form and dynamics. Geophysical Monograph 135, 103–132.

Dodds, R.R., 1987. Wadi Ziqlab Project 1987; Tabaqat al Buma- 200.

Donner, L., Schubert, W., 2011. The Development of Atmospheric General Circulation Models: Complexity, Synthesis, and Computation. Cambridge University Press.

Edwards, P.C., Thorpe, S., 1986. Surface lithic finds from Kharaysin, Jordan. paleo 12, 85–87.

Edwards, P.., Meadows, J., Sayej, G., Westaway, M., 2004. From the PPNA to the PPNB : new views from the Southern Levant after excavations at Zahrat adh-Dhra' 2 in Jordan. paleo 30, 21–60.

El-Naqa, A., 2001. Engineering geology assessment of El-Rabweh landslide, south-east of Amman City, Jordan. Bulletin of Engineering Geology and the Environment 60, 109–116.

Enloe, J.G., 2003. Food sharing past and present: archaeological evidence for economic and social interactions. Before Farming: the Archaeology and Anthropology of Hunter-Gatherers 1, 1–23.

Epstein, H., 1982. Awassi Sheep. World Animal Review 44, 11–27.

Eshed, A.N., Hershkovitz, I., Goring-Morris, A.N., 2008. A Re-Evaluation of Burial Customs in the Pre- Pottery Neolithic B in light of Paleodemographic Analysis of the Human Remains from Kfar HaHoresh, Israel. paleo 34, 91–103.

Eshed, V., Gopher, A., Gage, T.B., Hershkovitz, I., 2004. Has the transition to agriculture reshaped the demographic structure of prehistoric populations? New evidence from the Levant. American Journal of Physical Anthropology 124, 315–329.

Essa, S., 2004. GIS modeling of land degradation in Northern-Jordan using Landsat imagery, in: Proceedings of XXth ISPRS Congress. Istanbul.

Evans, T.P., Kelley, H., 2004. Multi-scale analysis of a household level agent-based model of land-cover change. Journal of Environmental Management 72, 57–72.

Fairbairn, S.L., Patience, J.F., Classen, H.L., Zijlstra, R.T., 1999. The energy content of barley fed to growing pigs: characterizing the nature of its variability and developing prediction equations for its estimation. J. Anim Sci. 77, 1502–1512.

Fall, P.L., Falconer, S.E., Lines, L., 2002. Agricultural intensification and the secondary products revolution along the Jordan Rift. Human Ecology 30, 445–482.

Farhan, Y., 1986. Landslides in Central Jordan with Special Reference to the March 1983 Rainstorm. Singapore Journal of Tropical Geography 7, 80–97.

Feinman, G., Neitzel, J.E., 1984. Too Many Types: An Overview of Sedentary Prestate Societies in the Americas. Advances in Archaeological Method and Theory 7, 39–102.

Fenner, J.N., 2005. Cross-cultural estimation of the human generation interval for use in genetics-based population divergence studies. American Journal of Physical Anthropology 128, 415–423.

Field, J., 1994. Rainfall patterns and landscape changes in Wadi Ziqlab, Jordan, in: Jamieson, R., Abonyi, S., Mirau, N. (Eds.), Archaeology and the Environment: A Fragile Coexistence. Proceedings of the 24th Annual Chacmool Conference. Department of Archaeology, University of Calgary, Calgary, pp. 257–59.

Field, J., Banning, E.B., 1998. Hillslope processes and archaeology in Wadi Ziqlab, Jordan. Geoarchaeology 13, 595–616.

Fisher, W., Atkinson, D., Beaumont, P., Coles, A., Gilchrist-Shirlaw, D., 1966. Soil Survey of Wadi Ziqlab, Jordan. Durham University, Durham.

Flanagan, Laflen, J.M., Meyer, L.D., 2003. Honoring the Universal Soil Loss Equation Booklet. American Society of Agricultural and Biological Engineers and Purdue University, West Lafayette, IN.

Flannery, K.V., 1993. Will the real model please stand up: comments on Saidel's "Round house or square". Journal of Mediterranean Archaeology 6, 109–117.

Fleuret, P.C., Fleuret, A.K., 1978. Fuelwood Use in a Peasant Community: A Tanzanian Case Study. The Journal of Developing Areas 12, 315–322.

Folke, C., 2006. Resilience: The emergence of a perspective for social-ecological systems analyses. Global environmental change 16, 253–267.

Folke, C., Carpenter, S., Walker, B., Scheffer, M., Elmqvist, T., Gunderson, L., Holling, C.S., 2004. Regime shifts, resilience, and biodiversity in ecosystem management. Annual Review of Ecology, Evolution, and Systematics 557–581.

Förster, H., Wunderlich, J., 2009. Holocene sediment budgets for upland catchments: The problem of soilscape model and data availability. CATENA 77, 143–149.

Foster, G.R., Meyer, L.D., Shen, 1972. A closed-form soil erosion equation for upland areas, in: Sedimentation: Symposium to Honor Professor HA Einstein. Ft. Collins, CO. pp. 12.1–12.19.

Fox, J., 1984. Firewood consumption in a Nepali village. Environmental Management 8, 243–249.

Fuller, D., Asouti, E., Purugganan, M., 2012. Cultivation as slow evolutionary entanglement: comparative data on rate and sequence of domestication. Vegetation History and Archaeobotany 21, 131–145.

Gaili, E.S., Ali, A.E., 1985. Meat from Sudan desert sheep and goats: Part 2–Composition of the muscular and fatty tissues. Meat Science 13, 229–236.

Galán, J.M., Izquierdo, L.R., Izquierdo, S.S., Santos, J.I., Del Olmo, R., López-Paredes, A., Edmonds, B., 2009. Errors and artefacts in agent-based modelling. Journal of Artificial Societies and Social Simulation 12, 1.

García Puchol, O., Baton, C.M., Bernabeu Aubán, J., 2008. Programa de prospección geofísica, microsondeos y catas para la caracterización de un gran foso del IV milenio cal AC en Alt del Punxó (Muro de l'Alcoi, Alacant). Trabajos de prehistoria 65, 143–154.

Garfinkel, Y., 1987. Yiftahel: a Neolithic village from the seventh millennium BC in Lower Galilee, Israel. Journal of Field Archaeology 14, 199–212.

Gasparini, N.M., Bras, R.L., Whipple, K.X., 2006. Numerical modeling of non-steady-state river profile evolution using a sediment-flux-dependent incision model. Special Paper - Geological Society of America 398, 127–141.

Gebel, H.G., 2004. Central to what? The centrality issue of the LPPNB Mega-Site phenomenon in Jordan, in: Bienert, H.-D., Gebel, H.G., Neef, R. (Eds.), Central Settlements in Neolithic Jordan, Studies in Early Near Eastern Production, Subsistence, and Environment. Ex oriente, Berlin, pp. 1–19.

Gibbon, D., 1981. Rainfed farming systems in the Mediterranean region. Plant Soil 58, 59–80.

Gibbs, K., 2008. Understanding Community: A Comparison of Three Late Neolithic Pottery Assemblages from Wadi Ziqlab, Jordan (Ph.D.). University of Toronto, Toronto.

Gibbs, K., Kadowaki, S., Banning, E.B., 2006. The Late Neolithic at al-Basatîn in Wadi Ziqlab, northern Jordan. Antiquity 80, http://antiquity.ac.uk/projgall/gibbs/index.html.

Gibbs, K., Kadowaki, S., Banning, E.B., 2010. Excavations at al-Basatîn, a Late Neolithic and Early Bronze I Site in Wadi Ziqlab, Northern Jordan. Annual of the Department of Antiquities of Jordan 54, 461–476.

Glaser, M., Ratter, B.M.W., Krause, G., Welp, M., 2012. New approaches to the analysis of human–nature relations, in: Glaser, M., Ratter, B.M.W., Krause, G., Welp, M. (Eds.), Human-nature Interactions in the Anthropocene: Potentials of Social-ecological Systems Analysis. Routledge, New York, pp. 1–12.

Goodale, N.B., 2009. Convergence in the Neolithic: Human population growth at the dawn of agriculture. Washington State University.

Goodale, N.B., Kuijt, I., 2006. Chronological Frameworks and Disparate Technology : an Exploration of Chipped Stone Variability and the Forager to Farmer Transition at 'Iraq ed-Dubb, Jordan. paleo 32, 27–45.

Goodchild, M., Haining, R., STEPHEN, W., 1992. Integrating GIS and spatial data analysis: problems and possibilities. International Journal of Geographical Information Systems 6, 407–423.

Gordon, R.L., Knauf, E.A., 1987. Er-Rumman Survey 1985. Annual of the Department of Antiquities of Jordan31 289–93.

Goring-Morris, A.N., Burns, R., Davidzon, A., Eshed, V., Goren, Y., Hershkovitz, I., Kangas, S., Kelecevic, J., 1998. The 1997 season of excavations at the mortuary site of Kfar HaHoresh, Galilee, Israel. Neo-Lithics 3, 1–4.

Goring-Morris, N., Belfer-Cohen, A., 2010. "Great Expectations," or the Inevitable Collapse of the Early Neolithic in the Near East Nigel Goring-Morris and Anna Belfer-Cohen, in: Brandy, M.S., Fox, J.R. (Eds.), Becoming Villagers: Comparing Early Village Societies. University of Arizona Press, Tucson, pp. 62–80.

Gotts, N.M., 2007. Resilience, panarchy, and world-systems analysis. Ecology and Society 12, 24.

Gould, R.A., 1978. Beyond analogy in ethnoarchaeology, in: Explorations in Ethnoarchaeology, SAR Advanced Seminars. University of New Mexico Press, Albuquerque, pp. 249–321.

GRASS Development Team, 2012. Geographic Resources Analysis Support System [WWW Document]. URL http://grass.osgeo.org (accessed 7.25.09).

Greer, J., Thorbecke, E., 1986. A methodology for measuring food poverty applied to Kenya. Journal of Development Economics 24, 59–74.

Gregg, M.W., Banning, E.B., Gibbs, K., Slater, G.F., 2009. Subsistence practices and pottery use in Neolithic Jordan: molecular and isotopic evidence. Journal of Archaeological Science 36, 937–946.

Griggs, D.J., Noguer, M., 2002. Climate Change 2001: The Scientific Basis. Contribution of Working Group I to the Third Assessment Report of the Intergovernmental Panel on Climate Change. Weather 57, 267–269.

Grisley, W., Kellogg, E.D., 1983. Farmers' Subjective Probabilities in Northern Thailand: An Elicitation Analysis. American Journal of Agricultural Economics 65, 74–82.

Gunderson, L.H., Allen, C.R., Holling, C.S., 2010. Foundations of ecological resilience. Island Press.

Gunderson, L.H., Holling, C.S. (Eds.), 2002. Panarchy: understanding transformations in human and natural systems. Island Press, Washington D.C.

Gustafson, E.J., Shifley, S.R., Mladenoff, D.J., Nimerfro, K.K., He, H.S., others, 2000. Spatial simulation of forest succession and timber harvesting using LANDIS. Canadian Journal of Forest Research 30, 32–43.

Halstead, P., 1999. Neighbours from hell? The household in Neolithic Greece. Neolithic society in Greece 77–95.

Hammad, A.A., Børresen, T., Haugen, L.E., 2006. Effects of rain characteristics and terracing on runoff and erosion under the Mediterranean. Soil and Tillage Research 87, 39–47.

Hammad, A.A., Lundekvam, H., Børresen, T., 2004. Adaptation of RUSLE in the Eastern Part of the Mediterranean Region. Environmental Management 34, 829–841.

Hartter, J., Boston, K., 2007. An integrated approach to modeling resource utilization for rural communities in developing countries. Journal of Environmental Management 85, 78–92.

Hartter, J., Boston, K., 2008. Consuming Fuel and Fuelling Consumption: Modelling Human Caloric Demands and Fuelwood Use. Small-scale Forestry 7, 1–15.

Hayden, B., Cannon, A., 1983. Where the garbage goes: Refuse disposal in the Maya Highlands. Journal of Anthropological Archaeology 2, 117–163.

Heckbert, S., Isendahl, C., Gunn, J., Brewer, S., Scarborough, V., Chase, A.F., Chase, D.Z., Costanza, R., Dunning, N., Beach, T., Luzzadder-Beach, S., Lentz, D., Sinclair, P., 2012. Growing the Maya social-ecological system from the bottom up: complex systems models of resilience, in: Isendahl, C., Stump, D. (Eds.), Handbook of Historical Ecology and Applied Archaeology. Oxford University Press, Oxford.

Hegmon, M., 1991. The Risks of Sharing and Sharing as Risk Reduction: Interhousehold Food Sharing in Egalitarian Societies, in: Gregg, S.A. (Ed.), Between Bands and States, Occasional Paper No. 9. Center for Archaeological Investigation, Southern Illinois University, Carbondale, pp. 309–332.

Heimsath, A.M., Chappell, J., Dietrich, W.E., Nishiizumi, K., Finkel, R.C., 2000. Soil production on a retreating escarpment in southeastern Australia. Geology 28, 787–790.

Heimsath, A.M., Chappell, J., Spooner, N.A., Questiaux, D.G., 2002. Creeping soil. Geology 30, 111–114.

Heimsath, A.M., Dietrich, W.E., Nishiizumi, K., Finkel, R.C., 1997. The soil production function and landscape equilibrium. Nature 338, 358–361.

Heimsath, A.M., Dietrich, W.E., Nishiizumi, K., Finkel, R.C., 2001. Stochastic Processes of Soil Production and Transport: Erosion Rates, Topographic Variation and Cosmogenic Nuclides in the Oregon Coast Range. Earth Surface Processes and Landforms 26, 531–552.

Heimsath, A.M., E. Dietrich, W., Nishiizumi, K., Finkel, R.C., 1999. Cosmogenic nuclides, topography, and the spatial variation of soil depth. Geomorphology 27, 151–172.

Henry, D.O., White, J.J., Beaver, J.E., Kadowaki, S., Nowell, A., Cordova, C.E., Dean, R.M., Ekstrom, H., McCorriston, J., Scott-Cummings, L., 2003. The Early Neolithic Site of Ayn Abu Nukhayla, Southern Jordan. Bulletin of the American Schools of Oriental Research 330, 1–30.

HilleRisLambers, R., Rietkerk, M., van den Bosch, F., Prins, H.H.T., de Kroon, H., 2001. Vegetation Pattern Formation in Semi-Arid Grazing Systems. Ecology 82, 50–61.

Hill, J.B., Miller, A.E., Wentz, E., Barton, C.M., 2008. Archaeoclimatology and Ancient Mediterranean Landscape Dynamics. Paper presented at Annual Meetings of the Society for American Archaeology. Presented at the The 74th Meeting of the Society for American Archaeology, Vancouver, Canada.

Hillman, G., 1973. Agricultural Productivity and Past Population Potential at Aşvan: An Exercise in the Calculation of Carrying Capacities. Anatolian Studies 23, 225–240.

Hirata, M., Fujita, H., Miyazaki, A., 1998. Changes in grazing areas and feed resources in a dry area of north-eastern Syria. Journal of Arid Environments 40, 319–329.

Hitchcock, R.K., 1987. Sedentism and site structure: Organizational changes in Kalahari Basarwa residential locations. Method and Theory for Activity Area Research 374–423.

Holling, C.S., 1973. Resilience and stability of ecological systems. Annual review of ecology and systematics 1–23.

Holling, C.S., Gunderson, L.H., 2002. Resilience and adaptive cycles, in: Gunderson, L.H., Holling, C.S. (Eds.), Panarchy: Understanding Transformations in Human and Natural Systems. Island Press, Washington D.C., pp. 25–62.

Holling, C.S., Gunderson, L.H., Peterson, G.D., 2002. Sustainability and panarchies, in: Gunderson, L.H., Holling, C.S. (Eds.), Panarchy: Understanding Transformations in Human and Natural Systems. Island Press, Washington D.C., pp. 63–102.

Horowitz, A., 2001. The Jordan Rift Valley. A.A. Balkema Publishers, Lisse ; Exton, PA.

Horwitz, L.K., Lernau, O., 2003. Temporal and spatial variation in Neolithic animal exploitation strategies: a case study of fauna from the site of Yiftah'el (Israel). Paléorient 29, 19–58.

Howard, A.D., Kerby, G., 1983. Channel changes in badlands. Geological Society of America Bulletin 94, 739–752.

Huston, M., Smith, T., 1987. Plant Succession: Life History and Competition. The American Naturalist 130, 168–198.

Ibáñez, J.J., González Urquijo, J., Rodríguez, A., 2007. The evolution of technology during the PPN in the Middle euphrates. A view from use wear analysis of lithic tools, in: Astruc, L., Binder, D., Briois, F. (Eds.), Technical Systems and Near Eastern PPN Communities. Editions APDCA, Antibes, pp. 153–165.

Ivanyi, M., Bocsi, R., Gulyas, L., Kozma, V., Legendi, R., 2007. The multi-agent simulation suite, in: Emergent Agents and Socialities: Social and Organizational Aspects of Intelligence. Papers from the 2007 AAAI Fall Symposium. pp. 57–64.

Janssen, M.A., Kohler, T.A., Scheffer, M., 2003. Sunk-Cost Effects and Vulnerability to Collapse in Ancient Societies. Current Anthropology 44, 722–728.

Janssen, M.A., Scheffer, M., 2004. Overexploitation of renewable resources by ancient societies and the role of sunk-cost effects. Ecology and Society 9, 6.

Johnson, A.L., 2002. Cross-Cultural Analysis of Pastoral Adaptations and Organizational States: A Preliminary Study. Cross-Cultural Research 36, 151–180.

Johnson, D.L., 1969. The Nature of Nomadism: A Comparative Study of Pastoral Migrations in Southwestern Asia and Northern Africa, Department of Geography Research Papers. The Department of Geography, The University of Chicago, Chicago.

Johnson, G., 1982. Organisational Structure and Scalar Stress, in: Renfrew, C. (Ed.), Theory & Explanation in Archaeology. Academic Press, New York, pp. 389–421.

Kadowaki, S., 2005. Designs and production technology of sickel elements in Late Neolithic Wadi Ziqlab, Northern Jordan. Paléorient 31, 69–85.

Kadowaki, S., 2007. Changing Community Life at a Late Neolithic Farmstead: Built environments and the use of Space at Tabaqat al-Bûma in Wadi Ziqlab, Northern Jordan (PhD Diss.). University of Toronto, Toronto.

Kadowaki, S., Gibbs, K., Allentuck, A., Banning, E.B., 2008. Late Neolithic Settlement in Wadi Ziqlab, Jordan: al-Basatîn. paleo 34, 105–129.

Kafafi, Z., 1992. Pottery Neolithic settlement patterns in Jordan, in: Studies in the History and Archaeology of Jordan IV. Department of Antiquities of Jordan, Amman, pp. 115–122.

Kafafi, Z., 1993. The Yarmoukians in Jordan. paleo 19, 101–114.

Kaliszan, L.R., Hermansen, B.D., Jensen, C.H., Skulbøl, T.B.B., Bille Petersen, M., Bangsgaard, P., Ihr, A., Sørensen Mette, L., Markussen, B., others, 2002. Shaqarat Mazyad-The village on the edge.

Kamp, K.A., 1987. Affluence and image: Ethnoarchaeology in a Syrian village. Journal of field archaeology 14, 283–296.

Kamp, K.A., 2000. From Village to Tell: Household Ethnoarchaeology in Syria. Near Eastern Archaeology 63, 84–93.

Karanth, K.K., Curran, L.M., Reuning-Scherer, J.D., 2006. Village size and forest disturbance in Bhadra Wildlife Sanctuary, Western Ghats, India. Biological Conservation 128, 147–157.

Keane, R.E., Cary, G.J., Davies, I.D., Flannigan, M.D., Gardner, R.H., Lavorel, S., Lenihan, J.M., Li, C., Rupp, T.S., 2004. A classification of landscape fire succession models: spatial simulations of fire and vegetation dynamics. Ecological Modelling 179, 3–27.

Kelly, R.L., 1983. Hunter-Gatherer Mobility Strategies. Journal of Anthropological Research 39, 277–306.

Kelly, R.L., 1991. Sedentism, socio-political inequality, and resource fluctuations, in: Gregg, S.A. (Ed.), Between Bands and States, Occasional Paper No.9. Center for Archaeological Investications, Southern Illinois University, Carbondale, pp. 135–158.

Kelly, R.L., 1995. The Foraging Spectrum: Diversity in Hunter-Gatherer Liveways, in: Foraging and Subsistence. Smithsonian Institution Press, Washington D.C., pp. 65–110.

Kent, S., 1993. Sharing in an Egalitarian Kalahari Community. Man 28, 479–514.

Kenyon, K.M., 1960. Archaeology in the Holy Land, 3d ed. Praeger, New York,.

Khazanov, A., 1994. Nomads and the Outside World. University of Wisconsin Press, Madison.

Khresat, S.A., Al-Bakri, J., Al-Tahhan, R., 2008. Impacts of land use/cover change on soil properties in the Mediterranean region of northwestern Jordan. Land Degradation & Development 19, 397–407.

Khresat, S.A., Rawajfih, Z., Mohammad, M., 1998a. Land degradation in north-western Jordan: causes and processes. Journal of Arid Environments 39, 623–629.

Khresat, S.A., Rawajfih, Z., Mohammad, M., 1998b. Morphological, physical and chemical properties of selected soils in the arid and semi-arid region in north-western Jordan. Journal of Arid Environments 40, 15–25.

Kim, S., Sarjoughian, H.S., Elamvazhuthi, V., 2009. DEVS-Suite: A Simulator for Visual Experimentation and Behavior Monitoring, in: High Performance Computing & Simulation Symposium, Proceedings of the Spring Simulation Conference. ACM Press.

Kinzig, A.P., Ryan, P.A., Etienne, M., Allison, H.E., Elmqvist, T., Walker, B.H., 2006. Resilience and regime shifts: assessing cascading effects. Ecology and Society 11.

Kirkby, M.J., 1971. Hillslope process-response models based on the continuity equation, in: Brunsden, D. (Ed.), Hillslopes: Form and Process, Institute of British Geographers Special Publications Series. Oxford, pp. 15–30.

Kohler-Rollefson, I., 1988. The Aftermath of the Levantine Neolithic Revolution in the Light of Ecological and Ethnographic Evidence. paleo 14, 87–93.

Kohler-Rollefson, I., 1992. A model for the development of nomadic pastoralism on the Transjordanian Plateau, in: Yosef, O.B., Khazanov, A. (Eds.), Pastoralism in the Levant: Archaeological Materials in Anthropological Perspectives, Monographs in World Archaeology. Prehistory Press, Madison, pp. 11–18.

Kohler-Rollefson, I., Rollefson, G.O., 1990. The impact of Neolithic subsistence strategies on the environment: The case of 'Ain Ghazal, Jordan, in: Bottema, S., Entjes-Nieborg, Zeist, W. van (Eds.), Man's Role in the Shaping of the Eastern Mediterranean Landscape. Balkema., Rotterdam, pp. 3–14.

Kohler, T.A., 2012. Complex Systems and Archaeology. Santa Fe Institute Working Papers.

Kohler, T.A., Johnson, C.D., Varien, M., Ortman, S., Reynolds, R., Kobti, Z., Cowan, J., Kolm, K., Smith, S., Yap, L., 2007. Settlement ecodynamics in the prehispanic central Mesa Verde region, in: Kohler, T.A., van der Leeuw, S. (Eds.), The Model-Based Archaeology of Socionatural Systems. SAR Press, Santa Fe, pp. 61–104.

Kohler, T.A., Varien, M.D., 2012. Emergence and Collapse of Early Villages: Models of Central Mesa Verde Technology. University of California Press.

Kohler, T., van der Leeuw (Eds.), 2007. The Model-Based Archaeology of Socionatural Systems. School for Advanced Research Press., Santa Fe, NM.

Koriat, A., Goldsmith, M., Pansky, A., 2000. Toward a Psychology of Memory Accuracy. Annual Review of Psychology 51, 481–537.

Kramer, C., 1980. Estimating prehistoric populations: An ethnoarchaeological approach, in: Barrelet, M.T. (Ed.), L'archéologie de l'Iraq: Du Début de L'époque Néolithique à 333 Avant Notre Ère, Perspectives Et Limites de L'interprétation Anthropologiques Des Documents. Colloques Internationaux du CNRS 580, Paris, pp. 315–334.

Kramer, C., 1982. Village Ethnoarchaeology: Rural Iran in Archaeological Perspective. Academic Press, New York.

Krysanova, V., Hattermann, F., Wechsung, F., 2005. Development of the ecohydrological model SWIM for regional impact studies and vulnerability assessment. Hydrological Processes 19, 763–783.

Kuijt, I., 2000a. Life in Neolithic Farming Communities: Social Organization, Identity, and Differentiation. Springer.

Kuijt, I., 2000b. People and Space in Early Agricultural Villages: Exploring Daily Lives, Community Size, and Architecture in the Late Pre-Pottery Neolithic. Journal of Anthropological Archaeology 19, 75–102.

Kuijt, I., 2004. Pre-Pottery Neolithic A and Late Natufian at 'Iraq ed-Dubb, Jordan. Journal of Field Archaeology 29, 291–308.

Kuijt, I., 2008a. The Regeneration of Life. CURR ANTHROPOL 49, 171–197.

Kuijt, I., 2008b. Demography and Storage Systems During the Southern Levantine Neolithic Demographic Transition, in: Bocquet-Appel, J.-P., Bar-Yosef, O. (Eds.), The Neolithic Demographic Transition and Its Consequences. Springer Netherlands, pp. 287–313.

Kuijt, I., 2009. What Do We Really Know about Food Storage, Surplus, and Feasting in Preagricultural Communities? Current Anthropology 50, 641–644.

Kuijt, I., Finlayson, B., 2009. Evidence for food storage and predomestication granaries 11,000 years ago in the Jordan Valley. PNAS 106, 10966–10970.

Kuijt, I., Goring-Morris, N., 2002. Foraging, Farming, and Social Complexity in the Pre-Pottery Neolithic of the Southern Levant: A Review and Synthesis. Journal of World Prehistory 16, 361–440.

Kuijt, I., Mabry, J., Palumbo, G., 1991. Early Neolithic use of upland areas of Wadi El-Yabis : preliminary evidence from the excavations of 'Iraq Ed-Dubb, Jordan. paleo 17, 99–108.

Kupfer, J., Farris, C., 2007. Incorporating spatial non-stationarity of regression coefficients into predictive vegetation models. Landscape Ecology 22, 837–852.

Laland, K.N., Odling-Smee, F.J., Feldman, M.W., 1999. Evolutionary consequences of niche construction and their implications for ecology. Proceedings of the National Academy of Sciences 96, 10242–10247.

Laland, K.N., Odling-Smee, F.J., Feldman, M.W., 2001. Niche construction, ecological inheritance, and cycles of contingency in evolution, in: Oyama, S., Griffiths, P.E., Gray, R.D. (Eds.), Cycles of Contingency: Developmental Systems and Evolution. The MIT Press, Cambridge, pp. 117–126.

Lamberson, P.J., Page, S.E., 2012. Tipping Points. Santa Fe Institute Working Papers.

Lansing, J.S., 2003. Complex adaptive systems. Annual Review of Anthropology 183–204.

Le Houérou, H.N., 1980. The role of browse in the management of natural grazing lands, in: Le Houérou, H.N. (Ed.), Browse in Africa: The Current State of Knowledge. International Livestock Center for Africa, Addis Ababa.

Lilburne, L., Hewitt, A., McIntosh, P., Lynn, I., 1998. GIS-driven models of soil properties in the high country of the south island, in: 10th Colloquium of the Spatial Information Research Centre, University of Otago, New Zealand. pp. 173–180.

Lim, K., Deadman, P.J., Moran, E., Brondizio, E., McCracken, S., 2002. Agent-based simulations of household decision making and land use change near Altamira, Brazil, in: Gimblett, H.R. (Ed.), Integrating Geographic Information Systems and Agent-Based Modeling: Techniques for Simulating Social and Ecological Processes. Oxford University Press, Cary, pp. 277–310.

Lovell, J., Dollfus, G., Kafafi, Z., 2007. The Ceramics of the Late Neolithic and Chalcolithic: Abu Hamid and the Burnished Tradition. paleo 33, 51–76.

Luke, S., Cioffi-Revilla, C., Panait, L., Sullivan, K., Balan, G., 2005. MASON: A multiagent simulation environment. Simulation 81, 517–527.

Maher, L.A., 2000. Analysing Quaternary Deposits: Problems in Determining Particle Size for Palaeosols at an Epipalaeolithic Site in Northern Jordan. York University.

Maher, L.A., 2005. The Epipalaeolithic in Context: Palaeolandscapes and Prehistoric Occupation of Wadi Ziqlab, Northern Jordan (PhD). University of Toronto.

Maher, L.A., 2007. 2005 Excavations at the Geometric Kebaran site of 'Uyun al-Hammam, al-Koura District, northern Jordan. Annual of the Department of Antiquities of Jordan 51, 263–272.

Maher, L.A., 2011. Reconstructing paleolandscapes and prehistoric occupation of Wadi Ziqlab, northern Jordan. Geoarchaeology 26, 649–692.

Maher, L.A., Banning, E.B., 2001. Geoarchaeological Survey in Wadi Ziqlab, Jordan, in: Zayadine, F. (Ed.), Annual of the Department of Antiquities of Jordan. Department of Antiquities of Jordan, Amman, pp. 61–69.

Maher, L.A., Banning, E.B., Chazan, M., 2011. Oasis or mirage? Assessing the role of abrupt climate change in the prehistory of the southern Levant. Cambridge Archaeological Journal 21, 1–29.

Maher, L.A., Löhr, M., Betts, M., Parslow, C., Banning, E.B., 2002. Middle Epipalaeolithic Sites in Wadi Ziqlab, Northern Jordan. Paléorient 27, 5–19.

Maltz, E., Shkolnik, A., 1980. Milk production in the desert: lactation and water economy in the black Bedouin goat. Physiological zoology 53, 12–18.

Marom, N., Bar-Oz, G., 2009. Culling profiles: the indeterminacy of archaeozoological data to survivorship curve modelling of sheep and goat herd maintenance strategies. Journal of Archaeological Science 36, 1184–1187.

Martínez-Casasnovas, J.A., Sánchez-Bosch, I., 2000. Impact assessment of changes in land use/conservation practices on soil erosion in the Penedès-Anoia vineyard region (NE Spain). Soil and Tillage Research 57, 101–106.

Martin, L., Edwards, Y.H., 2007. Fauna from the Natufian and PPNA Cave Site of Iraq ed-Dubb in Highland Jordan. paleo 33, 143–174.

Mavrogenis, A.P., Papachristoforou, C., 1988. Estimation of the energy value of milk and prediction of fat-corrected milk yield in sheep and goats. Small Ruminant Research 1, 229–236.

Mayer, G.R., Sarjoughian, H., 2007. Complexities of Simulating a Hybrid Agent-Landscape Model Using Multi-Formalism Composability, in: Spring Simulation Conference: Agent-Directed Simulation. IEEE Press, Norfolk, Virginia, pp. 161–168.

McBratney, A.B., Mendonca Santos, M.L., Minasny, B., 2003. On digital soil mapping. Geoderma 117, 3–52.

McCall, M.K., 1985. The significance of distance constraints in peasant farming systems with special reference to sub-Saharan Africa. Applied Geography 5, 325–345.

McIntosh, R.J., 1991. Early Urban Clusters in China and Africa: The Arbitration of Social Ambiguity. Journal of Field Archaeology 18, 199–212.

Mcshane, B.B., 2011. A statistical analysis of multiple temperature proxies: Are reconstructions of surface temperatures over the last 1000 years reliable? Ann. Appl. Stat. 5, 5–44.

Meged', S.S., Torkaev, A.N., Egorov, S.V., Storozhuk, S.I., 2008. Milk productivity of breeding sheep of the Altai finewool breed. Russ. Agricult. Sci. 34, 52–54.

Merah, O., Araus, J.L., Souyris, I., Nachit, M.M., Deléens, E., Monneveux, P., 2000. Carbon isotope discrimination: potential interest for grain yield improvement in durum wheat. Durum Wheat Improvement in the Mediterranean Region: New Challenges. Options MeÂditerraneÂennes 40.

Migowski, C., Stein, M., Prasad, S., Negendank, J.F.W., Agnon, A., 2006. Holocene climate variability and cultural evolution in the Near East from the Dead Sea sedimentary record. Quaternary Research 66, 421–431.

Miller, J., Franklin, J., 2002. Modeling the distribution of four vegetation alliances using generalized linear models and classification trees with spatial dependence. Ecological Modelling 157, 227–247.

Miller, J., Franklin, J., Aspinall, R., 2007. Incorporating spatial dependence in predictive vegetation models. Ecological Modelling 202, 225–242.

Miller, J.H., Page, S.E., 2007. Complex adaptive systems: An introduction to computational models of social life. Princeton University Press, Princeton.

Minasny, B., McBratney, A.B., 1999. A rudimentary mechanistic model for soil production and landscape development. Geoderma 90, 3–21.

Minasny, B., McBratney, A.B., 2006. Mechanistic soil-landscape modelling as an approach to developing pedogenetic classifications. Geoderma 133, 138–149.

Mitasova, H., Hofierka, J., Zlocha, M., Iverson, L.R., 1996a. Modelling topographic potential for erosion and deposition using GIS. International Journal of Geographical Information Systems 10, 629–641.

Mitasova, H., Mitas, L., 1993. Interpolation by Regularized Splines with Tension: I. Theory and implementation. Mathematical Geology 25, 641–655.

Mitasova, H., Mitas, L., Brown, W.M., 2001. Multiscale Simulation of Land Use Impact on Soil Erosion and Deposition Patterns, in: Stott, D.E., Mohtar, R.H., Steinhardt, G.C. (Eds.), Sustaining the Global Farm: 10th International Soil Conservation Organization Meeting Held May 24-29, 1999. Purdue University and the USDA-ARS National Soil Erosion Research Laboratory, pp. 1163–1169.

Mitasova, H., Mitas, L., Brown, W.M., Johnston, D., 1996b. Multidimensional Soil Erosion/Deposition Modeling Part III: Process based erosion simulation. Geographic Modeling and Systems Laboratory, University of Illinois at Urban-Champaign.

Mitchell, M., 2009. Complexity: a guided tour. Oxford University Press, Oxford.

Moore, I.D., Burch, G.J., 1986. Physical Basis of the Length-slope Factor in the Universal Soil Loss Equation. Soil Sci Soc Am J 50, 1294–1298.

Muheisen, M., Gebel, H.G., Hannss, C., Neef, R., 1988. Ain Rahub, a new final Natufian and Yarmoukian site near Irbid, in: Garrard, A., Gebel, Hans Georg (Eds.), The Prehistory of Jordan, British Archaeological Reports International Series. BAR, Oxford, pp. 572–502.

Murdock, G.P., White, D.R., 2006. Standard Cross-Cultural Sample: online edition, in: Social Dynamics and Complexity, Working Paper Series. Institute for Mathematical Behavioral Sciences, University of California Irvine, Irvine.

Nablusi, H., Ali, J.M., Abu Nahleh, J., 1993. Sheep and goat management systems in Jordan: traditional and feedlot, a case study. Task Force Documents, Amman.

Naughton-Treves, L., Kammen, D.M., Chapman, C., 2007. Burning biodiversity: Woody biomass use by commercial and subsistence groups in western Uganda's forests. Biological Conservation 134, 232–241.

Neteler, M., Mitasova, H., 2007a. Open Source GIS: A GRASS GIS Approach. The International Series in Engineering and Computer Science: Volume 773. New York.

Neteler, M., Mitasova, H., 2007b. Open Source GIS: A GRASS GIS Approach. The International Series in Engineering and Computer Science: Volume 773. New York.

Ngwa, A.T., Pone, D.K., Mafeni, J.M., 2000. Feed selection and dietary preferences of forage by small ruminants grazing natural pastures in the Sahelian zone of Cameroon. Animal Feed Science and Technology 88, 253 – 266.

Nordblom, T.L., Goodchild, A.V., Shomo, F., 1995. Livestock feeds and mixed farming systems in West Asia and North Africa.

Nyerges, A.E., 1980. Traditional pastoralism: an evolutionary perspective. Expedition 22, 36–41.

Oba, G., 2012. Harnessing pastoralists' indigenous knowledge for rangeland management: three African case studies. Pastoralism: Research, Policy and Practice 2, 1.

Odling-Smee, F.J., Laland, K.N., Feldman, M.W., 2003. Niche construction: the neglected process in evolution (MPB-37). Princeton University Press.

Onori, F., De Bonis, P., Grauso, S., 2006. Soil erosion prediction at the basin scale using the revised universal soil loss equation (RUSLE) in a catchment of Sicily (southern Italy). Environmental Geology 50, 1129–1140.

Osem, Y., Perevolotsky, A., Kigel, J., 2002. Grazing Effect on Diversity of Annual Plant Communities in a Semi-Arid Rangeland: Interactions with Small-Scale Spatial and Temporal Variation in Primary Productivity. The Journal of Ecology 90, 936–946.

Otto-Bliesner, B.L., Schulz, M., 2009. New Methods to Integrate Paleodata Into Climate Models: Data-Assimilation Techniques for Paleoclimate Data; Vienna, Austria, 25 April 2009. Eos Trans. AGU 90, 300.

Pachauri, R.K., 2007. Climate Change 2007: Synthesis Report. Contribution of Working Groups I, II and III to the Fourth Assessment Report of the Intergovernmental Panel on Climate Change. Intergovernmental Panel on Climate Change.

Parker, D.C., Manson, S.M., Janssen, M.A., Hoffmann, M.J., Deadman, P., 2003. Multi-agent systems for the simulation of land-use and land-cover change: a review. Annals of the Association of American Geographers 93, 314–337.

Park, H.-S., Jun, C.-H., 2009. A simple and fast algorithm for K-medoids clustering. Expert Systems with Applications 36, 3336–3341.

Pausas, J.G., 1999a. Response of plant functional types to changes in the fire regime in Mediterranean ecosystems: A simulation approach. Journal of Vegetation Science 10, 717–722.

Pausas, J.G., 1999b. Mediterranean vegetation dynamics: modelling problems and functional types. Plant Ecology 140, 27–39.

Payne, S., 1973. Kill-off patterns in sheep and goats: the mandibles from A\csvan Kale. Anatolian studies 281–303.

Perevolotsky, A., Seligman, N.G., 1998. Role of Grazing in Mediterranean Rangeland Ecosystems. BioScience 48, 1007–1017.

Phillips, S.J., Anderson, R.P., Schapire, R.E., 2006. Maximum entropy modeling of species geographic distributions. Ecological Modelling 190, 231–259.

Phillips, S.J., Dudik, M., Schapire, R., 2010. MaxEnt 3.3. Princeton University.

Prochnow, S.J., Mullins, M., Capello, S.V., Perry, A.F., Ahr, S.W., Westfield, I.T., Fallert, K.L., Gao, S., Hartzell, K.T., Lang, K.R., 2007. Gis Interpolation of Stratigraphic Contact Data to Reconstruct Paleogeography: Deriving a Paleolandscape Model of the Base Zuni Sequence and Subsequent Cretaceous Islands in Central Texas, in: 2007 GSA Denver Annual Meeting.

Pross, J., Kotthoff, U., Müller, U.C., Peyron, O., Dormoy, I., Schmiedl, G., Kalaitzidis, S., Smith, A.M., 2009. Massive perturbation in terrestrial ecosystems of the Eastern Mediterranean region associated with the 8.2 kyr B.P. climatic event. Geology 37, 887–890.

Pswarayi, A., van Eeuwijk, F.A., Ceccarelli, S., Grando, S., Comadran, J., Russell, J.R., Francia, E., Pecchioni, N., Li Destri, O., Akar, T., Al-Yassin, A., Benbelkacem, A., Choumane, W., Karrou, M., Ouabbou, H., Bort, J., Araus, J.L., Molina-Cano, J.L., Thomas, W.T.B., Romagosa, I., 2008. Barley adaptation and improvement in the Mediterranean basin. Plant Breeding 127, 554–560.

Quiroga, A., Funaro, D., Noellemeyer, E., Peinemann, N., 2006. Barley yield response to soil organic matter and texture in the Pampas of Argentina. Soil and Tillage Research 90, 63–68.

Rapp, M., Santa Regina, I., Rico, M., Gallego, H.A., 1999. Biomass, nutrient content, litterfall and nutrient return to the soil in Mediterranean oak forests. Forest Ecology and Management 119, 39–49.

Rawls, W.J., 1983. Estimating soil bulk denisty from particle size analysis and organic matter content. Soil Science 135, 123.

Reddy, A.K.N., 1981. An Indian village agricultural ecosystem- case study of Ungra village, Part II: Discussion. Biomass 1, 77–88.

Redman, C.L., 2005. Resilience Theory in Archaeology. American Anthropologist 107, 70–77.

Redman, C.L., Nelson, M.C., Kinzig, A.P., 2009. The resilience of socioecological landscapes: Lessons from the Hohokam, in: Fisher, C.T., Hill, J.B., Feinman, G.M. (Eds.), The Archaeology of Environmental Change: Socionatural Legacies of Degradation and Resilience. University of Arizona Press, Tucson.

Renard, K.G., Foster, G.R., Weesies, G.A., McCool, D.K., Yoder, D.C., 1997. Predicting soil erosion by water: a guide to conservation planning with the Revised Universal Soil Loss Equation (RUSLE), in: Agriculture Handbook. US Department of Agriculture, Washington, DC, pp. 1–251.

Renard, K.G., Foster, G.R., Weesies, G.A., Porter, J.P., 1991. RUSLE: Revised Universal Soil Loss Equation. Journal of Soil and Water Conservation 46, 30–33.

Renard, K.G., Freimund, J.R., 1994. Using monthly precipitation data to estimate the R-factor in the revised USLE. Journal of Hydrology 157, 287–306.

Řezanková, H., 2009. Cluster analysis and categorical data. Statistika 216–232.

Rhoton, F.E., Lindbo, D.L., 1997. A soil depth approach to soil quality assessment. Journal of soil and water conservation 52, 66–72.

Robinson, S.A., Black, S., Sellwood, B.W., Valdes, P.J., 2006. A review of palaeoclimates and palaeoenvironments in the Levant and Eastern Mediterranean from 25,000 to 5000 years BP: setting the environmental background for the evolution of human civilisation. Quaternary Science Reviews 25, 1517–1541.

Rogers, J.D., Nichols, T., Emmerich, T., Latek, M., Cioffi-Revilla, C., 2012. Modeling scale and variability in human–environmental interactions in Inner Asia. Ecological Modelling.

Rogosic, J., Pfister, J.A., Provenza, F.D., Grbesa, D., 2006. Sheep and goat preference for and nutritional value of Mediterranean maquis shrubs. Small Ruminant Research 64, 169–179.

Rollefson, G.O., 1989. The Aceramic Neolithic of the Southern Levant : The View from ’Ain Ghazal. paleo 15, 135–140.

Rollefson, G.O., 1990. Neolithic Chipped Stone Technology at ’Ain Ghazal, Jordan : The Status of the PPNC Phase. paleo 16, 119–124.

Rollefson, G.O., 1993. The Origins of the Yarmoukian at ’Ain Ghazal. paleo 19, 91–100.

Rollefson, G.O., 1997. Neolithic ’Ayn Ghazal in its landscape. Studies in the History and Archaeology of Jordan 6, 241–244.

Rollefson, G.O., 2001. The Neolithic Period, in: B. MacDonald, R.A., Bienkowski, P., Adams, R. (Eds.), The Archaeology of Jordan, Levantine Archaeology. Sheffield Academic Press, Sheffield, pp. 67–105.

Rollefson, G.O., 2004. A reconsideration of the PPN koine: Cultural diversity and centralities. Neo-Lithics 1, 46–48.

Rollefson, G.O., 2009. Slippery slope: the Late Neolithic rubble layer in the Southern Levant. Neo-Lithics 9.

Rollefson, G.O., Kafafi, Z., 2007. The rediscovery of the Neolithic Period in Jordan, in: Levy, T.E., Daviau, P.M.M., Younker, R.W., Shaer, M. (Eds.), Crossing Jordan. North American Contributions to the Archaeology of Jordan. Equinox Publishing, London, pp. 211–218.

Rollefson, G.O., Kohler-Rollefson, I., 1989. Collapse of Early Neolithic setttlements in the southern Levant, in: People and Culture in Change. Oxford : B.A.R, pp. 73–89.

Rollefson, G.O., Kohler-Rollefson, I., 1992. Early neolithic exploitation patterns in the Levant: Cultural impact on the environment. Population & Environment 13, 243–254.

Rollefson, G.O., Köhler-Rollefson, I., 1993. PPNC adaptations in the first half of the 6th millennium B.C. paleo 19, 33–42.

Rollefson, G.O., Schmandt-Besserat, D., Rose, J. c., 1998. A Decorated Skull from MPPNB ’Ain Ghazal. paleo 24, 99–104.

Rollefson, G.O., Simmons, A.H., Kafafi, Z., 1992. Neolithic Cultures at ’Ain Ghazal, Jordan. Journal of Field Archaeology 19, 443–470.

Ruter, A., Arzt, J., Vavrus, S., Bryson, R.A., Kutzbach, J.E., 2004. Climate and environment of the subtropical and tropical Americas (NH) in the mid-Holocene: comparison of observations with climate model simulations. Quaternary Science Reviews 23, 663–679.

Sadras, V.O., Calvino, P.A., 2001. Quantification of grain yield response to soil depth in soybean, maize, sunflower, and wheat. Agronomy Journal 93, 577–583.

Schacter, D.L., 1999. The seven sins of memory: Insights from psychology and cognitive neuroscience. American Psychologist 54, 182–203.

Scheffer, M., 2009. Critical transitions in nature and society, Princeton Studies in Complexity. Princeton University Press, Princeton.

Scheffer, M., 2010. Complex systems: Foreseeing tipping points. Nature 467, 411–412.

Scheffer, M., Bascompte, J., Brock, W.A., Brovkin, V., Carpenter, S.R., Dakos, V., Held, H., Nes, E.H. van, Rietkerk, M., Sugihara, G., 2009. Early-warning signals for critical transitions. Nature 461, 53–59.

Scheffer, M., Carpenter, S.R., 2003. Catastrophic regime shifts in ecosystems: linking theory to observation. Trends in Ecology & Evolution 18, 648–656.

Scheffer, M., Carpenter, S.R., Lenton, T.M., Bascompte, J., Brock, W., Dakos, V., Koppel, J. van de, Leemput, I.A. van de, Levin, S.A., Nes, E.H. van, Pascual, M., Vandermeer, J., 2012. Anticipating Critical Transitions. Science 338, 344–348.

Schiffer, M.B., 1987. Formation processes of the archaeological record. University of New Mexico Press, Albuquerque.

Schuldenrein, J., 2007. A Reassessment of the holocene stratigraphy of the Wadi Hasa Terrace and Hasa formation, Jordan. Geoarchaeology 22, 559–588.

Schulman, N., 1962. The geology of the central Jordan Valley. Hebrew University (Jerusalem).

Sen, A.R., Santra, A., Karim, S.A., 2004. Carcass yield, composition and meat quality attributes of sheep and goat under semiarid conditions. Meat Science 66, 757–763.

Shoup, J., 1990. Middle Eastern Sheep Production and the Hima System, in: Galaty, J.G., Johnson, D.L. (Eds.), World of Pastoralism: Herding Systems in Comparative Perspective. Guilford Press, New York, pp. 195–215.

Simmons, A.H., 2000. Villages on the edge: Regional settlement change and the end of the Levantine Pre-Pottery Neolithic, in: Kuijt, I. (Ed.), Life in Neolithic Farming Communities: Social Organization, Identiy and Differentiation. Kluwer Academic/Plenum Publishers, New York, pp. 211–230.

Simmons, A.H., 2007. The Neolithic Revolution in the Near East: Transforming the Human Landscape. University of Arizona Press, Tucson.

Simmons, A.H., Rollefson, G.O., Kafafi, Z., Mandel, R.D., Al-Nahar, M., Cooper, J., Kohler-Rollefson, I., Durand, K.R., 2001. Wadi Shu'eib, a large Neolithic community in central Jordan: final report of test investigations. Bulletin, American Schools of Oriental Research 321, 1–39.

Singh, R., Phadke, V.S., 2006. Assessing soil loss by water erosion in Jamni River Basin, Bundelkhand region, India, adopting universal soilloss equation using GIS. Current Science 90, 1431–1435.

Smith, A.B., 1992. Pastoralism in Africa : origins and development ecology. Christopher Hurst ; Ohio University Press, London : Athens :

Smith, M.L., 2006. How Ancient Agriculturalists Managed Yield Fluctuations through Crop Selection and Reliance on Wild Plants: An Example from Central India. Economic Botany 60, 39–48.

Sneh, A., Bartov, Y., Weissbrod, T., Rosensaft, M., 1998. Geological Map of Israel, 1:200,000. Israeli Geological Survey, (4 sheets).

Solomon, S., 2007. Climate change 2007: the physical science basis: contribution of Working Group I to the Fourth Assessment Report of the Intergovernmental Panel on Climate Change. Intergovernmental Panel on Climate Change.

Soto-Berelov, M., 2011. Vegetation Modeling of Holocene Landscapes in the Southern Levant (Ph.D., Geography). Arizona State University, United States -- Arizona.

Spielmann, K.A., Nelson, M., Ingram, S., Peeples, M.A., 2011. Sustainable small-scale agriculture in semi-arid environments. Ecology and Society 16, 26.

Staubwasser, M., Weiss, H., 2006. Holocene climate and cultural evolution in late prehistoric–early historic West Asia. Quaternary Research 66, 372–387.

Stewart, B.A., Woolhiser, D.A., Wischmeier, W.H., Caro, J.H., Frere, M.H., 1975. Control of Water Pollution from Cropland, Volume 1–A Manual for Guideline Development, EPA-600/2-75-026a. US Environmental Protection Agency, Washington D.C.

Stuth, J.W., Kamau, P.N., 1989. Influence of Woody Plant Cover on Dietary Selection by Goats in an Acacia senegal Savanna of East Aifrica. Small Ruminant Research 3, 211–225.

Stuth, J.W., Sheffield, W.J., 1991. Determining Carrying Capacity for Combinations of Livestock, White-tailed Deer and Exotic Ungulates, in: Wildlife Management Handbook. Texas A&M University Department of Wildlife and Fisheries Sciences, College Station, pp. 5–12.

Swarm Development Group, 1999. Swarm. www.swarm.org, Santa Fe.

Tabuti, J.R.S., Dhillion, S.S., Lye, K.A., 2003. Firewood use in Bulamogi County, Uganda: species selection, harvesting and consumption patterns. Biomass and Bioenergy 25, 581–596.

Tachikawa, T., Kaku, M., Iwasaki, A., Gesch, D., Oimoen, M., Zhang, Z., Danielson, J., Krieger, T., Curtis, B., Haase, J., others, 2011. ASTER Global Digital Elevation Model Version 2–Summary of Validation Results August 31, 2011.

Terradas, J., 1992. Mediterranean woody plant growth-forms, biomass and production in the eastern part of the Iberian Peninsula, in: Homage to Ramon Margalef or Why Is There Such Pleasure in Studying Nature. University of Barcelona, Barcelona, pp. 337–349.

Thomson, E.F., 1987. Feeding systems and sheep husbandry in the barley belt of Syria. ICARDA, Aleppo.

Thomson, E.F., Bahhady, F., 1983. Aspects of sheep husbandry systems in Aleppo Province of Northwest Syria, Farming systems program research reports. ICARDA, Aleppo.

Thomson, E.F., Bahhady, F., Termanini, A., Mokbel, M., 1986. Availability of home-produced wheat, milk products and meat to sheep-owning families at the cultivated margin of the NW Syrian steppe. Ecology of Food and Nutrition 19, 113–121.

Tucker, G., Lancaster, S., Gasparini, N., Bras, R., 2001. The Channel-Hillslope Integrated Landscape Development model (CHILD), Landscape erosion and evolution modeling. Kluwer Academic/Plenum Publishers, New York, NY.

Turner, M.G., Baker, W.L., Peterson, C.J., Peet, R.K., 1998. Factors influencing succession: lessons from large, infrequent natural disturbances. Ecosystems 1, 511–523.

Tversky, A., Kahneman, D., 1974. Judgment Under Uncertainty: Heuristics and Biases. Science 185, 1124–1131.

Twiss, K.C., 2007a. The Neolithic of the southern Levant. Evolutionary Anthropology: Issues, News, and Reviews 16, 24–35.

Twiss, K.C., 2007b. The Zooarchaeology of Tel Tif'dan (Wadi Fidan 001), Southern Jordan. Paléorient 33, 127–145.

Ullah, I.I.T., 2009. Within-room spatial analysis of activity areas at Late Neolithic Tabaqat Al-Buma, Wadi Ziqlab, Al Koura, Jordan, in: Studies in the History and Archaeology of Jordan, X. The Department of Antiquities of Jordan, Amman, pp. 87–95.

Ullah, I.I.T., 2011. A GIS method for assessing the zone of human-environmental impact around archaeological sites: a test case from the Late Neolithic of Wadi Ziqlâb, Jordan. Journal of Archaeological Science 38, 623–632.

Ullah, I.I.T., 2012. Particles from the past: microarchaeologial spatial analysis of ancient house floors, in: Parker, B.J., Foster, C.P. (Eds.), New Perspectives in Household Archaeology. Eisenbrauns, Winowna Lake, pp. 123–138.

Ullah, I.I.T., Bergin, S.M., 2012. Modeling the Consequences of Village Site Location: Least Cost Path Modeling in a Coupled GIS and Agent-Based Model of Village Agropastoralism in Eastern Spain, in: White, D.A., Surface-Evans, S.L. (Eds.), Least Cost Analysis of Social Landscapes: Archaeological Case Studies. University of Utah Press, Salt Lake City, pp. 155–173.

USDA, 2010. Nutrient Data Laboratory [WWW Document]. URL http://www.ars.usda.gov/main/site_main.htm?modecode=12-35-45-00 (accessed 12.9.10).

USDA, N.R.C. services, 2012. Soil Texture Calculator.

Usher, M.B., 1981. Modelling ecological succession, with particular reference to Markovian models. Plant Ecology 46-47, 11–18.

Van Dyke Parunak, H., Savit, R., Riolo, R., 1998. Agent-Based Modeling vs. Equation-Based Modeling: A Case Study and Users' Guide, in: Sichman, J., Conte, R., Gilbert, N. (Eds.), Multi-Agent Systems and Agent-Based Simulation, Lecture Notes in Computer Science. Springer Berlin / Heidelberg, pp. 277–283.

Van Nes, E.H., Scheffer, M., 2005. Implications of Spatial Heterogeneity for Catastrophic Regime Shifts in Ecosystems. Ecology 86, 1797–1807.

Varien, M.D., Ortman, S.G., Kohler, T.A., Glowacki, D.M., Johnson, C.D., 2007. Historical ecology in the Mesa Verde region: Results from the village ecodynamics project. American Antiquity 273–299.

Verhoeven, M., 2002. Transformations of society : the changing role of ritual and symbolism in the PPNB and the PN in the Levant, Syria and south-east Anatolia. paleo 28, 5–13.

Vigne, J.-D., 2011. The origins of animal domestication and husbandry: A major change in the history of humanity and the biosphere. Comptes Rendus Biologies 334, 171–181.

Vigne, J.-D., Helmer, D., 2007. Was milk a "secondary product" in the Old World Neolithisation process ? Its role in the domestication of cattle, sheep and goats. Anthropozoologica 42, 9–40.

Volohonsky, H., Kaplanovsky, A., Serruya, S., 1983. Storms on Lake Kinneret: Observations and mathematical model. Ecological Modelling 18, 141–153.

Wagner, W., 2011. Groundwater in the arab middle east. Springer Verlag.

Wainwright, J., 2008. Can modelling enable us to understand the rôle of humans in landscape evolution? Geoforum 39, 659–674.

Walker, B., Gunderson, L., Kinzig, A., Folke, C., Carpenter, S., Schultz, L., 2006. A Handful of Heuristics and Some Propositions for Understanding Resilience in Social-Ecological Systems. Ecology and Society 11, 13.

Warren, S.D., Mitasova, H., Hohmann, M.G., Landsberger, S., Skander, F.Y., Ruzycki, T.S., Senseman, G.M., 2005. Validation of a 3-D enhancement of the Universal Soil Loss Equation for preediction of soil erosion and sediment deposition. Catena 64, 281–296.

Wasse, A., 2002. Final results of an analysis of the sheep and goat bones from Ain Ghazal, Jordan. Levant 34, 59–82.

Watson, P.J., 1979. Archaeological Ethnography in Western Iran, Viking Fund Publications in Anthropology. University of Arizona Press, Tucson.

Weninger, B., Alram-Stern, E., Bauer, E., Clare, L., Danzeglocke, U., Jöris, O., Kubatzki, C., Rollefson, G., Todorova, H., van Andel, T., 2006. Climate forcing due to the 8200 cal yr BP event observed at Early Neolithic sites in the eastern Mediterranean. Quaternary Research 66, 401–420.

Weninger, B., Clare, L., Rohling, E.J., Bar-Yosef, O., Böhner, U., Budja, M., Bundschuh, M., Feurdean, A., Gebel, H.G., Jöris, O., 2009. The impact of rapid climate change on prehistoric societies during the Holocene in the Eastern Mediterranean. Documenta Praehistorica 36, 7–59.

Wilensky, U., 1999. NetLogo. Center for Connected Learning and Computer-Based Modeling, Northwestern University, Evanston, http://ccl.northwestern.edu/netlogo/.

Wilkinson, T.J., Gibson, M., Christiansen, J.H., Widell, M., Schloen, D., Kouchoukos, N., Woods, C., Sanders, J., Simumich, K.-L., Altaweel, M.R., Ur, J.A., Hritz, C., Lauinger, J., Paulette, T., Tenney, J., 2007. Modeling Settlement Systems in a Dynamic Environment, in: Kohler, T.A., van der Leeuw, S. (Eds.), The Model-Based Archaeology of Socionatural Systems. SAR Press, Santa Fe, pp. 175–208.

Wilk, R.R., Rathje, W.L., 1982. Household archaeology. American behavioral scientist 25, 617.

Wilson, J.P., 2012. Digital terrain modeling. Geomorphology 137, 107–121.

Wilson, R., Frank, D., Topham, J., Nicolussi, K., Esper, J., 2005. Spatial reconstruction of summer temperatures in Central Europe for the last 500 years using annually resolved proxy records: problems and opportunities. Boreas 34, 490–497.

Wilson, R.T., 1982. Husbandry, nutrition and productivity of goats and sheep in tropical Africa, in: Gatenby, R.M., Trail, J.C.. (Eds.), Small Ruminant Breed Productivity in Africa. International Livestock Center for Africa, ILCA, Addis Ababa.

Wischmeier, W.H., 1976. Use and Misuse of the Universal Soil Loss Equation. Journal of Soil and Water Conservation 31, 5–9.

Wischmeier, W.H., Johnson, C.B., Cross, B.V., 1971. A Soil Erodibility Nomograph for Farmland and Construction Sites. Journal of Soil and Water Conservation 26, 189–92.

Wischmeier, W.H., Smith, D.D., 1978. Predicting Rainfall-Erosion Losses - A Guide to Conservation Planning, USDA Agriculture Handbook.

Wolfram, S., 2002. A new kind of science.

Wong, M.T.F., Asseng, S., 2007. Yield and environmental benefits of ameliorating subsoil constraints under variable rainfall in a Mediterranean environment. Plant Soil 297, 29–42.

World Meteorological Organization, National Climatic Data Center (U.S.), 1998. 1961-1990 global climate normals.

Wright, K.I., 2000. The social origins of cooking and dining in early villages of Western Asia, in: Proceedings of the Prehistoric Society. pp. 89–122.

Wylie, A., 1985. The Reaction against Analogy. Advances in Archaeological Method and Theory 8, 63–111.

Yellen, J.E., 1977. Archaeological Approaches to the Present: Models for Reconstructing the Past. Academic Press, New York.

Zeder, M.A., 2008. Domestication and early agriculture in the Mediterranean Basin: Origins, diffusion, and impact. Proceedings of the National Academy of Sciences 105, 11597.

Zielhofer, C., Clare, L., Rollefson, G., Wächter, S., Hoffmeister, D., Bareth, G., Roettig, C., Bullmann, H., Schneider, B., Berke, H., Weninger, B., 2012. The decline of the early Neolithic population center of ʾAin Ghazal and corresponding earth-surface processes, Jordan Rift Valley. Quaternary Research.

APPENDIX A

SUBSIDIARY FORMULAS AND MODELING ROUTINES

A.1. Estimating Stream Depths

Depth of flow is difficult to estimate accurately because it is the depth of flowing water in a cell at any moment, and changes over the course of a rainfall event (Bledsoe, 2002). Iterative cellular automata routines, such as SIMWE (see Section 4.1.2, above), provide the most accurate way to estimate *h* in a GIS, but the are computationally very expensive, and thus impractical for long-term iterated landscape evolution simulations (such as that employed by the MML) where minimization of run-time length is important. Therefore MML estimates *h* in each cell from an idealized "unit hydrograph" for that cell, which is a graphical representation of flow depth over time during a simulation interval. Although a real unit hydrograph curve may take one of many different shapes (e.g., skewed, bimodal, etc.) the idealized unit hydrograph for a cell in the MML is assumed to be normally distributed with a base equal to the length of the time of a hydrologic event (such as a storm). The area under the curve is the total accumulated vertical meters of runoff from the event passing through the cell over the entire hydrological event, and the apex of the curve represents the the peak flow depth during the event (Figure A.1), which is a good estimation of *h*. Thus, *h* can be estimated according to the following function:

Eq. A.1
$$h = \frac{R_e \cdot A}{0.595 \cdot t}$$

In this equation, R_e [m] is the excess rainfall (meters precipitation minus infiltration) during the hydrologic event, and A [m^2] is the upslope accumulated area so that $R_e \cdot A$ is the accumulated runoff (vertical meters of water) that passed over the cell during the simulation interval[108]. The value of t is the number of "hydrologic instants" in the simulation interval. The hydrologic instant is the time it takes water to cross one cell of a raster DEM, which can be determined by multiplying the average velocity of flowing water in the watershed (e.g., as derived with Manning's equation) by the cell resolution.

108*A* is calculated by the GRASS hydrological modeling module "r.watershed". See Chapter 4, Section 4.5.2 for more information about the calculation of accumulated runoff

A.2. Determining Breakpoints in Net Accumulated Flow for Process Phase Changes

The location for surface process phase changes is based on the determination of series of breakpoints in net accumulated flow (A), which is the accumulated flow of all upslope precipitation minus infiltration (see Chapter 4, section 4.5.2). A series of three breakpoints are needed: on between diffusive soil creep and overland flow, the second between overland flow and rilling/gullying, and the third between rilling/gullying and channelized stream flow.

The first two breakpoints are determined by plotting A against local topographic curvatures in the direction of slope – the profile curvature (pc) – for each cell. Positive values of pc indicate a marked increase in slope (a convex profile), negative values indicate a marked decrease in slope (a concave profile), while values of $pc \sim 0$ represent cells where there is little change in slope. This is shown in Figure A.2a with A on the y-axis and pc on the x-axis. Drainage divides have little accumulation and little change of slope, plotting near 0 on the x and y axes; hillslopes also have little change in slope, but have higher accumulation, plotting near 0 on the x-axis but higher on the y-axis. The transition between the drainage divide and hillslopes has the maximum convex curvature (positive pc) and relatively low values of A, while the transition between hillslopes and gully heads at the base of slopes has concave curvature (negative pc) and higher accumulation values. Hence, for a given landscape and hydrologic regime, the value of A for the maximum value of pc is a good estimate for the transition from equation diffusion to USPED with exponents m and n for overland flow (sheetwash), and the value of A for the minimum value of pc is a good estimate for the transition from sheetwash to USPED with exponents m and n for rill/gully flow (Figure A.2a).

In a similar way, A can be plotted against the tangential curvature (tc) of each cell – the curvature perpendicular to the direction of slope – to identify the accumulation value for the transition from USPED to a shear-stress equation for channelized flow. The beginning of channelized flow can be identified as the location where very negative values of tc (concave) are associated with high values of A. Slightly negative values of tc that are associated with lower values of A represent the larger gullies and gully-heads (i.e., that occur higher in the drainage network than the real stream channels), and even higher values of A where tc has decreased indicate a widening channel carrying more water (Figure A.2b). Figure A.3 shows the locations of the transition points identified in Figure A.2 on the DEM for which they were derived.

A.3. The Adaptive "Soft-Knee" Net-dz Smoothing Algorithm

The smoothing procedure used to remove "spikes" from the net dz map is carried out over three stages. In the first stage, global univariate statistics are separately calculated for all values in the dz map below 0 (i.e., for all areas of net

erosion), and all areas in the *dz* map above 0 (i.e., for all areas of net deposition). Then, the routine identifies values from the 1st quartile of erosion to the minimum (i.e., the very large negative numbers) and values from the 3rd quartile of deposition to the maximum (i.e., the very large positive numbers). The numerical values in these areas are then linearly rescaled from the 1st quartile to the 1st percentile and the 3rd quartile to the 99th percentile respectively. Unlike "brick wall" single threshold limiting, this "soft-knee" style of limiting retains some of the original scaling at the ends of the distribution, but brings the highest values (i.e., the "spikes") into the range of a normally distributed dataset.

A.4. Calculation of Soil-Depth "Rates"

The soil depth "rate" maps are created in a two-stage process, illustrated in Figure A.4. First, the relationship between the slope of a cell and the base-line soil-depth is established using a "graphing function", which is a method that uses sequential linear equations to approximate the equation of a more complex curve. The segments of the linear graphing function are tied to breakpoints (Figure A.4, points a, b, c, and d), which control the shape of the curve they approximate, in this case, the base-line relationship between the topographic slope in the neighborhood of the raster cell and soil-depths. In the *r.soildepth.py* script, the modeler may adjust these breakpoints to suite the particular landscape in question. Once this baseline relationship is established, a localized "offset" of the soil depth curve is calculated based on the amount and type of average topographic curvature (i.e., the average of the profile and tangential curvatures) is present in the neighborhood of the raster cell. As the local curvature becomes increasingly concave, the curve is offset in the positive direction until the maximum positive offset is reached (points +b', +c', and +d' in Figure A.4), or, as the local curvature becomes increasingly concave, the curve is offset in the negative direction until the maximum negative offset is reached (points -a', -b', and -c' in Figure A.4). The relationship between the numerical amount of curvature and the numerical amount of offset is defined by a simple linear function, which can be adjusted by the modeler depending upon the particular landscape in question (which essentially changes the locations of +b', +c', +d', -a', -b', and -c' in Figure A.4). Once the localized "soil depth rate curve" is established for all cells in the input raster map, the "*r.soildepth.py*" script then converts these values to actual units of soil depth (meters of sediment) through a simple linear transformation. This transformation essentially sets the endpoints of the curve (points "a" and "d" in Figure A.4) to the actual maximum and minimum soil depths observed in the project area, and then estimates the depth of the particular raster cell based upon its position along the curve.

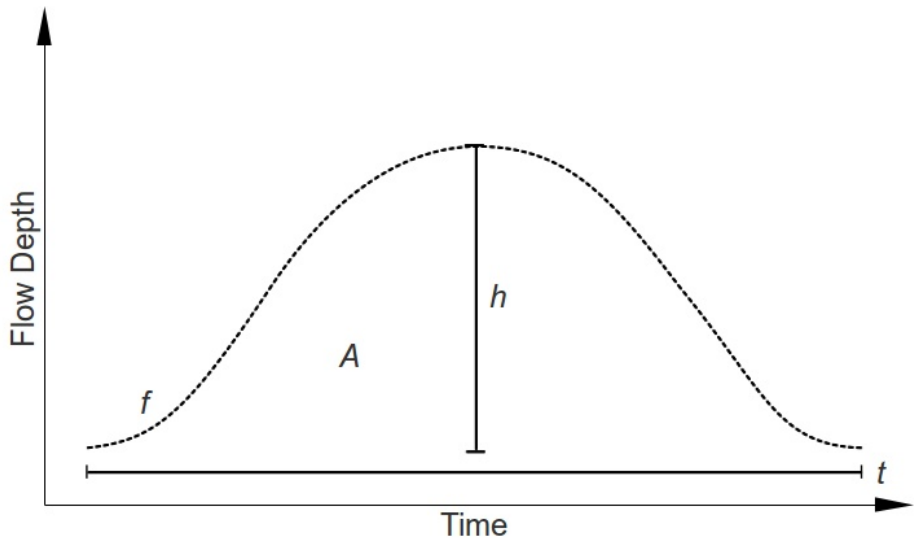

Fig. A.1. Method of approximation of peak flow depth from an idealize unit hydrograph. Dashed line "f" is flow depth over the course of a storm of time “t”. The area “A' under the curve is the total accumulated flow, and the length of the line at its peak, is the peak flow depth “h”.

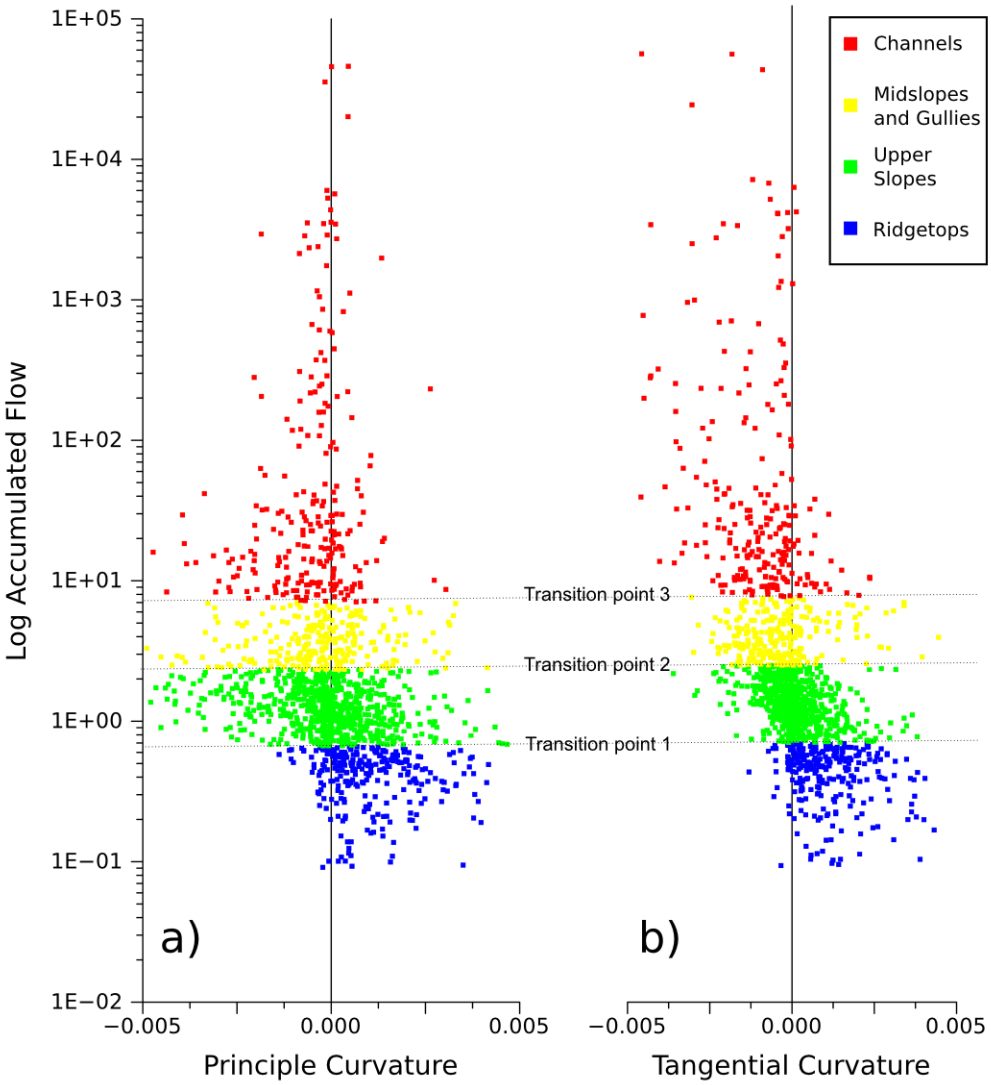

Fig. A.2. Graphical display of profile curvature and tangential curvature versus log flow accumulation.

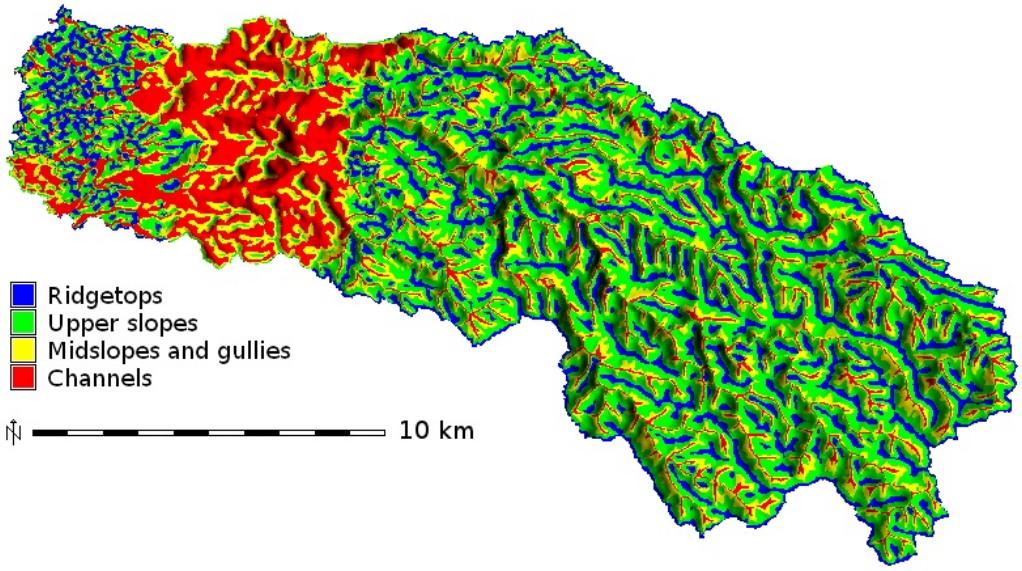

Fig. A.3. Map showing the locations of surface process transitions as determined from the graphs in figure A.2.

APPENDIX B

A GEOARCHAEOLOGICAL GAZETTEER OF THE WADI ZIQLAB REGION

B.1. Geoarchaeological Survey of Wadi-Ziqlab

In Wadi Ziqlab, the wadi-bottom and the lower and middle terraces were surveyed on foot from its outlet to about 1km beyond the confluence of the two main tributaries, Wadi ed-Dimna and Wadi 'Ain Zubiya. Portions of the upper regions of the Wadi, especially around the hilltop town of Tubna, were also visited, although contiguous survey of this region was not carried out. The purpose of this work was to better understand the relationship between the lower and middle terraces and the active channel in all parts of the Wadi, and to gain an understanding of the depth of soils/sediments on different landforms in the Wadi and the areas of the plateau and uplands associated with the Wadi.

Figure B.1 shows an overview of part of Wadi 'Ain Zubiya, above its confluence with Wadi ed-Dimna. The wadi is a seasonally inundated wash at this point, and the most prominent geomporphological features in this portion of the greater Ziqlab drainage are a series of small alluvial terraces right along the drainage channel in the narrow wadi-bottom (Figure B.1). These small terraces are actually Maher's "middle terrace", but are still partially fluvially connected to the current fluvial regime in this portion of the Wadi, mainly through lateral erosion (Figure B.2). Exposed profiles of this terrace show about 50 cm of interbedded alluvial pebbles, gravels, and sands with silt lenses, overlain by another 50 cm of lightly reworked colluvium with larger cobbles and boulders in a matrix of red clays and silts (Figure B.1). The color and consistency of the colluvial fines suggest a dual origin in the grey slope Rendzinas and the red Terra Rossa soils of the plateau region. Fluvial and colluvial processes seemed to be well balanced in this portion of the Wadi, resulting in minimal Holocene colluviation on terraces, and only minor Holocene channel incision. It is likely that much of the colluvial material that is deposited in this portion of the Wadi is incorporated into the sediment supply of the channel during winter storm events, and stored as a series of channel bars. These bars are the only equivalent of the lower terrace in this region. Also present in this portion of the Wadi are a series of small bench-terraces which occur intermittently at about 10 to 20 m above the current channel, occurring most frequently at the inside of bends in the wadi. These are Maher's "upper terrace", and many of them have been completely depleted of surface sediments, and are evidenced only by a mild break in the slope of the wadi walls (Figure B.2). The slopes above the upper terrace are covered in colluvium, and I found remnant, filled-in gully channels exposed in a road cut about half way up the slope (Figure B.3). This suggests that colluvial activity on the slope has alternated with gully erosion over time, but it is unclear if these gullies were active during the Neolithic.

At the confluence of Wadi 'Ain Zubiya and Wadi ed-Dimna (see Chapter 2, Figure 2.5), the channel becomes mildly incised, with banks of between 2-5 m. The lower terraces become more pronounced, and the system tends toward net erosion in this section of the Wadi. The middle terraces are now thickly mantled by colluvium, and several archaeological sites are preserved on them in this

portion of the Wadi, notably the Late Neolithic sites of Tabaqat al-Bûma and al Aqaba, and the Epipaleolithic site of 'Uyun al-Hammam (see Chapter 2). Excavation at these sites indicates that the red Epipaleolithic paleosol is present on most of the middle terrace remnants in this section of the wadi (Maher, 2011), and this was confirmed at several exposures (road cuts and agricultural terrace cuts) in this section of the Wadi (Figure B.5).

Below 'Uyun al-Hammam, the Wadi-bottom broadens significantly, the channel is no longer incised, and the channel itself is also much wider than in the upper portions of the Wadi system (Figure B.6). 'Uyun al-Hammam is an active spring, but is currently being pumped by the town of Dayr Abu Sa'id, and though water no longer flows perennially in this section of the Wadi, it certainly did so before the pumping began in modern times. The lower terrace is still in active connection with the channel, but it appears in larger sections. The middle terraces are now quite large and broad (Figure B.6), but retain similar bedding character to the lower terraces in the upper reaches of the wadi (Figure B.7). Portions of the middle terrace are being actively eroded by bank-undercut in this section of the Wadi, which has also led to large-scale stepped-slumping of the eroded edges of these terraces (Figure B.8). mass-wasting occurs very frequently on the slopes in this portion of the wadi, and there is a broad “piedmont” of colluvium at the base of these slopes in many parts of this portion of the Wadi, and can be seen directly overlaying the middle terrace in many cutbanks (Figure B.9). The Epipaleolithic paleosol can be also seen in many of the cutbanks of the middle terrace, sometimes overlain by massive amounts of Holocene colluvium (Figure B.10), and in some places, reworked deposits clearly derived from the paleosol occur in larger alluvial profiles (Figure B.11). Several large and sometimes cross-cutting rotational slumps are evident in this portion of the wadi, and some appear to be quite recent (Figure B.12). Rilling/gullying and associated translational sliding is also very common (Figures B.12 and B.13)

After almost 4 km, the wadi-bottom narrows again and, although the channel is not greatly incised in this section, it occupies the entirety of the wadi-bottom. The naturally flowing perennial spring of 'Ain Jahjah adds its waters to the Wadi about 1 km after the narrowing and, from this point onward, water flows in the wadi channel all year round. The upper of the two lower knick points occurs about 500 m past 'Ain Jahjah, forming a beautiful waterfall encrusted with travertines (Figure B.14). A smaller tributary wadi joins the main channel just past the 'Ain Jahjah knick point, and the site of Tell Rakkan I is located on the small promontory formed by this confluence (See Chapter 2, Figure 2.4). The Tell Rakkan promontory is also a remnant of the middle terrace, and, like other middle terrace remnants in this section of the Wadi, is covered by a substantial layer of colluvium (Figure B.15).

Below the 'Ain Jahjah knickpoint, the channel becomes very incised (Figure B.16), and the lower terraces are again mostly represented as sand and gravel bars, and the channel seems to be actively downcutting into bedrock in several areas. The middle terrace remnants are suspended perhaps 50-100 m

above the active channel, and are covered by thick deposits of colluvium. Excavations at the LN site of al-Basatîn, located on one of the middle terrace remnants in this section of the wadi, did not encounter the red paleosol, but the presence of small quantities of Epipaleolithic artifacts (Gibbs et al., 2006) at the site suggests that it does exist here too, but is likely very deeply buried. The modern surface of the al-Basatîn terrace is fairly steep: typically above 15 degrees, and approaching 30 degrees in its upper portions. Neolithic cobble surfaces discovered at the site (Banning et al., 2003, 2002; Gibbs et al., 2006) are relatively level, suggesting the terrace surface was flatter in the Neolithic. A ~2-meter deep geological sounding excavated on the upper portion of the terrace revealed that the colluvial deposits are at least that deep, and are likely several meters deeper. The buried remnants of ancient rills and gullies are preserved within the colluvium. Several of these ancient rills had cut into archaeological layers at the site, and could be traced horizontally for up to 30 m as they crossed through several of the excavation trenches (Figure B.17). Thus, it seems that, while colluviation at this location was likely fairly constant throughout the Holocene, there were episodes of increased fluvial rilling and gullying that occurred here some point after the Neolithic period.

The lowest and final knick point occurs about 1.7 km downstream from the 'Ain Jahjah knick point. This knick point is also marked by a magnificent waterfall, also shrouded in travertines. In 2004, the waterfall at this knick point had two tiers, first falling about 10 m over and into a small travertine cave, before falling another 5 m into a wide pool (Figure B.18, left side). By 2006, the cave had collapsed, and the head of the waterfall had retreated several meters upstream (Figure B.18, right side), confirming that headward channel incision at the knick points is still active, and is proceeding at a fairly rapid rate. Below this final knick point, for the remaining 3 km before its outlet into the Jordan Valley, the Wadi is at its most incised. Extensive remnants of the middle terrace exist along the northern edge of the wadi for about a kilometer below the knick point, but are stranded at least 60-80 m above the current channel. The lowest two kilometers of this section of the Wadi and the former Wadi-mouth are now covered by an artificial lake that forms behind a dam built in the 1960's, but apparently there were extensive sand and gravel delta deposits in this section of the wadi (Fisher et al., 1966). From the Wadi-mouth, the channel meanders across the floor of the Jordan Valley, flowing past the Chalcolithic site of Tell Fendi, until it empties into the Jordan River. In this section the channel margins are defined by levies covered in riparian vegetation, and surrounded by silty overbank deposits.

B.2. Geoarchaeological Survey of Wadi Tayyiba

A 4 km section of the middle and lower Wadi Tayyiba drainage—from the town of At-Tayyiba to the unexcavated Neolithic site of WT-4 (about 3 km from the outlet)—was surveyed mainly with pedestrian methods. The main purpose of the survey was to obtain GPS location information for the lower knick points in

Wadi Tayyiba, to study the WT-4 terrace landform noted in the 2000 geoarchaeological survey of the Wadi, and to assess the general terrace sequence in the Wadi. Although quite a bit narrower and deeper than the middle section of Wadi Ziqlab, there are some similarities between the two wadis. Tayyiba's wadi bottom is a more V-shaped in this section than is the U-shaped bottom of Ziqlab (Figure B.19), but, like Ziqlab, there is a "middle terrace" that seems to date from the Early to Middle Holocene. The remnants of this terrace are in a similar geomorphological context with regard to the current active channel (3-10 m above it) as can be seen in Figure B.20. Also like Ziqlab, this portion of the Wadi is currently a seasonally dry stream bed[109], and has an equivlaent "lower terrace", that is mainly composed of channel bars and spits. There may be some remnants of a highly eroded "upper terrace" in Tayyiba but, if it exists at all, it is rare, shallow, and difficult to differentiate from other breaks in slope on the Wadi flanks.

As in Wadi Ziqlab, the lower two knick points occur below the level of the currently-flowing perennial springs. Although the upper of the two Tayyiba knick points is shallower than the 'Ain Jahjah knick point in Ziqlab, it nevertheless marks the point of the same notable change in character of the Tayyiba drainage that occurs in the Ziqlab drainage; after this knick point it becomes moderately incised with perennial stream flow from a spring that bubbles up very close to the top of the knick point. The lower knick point is quite a bit steeper, and this was taken advantage of in the Ottoman period by the construction of a water driven mill (Figure B.21). The Wadi becomes quite deeply incised past this point, and access to the wadi-bottom from the middle terrace is very restricted (Figure B.22).

Interestingly, WT-4, the only known Neolithic site in Wadi Tayyiba (dated only by surface finds), is located in this lower region of the Wadi at a similar distance from the Wadi's outlet as Tell Rakkan I in Wadi Ziqlab. Similarly to Tell Rakkan I, WT-4 is situated on a hanging terrace framed by the confluence of a smaller tributary wadi that feeds from the north into the main Tayyiba drainage (Figure B.23). The WT-4 terraces is quite large (15 ha), and a very long north-south bulldozer cut has exposed a stratigraphic sequence along one of its edges (see Chapter 2, Figure 2.9). Interestingly, the strata are dipping to the north (i.e., away from the main Tayyiba drainage and against the direction of flow from the tributary wadi) at a 25-15 degree angle (Figure B.24). The stratigraphically lowest portion of the exposed profile appears at the southern end of the bulldozer cut, and consists of several 10-50 cm thick bands of greyish and buff colluvium with rounded to subangular pebbles and cobbles (Figure B.24). These layers are cut by a small normal fault, with an offset of about 65 cm, and a fault plane trending roughly east-west (i.e., perpendicular to the dip of the strata, and parallel with the flow of the Wadi) (Figure 2.24). Stratigraphically above these layers is a 3-4 m thick layer of red silts with abundant archaeological material (likely dating to the

109Although it likely was perennial in the past, before extensive groundwater pumping by the nearby town of at-Tayyiba.

Neolithic). There is a marked unconformity at the upper bound of this archaeological layer, which is topped by a massive layer of very lightly bedded tan silts with isolated cobbles and pebbles, which occupies the remainder of the very large exposed section. The severe "backwards" dip of all the layers suggests that this "terrace" may actually be a very large ancient rotational earth slump, of the type described by Field and Banning (1998). This hypothesis is supported by presence of microfaulting at the "toe" of the formation, and by the overall shape of the landform as seen on CORONA and GeoEye imagery (Figure B.23). The slump may have originally been a hanging alluvial terrace (perhaps the middle terrace?), left stranded and vulnerable to mass movement after the incision of the Tayyiba drainage in this section of the Wadi, which today is about 30-40 m below the edge of the terrace. The unconformal boundary of the archaeological layer with the massive silts suggests a period of post-Neolithic erosion of the surface of the ancient terrace, likely due to increased outwash from the small tributary wadi. This may have led to increased saturation, which induced the slump to occur. The slump would have created a "sediment trap", capturing silts carried by outwash from the small tributary. This would explain the accumulation of the massive silts behind the bedded front portion of the formation. Finally, an examination of the CORONA and GeoEye imagery (Figure B.23) suggests that it is also possible that the slump created a natural damn in the main Tayyiba channel[110], perhaps creating a small lake in this section of the Wadi, which may have been an attractive natural feature for later occupants of the region.

B.3. Geoarchaeological Survey of Wadi Abu Ziad

Wadi Abu Ziad differs from the previous two Wadis in that it is entirely located within the plateau region, and does not transgress into the uplands. There are also no knick points in Wadi Abu Ziad, and there is a relative lack of small alluvial terraces along most of the length of the Wadi. The Wadi has a more V-shaped profile than the other two wadis (Figure B.25), which likely has to do with two geomorphological aspects of the Wadi itself. Firstly the short traverse of the Wadi means that it has a relatively steeper fall from source to outlet, and thus is more likely to experience high-energy, erosive flow along its entire length. Thus, there was little chance for substantial alluvation to occur in the wadi-bottom. Secondly, one of the main tributaries of the Wadi sources at a high-flowing perennial spring, which is now located directly beneath the road just north of the main Masjid in the center of the town of Dayr Abu Sayeed, and which now supplies most of that town's water needs. The continual outflow from this spring, combined with the steep descent of the wadi channel, would have further exacerbated downcutting.

Another interesting feature of Wadi Abu Ziad is the presence of multiple types of tool-quality flint. Kadowaki et al. (2008) have identified two sources of

110It is also likely that a natural damn of this sort also occurred near the 'Ain Jahjah knick point in Wadi Ziqlab, and another in the upper part of Wadi Quseiba to the north of Wadi Tayyiba.

flint in Wadi Abu Ziad. The first is a band of fine- to medium-quality pinkish grey flint of the kind also appearing in outcrops in Wadi Ziqlab. In Abu Ziad, the main outcrop of this flint occurs in the lower stretch of the Wadi opposite one of the perennial springs ('Ain Beidah) near the Bronze Age site of 'Ain Beidah (see Chapter 2, Figure 2.2). The hillside where this outcrop occurs is scarred by half-moon-shaped quarry diggings (Figure B.26) that are likely contemporaneous with the site of 'Ain Beidah, but flint could have also been quarried there in the Neolithic. The second flint source identified by Kadowaki et al. (2008) is located a few hundred meters upstream from 'Ain Beidha (see map in Chapter 2, Figure 2.2), and is a source of fine-grained, lustrous, chocolate-brown, flint in nodule form. This type of fine-grained flint is required in order to make more technologically complex tool-forms, such as sickle-elements made on blades (Kadowaki, 2007).

It is only near the Wadi's outlet to the Jordan Valley that it widens sufficiently for alluviation to occur, and for terraces to develop. Thus, the main geoarchaeological work conducted in Wadi Abu Ziad took place at a large, stream-cut terrace riser on the south bank of the Wadi (Figure B.27), almost directly opposite the Bronze age site of 'Ain Beidha located on another small terrace on the northern side of the Wadi. This stream cut exposed roughly 5 m of alluvial deposits, grading into another overlaying 5-10 m of colluvium (Figure B.28). Close to the bottom of this stratigraphic sequence is a high-energy alluvial stratum composed of large imbricated cobbles, bounded below and above by thin fine-grained, low-energy alluvial layers that contained large amounts of organic materials and charcoal (Figure B.29). The upper alluvial layer also contained flints of indeterminate age or provenience. Radiocarbon samples collected from the low-energy organic-rich alluvial layers date the lower alluvial stratum at 20,550 (±410) cal BP, and the upper alluvial stratum 16,365 (±455) cal BP, suggesting that, in Wadi Abu Ziad, there were alternating periods of high- and low-energy alluviation in the Epipaleolithic. These layers thus predate the unconformity in Wadi Ziqlab, which Maher places some time between 14,600 and 11,500 cal BP (Maher, 2011, 2005), and, although it is impossible to be certain, the high charcoal content of the low-energy layers may relate to human alteration of the land-cover via burning in this early period, and which may have some implications for the causes of erosion at the end of this period.

Fig B.1. Upper section of Wadi 'Ayn Zubia. Arrow points to a good example of the middle terrace in this section of the Wadi.

Fig B.2. Cutbank into a middle terrace remnant in the Upper Ziqlab, showing the stratigraphy of the terrace.

Fig B.3. An example of a remnant of the upper terrace in the Upper Ziqlab region.

Fig B.4. A filled gully on the slopes of the Upper Ziqlab. Dotted line shows the outline of the ancient gully channel. Note that the fill derives from the red Terra Rossa soils of the upper plateau.

Fig B.5. This recent agricultural terrace cut in the Upper Ziqlab region has exposed a section showing the red Epipaleolithic paleosol directly (and unconformably) overlain by tan Holocene colluvium.

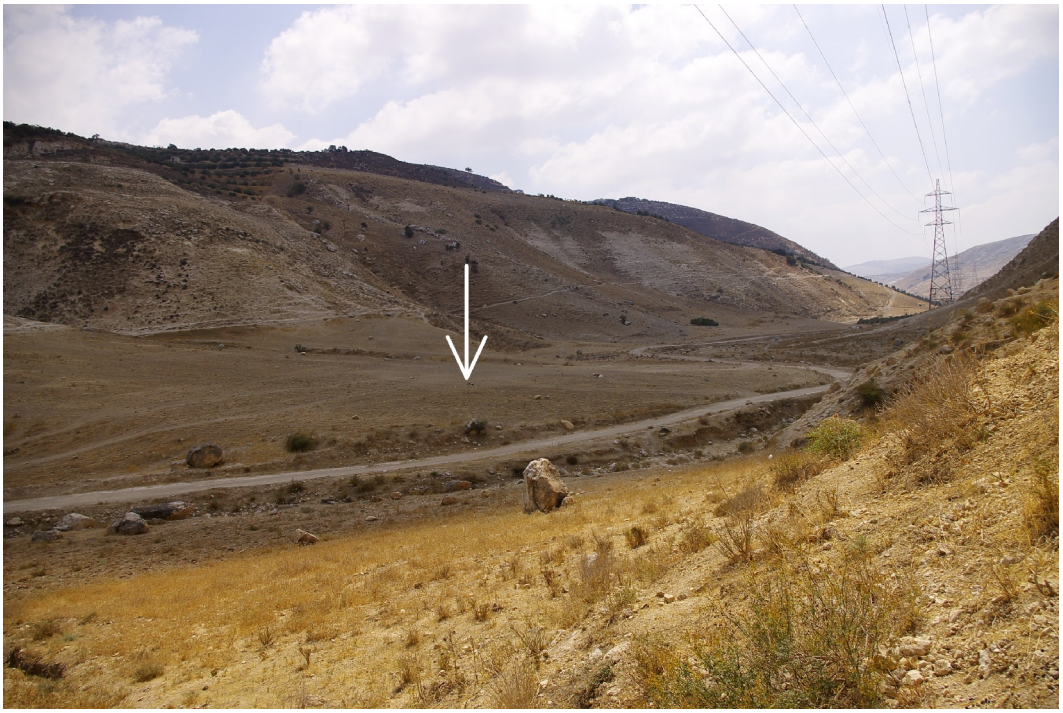

Fig B.6. Overview of the middle section of the Wadi Ziqlab drainage. The arrow points to a good example of the middle terrace in this section of the Wadi.

Fig B.7. This cutbank has exposed a small stratigraphic section of the middle terrace in the mid-reaches of the Ziqlab drainage.

Fig B.8. An excellent example of terrace edge-slump caused by bank undercut in the middle section of the Ziqlab drainage.

Fig B.9. An example of Late Holocene colluvium directly overlying alluvial deposits of the middle terrace in the mid-section of the Ziqlab drainage.

Fig B.10. An example of the Late Holocene colluvium directly and unconformably overlying the Epipaleolithic red paleosol in the middle section of the Wadi Ziqlab drainage.

Fig B.11. The outlined band of red alluvium likely represents reworked sediments eroded from the red Epipaleolithic paleosol further up the Wadi. This stratigraphic section was studied by Maher (2005, 2011).

Fig B.12. This photograph shows multiple slumps on the flank of the middle section of the Ziqlab drainage. The dotted lines outline the individual slump scars, and the arrow shows a small rill/gully that is forming on the same slope.

Fig B.13. This photograph shows a small alluvial fan in the middle section of the Ziqlab drainage. This fan was created by repeated translational debris flows. The arrow points to a small gully that is now forming at the head of the fan.

Fig B.14. A photograph of the spectacular waterfall that occurs at the Tell Rakkan knick point. Image courtesy of Seiji Kadowaki.

Fig B.15. This bulldozer cut on the Tell Rakkan terrace exposes a large section of the Late Holocene colluvium. Note the presence of a portion of stone LPPNB wall appearing in this section.

Fig B.16. An overview of the lower portion of the Ziqlab drainage, showing how incised the channel is at this point. The arrow points to the location of the Tell Rakkan terrace in the distance.

Fig B.17. Several ancient rills/gullies are preserved in the al-Basatin terrace. The dashed line outlines an ancient gully that cut into the Late Neolithic layers. The dotted line (back wall of excavation unit) outlines the remnants of a later gully that cut into the Early Bronze age layers at the site.

Fig B.18. Photographs of the waterfall that forms at the lower knick point in Wadi Ziqlab. The image on the left was taken in 2004, and the image on the right was taken in 2006. The arrow points to approximately the same location in both photographs, and indicates the amount of erosion that had occurred in the space of two years. Left image courtesy of Lisa Maher, right image courtesy of Adam Allentuck.

Fig B.19. Overview of the middle section of Wadi Tayyiba.

Fig B.20. Close up of a section of the middle Wadi Tayyiba drainage. The arrow points to a good example of the Tayyiba middle terrace, which is analogous to the middle terrace of Wadi Ziqlab.

Fig B.21. Overview of lower Tayyiba knickpoint. Notice the presence of an Ottoman period mill.

Fig B.22. Overview of the lower section of the Wadi Tayyiba drainage. Note how incised the channel is in this section.

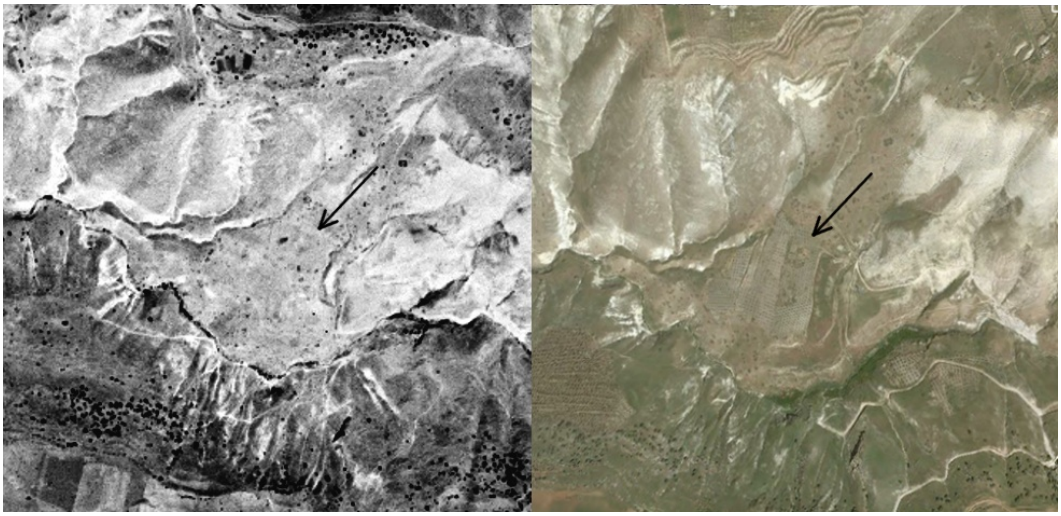

Fig B.23. CORONA (left) and GeoEye (right) imagery of the WT-4 terrace landform. The whole landform may be a rotational slump, and the arrow points to the possible point of detachment. Note that the slump may have originally blocked the entire Wadi channel.

Fig B.24. Close up of the stratigraphy of the "toe" of the WT-4 landform. The photo is looking downstream. Note the "backwards" dipping strata (outlined by the white dotted lines), and the fault (black dashed line). The arrow indicates the amount of slippage that has occurred along the fault line.

Fig B.25. Overview of the middle Wadi Abu Ziad drainage. Note the V-shape of the Wadi.

Fig B.26. Arrows point to probable ancient flint quarries at 'Ain Beidha.

Fig B.27. Overview of large alluvial deposits at the mouth of Wadi Abu Ziad.

Fig B.28. The large exposed section of alluvium at the mouth of Wadi Abu Ziad.

Fig B.29. Close up of the dated strata from the large alluvial deposit at the mouth of Wadi Abu Ziad. The upper dated strata had stone tools and abundant charcoal.

APPENDIX C

PERMISSIONS

Isaac Ullah <iullah@asu.edu>

Permission to use a figure from one of your articles in my dissertation...

Marco Janssen <Marco.Janssen@asu.edu> Mon, Nov 19, 2012 at 12:57 PM
To: "Isaac Ullah (Student)" <Isaac.Ullah@asu.edu>

Hi Isaac,

It is fine with me if you use the Figure 1 from Janssen, M. A. and M. Scheffer. 2004. Overexploitation of renewable resources by ancient societies and the role of sunk-cost effects. Ecology and Society 9(1): 6. [online] URL: http://www.ecologyandsociety.org/vol9/iss1/art6/ in your dissertation.

All the best

Marco Janssen

From: Isaac Ullah [mailto:isaac.ullah@asu.edu]
Sent: Monday, November 19, 2012 10:45 AM
To: Marco Janssen
Subject: Permission to use a figure from one of your articles in my dissertation

[Quoted text hidden]

Isaac Ullah <iullah@asu.edu>

PERMISSION REQUEST - SCIENCE AAAS copyright figure in my dissertation

1 message

Elizabeth Sandler <esandler@aaas.org> Tue, Dec 11, 2012 at 12:59 PM
To: isaac.ullah@asu.edu

Dear Isaac:

Thank you very much for your request and for your interest in our content.
Please feel free to include the figure in your thesis or dissertation subject to the guidelines listed on our website:

http://www.sciencemag.org/site/about/permissions.xhtml#thesis

If how you wish to use our content falls outside of these guidelines or if you have any questions please just let me know.

Best regards,

Liz Sandler
(Ms) Elizabeth Sandler
Rights and Permissions
The American Association for the Advancement of Science
1200 New York Ave., NW
Washington, DC 20005
+1-202-326-6765 (tel)
+1-202-682-0816 (fax)
esandler@aaas.org

>>> Isaac Ullah <isaac.ullah@asu.edu> 11/19/2012 1:38 PM >>>
Hello,

I'd like to request permission to use a figure from an AAAS publication in my dissertation. I'm including the request information here:

Name, Institution, Title, Address:
Isaac I Ullah, M.A.
Archaeology PhD Candidate,
School of Evolution and Social Change
Arizona State University
P.O. Box 2402
Tempe, AZ 85287-2402
tel: 650-201-0479
fax: 480-965-7671

ELSEVIER LICENSE
TERMS AND CONDITIONS

Nov 19, 2012

This is a License Agreement between Isaac I Ullah ("You") and Elsevier ("Elsevier") provided by Copyright Clearance Center ("CCC"). The license consists of your order details, the terms and conditions provided by Elsevier, and the payment terms and conditions.

All payments must be made in full to CCC. For payment instructions, please see information listed at the bottom of this form.

Supplier	Elsevier Limited The Boulevard,Langford Lane Kidlington,Oxford,OX5 1GB,UK
Registered Company Number	1982084
Customer name	Isaac I Ullah
Customer address	616 Flanner Hall Notre Dame, IN 46556-5611
License number	3032560512033
License date	Nov 19, 2012
Licensed content publisher	Elsevier
Licensed content publication	Trends in Ecology & Evolution
Licensed content title	Catastrophic regime shifts in ecosystems: linking theory to observation
Licensed content author	Marten Scheffer,Stephen R. Carpenter
Licensed content date	December 2003
Licensed content volume number	18
Licensed content issue number	12
Number of pages	9
Start Page	648
End Page	656
Type of Use	reuse in a thesis/dissertation
Intended publisher of new work	other
Portion	figures/tables/illustrations
Number of figures/tables /illustrations	3
Format	both print and electronic
Are you the author of this Elsevier article?	Yes
Will you be translating?	No

Order reference number	
Title of your thesis/dissertation	The Consequences of Human Landuse Strategies During the PPNB-LN Transition in Northern Jordan: A Simulation Modeling Approach.
Expected completion date	Dec 2012
Estimated size (number of pages)	400
Elsevier VAT number	GB 494 6272 12
Permissions price	0.00 USD
VAT/Local Sales Tax	0.0 USD / 0.0 GBP
Total	0.00 USD
Terms and Conditions	

INTRODUCTION

1. The publisher for this copyrighted material is Elsevier. By clicking "accept" in connection with completing this licensing transaction, you agree that the following terms and conditions apply to this transaction (along with the Billing and Payment terms and conditions established by Copyright Clearance Center, Inc. ("CCC"), at the time that you opened your Rightslink account and that are available at any time at http://myaccount.copyright.com).

GENERAL TERMS

2. Elsevier hereby grants you permission to reproduce the aforementioned material subject to the terms and conditions indicated.

3. Acknowledgement: If any part of the material to be used (for example, figures) has appeared in our publication with credit or acknowledgement to another source, permission must also be sought from that source. If such permission is not obtained then that material may not be included in your publication/copies. Suitable acknowledgement to the source

(Please contact Elsevier at permissions@elsevier.com)

6. If the permission fee for the requested use of our material is waived in this instance, please be advised that your future requests for Elsevier materials may attract a fee.

7. Reservation of Rights: Publisher reserves all rights not specifically granted in the combination of (i) the license details provided by you and accepted in the course of this licensing transaction, (ii) these terms and conditions and (iii) CCC's Billing and Payment terms and conditions.

8. License Contingent Upon Payment: While you may exercise the rights licensed immediately upon issuance of the license at the end of the licensing process for the transaction, provided that you have disclosed complete and accurate details of your proposed use, no license is finally effective unless and until full payment is received from you (either by publisher or by CCC) as provided in CCC's Billing and Payment terms and conditions. If full payment is not received on a timely basis, then any license preliminarily granted shall be deemed automatically revoked and shall be void as if never granted. Further, in the event that you breach any of these terms and conditions or any of CCC's Billing and Payment terms and conditions, the license is automatically revoked and shall be void as if never granted. Use of materials as described in a revoked license, as well as any use of the materials beyond the scope of an unrevoked license, may constitute copyright infringement and publisher reserves the right to take any and all action to protect its copyright in the materials.

9. Warranties: Publisher makes no representations or warranties with respect to the licensed material.

10. Indemnity: You hereby indemnify and agree to hold harmless publisher and CCC, and their respective officers, directors, employees and agents, from and against any and all claims arising out of your use of the licensed material other than as specifically authorized pursuant to this license.

11. No Transfer of License: This license is personal to you and may not be sublicensed, assigned, or transferred by you to any other person without publisher's written permission.

12. No Amendment Except in Writing: This license may not be amended except in a writing signed by both parties (or, in the case of publisher, by CCC on publisher's behalf).

13. Objection to Contrary Terms: Publisher hereby objects to any terms contained in any purchase order, acknowledgment, check endorsement or other writing prepared by you, which terms are inconsistent with these terms and conditions or CCC's Billing and Payment terms and conditions. These terms and conditions, together with CCC's Billing and Payment terms and conditions (which are incorporated herein), comprise the entire agreement between you and publisher (and CCC) concerning

this licensing transaction. In the event of any conflict between your obligations established by these terms and conditions and those established by CCC's Billing and Payment terms and conditions, these terms and conditions shall control.

14. Revocation: Elsevier or Copyright Clearance Center may deny the permissions described in this License at their sole discretion, for any reason or no reason, with a full refund payable to you. Notice of such denial will be made using the contact information provided by you. Failure to receive such notice will not alter or invalidate the denial. In no event will Elsevier or Copyright Clearance Center be responsible or liable for any costs, expenses or damage incurred by you as a result of a denial of your permission request, other than a refund of the amount(s) paid by you to Elsevier and/or Copyright Clearance Center for denied permissions.

LIMITED LICENSE

The following terms and conditions apply only to specific license types:

15. **Translation**: This permission is granted for non-exclusive world **English** rights only unless your license was granted for translation rights. If you licensed translation rights you may only translate this content into the languages you requested. A professional translator must perform all translations and reproduce the content word for word preserving the integrity of the article. If this license is to re-use 1 or 2 figures then permission is granted for non-exclusive world rights in all languages.

16. **Website**: The following terms and conditions apply to electronic reserve and author websites:
Electronic reserve: If licensed material is to be posted to website, the web site is to be password-protected and made available only to bona fide students registered on a relevant course if:
This license was made in connection with a course,
This permission is granted for 1 year only. You may obtain a license for future website posting,
All content posted to the web site must maintain the copyright information line on the bottom of each image,
A hyper-text must be included to the Homepage of the journal from which you are licensing at http://www.sciencedirect.com/science/journal/xxxxx or the Elsevier homepage for books at http://www.elsevier.com, and
Central Storage: This license does not include permission for a scanned version of the material to be stored in a central repository such as that provided by Heron/XanEdu.

17. **Author website** for journals with the following additional clauses:

All content posted to the web site must maintain the copyright information line on the bottom of each image, and the permission granted is limited to the personal version of your paper. You are not

allowed to download and post the published electronic version of your article (whether PDF or HTML, proof or final version), nor may you scan the printed edition to create an electronic version. A hyper-text must be included to the Homepage of the journal from which you are licensing at http://www.sciencedirect.com/science/journal/xxxxx . As part of our normal production process, you will receive an e-mail notice when your article appears on Elsevier's online service ScienceDirect (www.sciencedirect.com). That e-mail will include the article's Digital Object Identifier (DOI). This number provides the electronic link to the published article and should be included in the posting of your personal version. We ask that you wait until you receive this e-mail and have the DOI to do any posting.

Central Storage: This license does not include permission for a scanned version of the material to be stored in a central repository such as that provided by Heron/XanEdu.

18. **Author website** for books with the following additional clauses: Authors are permitted to place a brief summary of their work online only.
A hyper-text must be included to the Elsevier homepage at http://www.elsevier.com . All content posted to the web site must maintain the copyright information line on the bottom of each image. You are not allowed to download and post the published electronic version of your chapter, nor may you scan the printed edition to create an electronic version.

Central Storage: This license does not include permission for a scanned version of the material to be stored in a central repository such as that provided by Heron/XanEdu.

19. **Website** (regular and for author): A hyper-text must be included to the Homepage of the journal from which you are licensing at http://www.sciencedirect.com/science/journal/xxxxx. or for books to the Elsevier homepage at http://www.elsevier.com

20. **Thesis/Dissertation**: If your license is for use in a thesis/dissertation your thesis may be submitted to your institution in either print or electronic form. Should your thesis be published commercially please reapply for permission. These requirements include permission for the Library and Archives of Canada to supply single copies, on demand, of the complete thesis and include permission for UMI to supply single copies, on demand, of the complete thesis. Should your thesis be published commercially, please reapply for permission.

21. **Other Conditions**

v1.6

If you would like to pay for this license now, please remit this license along with your

payment made payable to "COPYRIGHT CLEARANCE CENTER" otherwise you will be invoiced within 48 hours of the license date. Payment should be in the form of a check or money order referencing your account number and this invoice number RLNK500900251.
Once you receive your invoice for this order, you may pay your invoice by credit card. Please follow instructions provided at that time.

Make Payment To:
Copyright Clearance Center
Dept 001
P.O. Box 843006
Boston, MA 02284-3006

For suggestions or comments regarding this order, contact RightsLink Customer Support: customercare@copyright.com or +1-877-622-5543 (toll free in the US) or +1-978-646-2777.

Gratis licenses (referencing $0 in the Total field) are free. Please retain this printable license for your reference. No payment is required.

ELSEVIER LICENSE
TERMS AND CONDITIONS

Nov 06, 2012

This is a License Agreement between Isaac I Ullah ("You") and Elsevier ("Elsevier") provided by Copyright Clearance Center ("CCC"). The license consists of your order details, the terms and conditions provided by Elsevier, and the payment terms and conditions.

All payments must be made in full to CCC. For payment instructions, please see information listed at the bottom of this form.

Supplier	Elsevier Limited The Boulevard,Langford Lane Kidlington,Oxford,OX5 1GB,UK
Registered Company Number	1982084
Customer name	Isaac I Ullah
Customer address	616 Flanner Hall Notre Dame, IN 46556-5611
License number	3023170866488
License date	Nov 06, 2012
Licensed content publisher	Elsevier
Licensed content publication	Geomorphology
Licensed content title	Towards the identification of scaling relations in drainage basin sediment budgets
Licensed content author	Olav Slaymaker
Licensed content date	20 October 2006
Licensed content volume number	80
Licensed content issue number	1–2
Number of pages	12
Start Page	8
End Page	19
Type of Use	reuse in a thesis/dissertation
Intended publisher of new work	other
Portion	figures/tables/illustrations
Number of figures/tables /illustrations	1
Format	both print and electronic
Are you the author of this Elsevier article?	No
Will you be translating?	No
Order reference number	
Title of your thesis/dissertation	The Consequences of Human Landuse Strategies During the PPNB-LN Transition in Northern Jordan: A Simulation Modelling Approach.
Expected completion date	Dec 2012
Estimated size (number of pages)	400
Elsevier VAT number	GB 494 6272 12
Permissions price	0.00 USD
VAT/Local Sales Tax	0.0 USD / 0.0 GBP
Total	0.00 USD
Terms and Conditions	

INTRODUCTION

1. The publisher for this copyrighted material is Elsevier. By clicking

"accept" in connection with completing this licensing transaction, you agree that the following terms and conditions apply to this transaction (along with the Billing and Payment terms and conditions established by Copyright Clearance Center, Inc. ("CCC"), at the time that you opened your Rightslink account and that are available at any time at http://myaccount.copyright.com).

GENERAL TERMS

2. Elsevier hereby grants you permission to reproduce the aforementioned material subject to the terms and conditions indicated.

3. Acknowledgement: If any part of the material to be used (for example, figures) has appeared in our publication with credit or acknowledgement to another source, permission must also be sought from that source. If such permission is not obtained then that material may not be included in your publication/copies. Suitable acknowledgement to the source must be made, either as a footnote or in a reference list at the end of your publication, as follows:

"Reprinted from Publication title, Vol /edition number, Author(s), Title of article / title of chapter, Pages No., Copyright (Year), with permission from Elsevier [OR APPLICABLE SOCIETY COPYRIGHT OWNER]." Also Lancet special credit - "Reprinted from The Lancet, Vol. number, Author(s), Title of article, Pages No., Copyright (Year), with permission from Elsevier."

4. Reproduction of this material is confined to the purpose and/or media for which permission is hereby given.

5. Altering/Modifying Material: Not Permitted. However figures and illustrations may be altered/adapted minimally to serve your work. Any other abbreviations, additions, deletions and/or any other alterations shall be made only with prior written authorization of Elsevier Ltd. (Please contact Elsevier at permissions@elsevier.com)

6. If the permission fee for the requested use of our material is waived in this instance, please be advised that your future requests for Elsevier materials may attract a fee.

7. Reservation of Rights: Publisher reserves all rights not specifically granted in the combination of (i) the license details provided by you and accepted in the course of this licensing transaction, (ii) these terms and conditions and (iii) CCC's Billing and Payment terms and conditions.

8. License Contingent Upon Payment: While you may exercise the rights licensed immediately upon issuance of the license at the end of the licensing process for the transaction, provided that you have disclosed complete and accurate details of your proposed use, no license is finally effective unless and until full payment is received from you (either by publisher or by CCC) as provided in CCC's Billing and Payment terms and conditions. If full payment is not received on a timely basis, then any license preliminarily granted shall be deemed automatically revoked and shall be void as if never granted. Further, in the event that you breach any of these terms and conditions or any of CCC's Billing and Payment terms and conditions, the license is automatically revoked and shall be void as if never granted. Use of materials as described in a revoked license, as well as any use of the materials beyond the scope of an unrevoked license, may constitute copyright infringement and publisher reserves the right to take any and all action to protect its copyright in the materials.

9. Warranties: Publisher makes no representations or warranties with respect to the licensed material.

10. Indemnity: You hereby indemnify and agree to hold harmless publisher and CCC, and their respective officers, directors, employees and agents, from and against any and all claims arising out of your use of the licensed material other than as specifically authorized pursuant to this license.

11. No Transfer of License: This license is personal to you and may not be sublicensed, assigned, or transferred by you to any other person without publisher's written permission.

12. No Amendment Except in Writing: This license may not be amended except in a writing signed by both parties (or, in the case of publisher, by CCC on publisher's behalf).

13. Objection to Contrary Terms: Publisher hereby objects to any terms contained in any purchase order, acknowledgment, check endorsement or other writing prepared by you, which terms are inconsistent with these terms and conditions or CCC's Billing and Payment terms and conditions. These terms and conditions, together with CCC's Billing and Payment terms and conditions (which are incorporated herein), comprise the entire agreement between you and publisher (and CCC) concerning this licensing transaction. In the event of any conflict between your obligations established by these terms and conditions and those established by CCC's Billing and Payment terms and conditions, these terms and conditions shall control.

14. Revocation: Elsevier or Copyright Clearance Center may deny the permissions described in this License at their sole discretion, for any reason or no reason, with a full refund payable to you. Notice of such denial will be made using the contact information provided by you. Failure to receive such notice will not alter or invalidate the denial. In no event will Elsevier or Copyright Clearance Center be responsible or liable for any costs, expenses or damage incurred by you as a result of a denial of your permission request, other than a refund of the amount(s) paid by you to Elsevier and/or Copyright Clearance Center for denied permissions.

LIMITED LICENSE

The following terms and conditions apply only to specific license types:

15. **Translation**: This permission is granted for non-exclusive world **English** rights only unless your license was granted for translation rights. If you licensed translation rights you may only translate this content into the languages you requested. A professional translator must perform all translations and reproduce the content word for word preserving the integrity of the article. If this license is to re-use 1 or 2 figures then permission is granted for non-exclusive world rights in all languages.

16. **Website**: The following terms and conditions apply to electronic reserve and author websites:
Electronic reserve: If licensed material is to be posted to website, the web site is to be password-protected and made available only to bona fide students registered on a relevant course if:
This license was made in connection with a course,
This permission is granted for 1 year only. You may obtain a license for future website posting,
All content posted to the web site must maintain the copyright information line on the bottom of each image,
A hyper-text must be included to the Homepage of the journal from which you are licensing at http://www.sciencedirect.com/science/journal/xxxxx or the Elsevier homepage for books at http://www.elsevier.com , and
Central Storage: This license does not include permission for a scanned version of the material to be stored in a central repository such as that provided by Heron/XanEdu.

17. **Author website** for journals with the following additional clauses:

All content posted to the web site must maintain the copyright information line on the bottom of each image, and the permission granted is limited to the personal version of your paper. You are not allowed to download and post the published electronic version of your article (whether PDF or HTML, proof or final version), nor may you scan

the printed edition to create an electronic version. A hyper-text must be included to the Homepage of the journal from which you are licensing at http://www.sciencedirect.com/science/journal/xxxxx . As part of our normal production process, you will receive an e-mail notice when your article appears on Elsevier's online service ScienceDirect (www.sciencedirect.com). That e-mail will include the article's Digital Object Identifier (DOI). This number provides the electronic link to the published article and should be included in the posting of your personal version. We ask that you wait until you receive this e-mail and have the DOI to do any posting.

Central Storage: This license does not include permission for a scanned version of the material to be stored in a central repository such as that provided by Heron/XanEdu.

18. **Author website** for books with the following additional clauses: Authors are permitted to place a brief summary of their work online only.
A hyper-text must be included to the Elsevier homepage at http://www.elsevier.com . All content posted to the web site must maintain the copyright information line on the bottom of each image. You are not allowed to download and post the published electronic version of your chapter, nor may you scan the printed edition to create an electronic version.

Central Storage: This license does not include permission for a scanned version of the material to be stored in a central repository such as that provided by Heron/XanEdu.

19. **Website** (regular and for author): A hyper-text must be included to the Homepage of the journal from which you are licensing at http://www.sciencedirect.com/science/journal/xxxxx. or for books to the Elsevier homepage at http://www.elsevier.com

20. **Thesis/Dissertation**: If your license is for use in a thesis/dissertation your thesis may be submitted to your institution in either print or electronic form. Should your thesis be published commercially, please reapply for permission. These requirements include permission for the Library and Archives of Canada to supply single copies, on demand, of the complete thesis and include permission for UMI to supply single copies, on demand, of the complete thesis. Should your thesis be published commercially, please reapply for permission.

21. **Other Conditions**

v1.6

If you would like to pay for this license now, please remit this license along with your payment made payable to "COPYRIGHT CLEARANCE CENTER" otherwise you will be invoiced within 48 hours of the license date. Payment should be in the form of a check or money order referencing your account number and this invoice number RLNK500891923.
Once you receive your invoice for this order, you may pay your invoice by credit card. Please follow instructions provided at that time.

Make Payment To:
Copyright Clearance Center
Dept 001
P.O. Box 843006
Boston, MA 02284-3006

For suggestions or comments regarding this order, contact RightsLink Customer Support: customercare@copyright.com or +1-877-622-5543 (toll free in the US) or +1-978-646-2777.

Gratis licenses (referencing $0 in the Total field) are free. Please retain this printable license for your reference. No payment is required.

ELSEVIER LICENSE
TERMS AND CONDITIONS

Nov 06, 2012

This is a License Agreement between Isaac I Ullah ("You") and Elsevier ("Elsevier") provided by Copyright Clearance Center ("CCC"). The license consists of your order details, the terms and conditions provided by Elsevier, and the payment terms and conditions.

All payments must be made in full to CCC. For payment instructions, please see information listed at the bottom of this form.

Supplier	Elsevier Limited The Boulevard,Langford Lane Kidlington,Oxford,OX5 1GB,UK
Registered Company Number	1982084
Customer name	Isaac I Ullah
Customer address	616 Flanner Hall Notre Dame, IN 46556-5611
License number	3023171060526
License date	Nov 06, 2012
Licensed content publisher	Elsevier
Licensed content publication	Geomorphology
Licensed content title	The potential contribution of geomorphology to tropical mountain development: The case of the MANRECUR project
Licensed content author	Olav Slaymaker
Licensed content date	1 June 2007
Licensed content volume number	87
Licensed content issue number	1–2
Number of pages	11
Start Page	90
End Page	100
Type of Use	reuse in a thesis/dissertation
Intended publisher of new work	other
Portion	figures/tables/illustrations
Number of figures/tables /illustrations	1
Format	both print and electronic
Are you the author of this Elsevier article?	No
Will you be translating?	No
Order reference number	
Title of your thesis/dissertation	The Consequences of Human Landuse Strategies During the PPNB-LN Transition in Northern Jordan: A Simulation Modelling Approach.
Expected completion date	Dec 2012
Estimated size (number of pages)	400
Elsevier VAT number	GB 494 6272 12
Permissions price	0.00 USD
VAT/Local Sales Tax	0.0 USD / 0.0 GBP
Total	0.00 USD
Terms and Conditions	

INTRODUCTION

1. The publisher for this copyrighted material is Elsevier. By clicking

"accept" in connection with completing this licensing transaction, you agree that the following terms and conditions apply to this transaction (along with the Billing and Payment terms and conditions established by Copyright Clearance Center, Inc. ("CCC"), at the time that you opened your Rightslink account and that are available at any time at http://myaccount.copyright.com).

GENERAL TERMS

2. Elsevier hereby grants you permission to reproduce the aforementioned material subject to the terms and conditions indicated.

3. Acknowledgement: If any part of the material to be used (for example, figures) has appeared in our publication with credit or acknowledgement to another source, permission must also be sought from that source. If such permission is not obtained then that material may not be included in your publication/copies. Suitable acknowledgement to the source must be made, either as a footnote or in a reference list at the end of your publication, as follows:

"Reprinted from Publication title, Vol /edition number, Author(s), Title of article / title of chapter, Pages No., Copyright (Year), with permission from Elsevier [OR APPLICABLE SOCIETY COPYRIGHT OWNER]." Also Lancet special credit - "Reprinted from The Lancet, Vol. number, Author(s), Title of article, Pages No., Copyright (Year), with permission from Elsevier."

4. Reproduction of this material is confined to the purpose and/or media for which permission is hereby given.

5. Altering/Modifying Material: Not Permitted. However figures and illustrations may be altered/adapted minimally to serve your work. Any other abbreviations, additions, deletions and/or any other alterations shall be made only with prior written authorization of Elsevier Ltd. (Please contact Elsevier at permissions@elsevier.com)

6. If the permission fee for the requested use of our material is waived in this instance, please be advised that your future requests for Elsevier materials may attract a fee.

7. Reservation of Rights: Publisher reserves all rights not specifically granted in the combination of (i) the license details provided by you and accepted in the course of this licensing transaction, (ii) these terms and conditions and (iii) CCC's Billing and Payment terms and conditions.

8. License Contingent Upon Payment: While you may exercise the rights licensed immediately upon issuance of the license at the end of the licensing process for the transaction, provided that you have disclosed complete and accurate details of your proposed use, no license is finally effective unless and until full payment is received from you (either by publisher or by CCC) as provided in CCC's Billing and Payment terms and conditions. If full payment is not received on a timely basis, then any license preliminarily granted shall be deemed automatically revoked and shall be void as if never granted. Further, in the event that you breach any of these terms and conditions or any of CCC's Billing and Payment terms and conditions, the license is automatically revoked and shall be void as if never granted. Use of materials as described in a revoked license, as well as any use of the materials beyond the scope of an unrevoked license, may constitute copyright infringement and publisher reserves the right to take any and all action to protect its copyright in the materials.

9. Warranties: Publisher makes no representations or warranties with respect to the licensed material.

10. Indemnity: You hereby indemnify and agree to hold harmless publisher and CCC, and their respective officers, directors, employees and agents, from and against any and all claims arising out of your use of the licensed material other than as specifically authorized pursuant to this license.

11. No Transfer of License: This license is personal to you and may not be sublicensed, assigned, or transferred by you to any other person without publisher's written permission.

12. No Amendment Except in Writing: This license may not be amended except in a writing signed by both parties (or, in the case of publisher, by CCC on publisher's behalf).

13. Objection to Contrary Terms: Publisher hereby objects to any terms contained in any purchase order, acknowledgment, check endorsement or other writing prepared by you, which terms are inconsistent with these terms and conditions or CCC's Billing and Payment terms and conditions. These terms and conditions, together with CCC's Billing and Payment terms and conditions (which are incorporated herein), comprise the entire agreement between you and publisher (and CCC) concerning this licensing transaction. In the event of any conflict between your obligations established by these terms and conditions and those established by CCC's Billing and Payment terms and conditions, these terms and conditions shall control.

14. Revocation: Elsevier or Copyright Clearance Center may deny the permissions described in this License at their sole discretion, for any reason or no reason, with a full refund payable to you. Notice of such denial will be made using the contact information provided by you. Failure to receive such notice will not alter or invalidate the denial. In no event will Elsevier or Copyright Clearance Center be responsible or liable for any costs, expenses or damage incurred by you as a result of a denial of your permission request, other than a refund of the amount(s) paid by you to Elsevier and/or Copyright Clearance Center for denied permissions.

LIMITED LICENSE

The following terms and conditions apply only to specific license types:

15. **Translation**: This permission is granted for non-exclusive world **English** rights only unless your license was granted for translation rights. If you licensed translation rights you may only translate this content into the languages you requested. A professional translator must perform all translations and reproduce the content word for word preserving the integrity of the article. If this license is to re-use 1 or 2 figures then permission is granted for non-exclusive world rights in all languages.

16. **Website**: The following terms and conditions apply to electronic reserve and author websites:
Electronic reserve: If licensed material is to be posted to website, the web site is to be password-protected and made available only to bona fide students registered on a relevant course if:
This license was made in connection with a course,
This permission is granted for 1 year only. You may obtain a license for future website posting,
All content posted to the web site must maintain the copyright information line on the bottom of each image,
A hyper-text must be included to the Homepage of the journal from which you are licensing at http://www.sciencedirect.com/science/journal/xxxxx or the Elsevier homepage for books at http://www.elsevier.com , and
Central Storage: This license does not include permission for a scanned version of the material to be stored in a central repository such as that provided by Heron/XanEdu.

17. **Author website** for journals with the following additional clauses:

All content posted to the web site must maintain the copyright information line on the bottom of each image, and the permission granted is limited to the personal version of your paper. You are not allowed to download and post the published electronic version of your article (whether PDF or HTML, proof or final version), nor may you scan

the printed edition to create an electronic version. A hyper-text must be included to the Homepage of the journal from which you are licensing at http://www.sciencedirect.com/science/journal/xxxxx . As part of our normal production process, you will receive an e-mail notice when your article appears on Elsevier's online service ScienceDirect (www.sciencedirect.com). That e-mail will include the article's Digital Object Identifier (DOI). This number provides the electronic link to the published article and should be included in the posting of your personal version. We ask that you wait until you receive this e-mail and have the DOI to do any posting.

Central Storage: This license does not include permission for a scanned version of the material to be stored in a central repository such as that provided by Heron/XanEdu.

18. **Author website** for books with the following additional clauses: Authors are permitted to place a brief summary of their work online only.
A hyper-text must be included to the Elsevier homepage at http://www.elsevier.com . All content posted to the web site must maintain the copyright information line on the bottom of each image. You are not allowed to download and post the published electronic version of your chapter, nor may you scan the printed edition to create an electronic version.

Central Storage: This license does not include permission for a scanned version of the material to be stored in a central repository such as that provided by Heron/XanEdu.

19. **Website** (regular and for author): A hyper-text must be included to the Homepage of the journal from which you are licensing at http://www.sciencedirect.com/science/journal/xxxxx. or for books to the Elsevier homepage at http://www.elsevier.com

20. **Thesis/Dissertation**: If your license is for use in a thesis/dissertation your thesis may be submitted to your institution in either print or electronic form. Should your thesis be published commercially please reapply for permission. These requirements include permission for the Library and Archives of Canada to supply single copies, on demand, of the complete thesis and include permission for UMI to supply single copies, on demand, of the complete thesis. Should your thesis be published commercially, please reapply for permission.

21. **Other Conditions**

v1.6

If you would like to pay for this license now, please remit this license along with your payment made payable to "COPYRIGHT CLEARANCE CENTER" otherwise you will be invoiced within 48 hours of the license date. Payment should be in the form of a check or money order referencing your account number and this invoice number RLNK500891927.
Once you receive your invoice for this order, you may pay your invoice by credit card. Please follow instructions provided at that time.

Make Payment To:
Copyright Clearance Center
Dept 001
P.O. Box 843006
Boston, MA 02284-3006

For suggestions or comments regarding this order, contact RightsLink Customer Support: customercare@copyright.com or +1-877-622-5543 (toll free in the US) or +1-978-646-2777.

Gratis licenses (referencing $0 in the Total field) are free. Please retain this printable license for your reference. No payment is required.